

Investigating Biofumigation for the Control of Plant-Parasitic Nematodes

John William Harry Lennon

Submitted in accordance with the requirements for the degree of
Doctor of Philosophy

The University of Leeds

School of Biology

September 2018

The candidate confirms that the work submitted is his own and that appropriate credit has been given where reference has been made to the work of others.

This copy has been supplied on the understanding that it is copyright material and that no quotation from the thesis may be published without proper acknowledgement.

The right of John William Harry Lennon to be identified as Author of this work has been asserted by him in accordance with the Copyright, Designs and Patents Act 1988.

Dedicated to my grandfather, Harry Graham Wallace.

Acknowledgements

First and foremost I would like to thank my supervisor, Professor Urwin, for giving me the opportunity to undertake my PhD and for providing guidance and support over the years.

I would also like to thank my co-supervisor Dr Kelly Redeker for his support and expertise, which proved invaluable.

Thanks go to Dr Catherine Lilley for her words of wisdom and wealth of knowledge.

The Plant Nematology group, past and present, earn thanks not only through the support and assistance offered in the lab, but for creating a fantastic, friendly environment to work in. Friday cakes will be missed!

I'd like to thank Chris Bell for being a great lab mate and mate in general, and all the friends I've made over the past 4 years, both within university walls and without.

Finally, I'd like to thank my family for spurring me on over the years, and for inspiring me to begin with.

ABSTRACT

The white potato cyst nematode, *Globodera pallida*, is an important pest of potato in all potato-growing regions of the world and is of particular importance to UK agriculture, found in 48-64 % of UK potato fields and incurring costs related to management and yield losses. Biofumigation is a pest management practice that seeks to exploit the production of bioactive compounds, isothiocyanates, from disrupted brassica tissues incorporated into soil. Aspects of biofumigation as they relate to control of *G. pallida* were investigated.

The xenobiotic metabolism of *G. pallida* juveniles in response to contact with isothiocyanates was investigated through RNAseq analysis of nematodes exposed to Dazomet, an isothiocyanate generator. The roles of genes implicated in this response were investigated and their up-regulation confirmed, identifying several genes directly implicated in detoxification of xenobiotic compounds, presenting targets for development of future controls.

A screening system for evaluation of novel biofumigant crops was developed, utilising *Caenorhabditis elegans* reporter lines that indicated the presence of isothiocyanates through induced expression of green fluorescent protein (GFP). Attempts to generate novel *C. elegans* reporters for *G. pallida* genes were unsuccessful, but progress was made towards generation of transgenic root-knot nematodes, a step towards a plant-parasitic nematode model system.

The volatile emissions given off by brassicas as they grow were measured and a number of bioactive compounds were identified. New estimates of the contributions of brassicas to atmospheric methyl bromide concentrations were generated. A system was developed to test the toxicity of volatile compounds as given off by the above- and belowground biomass of brassicas, and toxicity was observed in *C. elegans* adults and *G. pallida* juveniles and encysted eggs.

The approaches taken to investigate biofumigation are novel and support expansion of the scope of future biofumigation research in line with the findings presented.

Table of Contents

Acknowledgements.....	i
ABSTRACT.....	ii
Table of Contents.....	iii
List of Figures.....	viii
List of Tables.....	xi
Glossary.....	xii
Chapter 1 Introduction.....	1
1.1 The potato.....	1
1.2 Plant-parasitic nematodes.....	2
1.2.1 Cyst nematodes.....	2
1.2.3 Potato cyst nematodes.....	3
1.2.4 The life cycle of potato cyst nematodes.....	5
1.2.5 The syncytium.....	10
1.2.6 Potato cyst nematode genomics.....	11
1.3 Control of potato cyst nematodes.....	15
1.3.1 Resistant potato cultivars.....	15
1.3.2 Chemical control of nematode pests of potato.....	16
1.4 Biofumigation.....	20
1.4.1 Glucosinolates and the production of isothiocyanates.....	20
1.4.2 The glucosinolate-myrosinase defence system.....	24
1.4.3 Biofumigation in agricultural practice.....	25
1.5 Aims.....	32
Chapter 2 General Materials & Methods.....	33
2.1 Biological Materials.....	33

2.2	Cultivation of nematodes	33
2.2.1	Cultivation of cyst nematode populations.....	33
2.2.2	Extraction of cysts from soil	34
2.2.3	Performing egg counts	34
2.2.4	Hatching <i>Globodera pallida</i> cysts.....	34
2.2.5	Plate cultivation of <i>Caenorhabditis elegans</i>	35
2.2.6	<i>Caenorhabditis elegans</i> liquid cultures.....	35
2.3	Bacterial cultivation.....	36
2.3.1	Preparation of <i>E. coli</i> HT115 as a food source for <i>C. elegans</i> liquid culture 36	
2.3.2	Preparation of ultra-competent <i>E. coli</i> DH5 α	36
2.4	Molecular Biological Techniques.....	37
2.4.1	Transformation of ultra-competent cells.....	37
2.4.2	Extraction of plasmid DNA from bacterial cultures	37
2.4.3	Extraction of nematode genomic DNA	38
2.4.4	Phenol-chloroform extraction of nucleic acids.....	39
2.4.5	Ethanol precipitation of nucleic acids.....	39
2.4.6	Polymerase chain reaction.....	39
2.4.7	Colony PCR	42
2.4.8	Agarose gel electrophoresis.....	43
Chapter 3	<i>Globodera pallida</i> xenobiotic metabolism in the context of biofumigation 44	
3.1	Introduction.....	44
3.2	Aims	48
3.3	Materials & methods.....	49
3.3.1	RNAseq analysis of <i>Globodera pallida</i> xenobiotic metabolism	49

3.3.2	Confirming gene models and cloning promoter regions	49
3.3.3	Bioinformatic analysis of genes	50
3.3.4	RNA extraction and reverse transcription	50
3.3.5	Quantitative PCR	51
3.4	Results	54
3.4.1	RNAseq analysis	54
3.4.2	Confirmation of gene models and bioinformatics	54
3.4.5	Quantification of expression in Dazomet-treated second-stage juveniles 78	
3.5	Discussion	81
3.5.1	Genes implicated in <i>Globodera pallida</i> xenobiotic metabolism	81
3.5.2	Identification of genes through exposure to known xenobiotics	83
3.5.3	Potential for RNAi-based control of <i>G. pallida</i>	84
3.5.4	Differences in fold-change observed from RNAseq and qPCR data	84
3.5.5	Conclusions	85
3.6	Summary	86
4	Utilising <i>C. elegans</i> reporter lines to identify xenobiotic activity in plants	87
4.1	Introduction	87
4.2	Aims	90
4.3	Materials & methods	91
4.3.1	Source of reporter lines	91
4.3.2	Toxicity of isothiocyanates to <i>C. elegans</i>	91
4.3.3	Reporter line chemical exposures	91
4.3.4	Imaging fluorescent nematodes	91
4.3.5	Quantification of GFP response	92
4.3.6	Generating leaf extracts	92

4.3.7	Plant tissue extract exposures	93
4.3.8	Generation of transformation vectors for nematode bombardment	93
4.3.9	Preparation of vector for transformation of nematodes	95
4.3.10	Bombardment protocol	96
4.3.11	Selection of positive transformants	97
4.3.12	Double plasmid bombardment protocol	97
4.3.13	Data analysis	97
4.4	Results	103
4.4.1	Toxicity of isothiocyanates to <i>C. elegans</i> N2 adults.....	103
4.4.2	<i>gst-31::gfp</i> reporter lines	103
4.4.3	Transforming <i>C. elegans</i> with GFP under control of exogenous promoters 113	
4.4.4	Transforming <i>C. elegans</i> by microparticle bombardment with two vectors 113	
4.4.5	Attempts to transform <i>Globodera pallida</i> and <i>Meloidogyne incognita</i> .	118
4.5	Discussion	120
4.5.1	<i>C. elegans</i> reporter lines as reporters of biofumigant activity	120
4.5.2	Generation of <i>C. elegans</i> reporters for <i>G. pallida</i> xenobiotic metabolism 121	
4.5.3	Double bombardment of <i>C. elegans</i>	121
4.5.4	Transgenesis of plant-parasitic nematodes	123
4.5.5	Conclusions	123
4.6	Summary.....	125
Chapter 5 Investigating the volatile emissions of brassicas as a source of pest management		126
5.1	Introduction.....	126
5.2	Aims	129

5.3	Materials & methods.....	130
5.3.1	Growth of plants for volatile sampling	130
5.3.2	Sampling plant volatiles	130
5.3.3	Analysis of volatile samples and calculation of flux.....	133
5.3.4	Estimating contributions of brassicas to global methyl bromide budgets 133	
5.3.5	Volatile toxicity assays	134
5.3.6	Statistical analyses	137
5.4	Results	138
5.4.1	Gaseous compounds emitted by brassicas in a closed environment	138
5.4.2	Toxicity of emitted compounds to nematodes.....	155
5.5	Discussion.....	160
5.5.1	Brassicas produce bioactive methyl halides and dimethyl sulphide.....	160
5.5.1.2	Negative flux values.....	161
5.5.2	Atmospheric impacts of brassicaceous crops.....	161
5.5.3	Toxicity of volatile compounds emitted by brassicas.....	162
5.6	Summary	164
Chapter 6	General Discussion	165
6.1	Investigating xenobiotic metabolism of <i>Globodera pallida</i>	165
6.2	Screening plant extracts for biofumigant activity	167
6.3	Developing transgenesis of plant-parasitic nematodes.....	169
6.4	Bioactivity of volatile compounds released by plants.....	171
6.5	Environmental impacts of biofumigation.....	173
Chapter 7	References.....	176

List of Figures

Figure 1.1 Simplified life cycle of a cyst nematode.	9
Figure 1.2 The general structure of glucosinolates and their breakdown products.	22
Figure 3.1 Fold changes of genes of interest identified from RNAseq analysis.	55
Figure 3.2 Heatmap and principal components analysis showing clustering of gene regulation in Dazomet-exposed <i>G. pallida</i>.	56
Figure 3.3 Amino acid sequence alignment for GP01278.	57
Figure 3.4 Comparison of cloned and predicted amino acid sequences for GP02040.	58
Figure 3.5 GP02405 sequence homology with <i>M. incognita</i> GST-1.	60
Figure 3.6 Amino acid sequence alignment for GP03693.	61
Figure 3.7 GP04700 predicted ORFs.	64
Figure 3.8 Comparison of predicted and sequenced protein models for GP04723.	65
Figure 3.9 GP07079 amino acid sequence alignment.	66
Figure 3.10 Signal peptide identified in the GP08126 sequence.	67
Figure 3.11 GP08879 sequence alignments.	68
Figure 3.12 GP09707 sequence alignment.	70
Figure 3.13 Cloned GP10083 sequence aligns well with the predicted sequence, post-translation.	71
Figure 3.14 GP10467 compared with <i>G. rostochiensis</i> g04732.	72
Figure 3.15 GP10686 structural features.	74
Figure 3.16 GP11840 sequence alignments.	75
Figure 3.17 Predicted GP11984 amino acid sequence compared with the cloned GP02405 sequence.	76

Figure 3.18 GP12030 sequence and signal peptide prediction.....	77
Figure 3.19 Fold change in gene expression in <i>G. pallida</i> second-stage juveniles following exposure to Dazomet.....	79
Figure 4.1 annotated schematic of the pJM119 vector backbone	98
Figure 4.2 pPD95_75 vector backbone with restriction sites highlighted.	99
Figure 4.3 structure of plasmid pBCN22.....	100
Figure 4.4 Viability of <i>C. elegans</i> N2 adults after 16h exposure to isothiocyanates.	104
Figure 4.5 Quantification of GFP response in allyl isothiocyanate and Dazomet-exposed <i>gst-31::gfp</i> reporters over time.	105
Figure 4.6 Dose-dependent response of <i>C. elegans gst-31::gfp</i> reporters to methyl isothiocyanate and Dazomet.	106
Figure 4.7 Differential sensitivity of <i>gst-31::gfp</i> reporters to isothiocyanates.....	108
Figure 4.8 Non-brassicaceous leaf extracts induced no up-regulation of <i>gst-31</i>	110
Figure 4.9 Brassicaceous leaf extracts induce a dose-dependent up-regulation of <i>gst-31</i>	111
Figure 4.10 Schematic diagram of the generation of pPDmCh.....	115
Figure 4.11 <i>C. elegans unc-119</i> mutants bombarded simultaneously with pPDmCh-my0-2 and pPD95_75-Ce-my0-2 showed red and green fluorescence in the pharynx.	116
Figure 4.12 Transgenic <i>Meloidogyne incognita</i> egg with GFP under control of a <i>G. pallida GAPDH1</i> promoter.....	119
Figure 5.1 Plant volatile sampling chamber.	132
Figure 5.2 The nested dish system used to assay toxicity of volatile compounds. ...	135

Figure 5.3 Gas fluxes from <i>Brassica juncea</i> cv. 'ISCI99' roots and aboveground biomass over 3 growth stages.	143
Figure 5.4 Gas fluxes from <i>Raphanus sativus</i> cv. 'WeedCheck' roots and aboveground biomass over 3 growth stages.	145
Figure 5.5 Gas fluxes from <i>Raphanus sativus</i> cv. 'Diablo' roots and aboveground biomass over 3 growth stages.	148
Figure 5.6 Gas fluxes from <i>Eruca sativa</i> cv. 'Nemat' roots and aboveground biomass over 3 growth stages.	151
Figure 5.7 Toxicity of methyl iodide to <i>C. elegans</i> N2 adults in solution and in volatile form.	156
Figure 5.8 Inactivity in <i>Globodera pallida</i> J2s after 18h incubation with volatile methyl iodide, with or without additional chloroform.	157
Figure 5.9 Inactivity in <i>Globodera pallida</i> J2s after incubation with volatile dimethyl sulphide.	158
Figure 5.10 Toxicity of methyl iodide and dimethyl sulphide to <i>Globodera pallida</i> encysted eggs.	159

List of Tables

Table 3.1 Primers for sequencing of <i>G. pallida</i> genes	52
Table 3.2 qPCR primers.	53
Table 3.3 Comparison of the fold changes reported by RNAseq and qPCR77	
Table 4.1 Isothiocyanates used in ITC-screens with reporters.	101
Table 4.2 Primers used for generating and checking promoter constructs.	102
Table 4.3 Transformation vectors generated for each vector backbone.	114
Table 4.4 Rates of transformation and of inheritance in subsequent generations following double bombardment.	115
Table 5.1 Compounds investigated in Chapter 5	136
Table 5.2 One-way ANOVA of compound fluxes against growth stages	139
Table 5.3 One-way ANOVA comparing flux of compounds against cultivar	140
Table 5.4 Total flux per plant, based on average dry biomass	153
Table 5.5 Estimates of the global yearly methyl bromide flux due to growth of mustard and radish as cash crops	154

Glossary

ABC	ATP-binding cassette
AHDB	Agriculture and Horticulture Development Board
ANOVA	Analysis of variance
ATP	Adenosine triphosphate
BLAST	Basic local alignment search tool
CCD	Charge-coupled device
CDS	Coding DNA sequence
CFC	Chlorofluorocarbon
CRISPR	Clustered regularly interspaced short palindromic repeats
CYP	Cytochrome P450 protein
DMDS	Dimethyl disulphide
DMS	Dimethyl sulphide
DMSO	Dimethyl sulphoxide
DNA	Deoxyribonucleic acid
DZM	Dazomet
EC	Enzyme Commission
EDTA	Ethylenediaminetetraacetic acid
ESP	Epithiospecifier protein
EU	European Union
EUR	Euro, €
FAO	Food and Agricultural Organisation of the United Nations
GAPDH	Glyceraldehyde 3-phosphate dehydrogenase
GBP	Pounds sterling, £
GC/MS	Gas chromatography/mass spectrometry

GFP	Green fluorescent protein
GM	Genetically modified
GSH	Glutathione (reduced)
GSL	Glucosinolate
GST	Glutathione S-transferase
HOL	Harmless to ozone layer
HTMT	Halide transferase/methyl transferase
IAA	Isoamyl alcohol
IPM	Integrated pest management
ISC	Initial syncytial cell
ITC	Isothiocyanate (see page 98 for a complete list of ITCs used in this study)
IUPAC	International Union of Pure and Applied Chemistry
LB	Lysogeny broth
MeBr	Methyl bromide
MeCl	Methyl chloride
MeI	Methyl iodide
MeSH	Methane thiol
NGM	Nematode growth medium
NSP	Nitrile-specifier protein
ORF	Open reading frame
PCN	Potato cyst nematode
PCR	Polymerase chain reaction
PEP	Phosphoenol pyruvate
PIPES	Piperazine-N,N'-bis(2-ethanesulfonic acid)
PMT	Phosphoethanolamine methanol transferase

PPN	Plant-parasitic nematodes
PVC	Polyvinyl chloride
RFP	Red fluorescent protein
RISC	RNA-induced silencing complex
RKN	Root-knot nematode
RNA	Ribonucleic acid
RNAi	RNA interference
SAM	S-adenosyl-L-methionine
SD	Standard deviation
SDS	Sodium dodecyl sulphate
SEM	Standard error in the mean
SOB	Super optimal broth
SXC	Six cysteine domain
TAE	Tris-acetate EDTA
TAT	Tyrosine aminotransferase
TB	Transformation buffer
TBE	Tris-borate EDTA
TFP	Thiocyanate-forming protein
UGT	Uridine 5'-diphospho-glucuronosyltransferase
UNEP	United Nations Environment Programme
US(A)	United States (of America)
USD	US Dollars, \$
UV	Ultraviolet
XME	Xenobiotic metabolism enzyme

Chapter 1 Introduction

1.1 The potato

The potato, *Solanum tuberosum*, is a tuberous vegetable of the family Solanaceae, originating in the Andes and now a staple foodstuff around the world. It is the 4th highest produced food crop and 5th most produced crop globally, following sugarcane (grown principally for processing and industrial usage), maize, wheat and rice (FAOSTAT, 2017). Genomic analysis of cultivated and wild potato relatives have found evidence for a single origin for cultivated potato in the southern regions of Peru, some time before the expansion of European cultures into South America (Spooner et al., 2005). In Europe, potatoes are an important cash crop supporting an international industry based around ware potatoes for eating and processing, and seed potatoes for tuber production: over 56 million tonnes of potatoes were produced in the EU in 2016 (FAOSTAT, 2017), for a production value of around EUR 12.7 billion (Eurostat, 2017). Total potato production in the UK was worth GBP 747 million in 2016 (Eurostat, 2017).

One of the major associated costs for UK potato production is the application of pesticides. The major pathogens associated with potato in the UK are late blight, caused by the oomycete *Phytophthora infestans*, and the potato cyst nematodes, *Globodera pallida* and *G. rostochiensis*. Management of late blight requires repeated prophylactic application of costly fungicides (Liljeroth et al., 2016). Nematode management includes use of soil fumigants, which may account for 17% of the total production cost of a crop (Kerry et al., 2003). As well as monetary costs, pesticides contribute to the carbon emissions of potato production, accounting for up to 14 % of the emitted CO₂ associated with a potato crop (Haverkort and Hillier, 2011). For growers, it is important to be able to manage the impact of pathogens and pests in order to protect their crops, while governments are concerned both with the reduction of CO₂ emissions in order to limit the impacts of climate change (in accordance with the Paris agreement (UNFCC, 2016)), and with regulating the use of crop treatments with other negative environmental effects (e.g. ozone depletion, according to the Montreal Protocol (UNEP, 2012)). Much research is therefore focused on generating methods of pest control that are both cost-effective and environmentally sound.

1.2 Plant-parasitic nematodes

Plant-parasitic nematodes are agricultural pests of great economic importance, with global annual crop losses estimates running from 80 billion USD (Nicol et al., 2011) to as high as 157 billion USD (Abad et al., 2008). It is suggested that such losses may be underestimated (De Waele and Elsen, 2007), due to under-reporting of nematode damage by growers – particularly in developing nations – due to a lack of knowledge leading to incorrect diagnosis. Plant parasitism has evolved independently a number of times in the phylum Nematoda (Kikuchi et al., 2017, van Megen et al., 2009), and a number of plant-parasitic feeding strategies are therefore represented among nematodes; the most economically important of these is sedentary endoparasitism. Sedentary endoparasites are those nematodes of the family Heteroderidae that adopt a fixed feeding site in the roots of the host plant, and are represented by the root-knot nematodes and the cyst nematodes, considered the two most important plant-parasitic nematodes in plant pathology, respectively (Jones et al., 2013a).

1.2.1 Cyst nematodes

Cyst nematodes comprise 8 genera and 114 described species, the most important of which fall into the genera *Globodera* (12 species) and *Heterodera* (82 species) (Turner and Subbotin, 2013). Species of the genus *Meloidogyne*, the root-knot nematodes, also belong to the Heteroderidae but are not classified as cyst nematodes as they do not form cysts, as do the adult females that typify the group. Cyst nematodes are found in most crop-growing regions of the world, although they are typically restricted to temperate climates (Turner and Subbotin, 2013); there are, however, reports of cyst nematodes in tropical regions, such as *Globodera rostochiensis* found on potato in East Java, Indonesia (Indarti et al., 2004), and *Heterodera avenae* found on cereal crops in northern and central India (Rao et al., 2013).

The host ranges of cyst nematodes are typically narrow, especially with respect to the broad host ranges exhibited by parthenogenetic *Meloidogyne* species (Trudgill, 1997). The cyst nematode species of greatest economic importance are those that affect those crop species that are grown most widely. Soybean cyst nematodes (*Heterodera glycines*) cause up to 1.5 billion USD in crop losses in the US each year and were responsible for yield losses of 9 million metric tons worldwide in 1998 (Wrather et al., 2001). Cereal cyst

nematodes (*H. avenae* and *H. filipjevi*) affect cereal grains such as wheat and barley and can cause yield losses of up to 90 % in affected fields (Nicol et al., 2011). The potato cyst nematodes (*Globodera pallida* and *G. rostochiensis*) affect crops of the family Solanaceae and are found in most potato-growing regions of the world (Turner and Subbotin, 2013). The sugarbeet nematode (*H. schachtii*) is atypical among cyst nematodes in that it has a relatively broad host range, able to parasitise plants of the Brassicaceae (mustards) including *Arabidopsis thaliana*, as well as sugar beet (Nielsen et al., 2003, Sijmons et al., 1991); losses to European sugar beet production in 1999 due to *H. schachtii* were estimated at 90 million EUR (Müller, 1999). Other cyst nematodes of note are the rice cyst nematode, *Heterodera oryzae* (ref), and the corn cyst nematode, *H. zaeae*, which parasitises the grains grown in greatest quantity around the world: maize, wheat, and rice (IGC, 2017).

1.2.3 Potato cyst nematodes

Potato cyst nematodes belong to the genus *Globodera*: as important pests of potato, they are quarantine pathogens in most temperate potato-growing regions of the world (Nicol et al., 2011, Turner and Subbotin, 2013). *Globodera* spp. have a narrow host range, limited to plants of the family Solanaceae, but cause crop losses totalling ~9 % of all global potato production (Turner and Subbotin, 2013). Assessed almost 20 years ago, potato cyst nematodes were present in 64% of English and Welsh potato fields, represented by *Globodera pallida* and *G. rostochiensis*, found in 92 % and 33 % of contaminated fields respectively (Minnis et al., 2002). A more recent investigation into potato fields in England and Wales found that PCN were present in 48 % of the 491 tested sites; of these, mixed populations made up 5 %, while *G. pallida* and *G. rostochiensis* were detected in isolation in 89 % and 6 %, respectively (Lima-Dybal, 2016, unpublished). The decline of *G. rostochiensis* incidence relative to *G. pallida* can be largely attributed to the wide availability of *G. rostochiensis*-resistant potato cultivars (Minnis et al., 2002). A survey of potato fields in Scotland found *G. pallida* in 76 % of 687 tested (Eves-van den Akker et al., 2015). These two species are the most economically significant species of potato cyst nematodes globally (Bohlmann and Sobczak, 2014, Jones et al., 2013a), costing UK agriculture an estimated 50 million GBP per annum (Jones et al., 2017b). Other PCN species of note include *G. ellingtonae*, a potato cyst

nematode identified in US potato fields in 2008 (Handoo et al., 2012, Skantar et al., 2011), and *G. tabacum*, the tobacco cyst nematode, a pest of tobacco production in both North America and mainland Europe (Bardou-Valette et al., 2016, Mota and Eisenback, 1993).

The origin of potato cyst nematodes can be traced to the Andes, in the regions broadly around the Peru-Bolivia border (Grenier et al., 2010, Mai, 1977). Evolution is thought to have occurred concurrently with the wild potato for 15-21 million years, highlighting the intimate relationship between parasite and host (Jones et al., 2018a). Populations of the two species are separated by latitude and altitude, with *G. pallida* occurring in the cooler regions north of Lake Titicaca, with *G. rostochiensis* found in the lower southern regions (Grenier et al., 2010). This geographical separation is thought to have been a factor in their differentiation, and has impacts on their respective heat tolerances: *G. pallida*, being adapted to cooler climates, is more sensitive to heat stress than *G. rostochiensis*, with implications for their future survivability in the face of rising global temperatures (Jones et al., 2017b). European populations of *Globodera pallida* have been traced back to a single contamination event from a southern Peruvian population, imported on infested potato, from which it has spread across the continent (Plantard et al., 2008). Contamination of North America has occurred on at least two occasions: microsatellite analysis of 15 geographically distinct *G. rostochiensis* populations suggested that it was brought to Europe around the same time as *G. pallida*, and was then introduced to Canada and the US from at least two distinct European populations (Boucher et al., 2013). Suggested mechanisms for these contamination events include contaminated soil brought over on flower bulbs (Rott et al., 2010) and on returning military equipment in the aftermath of World War II (Boucher et al., 2013).

On a regional scale, potato cyst nematodes are spread largely through agricultural activity – the movement of infested plant material and of farm equipment carrying infested soil – giving a dispersal rate of 5.3 km per year from any given field, based on modelling of historical dispersal data (Banks et al., 2012). Detection of low density field populations can be incredibly difficult (Banks et al., 2012), even in fields that have previously tested positive for *Globodera* infestation (Eves-van den Akker et al., 2015). While low density populations may be difficult to detect, they may lead to devastating

impacts on a crop due to the potential for populations to increase 60-fold over the course of one cropping season (Moxnes and Hausken, 2007).

Both *Globodera pallida* and *G. rostochiensis* are quarantine pests in the EU. As such, there are directives in place to monitor populations and limit or prevent the spread of *Globodera* species from known sites of infection to uncontaminated fields. The European Union's Regulation (EU) 2016/2031 sets out requirements for the testing of fields for the presence of potato cyst nematodes and bans the growing of seed potatoes, or other plants grown for planting, on fields in which cyst nematodes are detected. This aims to limit the spread of cyst nematodes beyond fields where they are already present. Efforts to control potato cyst nematodes are discussed further in a later section (Chapter 1.3)

1.2.4 The life cycle of potato cyst nematodes

All cyst nematodes follow a similar life cycle, with some variation in timings and population dynamics. Encysted eggs hatch principally when induced by signals indicating the presence of a potential host plant, and at a lower rate at random. Second-stage juveniles (J2s) emerge from eggs within the cyst, then migrate towards and infiltrate host roots. When a suitable feeding site is found, the nematode forms a fixed feeding site and from there progresses through J3 and J4 stages to adulthood. Adult males leave the feeding site to find sedentary adult females with which to mate. After production of viable eggs, the female dies and encysts around the eggs – the nematodes within develop into first-stage juveniles and moult to the J2 stage before they are ready to hatch. Details specific to potato cyst nematode follow; a schematic diagram is given in Figure 1.1.

Among cyst nematodes, *Globodera* species are classed as having a low random hatch rate (Perry, 2002) – population decline within cysts in fallow fields may be as low as 10% per year, meaning that viable eggs can persist in a field for over 20 years (Turner, 1996). Soil conditions, including pH, moisture content and ambient temperatures, influence the rate of population decline, with higher temperatures in particular leading to a greater falloff over time (Perry, 2002). Hatching is strongly induced by root exudate from a suitable host, such as potato (*Solanum tuberosum*) or tomato (*S. lycopersicum*), though only after a period of diapause typically lasting approximately 6 months (Palomares-Rius

et al., 2013): this means that the next generation of nematodes remains viable until the next host crop is planted, and that non-host cropping and periods of fallow do little to reduce population numbers in an affected field (Turner and Subbotin, 2013). Potato cyst nematode eggs undergo two forms of dormancy before hatching. The first, diapause, requires a period of cold soil temperatures to pass (Palomares-Rius et al., 2013). The length of diapause is dependent on the growth conditions in which the eggs were produced (Salazar and Ritter, 1993). Upon completing diapause, the eggs enter the second dormant phase: quiescence, a reversible state of dormancy that is broken by the presence of suitable host root exudates (Perry and Moens, 2011). An advantage of the longevity of encysted eggs and the specificity of hatching induction is that infested soil samples can be stored for research purposes over long periods, and hatching can therefore be intentionally induced to obtain live J2s for experimentation (Heungens et al., 1996).

After induction of hatching in the field, the infective second-stage juveniles will move towards the source of the hatching stimulus. Individual nematodes move towards plant roots based on concentration gradients of a number of factors associated with the rhizosphere, likely to include CO₂ and sugar concentrations, and pH, and possibly also involving host species-specific cues (Lilley et al., 2005, Perry, 1997). On finding the host plant, the J2 will pierce the root with its stylet and migrate destructively through the root cortex to the vascular cylinder (Kyndt et al., 2013). Here it will penetrate cells with its stylet until a cell suitable for the formation of a feeding site is formed (Jones et al., 2013a, Kyndt et al., 2013). The formation and maintenance of the syncytium is a complex process, and integral to the success of an individual nematode; this is discussed in greater detail in the following section (1.2.5).

Potato cyst nematodes reproduce sexually, and sex determination occurs at the end of the J2 stage. Third-stage (J3) juveniles are superficially similar, but can be sex differentiated through inspection of their genital primordia (Lilley et al., 2005). Where past studies have suggested that sex is genetically determined, evidence points toward determination based on environmental conditions (Lilley et al., 2005). The proportions of males and females in the adult population is determined by nutrient availability: greater nutrition leads to a greater proportion of females, while lower nutrients and

higher levels of intraspecific competition lead to a greater adult population of males (Lilley et al., 2005, Sobczak and Golinowski, 2011). When tested *in vitro*, higher sucrose content in plant growth medium led to a greater proportion of applied J2s of *Heterodera schachtii* developing into females (Grundler et al., 1991).

The feeding site for the nematode is fixed until the J4 stage, after which adult males will leave the root while adult females remain sedentary until the end of their life cycle (Lilley et al., 2005, Sobczak and Golinowski, 2011). Adult males are short-lived and non-feeding (Turner and Subbotin, 2013). Males migrate through the soil towards females, attracted by chemical cues that likely include sex pheromones (Turner and Subbotin, 2013). Vanillic acid has been identified as a cyst nematode sex pheromone, released by *Heterodera glycines* females and acting to attract males (Jaffe et al., 1989). Pheromone specificity has been observed: vanillic acid did not act as an attractant to males of *H. schachtii* (Auma and Hashem, 1993), *G. rostochiensis* or *G. pallida* (Perry, 1996). Analysis of mitochondrial DNA from eggs within single cysts has confirmed that cyst nematodes are polyandrous, with each cyst potentially containing progeny from multiple mating events (Eves-van den Akker et al., 2015).

The defining characteristic of cyst nematodes is that of cyst formation by the adult female. Following mating, the fertile eggs then develop through embryogenesis and through the first moult to the J2 stage (Turner and Subbotin, 2013). The female then dies and encysts around them, forming a protective casing that can persist in the soil for upwards of 20 years (Turner, 1996). The cyst forms through the action of polyphenol oxidase on the wall of the adult female's body (Ellenby, 1946) and acts to protect the eggs within, principally shielding them from desiccation, as the outer wall becomes less permeable to water as it dries (Ellenby, 1968). Development time differs between plant-parasitic nematode species (Jones et al., 1998, Turner and Subbotin, 2013). The link between temperature and development at all stages has been established since the 1930s: development progresses only above a base temperature, which varies by species, and above which the rate of development will increase up to a thermal optimum (Tyler, 1933), for potato cyst nematodes, this optimum is 16 °C for *G. pallida* and 20 °C for *G. rostochiensis* (Turner and Subbotin, 2013). A recent assessment found that female fecundity for *G. pallida* was significantly reduced when temperatures were increased

from 15 °C to 25 °C, while *G. rostochiensis* fecundity increased from 15 °C up to 22.5 °C, but declined at 25 °C (Jones et al., 2017b). The difference in thermotolerance between the two species, ascribed to their adaptations to their native ranges, has been attributed at least partially to the presence of hsp-110, a thermoregulatory element that is activated under heat stress in *G. rostochiensis* but not in *G. pallida*, and correlates with the greater ability of *G. rostochiensis* juveniles to recover from heat stress (Jones et al., 2018a). Predicted increases in global temperatures may influence the survivability of each of these species in the UK: one study modelled soil temperatures in near-future medium and high-emission scenarios and found that populations of *G. pallida* would likely decline, particularly in the south of England (Jones et al., 2017b). The authors suggest that increased temperatures combined with the exploitation of widely available *G. rostochiensis*-resistant cultivars could lead to an overall decline in PCN populations in the UK (Jones et al., 2017b). A second group combined *in planta* experimentation, with three distinct PCN populations grown on potato roots in different soil temperatures, with low- and high-emission future temperature models to similarly predict that conditions could become more favourable for *G. rostochiensis* relative to *G. pallida* (Skelsey et al., 2018). However, the authors found that the shift in growing season and available potato growing area resulting from increased temperatures would effectively negate the potential increased risk of PCN proliferation (Skelsey et al., 2018).

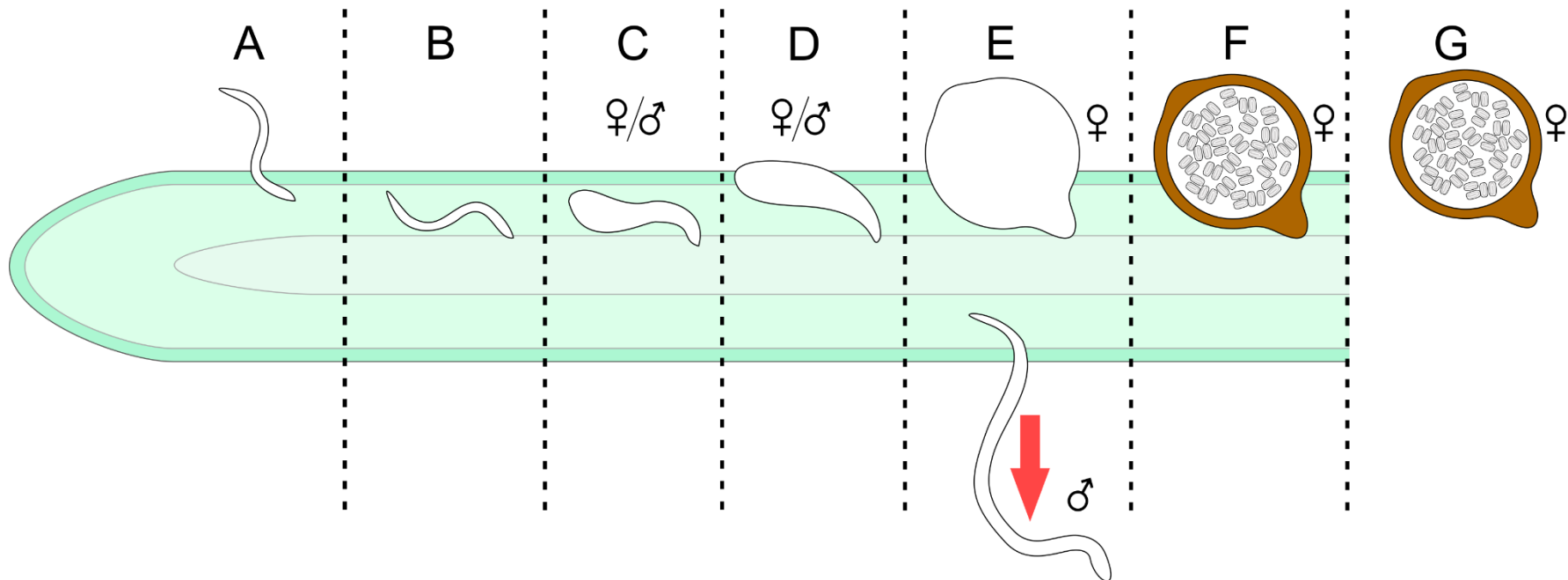


Figure 1.1 Simplified life cycle of a cyst nematode. A, after hatching, the infective second-stage juvenile (J2) migrates towards the root of a host plant, penetrates the dermis and moves destructively through the cortex towards the vascular cylinder. B, having found a suitable site, the J2 selects the initial syncytial cell (ISC) that will form the beginnings of the syncytium; the sex of the nematode is determined before moulting to the J3 stage. C, at the J3 stage, males and females continue to feed from the growing syncytium; they are superficially similar but can be differentiated by observation of their genital primordia. D, at the J4 stage, female nematodes continue to feed and develop, while males cease feeding and begin development of the adult vermiform body within the J4 outer cuticle. E, adult males leave the root to find sedentary adult females with which to mate. F, following mating and the development of the eggs, the adult female dies and the cuticle encysts around the eggs within. G, after death of the adult female, the eggs remain in the soil protected by the cyst; hatching will only begin after a period of diapause, generally in response to external stimuli such as host root exudate. Following this, nematodes hatch as J2s and migrate through the soil, beginning the cycle again.

On reaching the unhatched J2 stage, the nematode enters a state of diapause – dormancy that requires a set period of time as well as other cues before it will come to an end – and after diapause enters quiescence – a second period of dormancy that ends in response to hatching stimulus, i.e. host root exudate (Palomares-Rius et al., 2016). The requirements of the diapause phase are dependent upon the growing conditions of the host plant during formation of the cyst: increased day length led to a shorter diapause period in eggs of both *G. pallida* and *G. rostochiensis* (Salazar and Ritter, 1993). Once diapause is complete, the life cycle begins again: *G. pallida* typically requires a full potato-growing season to produce a single generation of progeny, which complete diapause in the following spring (Lilley et al., 2005); there is some evidence of *G. rostochiensis*, being better adapted to warmer climates, producing two generations over the course of a warmer growing period (Jones et al., 2017b).

1.2.5 The syncytium

Formation and maintenance of a potato cyst nematode's feeding site is intrinsic to its parasitic life stages. The cell first chosen by the J2 nematode is termed the initial syncytial cell (ISC). The nematode injects secretions known as effectors into the ISC, inducing metabolic changes that lead to the development of the syncytium. Effectors mediate the parasite's interactions with the host plant, suppressing host defences, and developing and maintaining the feeding cell environment (Kyndt et al., 2013). The profile of effectors introduced into the cell changes throughout the different life stages of the nematode (Palomares-Rius et al., 2012), as the demands of the parasite on the host change over time. The effectors secreted into the cell stimulate the expansion of the plasmodesmata between the ISC and the surrounding cells and induce production of cell-wall degrading enzymes (Grundler et al., 1998), leading to the amalgamation of neighbouring cells into a single, multinucleate whole. Observation of parallel changes in the surrounding cells suggests communication between them (Thorpe et al., 2014). Expansion of the syncytium continues such that a single syncytium may comprise more than a hundred cells fused together in this way (Bohlmann and Sobczak, 2014). The syncytium is the sole source of nutrition for the nematode, acting as a nutrient sink, diverting nutrients from the host plant (Kyndt et al., 2013) – cytoplasmic concentrations of sucrose and amino acids in syncytia are elevated relative to surrounding cells

(Hofmann et al., 2010). It is this diversion of nutrients from the host plant that leads to the disease symptoms associated with cyst nematode infection.

Effectors are the subject of a great deal of recent research, in an effort to better understand the interactions between parasite and host. In potato cyst nematodes, effectors are produced in the subventral and dorsal gland cells and injected into the syncytium via the stylet (Thorpe et al., 2014). Identification of effectors implicated in processes such as: cell wall degradation (Smant et al., 1998); suppression of host defences (Jaouannet et al., 2013, Postma et al., 2012); and in formation of the feeding site through manipulation of native cell signalling pathways – through mimicry of proteins involved in cell division and differentiation (Clark et al., 1995, Wang et al., 2005) or auxin signalling (Lee et al., 2011); demonstrate the significance of effectors to establishment of the feeding site.

Research into effectors has employed a number of techniques aiming to identify and characterise the broad array of molecules that may act as effectors, including proteomic analysis of induced stylet secretions (Bellafiore et al., 2008) and transcriptomics performed on gland cell RNA (Maier et al., 2013). The publication of genomes for the two major potato cyst nematodes (Cotton et al., 2014, Eves-van den Akker et al., 2016) has provided powerful tools for the discovery of novel effectors in the two species, resulting in the identification of a family of SPRY-domain proteins in *G. pallida*, of which a subset are confirmed as effectors (Mei et al., 2015), and of a regulatory element in the genome of *G. rostochiensis* that is implicated in the regulation and tissue-specific expression of dorsal gland effectors, termed the DOG Box (Eves-van den Akker et al., 2016).

1.2.6 Potato cyst nematode genomics

As significant pests of a globally important cash crop, both *Globodera pallida* and *G. rostochiensis* are well-studied organisms (Jones et al., 2013a) for which genomes have been published (Cotton et al., 2014, Eves-van den Akker et al., 2016). The genomes for each of these *Globodera* species are fragmented and somewhat incomplete. The *G. pallida* assembly consists of 6873 scaffolds (covering 124.6 megabases) while for *G. rostochiensis* there are 4377 scaffolds (95.9 Mb), each corresponding to genomes of 9 chromosomes ($2n=18$); this contrasts with the genome assembly available for

Caenorhabditis elegans, for which there are 7 scaffolds, corresponding to 6 chromosomes ($2n=12$) and the mitochondrial genome (Spieth et al., 2014). Based on representation of 458 conserved eukaryotic genes, used as a proxy for total genome completeness (Parra et al., 2009), the *G. pallida* genome is rated as 81 % complete (Cotton et al., 2014) and the *G. rostochiensis* genome as 94 % complete (Eves-van den Akker et al., 2016). The number of genes predicted for each species are 16,466 and 14,309, respectively, with the larger number of genes predicted for *G. pallida* corresponding to the larger genome assembly (Cotton et al., 2014, Eves-van den Akker et al., 2016). Using the presence or absence of start and stop codons as a measure of predicted protein completeness, 88.8 % of *G. pallida* and 91.4 % of *G. rostochiensis* predicted proteins were complete (Eves-van den Akker et al., 2016).

Comparison of the locations of *G. pallida* genes relative to one another with the clustering of genes on *C. elegans* chromosomes suggests that there is little conservation of gene order: orthologous genes found on a single scaffold (representing a portion of a single chromosome) from the potato cyst nematode genome are not clustered in the same way as in the *C. elegans* genome, but may be found spread across several chromosomes (Cotton et al., 2014). Comparison of the two potato cyst nematode genomes, however, found greater synteny between the two, with gene clusters found in similar regions (Eves-van den Akker et al., 2016). This is congruent with the degree of evolutionary divergence between the three species: where the two potato cyst nematodes (of nematode clade IV) are estimated to have diverged approximately 18 million years ago (Plantard et al., 2008), they are each much more distantly related to *C. elegans* (clade V) (Blaxter, 2011). The timings of ancient nematode divergences are not often given estimates, owing to inconsistent conservation among different gene families and to the lack of a reliable molecular clock for nematodes (Kiontke and Fitch, 2005).

Alongside sequencing of each of the potato cyst nematode genomes, transcriptomic analysis was performed on nematodes of different life stages. RNA-seq was performed on *Globodera pallida* to determine changes in gene expression across eight lifecycle stages: J2s within unhatched eggs, hatched J2s, adult males, and parasitic females at 7, 14, 21, 28, and 35 days post infection (dpi) (Cotton et al., 2014). Based on the observed

changes in expression from this analysis, *G. rostochiensis* gene expression was analysed in dehydrated cysts, hydrated eggs, hatched J2s and in 14 dpi sedentary females (Eves-van den Akker et al., 2016).

The 16419 predicted proteins encoded by the *G. pallida* genome were analysed and their roles inferred from similarity to known proteins: predicted proteins could be placed into 6174 known gene families, 3890 genes did not fit into any family, and 825 gene families unique to *G. pallida* were identified (Cotton et al., 2014). Proteins with no functional annotation were enriched among the genes unique to *G. pallida*, and a unique expansion of the glutathione synthetase gene family was found: a complement of 52 glutathione synthetases, dwarfing the usual number of 1 to 4 typically found in nematodes, were also found to be up-regulated in the early stages of parasitism, suggesting a novel function for the enzymes (Cotton et al., 2014). *Globodera pallida* has a reduced complement of genes involved in xenobiotic metabolism when compared with *C. elegans* (Cotton et al., 2014), a trait often observed in endoparasites, including among nematodes (Barrett, 2009), perhaps due to the risk of encountering various toxins (aside from host defences) being reduced in a sedentary endoparasitic lifestyle. The genome also features an expansion of proteins with SPRY domains, 299 genes compared with 8 in *C. elegans* and 27 in *Meloidogyne incognita* (Cotton et al., 2014). Among these are the SPRYSECs, SPRY proteins that are secreted and have been implicated as effectors: subcellular localisation assays with *Nicotiana benthamiana* leaves found that two SPRYSEC proteins localised to the nucleus and nucleolus, suggesting a role in manipulation of gene regulation in the host (Jones et al., 2009). Further studies have confirmed that some SPRYSECs suppress host defences, but suggested that less than 10 % of the SPRY domain gene family are expected to function as effectors (Mei et al., 2015).

The mitochondrial genomes of potato cyst nematodes are unique among higher animals in their organisation. Where metazoan mitochondria typically contain 2-10 copies of a single genome (Wiesner et al., 1992), *G. pallida* mitochondria were found to have several smaller subgenomes (Armstrong et al., 2000) with evidence of frequent recombination events such that many of these subgenomes were mosaics featuring genes with deleterious alterations (Gibson et al., 2007b). Broadly similar organisation of

mtDNA was observed in *G. rostochiensis*, though while there was conservation between the subgenomes of the two species, there were subgenomes unique to each species (Gibson et al., 2007a). Organisation and recombination of mtDNA in this way is atypical in animals, but bears some similarity to that found in plants and fungi (Armstrong et al., 2000).

Potato cyst nematodes have been classified into a number of pathotypes based on their relative virulence towards seven different *Solanum* accessions (Kort et al., 1977), giving three pathotypes for *G. pallida* (Pa1, Pa2, and Pa3) and five for *G. rostochiensis* (Ro1 through Ro5), though the boundaries between these are not always clear (Phillips and Trudgill, 1998). In the UK, *G. pallida* populations are typically classified into pathotype Pa1 or Pa2/3 (a Pa2/3 population provided the material for generation of the genome assembly (Cotton et al., 2014)), and *G. rostochiensis* populations are typically identified as pathotype Ro1 (Eves-van den Akker et al., 2016). These classifications are difficult to separate from one another, and efforts have been made to identify genetic markers for the various pathotypes, with a region of mitochondrial DNA encoding cytochrome B identified as a useful proxy marker for the three *G. pallida* pathotypes found in the UK (Eves-van den Akker et al., 2015) – it is noted, however, that there is likely no causal relationship between these mitotypes and the pathotypes with which they were associated. The variations in virulence between species and pathotypes complicate the use of resistant cultivars for management of potato cyst nematodes – planting of the popular and *G. rostochiensis*-resistant potato cultivar ‘Maris Piper’ has inadvertently led to selection of *G. pallida* in fields in the UK (Minnis et al., 2002, Whitehead et al., 1984).

1.3 Control of potato cyst nematodes

Control of plant-parasitic nematodes is generally achieved through combination of a variety of available practices, including crop rotations, intercropping, resistant or tolerant cultivars, chemical pesticides, and alternative strategies such as green mulching or biofumigation, the focus of Chapter 1.4.

Crop rotation, a technique employed in the management of most plant pathogens including root-knot nematodes (*Meloidogyne spp.*) (McSorley, 2011), is considered limited in efficacy for control of potato cyst nematodes, due to the low rate of population decline between cropping seasons (Turner, 1996). Ware potatoes grown on fields in which *Globodera spp.* have been detected are typically not planted with potato again for 5 – 8 years (McSorley, 2011). EU legislation prevents the planting of seed potatoes or any other crop that is to be replanted on soil that has not been certified PCN-free in the past 4 years (Regulation (EU) 2016/2031).

1.3.1 Resistant potato cultivars

Where potatoes are to be grown in fields with a history of PCN-infestation, resistant or tolerant cultivars are employed, if possible, to limit population growth and protect yields. Resistance genes for potato cyst nematodes are available but are not comprehensive. Of planted potato cultivars in the year 2000, 43 % were resistant to *Globodera rostochiensis* while 6 % had resistance to *G. pallida* (Evans and Haydock, 2000). The top 10 planted cultivars in British fields in 2018 are still dominated by H1 carrying cultivars such as Maris Piper, Markies, and Melody, but show increased planting of *G. pallida*-resistant varieties such as Innovator (AHDB, 2018). Online tools are available to select potato cultivars based on resistance to a range of pests, including potato cyst nematodes, such as that provided by the Agriculture and Horticulture Development Board in the UK (AHDB, 2018). However, cultivars that are resistant to one potato cyst nematode are rarely resistant to others. The H1 gene is a resistance (R) gene identified in an Andean subspecies of potato (*Solanum tuberosum ssp. andigena*) that conveys resistance to *Globodera rostochiensis* but only partial resistance to *G. pallida* and has been successfully crossed into the Maris Piper potato cultivar (Finkers-Tomczak et al., 2010). The prevalence of *G. pallida* in British potato fields is in part ascribed to the widespread use of potato cultivars containing the H1 gene – growing *G. rostochiensis*-

resistant varieties in fields with mixed populations selects for *G. pallida* population growth (Minnis et al., 2002, Whitehead et al., 1984). Partial resistance to PCN, as found in Maris Piper, can refer either to limited resistance of the crop to infection, resulting in smaller increases in PCN population over the growth period, or tolerance to infection, in which varieties may still produce good crop yields in moderately-infested fields (Pylypenko, 2002). Partially resistant potato varieties may limit increases in population size when the initial population density is low, but are not suitable for growth in heavily-infested fields, where even tolerant varieties will suffer significant yield losses (Phillips & Trudgill, 1998).

Transgenic potatoes have been developed that carry resistance-enhancing genes. Root-specific expression of a cystatin from rice (previously shown to provide resistance in transgenic hairy roots (Urwin et al., 1995)) was found to up-regulate at the site of nematode feeding and result in increased resistance (Lilley et al., 2004). Secretion of nematode neuropeptides from plants has been explored as an avenue of control, with transgenic potatoes that secreted a peptide inhibiting chemoreception in cyst nematodes provided up to 75% resistance (Green et al., 2012); this technology was later investigated outside of the plant, with transgenic soil microbes secreting neuropeptide-like proteins reducing infection levels in tomato roots by up to 90% (Warnock et al., 2017).

However, UK markets cannot benefit from transgenic potato cultivars as genetically modified (GM) crops are not approved for commercial growth in the UK, and GM foods are limited to imports of oilseed rape, soybean, cotton-seed oil, maize, and sugar beet (Gov.uk, 2018).

1.3.2 Chemical control of nematode pests of potato

Chemical control of plant-parasitic nematodes has historically been achieved through application of nematicidal chemicals, typically classified as either fumigant (Lembricht, 1990) or non-fumigant (Apt and Caswell, 1988), which differ in their methods of application. Chemicals may be further described as: nematicidal, those that directly kill nematodes; nematostatic, chemicals that impede the infective stages of a nematode for long enough to protect most of the value of a crop; and multi-purpose, chemicals that

are rarely applied solely for nematode control due to high costs but may have broad-spectrum activity.

Soil fumigants are volatile compounds that are injected into the soil, either in solution or as a liquid under pressure, and rapidly volatilise, spreading through the soil via the gas phase and either dissolving in water films on soil surfaces or adsorbing into organic matter within the soil (Lembricht, 1990). Many soil fumigants, such as methyl bromide (bromomethane), DBCP (1,2-dibromo-3-chloropropane), and ethylene bromide (1,2-dibromoethane), have been phased out due to their detrimental effects on non-target organisms and the environment (Qin et al., 2004). Methyl bromide has frequently been used for research purposes as a benchmark against which to test novel control methods (McSorley, 2011), but has been withdrawn from agricultural use (as per the Montreal Protocol on Substances that Deplete the Ozone Layer, 1987) as it breaks down to form elemental bromine, a potent ozone depletion agent (Noling and Becker, 1994). However, dependence on methyl bromide persists such that it can still be applied to fields when critical use exemptions are granted, which continue through 2018 and 2019 (UNEP, 2017). The need for adequate replacements for methyl bromide has been recognised for as long as the need to regulate its use (Noling, 2002, Noling and Becker, 1994).

Non-fumigants are applied in liquid or granular form, and may act through the proliferation of volatile breakdown products, or otherwise require contact with nematodes to be effective (Apt and Caswell, 1988). Two principal classes of compounds make up the non-fumigant nematicides: carbamates and organophosphates, each acting through inhibition of acetylcholinesterase (Gupta et al., 2018). The carbamate aldicarb (previously sold as Temik™ by Bayer CropScience) has been withdrawn from use in the EU due to non-target toxicity, despite its low potential for bioaccumulation (European Commission, 2003). However, evidence of unlawful applications of aldicarb suggest it has not yet been removed from markets (Ruiz-Suárez et al., 2015). Fosthiazate ((*RS*)-[*S*-(*RS*)-*sec*-butyl *O*-ethyl 2-*oco*-1,3-thiazolidin-3ylphospho-nothioate]), marketed as Nemathorin, is an organophosphate treatment that effective at much lower doses in nematodes than in other animals, but is hampered by its potential for leaching into waters around places of application (Karpouzias et al., 2007), and its relatively quick

degradation by microbes present in the soil: leaching was increased in acidic soils, while persistence increased in soils with high organic matter content (Qin et al., 2004). Fenamiphos ((*RS*)-(ethyl 4-methylthio-m-tolyl isopropylphosphoramidate)) is an organophosphate used for control of nematodes (Oka et al., 2009) but is limited in effectiveness against nematodes other than *Meloidogyne* species (Oka, 2014). As non-fumigant nematicides may persist in the soil, they run the risk of exposing target nematodes to sublethal concentrations at which they may only have a nematostatic effect. Fluopyram (*N*-[2-[3-Chloro-5-(trifluoro-methyl)-2-pyridinyl]ethyl]-2-(trifluoro-methyl) benzamide, marketed as Velum One™ by Bayer CropScience) is a non-fumigant pesticide first developed as a fungicide but now marketed as a multipurpose chemical with nematicidal effects. It was found to be effective against *Meloidogyne incognita* on lima bean (Jones et al., 2017a) but no published data exists on its efficacy for cyst nematode control, and it has been suggested that it acts as an effective nematostat rather than a nematicide (Faske and Hurd, 2015). Oxamyl (methyl 2-(dimethyl amino)-*N*-[(methylcarbamoyl)oxy]-2-oxoethanimidothioate), is a carbamate, marketed as Vydate, that is more effective at controlling *G. rostochiensis* than *G. pallida* (Whitehead et al., 1984). It is broadly effective against nematodes (Jones et al., 2017a), resulting in off-target effects and the risk of bioaccumulation in treated foodstuffs (Osman et al., 2009). The granular form of oxamyl is banned and use of the liquid form is heavily regulated to limit potential for bioaccumulation (UNEP, 2005). Fluensulfone (5-chloro-2-(3,4,4-trifluorobut-3-enylsulfonyl)-1,3-thiazole) is a non-fumigant that has been shown to act specifically on nematodes, resulting in irreversible detrimental impacts on development at all stages of life (Kearn et al., 2014). However, it has also been found only to affect certain genera of plant-parasitic nematodes, effective against root-knot nematodes, but ineffective against the pine wood nematode, *Bursaphelenchus xylophilii* (Oka, 2014). Fluensulfone compared poorly with other available non-fumigants when trialled on *Globodera* spp., including oxamyl and fosthiazate (Norshie et al., 2016).

Dazomet (3,5-dimethyl-1,3,5-thiadiazinane-2-thione) is a multipurpose chemical that has largely replaced use of methyl bromide – it is less effective but also carries lower risk to wildlife and the environment (Lewis et al., 2016). Dazomet is applied in granular form but degrades in the soil generating methyl isothiocyanate (MITC), a bioactive,

sulphurous volatile to which the pesticidal activity of dazomet is ascribed (Mao et al., 2014). When applied to root-knot nematode-infested cucumber fields in combination with dimethyl disulphide (DMDS) or 1,3-dichloropropene, dazomet was found to have nematicidal activity comparable to methyl bromide, while dazomet alone was less effective but performed better than untreated controls (Mao et al., 2014, Mao et al., 2012). Metam sodium is a dithiocarbamate that also acts to generate MITC, and was the third most commonly applied pesticide in the US in 2000 (Pruett et al., 2001).

The number of available chemical controls and the degrees to which these can be employed have become limited by regulations over the past few decades (Starr et al., 2007). The development of novel synthetic nematicides, however, is a long and expensive process, made difficult by the protective cuticle of nematodes and their unpredictable dispersal throughout the soil, as well as their protected environment in the plant root (Chitwood, 2002). Regulatory barriers also limit the development of novel nematicides, as ideally any new chemical will be target specific, will not persist in the soil, will not endanger local ecosystem, and will not negatively impact the environment. The Montreal Protocol restricts application of any chemical that acts to deplete the ozone layer (UNEP, 2002). Further EU regulations limit the application of potentially harmful nematicides, operating under the precautionary principle: any treatment cannot be applied if the potential for harm cannot be ruled out (Erbach, 2012, European Union, 1957). Many growers therefore implement integrated pest management (IPM) strategies, utilising chemical control alongside other methods (Starr et al., 2007).

1.4 Biofumigation

Due to both the difficulties associated with potato cyst nematode management and the regulation of the more effective chemical treatments once used for their control, growers frequently look to alternative pest management strategies, in order to increase yields and reduce costs and losses associated with the crop. One such strategy that has received attention in recent years is that of biofumigation – the exploitation of bioactive compounds generated from disrupted brassicaceous plant tissues to control pests. This typically focuses on generating isothiocyanates: sulphurous, bioactive compounds produced from the breakdown of glucosinolates.

1.4.1 Glucosinolates and the production of isothiocyanates

Glucosinolates are sulphurous secondary metabolites found in plants of the order Brassicales, including the family Brassicaceae which features crops such as Indian mustard, *Brassica juncea*; cabbage, *Brassica oleracea*; oilseed rape, *Brassica napus*; radish, *Raphanus sativus*; as well as the important model plant *Arabidopsis thaliana*. Over 120 distinct glucosinolates have been identified among the Brassicales, with each species producing a specific subset of these (Fahey et al., 2001). *Arabidopsis* is known to produce at least 34 different glucosinolates (Kliebenstein et al., 2001). Many of the pathways of glucosinolate biosynthesis have been elucidated through work with *Arabidopsis*, with over 20 biosynthesis genes discovered, such that glucosinolates are regarded by some as “model secondary metabolites” (Sønderby et al., 2010).

The structure of a glucosinolate comprises three moieties (Figure 1.2 A): a β -thioglucose linked via sulphur to a sulfonated oxime moiety, in turn linked via carbon to a variable (R group) side chain derived from an α -amino acid (Ishida et al., 2014). The R group distinguishes different glucosinolates from one another, is used to classify them into three groups (aliphatic, aromatic or indolic), and determines the chemistry of their breakdown products (Fahey et al., 2001). Glucosinolate biosynthesis begins with an amino acid: aliphatic glucosinolates being derived from alanine, leucine, isoleucine, valine and methionine; aromatic from phenylalanine or tyrosine; and indolic glucosinolates from tryptophan. The amino acid may be chain-elongated (methionine and phenylalanine only) before formation of the glucosinolate structure and subsequent

modification of the R group (Sønderby et al., 2010); it is this side chain modification that gives rise to the great diversity of known glucosinolates (Fahey et al., 2001).

In the host plant, glucosinolates are found in the vacuoles of most cells (Kelly et al., 1998), though the distribution of different glucosinolates and their respective abundances may differ from organ to organ and within an organ (Shroff et al., 2008). These abundances may change in response to external stimuli, such as increased concentrations following herbivore attack, or temporally, with senescent leaves having greatly reduced glucosinolate content (Brown et al., 2003). The primary function of glucosinolates within the host is in the glucosinolate-myrosinase defence system. As whole molecules, glucosinolates are relatively chemically inert. When plant tissues are disrupted, local glucosinolates are allowed to come into contact with native myrosinase enzymes. Hydrolysis catalysed by myrosinase (also termed β -thioglucoside glucohydrolase) leads to the liberation of a glucose molecule and production of an unstable thiohydroximate (Figure 1.2 B), which then degrades to form one of a range of active compounds (Figure 1.2 C) in a pH and enzyme dependent manner (Bones and Rossiter, 2006). These active compounds then act to harm or deter the pathogen or herbivore that has attacked the plant. The principal products generated from the degradation of glucosinolates are isothiocyanates, followed by nitriles and thiocyanates (Figure 1.2 C i., iii., and iv.).

The principal glucosinolates found in brassicas of commercial value are: sinigrin, which gives allyl isothiocyanate, found in most brassicas and the principal GSL identified in *Brassica spp.*; glucoraphanin, found abundantly in radishes; and glucoerucin, identified in rocket (Kirkegaard and Sarwar, 1998). The majority of field trials focus on the use of *Brassica juncea* cultivars with high sinigrin content (discussed in Chapter 1.4.3).

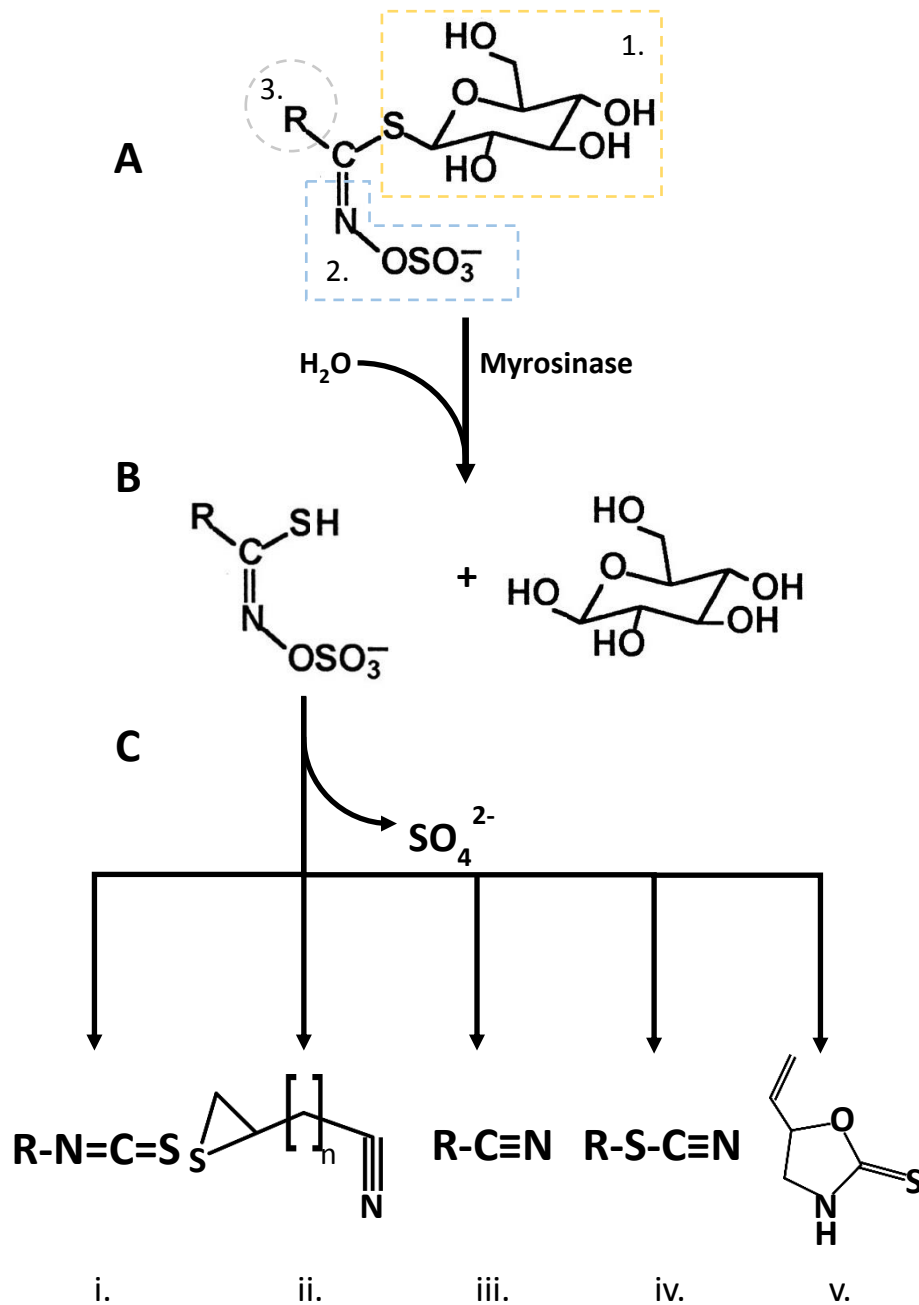


Figure 1.2 The general structure of glucosinolates and their breakdown products. A, general structure of a glucosinolate, highlighting the β -thioglucoside (1) and sulfonated oxime (2) moieties and the R side chain (3). B, hydrolysis by myrosinase, liberating a glucose molecule and an unstable thiohydroximate. C, subsequent degradation products under different conditions: i, isothiocyanate; ii, epithionitrile; iii, nitrile; iv, thiocyanate; and v, goitrin. Adapted from: (Bones and Rossiter, 2006, Ishida et al., 2014, Shapiro et al., 2001)

Isothiocyanates form naturally from the spontaneous degradation of the unstable thiohydroximate residue left after hydrolysis of the glucose moiety (figure 1.2 B); this occurs through a process termed a Lossen rearrangement (Ettlinger et al., 1961, Ettlinger and Lundeen, 1957), wherein the bond between the R-group and the central carbon shifts to the nitrogen, the sulphate anion is released and the hydrogen bound to sulphur is liberated, forming a double bond between sulphur and carbon (Bones and Rossiter, 2006).

Myrosinases (EC 3.2.1.147) are a class of enzymes in the β -glycosidase family, forming a distinct phylogenetic subgroup amongst glycoside hydrolase family 1 enzymes (Xu et al., 2004). Compared to O-glycosidase enzymes found widely in nature, myrosinases are the only known S-glycosidases (Burmeister et al., 2000). As all studied members of the Brassicaceae produce glucosinolates, they also express myrosinase, with each species expressing several distinct myrosinase enzymes, classified into three subfamilies, MA, MB, and MC, which may have different functions (Xue et al., 1992, Eriksson et al., 2002). Recombinant myrosinase enzymes from the roots and shoots of *A. thaliana* were found to have slightly differing catalytic activities with regards to pH and ascorbic acid concentrations, but were all found to catalyse the hydrolysis of sinigrin across a range of conditions (Andersson et al., 2009). An analysis of the myrosinases found in a range of brassicas found that all those analysed had classic myrosinase activity, converting sinigrin to allyl isothiocyanate and glucotropaeolin to benzyl isothiocyanate (Piekarska et al., 2013). Structurally, MA-type myrosinases typically occur as a homodimer, while MB and MC myrosinases are often found in complex with myrosinase-binding proteins that may affect the final breakdown product of glucosinolate hydrolysis (Eriksson et al., 2002, Rask et al., 2000). Natively expressed myrosinase has been found to be heavily glycosylated, which may aid in protein stability (Halkier and Gershenzon, 2006) or in cellular localisation (Bones and Rossiter, 1996) – the activity of recombinant myrosinases without glycosylation suggests that it is not necessary for the function of the enzyme.

While isothiocyanates are the principal breakdown product of glucosinolate hydrolysis, formation of alternative breakdown products can occur either at low pH (pH<5 for formation of nitriles (Bones and Rossiter, 2006)) or in the presence of specifier proteins.

Epithiospecifier protein (ESP), first isolated in crambe, *Crambe abyssinica*, was found to interact with the enzymatic hydrolysis of glucosinolates and generate epithionitriles alongside isothiocyanate production (Tookey, 1973), and was later found in other members of the Brassicales (*Brassica napus* and *B. campestris*), with Fe^{2+} identified as a non-essential promoter of the reaction (MacLeod and Rossiter, 1985). When epithiospecifier proteins interact with the hydrolysis of either non-alkenyl or indolic glucosinolates, a nitrile is formed rather than an epithionitrile (Wittstock and Burow, 2007). Thiocyanates are formed in the presence of thiocyanate-forming protein (TFP), theorised for some time before the identification of a TFP in cress, *Lepidium sativum* (Burow et al., 2007). Thiocyanate-forming proteins have been found to produce thiocyanates only from certain glucosinolates, such as allylglucosinolate (sinigrin) and benzylglucosinolate, with other substrates resulting in the production of simple nitriles (Kuchernig et al., 2011). A third class of enzymes, nitrile-specifier proteins (NSPs), alter glucosinolate breakdown to preferentially generate nitriles. Three Fe^{2+} -dependent NSPs have been characterised in arabidopsis, with a further two identified based on sequence information (Kong et al., 2012). Interestingly, an NSP is produced by larvae of the cabbage white moth, *Pieris rapae*, which feeds on brassicas – the larvae are vulnerable to isothiocyanates but are not harmed by nitriles, suggesting that the NSP acts to undermine the defence system (Wittstock et al., 2004). The crystal structures of *Arabidopsis thaliana* ESP (AtESP) (Zhang et al., 2016), *A. thaliana* NSP1 (AtNSP1) (Zhang et al., 2017), and *Thlaspi arvense* TFP (TaTFP) (Gumz et al., 2015) have been resolved. Resolved structures for ESP and TFP are broadly similar, though TaTFP dimerises differently to AtESP and has a smaller active site, while AtNSP1 is more structurally distinct (Gumz et al., 2015, Zhang et al., 2016, Zhang et al., 2017). Goitrin (Figure 1.2 C v.) is formed only from the hydrolysis of the glucosinolate progoitrin, being the end result of hydrolysis instead of an isothiocyanate (van Doorn et al., 1998). The biological functions of these alternative end products are less well understood than those of the isothiocyanates, due to lower toxicity (Wittstock and Burow, 2007).

1.4.2 The glucosinolate-myrosinase defence system

Glucosinolates are typically posited as being involved in defence against herbivory and pathogen attack, in a defence scheme termed the glucosinolate-myrosinase system or

the mustard oil bomb (Matile, 1980). Studies intended to determine whether or not glucosinolates were utilised as a sulphur-storage system have found that glucosinolate content is dependent on sulphur provision and that sulphur-deficient conditions reduce glucosinolate content (Falk et al., 2007). However, glucosinolates were not used as a storage sink when brassicas were exposed to excess sulphur (Aghajanzadeh et al., 2014), suggesting a limited role in sulphur-storage.

As glucosinolates become highly reactive upon hydrolysis by myrosinase, it is necessary for brassicas to keep these elements separate from one another until they are needed. Glucosinolates are found within cells throughout the tissues of a plant (Shroff et al., 2008), so this is achieved through compartmentalising myrosinase in specialised idioblasts (cells that are distinct from their surrounding tissue) termed myrosinoblasts or myrosin cells (Andreasson et al., 2001). This physical separation is broken when the tissues of a brassica are disrupted, for instance when under herbivore attack; the release of myrosinase from the myrosin cells allows the enzymatic degradation of the plant's glucosinolates into the bioactive compounds described above. This phenomenon has been shown to aid in defence against a number of herbivores and pathogens. Herbivory by cabbage moth larvae (*Mamestra brassicae*) was increased when two transcription factors associated with the biosynthesis of aliphatic glucosinolates (MYB28 and MYB29) were knocked down in arabidopsis (Beekwilder et al., 2008). Studies with various arabidopsis mutants found that growth of a brassica-specific fungal pathogen, *Alternaria brassicicola*, was inhibited by aliphatic and aromatic isothiocyanates, while a generalist fungus, *Botrytis cinerea*, was sensitive to various breakdown products dependent on their source glucosinolate (Buxdorf et al., 2013). It has been suggested that the glucosinolate-myrosinase system is also used to influence larger herbivores. *Ochradenus baccatus* manipulates rodents that feed on its fruits by compartmentalising glucosinolates in the flesh and myrosinase in the seeds – this encourages herbivores to eat the flesh and spit out the seeds in order to avoid the production of isothiocyanates, thereby aiding in seed dispersal (Samuni-Blank et al., 2012).

1.4.3 Biofumigation in agricultural practice

The ability of disrupted brassica tissues to generate bioactive compounds has been exploited in agricultural settings for the management of pests. This is termed

biofumigation, and the typical methodology employed is to grow the biofumigant crop or crop mix in the field to be treated until an optimal time point is reached, after which the crop is macerated and incorporated into the soil (McSorley, 2011). This is performed before planting of a cash crop, in order to reduce or control the populations of soilborne pests, thereby limiting their effects on the yield and value of the crop. Other biofumigation methodologies include application of a brassicaceous green mulch, or growing brassicas between the primary crop as a living mulch (Marahatta et al., 2010) and the sowing of brassica seed meal into the soil (Zasada et al., 2009). Brassicas may also be grown as “catch crops”: in theory, nematodes may invade the roots and fail to reproduce due to the production of low-volatility isothiocyanates that persist in the damaged root environment (Lazzeri et al., 2013). Among the potential benefits of biofumigation are its potential low environmental impact, and its regulatory simplicity – crop species employed for their biofumigant effects are already grown for other purposes around the world. While it might be assumed that biofumigation could be a relatively cheap management choice, the cost per hectare can include £40-100 in seeds, £200-300 in planting and maintenance of the crop, and may incur the cost of hiring machinery for incorporation of the crop (Lord et al., 2011). A typical granular nematicide costs around £300 per hectare, e.g. Dazomet. Further, a brassica crop grown for biofumigation may provide a habitat for pests and pathogens that later affect the cash crop (Lu et al., 2010), and could impact a grower’s profits by occupying land that could be used for growth of a cash crop. The case for biofumigation must be strong enough, therefore, to justify any extra costs.

The effectiveness of biofumigation for control of nematodes is the subject of a great deal of sometimes contradictory research: a recent meta-analysis of field trials refutes the efficacy of brassicas when compared with fallow treatments (McSorley, 2011), while a number of studies suggest that biofumigation may form an important role in future management of nematodes (Chan and Close, 1987, Kirkegaard and Sarwar, 1998, Mojtahedi et al., 1993).

Pure isothiocyanates are certainly toxic to nematodes and other plant pathogens *in vitro*, but consistently translating this toxicity into a biofumigation scheme applied in the field can prove challenging (Morra and Kirkegaard, 2002). Presented in the context of

biofumigation, there have been numerous studies into the toxicity of isothiocyanates to plant-parasitic nematodes. *Meloidogyne incognita* J2s incubated with glucosinolates were unaffected, but when incubated with those same glucosinolates with added myrosinase, all tested glucosinolates resulted in immobilisation and mortality (Lazzeri et al., 2004). Allyl isothiocyanate was shown to be toxic to hatched *Globodera pallida* J2s and to suppress induced hatching from cysts *in vitro* (Wood et al., 2017). Recovery of *G. pallida* J2s from sand columns was reduced by up to 100% after 24 h exposure to aqueous leaf extracts, relative to a water control treatment (Lord et al., 2011). It is notable that the greatest level of control was not achieved with leaf extract from the plants with highest glucosinolate leaf content, and a degree of control was also observed with non-brassicaceous leaf extracts (Lord et al., 2011).

Isothiocyanates are not equally bioactive: in a number of *in vitro* assays allyl isothiocyanate, the breakdown product of one of the more prevalent glucosinolates, sinigrin, has been shown to be highly toxic to both *M. incognita* and *M. javanica*, alongside other effective ITCs such as 2-phenylethyl ITC and methyl ITC (MITC) (Aissani et al., 2013, Lazzeri et al., 2004, Wu et al., 2011, Zasada and Ferris, 2003); phenyl ITC was found to have low toxicity to both species (Aissani et al., 2013, Wu et al., 2011); while a number of compounds were differentially toxic, with butenyl ITC and 4-methylthiobutyl ITC having high bioactivity against *M. incognita* (Lazzeri et al., 2004) but lower bioactivity with *M. javanica* (Wu et al., 2011). This discrepancy between closely related nematode species indicates that results from studies on one plant-parasitic nematode may not apply to others, suggesting that achieving a “one size fits all” biofumigation protocol may not be a plausible goal.

Attempts to translate effective *in vitro* trials with biofumigation into efficacy *in planta* have seen some success. Pot trials with three *B. juncea* cultivars incorporated into soil containing *G. pallida* cysts found that egg viability was reduced by 70-85 % in uncovered pots and by up to 95 % when the soil was covered with polyethylene – other brassica species reduced viability to lesser extents while a wheat treatment also reduced levels relative to a mock treated control (Lord et al., 2011). Incorporated green tissues of *Brassica rapa* (turnip), *B. oleracea* (kale, cauliflower, broccoli and Portuguese cabbage), and *Nasturtium officinalis* (watercress) significantly reduced cyst-formation in potatoes

grown in *G. rostochiensis*-infested pots, to less than 7% of the untreated control in the case of the watercress amendment (Aires et al., 2009). Reduction in hatching was observed in *G. pallida* cysts exposed to allyl isothiocyanate *in vitro*, but this could not then be replicated in pot trials using infested field soil (Brolsma et al., 2014). Tissue extracts from three *Brassica oleracea* varieties, *B. rapa* (turnip) and *Nasturtium officinale* (watercress) were added to pots in which *G. rostochiensis* were growing on susceptible potato; population growth was significantly reduced relative to a control treatment (Aires et al., 2009). However, extracts were made by freeze-drying and grinding the green tissues of the plants before addition to the pots in which juveniles had already hatched from cysts, conditions that do not represent a standard biofumigation protocol, and the biomasses required of each tested cultivar in a given field would require addition of green tissues grown separately to the field to be tested (Aires et al., 2009).

Direct applications of isothiocyanates to infested fields have demonstrated the toxicity of these compounds in an agricultural context. Application of allyl and acryloyl isothiocyanates to *M. javanica*-infested cucumber plots resulted in reduced galling to near zero at higher concentrations ($\geq 1 \text{ kg ha}^{-1}$), comparing favourably with metam sodium (Wu et al., 2011), though no comparison was made between the concentrations of ITCs added to the plots and the potential output from incorporation of a biofumigant crop. Biofumigation by incorporation of yellow mustard, *Brassica juncea* cv. Zlata, significantly reduced *G. rostochiensis* population levels in two fields in Belgium compared with growing but not incorporating the mustard and with fallow – combining mustard incorporation with plastic mulching further reduced the viable nematode populations (Valdes et al., 2012). Application of *B. juncea* seed meal to *Meloidogyne incognita*-infested soil reduced viable J2 populations to near zero, without negatively impacting the growth of pepper (*Capsicum annuum*) seedlings transplanted into the soil later on (Meyer et al., 2011). Field trials performed in Shropshire, UK, found that summer-grown *B. juncea* cv. Caliente 99 and *Raphanus sativus* cv. Bento reduced *G. pallida* egg viability, and that total glucosinolate content in the plants correlated with reduction in viability (Ngala et al., 2014). Analysis of host status and effects of green manure incorporation of a number of crops in *M. chitwoodi*-infested potato fields found

that *R. sativus* cvs. Melodie and Trez were both poor hosts for the root-knot nematode and that green tissue incorporation resulted in nematode populations falling by 65-79% and reduced galling in the following crop (Al-Rehiayani and Hafez, 1998). As well as acting to control nematode populations, brassicaceous green tissue amendments have been demonstrated to reduce the impact of soil-borne fungal disease on subsequent potato crops (Larkin and Griffin, 2007).

Conversely, a number of studies have demonstrated “biofumigant” effects separate from glucosinolate content or isothiocyanate production, or the simple absence of any nematode-controlling effect, attributing suppressive effects or improvements to crop yield to the benefits of a green tissue incorporation more generally. Green manures are thought to benefit subsequent crops by providing greater available nutrients and to boost soil microbial communities, potentially increasing the abundance of organisms that help fight plant pathogens (dos Santos Marques et al., 2017). Analysis of a number of studies on various non-brassica rotation crops found that nematode numbers were suppressed at a rate similar to application of aldicarb and to a season of clean fallow, but performed poorly compared to fumigation with methyl bromide (McSorley, 2011). A reduction in *G. rostochiensis* populations was observed when brown mustard was grown in rotation for 3 consecutive years in infested fields in Canada, but this effect was mirrored by corn and millet rotations, and a greater population reduction was observed in plots in which resistant potato cultivars were planted (Bélair et al., 2016). An experimental field in Germany that was host to several plant-parasitic nematode genera (*Meloidogyne*, *Heterodera*, *Trichodorus*, *Tylenchorynchus*, and *Pratylenchus*) was separately treated with amendments of four *B. juncea* cultivars as well as with wheat with and without added allyl isothiocyanate, as positive and negative controls; no significant impact on population densities of the monitored plant-parasitic nematode genera was recorded following incorporation of brassicas or of wheat with added isothiocyanates (Vervoort et al., 2014). However, owing to the low initial densities of *Meloidogyne*, *Heterodera*, and *Pratylenchus* found in the field, only the ectoparasitic *Trichodorus* and *Tylenchorynchus* genera were assessed post-incorporation, so impacts on sedentary and migratory endoparasites cannot be inferred from the results (Vervoort et al., 2014). Rapeseed was found to be a poor host for both *M. incognita* and

M. javanica but population growth on the following squash crop was unaffected by incorporation of the brassica green manure (Johnson et al., 1992). In a number of field trials performed in Georgia, USA, growth of *M. incognita* populations on a number of biofumigants counteracted the reduction observed after incorporation of green tissues, such that the cash crop was exposed to higher nematode populations than before the trials began (Monfort et al., 2007). Realisation of any potential biofumigant effect from a crop depends on translating glucosinolate concentrations in the plant into isothiocyanate concentrations in the soil. A study performed on two commercial biofumigant crops found that tissue disruption and incorporation using a rotary hoe resulted in only 1.0 ± 0.08 % of the potential isothiocyanate release detected in soils after 24 hours (Morra and Kirkegaard, 2002). The concentrations of isothiocyanates in the soil were found to be highest immediately after incorporation of high-glucosinolate *Brassica juncea*, reaching a maximum of 56% ITC release efficiency, but concentrations tailed off thereafter, though some isothiocyanates were detected at low levels up to 12 days after incorporation (Gimsing and Kirkegaard, 2006).

A potential issue with the application of biofumigation to control some nematode species is that, regardless of any population-controlling effect of green tissue incorporation, polyphagous nematode species may increase in numbers over the growth period of the biofumigant crop by utilising the biofumigant as a host. An assessment of the host status of 31 brassica cultivars across 8 species for *Meloidogyne incognita*, *M. hapla*, and *M. javanica* found that the majority of the plants tested had significant root galling (Edwards and Ploeg, 2014), according to an established root galling index (Bridge and Page, 1980). Glasshouse experiments with *M. javanica* grown on *B. juncea*, *B. napus*, and a commercial biofumigant mix of *B. napus* and *B. campestris* found that, though population increases were only 3-23% of those found on a susceptible tomato cultivar, they were enough that the authors recommended against summer growing of these plants for biofumigation in subtropical climates, as any positive effects would be undone by the increase in nematode numbers (Stirling and Stirling, 2003). However, this should not be an issue for control of host-specific cyst nematodes such as *Globodera*.

A further issue is that of target specificity, though this also applies to chemical nematicides. Entomopathogenic nematodes are thought to help protect crops from

insect pests and are sometimes intentionally applied to fields as a biocontrol measure – infection of *Galleria mellonella* larvae by native entomopathogenic nematodes was reduced in potato fields that had had biofumigant amendments, and glasshouse trials showed that entomopathogenic nematode activity was more affected by brassica amendments with higher glucosinolate content (Ramirez et al., 2009). Conversely, a mixed system containing Colorado potato beetle (*Leptinotarsa decemlineata*), *Steinernema* spp. entomopathogenic nematodes, and *Meloidogyne chitwoodi*, grown on potato in pots, found that biofumigation interrupted the effectiveness of entomopathogenic nematode-based insect control, but ultimately led to greater potato yields as root-knot nematode populations were decreased and Colorado potato beetles were discouraged from egg-laying (Henderson et al., 2009).

A review of the literature suggests that the science of biofumigation is far from settled. While the toxicity of isothiocyanates and the generation of isothiocyanates from disrupted brassica tissues are both well documented, the question of how to translate this into an effective and consistent nematode management technique remains unanswered.

1.5 Aims

A great deal of research has focused on the potential for biofumigation as a method of pest control, but the number of conflicting reports and the lack of a full understanding of the mechanisms of the technique leave several questions unanswered. The effects of exposure to isothiocyanates on plant-parasitic worms were investigated to better understand variations in susceptibility to biofumigation and to isothiocyanates, and to provide a basis upon which further research can be built. To increase the number of tools available to crop growers, a method for screening plant species for potential biofumigant effects was developed. As glucosinolate content is not always linked to biofumigant efficacy, the volatile emissions of a number of brassicas were investigated to determine if brassicas offer a source of nematode control separate to the glucosinolate-myrosinase system.

Chapter 2 General Materials & Methods

2.1 Biological Materials

Plants:

- Potato – *Solanum tuberosum* cv. Désirée
- Yellow mustard – *Brassica juncea* cv. ISCI99
- Radish – *Raphanus sativus* cv. WeedCheck, Diablo
- Rocket – *Eruca sativa* cv. Nemat
- Tomato – *Solanum lycopersicum* cv. Ailsa Craig

Nematodes:

- White potato cyst nematode – *Globodera pallida* LINDLEY (Pa2/3)
- *Caenorhabditis elegans*
 - N2 (wild-type)
 - unc119
 - *gst-31::gfp* reporter strain (Jones et al., 2013b)

Bacteria:

- *Escherichia coli*
 - Ultra-competent DH5 α (Inoue et al., 1990)
 - HT115(DE3)

2.2 Cultivation of nematodes

2.2.1 Cultivation of cyst nematode populations

Cysts of *Globodera pallida* were stored long-term in soil at 4 °C. Cyst populations were replenished by growing susceptible potato cultivars in 50:50 sand/loam soil containing cysts to give approximately 50 eggs g⁻¹ soil. Tubers of the potato cultivar Désirée were allowed to chit by incubating in an open tray at room temperature. Tuber cuttings containing one chit were taken and planted in 15 cm pots. These were watered every other day for approximately 12 weeks when the foliar parts of the plants were clipped

and the soil was left to dry. After drying, egg counts were performed on 100 g soil samples (section 2.1.4) and the soil was stored at 4 °C.

2.2.2 Extraction of cysts from soil

Cysts were extracted from soil using the Fenwick can method (Fenwick, 1940). Soil samples infested with cysts were washed through an 800 µm steel mesh sieve into the Fenwick can, removing larger pieces of detritus, where the buoyant cysts are separated from heavier soil particles by flotation. The effluent from the can was then sieved through a 500 µm mesh and collected in a 150 µm mesh sieve, removing particles larger and smaller than the cysts. The contents of the sieve were then rinsed into a medium flow filter paper (GE Whatman, UK) in a sealed funnel. The contents of the filter paper were allowed to settle before slowly draining, leaving the cysts in the outer ring of sediment collected on the paper. Cysts were then collected from filter papers using fine forceps under a dissecting microscope. Cysts were stored in sterile distilled water at 4 °C before use.

2.2.3 Performing egg counts

Egg counts were performed by extracting all cysts from 100 g infested soil samples (section 2.2.2) before crushing the cysts and resuspending the eggs in water. Subsamples from each egg suspension could then be counted using a counting chamber slide and from there the number of eggs per gram of soil calculated.

2.2.4 Hatching *Globodera pallida* cysts

In order to sterilise the cysts and induce hatching of second stage juveniles (J2s), cysts of *Globodera pallida* were first washed in absolute ethanol for 30 seconds, then with 1% sodium hypochlorite solution for up to 20 minutes, frequently inverting to ensure good mixing, until the cysts lost their brown colouration (Heungens et al., 1996). This causes the walls of the cysts to rupture, releasing eggs and encouraging hatching. Cysts were then washed thoroughly with sterilised tap water, to ensure no bleach remained. After washing, cysts were placed in a hatching jar consisting of a small, thick-walled glass jar covered with tinfoil to block light and containing a plastic ring holding a 30 µm nylon mesh, all autoclaved before use, onto which the cysts were placed. The mesh keeps eggs and cysts within the plastic ring but allows hatched juveniles through, to collect in the glass jar. Potato root diffusate was added to each jar to further encourage hatching, and

the jar was stored at 20 °C in the dark. After an initial 4 day incubation, juveniles were collected from the jar and the removed potato root diffusate was replaced each day for a period of 2 weeks. Any juveniles not immediately used were stored in non-stick 15 ml centrifuge tubes at 10 °C.

2.2.5 Plate cultivation of *Caenorhabditis elegans*

Caenorhabditis elegans cultures were maintained on 50 mm petri dishes with Nematode Growth Medium Lite (NGM Lite) + tetracycline, seeded with a lawn of *Escherichia coli* strain HT115, sealed with Parafilm M paraffin film (Bemis NA, Wisconsin, USA). Plates were incubated at 20 °C to encourage population growth or at 10 °C for longer term storage. When the bacterial lawn of plates was depleted, nematodes were transferred to new plates using a WormStuff worm pick with a flattened platinum tip (GeneSee Scientific, California, USA). When plates were contaminated with foreign bacteria or fungi, cultures could be axenised (Stiernagle, 1999). Gravid hermaphrodites were first rinsed from contaminated plates with sterile distilled water and collected in a 3.5 ml total volume in a 15 ml centrifuge tube. A mixture of 0.5 ml 5 M NaOH and 1 ml household bleach was then made up and added to the nematode suspension, which was vortexed for a few seconds every 2 minutes for a period of 10 minutes. This breaks down the bodies of the adults and sterilises the surfaces of released eggs. The tube was then centrifuged at 1500 rcf for 30 seconds to collect released eggs, and the supernatant removed and replaced with sterile distilled water. The centrifugation was repeated, the supernatant removed, and the remaining concentrated volume of eggs added to a fresh NGM Lite plate seeded with *E. coli* HT115.

2.2.6 *Caenorhabditis elegans* liquid cultures

In order to grow larger populations, *C. elegans* was grown in liquid culture. To start a liquid culture from a plate, nematodes of all stages were rinsed from the surface of the media using sterile M9 buffer. The nematode suspension was then added to a 250 ml conical flask containing 50 ml sterile M9 buffer, 300 µl 0.5 M CaCl₂, 150 µl 1.0 M MgSO₄, 50 µl 8 mg/ml cholesterol in ethanol, 500 µl antibiotic mix (penicillin, streptomycin, and neomycin, at 10 mg/ml, 10 mg/ml, and 5 mg/ml respectively), and 50 µl 10 mg/ml nystatin. To this was added 3 ml of a condensed *E. coli* HT115 food source. Cultures were

checked periodically for population status and food availability, adding more HT115 as necessary.

2.3 Bacterial cultivation

2.3.1 Preparation of *E. coli* HT115 as a food source for *C. elegans* liquid culture

An overnight culture of *E. coli* HT115 in 5 ml LB media (10 g tryptone, 10 g NaCl, and 5 g yeast extract per litre, autoclaved) was added to 1.4 l superbrot media (15.68 g K₂HPO₄, 2.89 g KH₂PO₄, 15 g tryptone, 30 g yeast extract, 1.4 l distilled water, with 10 ml 50 % glycerol added after autoclaving) in a 2 l conical flask. The flask was incubated at 37 °C, 150 rpm for 24 hours. After incubation, the culture was split between six 250 ml centrifuge bottles and pelleted by centrifugation at 8000 rcf, 4 °C for 15 min. The supernatant was discarded and each pellet re-suspended by addition of 12 ml M9 buffer followed by shaking on ice at 200 rpm for 20 min, or until the pellets were fully re-suspended. The suspension was then aliquoted into 15 ml sterile tubes before freezing at -20 °C. This suspension could then be defrosted as necessary for feeding *C. elegans* liquid cultures.

2.3.2 Preparation of ultra-competent *E. coli* DH5 α

Cell cultures were generated from existing frozen aliquots of *E. coli* DH5 α cells, using a modified method based on Inoué *et al.*, 1990. Cells were streaked on 90mm LB-agar plates (10 g tryptone, 10 g NaCl, 5 g yeast extract, and 15 g bacteriological agar per litre, autoclaved) and incubated overnight at 37 °C to achieve single colonies. Three liquid cultures were set up, staggered at 6 hour intervals, in 1 l conical flasks containing 250 ml SOB media (Super-optimal broth: 5 g yeast extract, 20 g tryptone, 0.584 g NaCl, 0.188 g KCl, 2.032 g MgCl₂, 2.464 g MgSO₄ per litre, autoclaved) by picking 10 individual colonies and adding them to each flask. These were incubated at 19 °C and 250 rpm for at least 24 hours, after which samples were taken to assess absorbance at λ 600 nm (A_{600}), using sterile SOB media as a blank. When the A_{600} came into the 0.5-0.6 range, the flask was taken out of the incubator and placed on ice for ten minutes – preparation of three staggered cultures was done so that if the first culture reached $A_{600}>0.6$, the second or third could still be used. The liquid culture was then centrifuged at 4000 rpm, 4 °C for 10 min and the supernatant removed. The cell pellet was then re-suspended in 80 ml TB (Transformation buffer: 10 mM PIPES, 15 mM CaCl₂, 250 mM KCl, adjusted to pH 6.7

with KOH and HCl, before adding 55 mM $\text{MnCl}_2 \cdot 4\text{H}_2\text{O}$ and sterilising by filtration through a 0.45 μm syringe filter, to be stored at 4 °C). After re-suspension, the cells were stored on ice for a further 10 min before repeating centrifugation as above. The supernatant was removed and the cells gently re-suspended, on ice, in a solution of 1.4 ml ice cold DMSO and 18.4 ml TB. Cells were then dispensed in 100 μl aliquots into pre-chilled, sterile microcentrifuge tubes and snap frozen in liquid nitrogen. Tubes containing ultra-competent DH5 α cells could then be stored at -80 °C indefinitely.

2.4 Molecular Biological Techniques

2.4.1 Transformation of ultra-competent cells

After defrosting ultra-competent *E. coli* DH5 α cells (prepared according to methods section 2.1.9), plasmid DNA was pipetted into the tube containing the cells. After incubating on ice for 5 minutes, cells could then be plated on LB-Agar plates. To select for positive transformants when the added plasmid contained antibiotic resistance genes, the relevant antibiotics were added into the LB-Agar solution before pouring into the plates. The transformation efficiency of the cells could be tested by adding a known mass of purified plasmid DNA to an aliquot of cells, preparing a dilution series from that aliquot and then plating the different dilutions (on antibiotic-selective LB-Agar) and growing overnight at 37 °C. Transformation efficiency, expressed as colonies/ μg DNA, could be calculated by dividing the number of colonies counted on a plate, divided by the mass of DNA added to the original cell aliquot and then divided again by the dilution factor relevant to the plate counted.

2.4.2 Extraction of plasmid DNA from bacterial cultures

Depending on the application for which the plasmid DNA was intended, two separate methods of plasmid extraction were routinely performed. When checking a number of colonies for the presence of a plasmid with insert for which there was no trivial selection criteria (e.g. blue-white screening), an alkaline lysis minipreparation was performed as follows: colonies were picked and transferred to Universal containers with 5 ml LB media and the relevant antibiotic for selection; these were then incubated overnight at 37 °C, 200 rpm. From each liquid culture, a 1.5 ml aliquot was pipetted into a microcentrifuge tube and centrifuged at 14,100 rpm for 15 s – the supernatant was then discarded and a second 1.5 ml aliquot added to the same tube and centrifuged again under the same

conditions. Each pellet was then re-suspended in 100 µl miniprep solution 1 (50 mM Tris-HCl, 10 mM EDTA, pH 8.0, with 100 µg/ml RNase A added after autoclaving) and vortexed to break up any clumps. To each tube was then added 200 µl solution 2 (1% SDS, 0.2M NaOH), followed by mixing without vortexing, to avoid shearing of genomic DNA. This was then incubated on ice for 5 minutes, after which 150 µl solution 3 (3.0 M potassium acetate, pH 5.5, ice cold) was added, followed again by gentle mixing and incubation on ice for 5 minutes. To remove the white precipitate that forms, the tubes are centrifuged at 14,100 rpm for 5 minutes and the supernatant pipetted into sterile microcentrifuge tubes. One volume of isopropanol was then added and the tubes are mixed vigorously before letting stand for 2 minutes at room temperature and centrifuging at 14,100 rpm for 5 minutes. The supernatant was then discarded, taking care not to disturb the pellet, and 200 µl absolute ethanol was added. The tubes are then mixed by inversion and centrifuged once again at 14,100 rpm for 3 minutes. The ethanol was then discarded and any remnants allowed to evaporate, before re-suspending the pellet in 30 µl TE buffer (10 mM Tris-HCl, 1mM EDTA, pH 8.0).

After identifying colonies of interest either through selection criteria like blue-white screening, or through analysis of the crude plasmid DNA from the above method, purified plasmid DNA could be obtained by growing an overnight culture, as above, and performing a miniprep using a QIAprep Spin Miniprep Kit (QIAGEN, 27106). Crude miniprep plasmids could also be purified by using a modified method provided in the QIAprep Spin Miniprep Kit.

2.4.3 Extraction of nematode genomic DNA

Extraction of *Globodera pallida* genomic DNA was performed according to a protocol for *C. elegans* total DNA extraction (Johnstone, 1999). Briefly, clean cysts were crushed to obtain eggs as in method 2.2.3, or J2s were collected from hatching jars, as in method 2.2.4. These were pelleted and the supernatant removed. The juveniles or eggs were then re-suspended in 10 volumes of extraction buffer (0.1 M NaCl, 10 mM Tris-HCl, pH 8.0, 10 mM EDTA, 1 % SDS, autoclaved, to which 1% β-mercaptoethanol and 100 µg/ml proteinase K are added before use, preheated to 60 °C). This was then incubated at 60 °C for 1-3 hours with occasional mixing by gentle inversion. Degradation was checked by viewing 5 µl aliquots of the mixture under magnification. Once worms

were visibly degraded, leaving only remnants of cuticle, the DNA was separated from proteins, etc., by phenol-chloroform extraction (method 2.4.4), performing this twice with phenol:chloroform:IAA and then once with chloroform only. The resulting DNA solution could then be cleaned and concentrated by ethanol precipitation.

2.4.4 Phenol-chloroform extraction of nucleic acids

Phenol-chloroform extraction was performed in order to purify nucleic acids extracted from whole organisms, removing cellular debris. To a given volume of DNA to be purified, an equal volume of phenol:chloroform:isoamyl alcohol (in a 25:24:1 ratio) was added. This was then vortexed until an emulsion was formed then centrifuged in a microcentrifuge at maximum speed for 5 minutes. The aqueous phase was then pipetted into a new tube, taking care not to take up any of the interphase or the lower phenol phase. The extraction could then be repeated on the aqueous phase by adding another volume of phenol:chloroform:isoamyl alcohol. Chloroform could then be used alone for a further extraction, following the same protocol. Ethanol precipitation of the DNA could then be performed by addition of 0.7 volumes of isopropanol and 0.1 volumes of sodium acetate.

2.4.5 Ethanol precipitation of nucleic acids

In order to clean and concentrate DNA, ethanol precipitation was performed as follows: 0.1 volumes 3 M sodium acetate, pH 5.5, and 0.7 volumes isopropanol were added, the tube mixed by inversion, then incubated at room temperature for 5 minutes. DNA was then pelleted by centrifugation at maximum speed for 5 minutes, and the supernatant was removed. The pellet was then washed with filter-sterilised 70 % ethanol, by adding a 200 µl aliquot, pipetting to float the pellet from the bottom of the tube, and centrifuging at max speed for 3 minutes. After this, the ethanol was pipetted off and the pellet was allowed to air dry for 3 minutes. The pellet was then rehydrated by addition of 80 µl TE buffer and resting for 1 hour at room temperature and then overnight at 4 °C before being re-suspended by gently mixing. If required, 1 µl 10 mg/ml RNase A could then be added to the DNA solution.

2.4.6 Polymerase chain reaction

The polymerase chain reaction was used extensively throughout the project. Where the purpose of the PCR was to identify the presence or absence of a specific sequence,

standard PCR was performed using MyTaq™ Red Mix (Bio-Line, BIO-25044). Reaction mixtures were set up according to the following scheme:

20.0 μ l	Total reaction volume
10.0 μ l	MyTaq™ Red 2X Mix
0.5 μ l	Forward primer
0.5 μ l	Reverse primer
x μ l	DNA
$(9.0 - x)$ μ l	ddH ₂ O

Where x is the variable concentration of the DNA source to be amplified. PCR was then performed on a Bio-Rad T100 Thermal Cycler (Bio-Rad, 186-1096). The annealing temperature (T_A) used was typically set at 5 °C below the lower melting temperature (T_m) of the primer pair. The protocol used was as follows:

Cycles	Temp (°C)	Time (min:s)
1x	95	0:30
	95	0:15
35x	$(T_m - 5)^*$	0:15
	72	0:30 per kb**
1x	72	3:00

* annealing temp based on primer T_m ;

** extension time based on fragment length, kilobases

High-fidelity PCR was performed when high quality amplification was desired, such as when a DNA fragment was to be amplified for later sequencing. For this purpose, Phusion High-Fidelity DNA Polymerase (New England BioLabs, M0530) was used, with each reaction mixture set up as follows:

25.0 μ l	Total reaction volume
5.0 μ l	5X Phusion HF or GC buffer
0.5 μ l	10mM dNTP mix
0.25 μ l	HiFi Platinum <i>Taq</i> (5U/ μ l)
x μ l	Template DNA (<250ng)
1.25 μ l	Forward primer, 10 μ M
1.25 μ l	Reverse primer, 10 μ M
(17.75- x) μ l	ddH ₂ O

The reaction was then cycled according to the following protocol, using the same Bio-Rad T100 Thermal Cycler:

Cycles	Temp ($^{\circ}$ C)	Time (min:s)
1x	98	0:30
	98	0:10
35x	(T_m+3)*	0:10 – 0:30
	72	0:30 per kb**
1x	72	3:00

* annealing temp based on primer T_m ;

** extension time based on fragment length, kilobases

Where amplification of a fragment was expected but was not achieved, optimisation of the PCR reaction could be performed for both standard and high-fidelity reactions. In some cases, addition of 5% DMSO to the reaction mixture (with an associated reduction in the volume of added ddH₂O) helped improve amplification. Optimisation of annealing temperature was performed by making up replicates of individual reactions and cycling the reactions through identical schemes with only the annealing temperature altered. Analysis of the products on an agarose gel (Method 2.4.8) would then allow selection of the optimal annealing temperature for future reactions.

2.4.7 Colony PCR

In order to test for the presence of the desired transgene in transformed bacterial cultures before growth of overnight cultures, colony PCR was performed. If the DNA fragment of interest was expected to fall between conserved regions of a plasmid, generic primers could be used; otherwise, transgene sequence-specific primers were used. Individual colonies from a plate of transformants were picked using a sterile yellow pipette tip and transferred to a 50 μ l aliquot of autoclaved, distilled water. This could then be used in place of the DNA template when setting up the PCR reaction. Colony PCR reactions were set up as follows:

10.0 μ l	Total reaction volume
5.0 μ l	MyTaq™ Red 2X Mix
0.5 μ l	Forward primer
0.5 μ l	Reverse primer
2 μ l	Bacterial cell suspension
3 μ l	ddH ₂ O

Reactions were then cycled similarly to standard PCR conditions, with an extended initial denaturing step at 95 °C in order to breakdown bacteria and release the plasmid DNA:

Cycles	Temp (°C)	Time (min)
1x	95	10:00
	95	0:15
35x	55	0:15
	72	0:30 per kb*
1x	72	10:00

*extension time based on fragment length, kilobases

Reaction mixtures could then be analysed by agarose gel electrophoresis (Method 2.4.8). Where the PCR of a colony generated an amplicon of the desired size, the remainder of the cell suspension could be added to 5 ml LB media (with relevant antibiotic for selection) in a 30 ml Universal container, then incubated overnight at 37 °C, 200 rpm, to generate sufficient quantities of plasmid DNA for downstream applications.

2.4.8 Agarose gel electrophoresis

In order to analyse the products of PCR reactions, restriction digests, and other techniques that generate linear DNA, agarose gel electrophoresis of the DNA was performed. Typically, 1.0 % w/v agarose (molecular biology reagent grade) was added to a volume of TAE buffer (40 mM Tris-acetate, 1 mM EDTA) and dissolved by heating in an 800W microwave at full power for 60 seconds; the volume required was determined based on the number of gels desired and the size of the gel trays to be used. The heated solution was then allowed to cool to approximately 60 °C before adding 1/20,000 volume of GelRed Nucleic Acid Stain (Biotium, 41003). The gel was then gently poured into gel trays that had been sealed at each end, ensuring that no bubbles are formed while pouring. A well comb with a number of teeth appropriate to the number of samples to be analysed was then added, before leaving the gel to cool and set. Once cooled, autoclave tape was removed, gels were placed into the electrophoresis tank and the combs carefully removed, and the gel could be loaded with samples. If necessary, loading buffer was added to DNA samples before pipetting into wells, alongside wells dedicated to a DNA marker, typically 1.5 µl 1 Kb Plus DNA Ladder (Invitrogen, 10787018), spaced appropriately among sample wells to allow for visualisation after electrophoresis. Electrophoresis was then performed in Bio-Rad horizontal gel electrophoresis tanks, using the Bio-Rad PowerPac 300 power system (Bio-Rad, 31453), typically performed at 70 V for 45 minutes. Where higher resolution gel images were required, a higher percentage of agarose was added to the gel, while a lower agarose percentage was used to achieve greater separation of bands at the cost of resolution. Gels were imaged and photographed under UV illumination using a Syngene U:Genius 3 gel imager.

Chapter 3 *Globodera pallida* xenobiotic metabolism in the context of biofumigation

3.1 Introduction

The cellular mechanisms by which organisms detoxify foreign compounds (xenobiotics) are collectively termed the xenobiotic metabolism. Xenobiotic metabolism and the enzymes associated with it (XMEs) are classified into three phases: modification, conjugation, and excretion. Phase I – modification typically involves recruitment of cytochrome P450 (CYP) enzymes, resulting in oxidation, reduction, or hydrolysis of xenobiotic compounds, priming them for the next phase (Omiecinski et al., 2011); over 21,000 CYPs have been described across all domains of life (Nelson, 2009). Phase II metabolism is the conjugation of charged species to the products of phase I metabolism. Enzymes such as glutathione S-transferases (GSTs, which conjugate reduced glutathione, GSH), UDP-glucuronosyltransferases (UGTs), and methyltransferases produce conjugated compounds that are higher in molecular weight and have reduced reactivity and toxicity (Jancova et al., 2010). The distinction between the first two phases of xenobiotic metabolism was first made in the 1950s, though conjugation as a method of detoxification had been observed in decades prior (Williams, 1959). Phase III encompasses a broader range of enzymes that recognise, and may modify further, the products of phase II before transporting them from the cell into the extracellular matrix, via ATP-binding cassette transporters (ABCs), where they undergo further modification and eventual degradation (Omiecinski et al., 2011). The modes of action of some drugs, including drugs designed to treat nematode parasites in mammals, depend on activation by the xenobiotic metabolism of the target: the drug as administered may not be bioactive until it has been altered through interaction with XMEs (Matoušková et al., 2016). Xenobiotic metabolism also plays an important part in the development of resistance to drugs: *C. elegans* lines that were selected for resistance to ivermectin and moxidectin constitutively over-expressed XMEs and transporters compared to susceptible lines (Menez et al., 2016). The processes that manage toxic compounds generated during the normal function of the cell are considered distinct from the xenobiotic metabolism, and comprise the glyoxalase system (part of the metabolic

pathway that generates GSH (Thornalley, 2003)) and the various systems of antioxidant metabolism (Sies, 1997).

Investigation of the xenobiotic metabolism of an organism has the potential to provide targets for control. Endoparasites are protected from many foreign compounds by the body of their host, reflected by reduced complements of XMEs observed in a number of parasitic nematode species (Abad et al., 2008, Cotton et al., 2014, Ghedin et al., 2007). However, they must combat the defences of the host for the duration of parasitism. Inhibition of a parasite's ability to avoid host defences should therefore have a detrimental effect on continued parasitism. The xenobiotic metabolisms of animal-parasitic nematodes have long been investigated as potential drug targets (Brophy and Barrett, 1990). Drugs that inhibit GSTs have been trialled against filarial nematodes (Ahmad and Srivastava, 2008), while cattle were protected against infection by *Fasciola hepatica* by immunisation with GST (Morrison et al., 1996). Plant-parasitism presents similar challenges for the parasite: following infection by *M. incognita*, tomato cells produced increased levels of nitric oxide, reactive oxygen species, and other defence compounds (Melillo et al., 2011), that are implicated both in direct toxicity to the invading organism, and in activation of further defence mechanisms including generation of toxic secondary metabolites (Torres et al., 2006). Transcription factors conserved with animal-parasitic nematodes and associated with xenobiotic metabolism have been implicated in successful maintenance of plant-parasitism (Gillet et al., 2017). Modulation of transcription factors involved in arabidopsis stress responses was observed in cases of *Heterodera schachtii* infection (Ali et al., 2014) and study of root-knot nematode effectors has identified manipulation of host defences as a major role (Quentin et al., 2013).

Of relevance to biofumigation are the xenobiotic metabolic elements involved in detoxification of isothiocyanates. The enzymes most closely associated with detoxification of isothiocyanates are glutathione S-transferases: numerous studies have demonstrated that isothiocyanates are sequestered in mammalian cells by conjugation with glutathione (Jiao et al., 1996, Kolm et al., 1995, Zhang, 2000). This mode of detoxification is conserved across diverse phyla: arabidopsis with reduced glutathione levels were more sensitive to allyl isothiocyanate, exposure to which induced up-

regulation of GSTs in both mutants and wild type (Øverby et al., 2015); exposure to Dazomet induced the specific up-regulation of a *C. elegans* glutathione S-transferase, GST-31 (Jones et al., 2013b). The *Globodera pallida* genome publication highlighted the limited repertoire of genes involved in xenobiotic metabolism (Cotton et al., 2014), a feature commonly observed in endoparasitic animals due to the protective nature of living within another organism. GSTs in parasitic nematodes have been shown to have roles in detoxifying endogenous cytotoxins as well as xenobiotic compounds (Ahmad and Srivastava, 2008), therefore contributing to normal cell function in the absence of xenobiotics. This is in-line with the trend among parasitic animals towards reduction and compaction of the genome (Poulin and Randhawa, 2015). This reduced complement of XME genes could result in each gene having a greater number of roles, such that knocking out expression of a single gene could have important effects.

The silencing of genes by RNA interference (RNAi) was developed in *C. elegans* (Fire et al., 1998) and has been subsequently demonstrated in a number of plant-parasitic nematodes including *Globodera pallida* (Lilley et al., 2012). The classical RNAi pathway occurs when exogenous dsRNA is recognised by the target organism and processed by the Dicer complex into small interfering RNAs (siRNA) (Grishok, 2005). The RNA-induced silencing complex (RISC) is then guided by these siRNAs to homologous mRNAs, which are then cleaved by an Argonaute protein, a class of ribonucleases integral to the function of the RISC (Sontheimer, 2005). Study of the genome of *G. pallida* has revealed that many of the components of the RNAi machinery described in *C. elegans* are conserved, though genes involved in the spreading of dsRNA between cells, enabling systemic RNAi, are missing (Cotton et al., 2014). The fixed feeding site induced by sedentary endoparasitic plant parasitic nematodes is ideal for the targeted delivery of silencing dsRNA (Lilley et al., 2012); as the interface between host and parasite, the feeding site is also the frontier at which the nematode faces host defences. Transgenes under control of root-specific promoters that are up-regulated in the giant cells of *Meloidogyne spp.* and the syncytia induced by *Globodera spp.* have been previously used to deliver an anti-feeding cystatin in potato roots (Lilley et al., 2004). Resistance to multiple *Meloidogyne spp.* was achieved in arabidopsis expressing dsRNA homologous to a parasitism gene, *16D10* (Huang et al., 2006). Tomato plants expressing dsRNA

targeting *M. incognita* cuticle collagen genes reduced the numbers of females per plant by up to 38 % and the number of eggs in each egg mass by as much as 82 % (Banerjee et al., 2017). RNAi targeting plant-parasitic nematodes has been most effective when the target is essential to normal cellular function in the target (Lilley et al., 2012). Targeted silencing of particular *G. pallida* genes could therefore elucidate the importance of xenobiotic metabolism to maintenance of sedentary endoparasitism, and potentially provide a new method of control. The ability to generate sequence-specific silencing induced only at nematode feeding sites should allow for generation of biosafe transgenic plants (Roberts et al., 2015).

3.2 Aims

1. Investigate genes potentially involved in *Globodera pallida* xenobiotic metabolism in response to the ITC-generator Dazomet
2. Substantiate gene models present in the *G. pallida* genome assembly and analyse sequences to identify potential roles
3. Confirm the up-regulation of identified genes of interest in order to identify candidates for targeting by RNA interference

3.3 Materials & methods

3.3.1 RNAseq analysis of *Globodera pallida* xenobiotic metabolism

RNAseq analysis was performed on triplicate treatments of 5000 second-stage juveniles, exposed to 0.12 mM Dazomet for 24 h and incubated with 0.5 % DMSO for 24 h as a solvent control, at the Wellcome Trust Sanger Institute (Wellcome Trust Genome Campus, Cambridgeshire, UK). Using an Illumina HiSeq instrument, 100 bp paired-end reads were generated from RNA extracted from treated nematodes, and were mapped to 16403 genes from the *G. pallida* genome assembly (hosted by the James Hutton Institute, UK http://ppcollab.hutton.ac.uk/cgi-bin/gb2/gbrowse/Gp_ass_2012_04/ (Cotton et al., 2014)). Genes for which there were no reads from either Dazomet or mock-treated RNA extractions were excluded from further analysis. Normalised expression values were analysed using the DESeq2 package (Love et al., 2014) for R (R Core Team, 2018) to give fold-changes in expression of genes between DMSO-treated and Dazomet-treated nematodes that were differentially regulated, based on a confidence value of $P < 0.01$. Genes of interest from among this subset were selected by limiting the confidence level to $P < 0.005$ for genes up-regulated under Dazomet exposure, with a 10-fold lower limit for change in expression. A heatmap was generated using the pheatmap package (Kolde, 2018) and principal components analysis was plotted using the Bioconductor package (Huber et al., 2015).

3.3.2 Confirming gene models and cloning promoter regions

Primers for sequencing genes were designed based on the gene models present on the *Globodera pallida* genome assembly, checking the melt temperature and potential for primer dimers using the Multiple Primer Analyzer from ThermoFisher Scientific (with T_m estimation based on a modified nearest neighbour method (Breslauer et al., 1986)). Sequencing primers are given in Table 3.1.

Primers were first checked using standard PCR, to ensure amplification of an amplicon from the *G. pallida* genome. High-fidelity PCR (Method 2.4.6) was then performed on cDNA extracted from Dazomet-exposed *G. pallida* J2s (Method 3.3.4).

3.3.3 Bioinformatic analysis of genes

Gene sequences were analysed to identify potential roles in *G. pallida* xenobiotic metabolism or gene regulation. BLAST alignments (Altschul et al., 1990, Madden et al., 1996, States and Gish, 1994) were combined with InterPro homology analysis (Finn et al., 2017), SignalP signal peptide predictions (Petersen et al., 2011) and Phobius transmembrane topology prediction (Kall et al., 2004) to inform assignment of putative roles for the enzymes encoded by the sequenced genes.

3.3.4 RNA extraction and reverse transcription

To confirm the changes in gene expression identified through RNAseq, qPCR was performed. *Globodera pallida* J2s were collected from hatching jars (Method 2.2.4), over a period not exceeding 7 days. The nematodes were collected in a single 15 ml maximum recovery centrifuge tube, and cleaned by allowing them to settle, removing the potato diffusate and re-suspending in sterile tap water. This was repeated three times. Nematodes were then re-suspended in water to give approximately 5000 individuals per 1 ml. Three experimental tubes were set up with 120 μ M Dazomet (final concentration, applied in 0.25 μ l DMSO) and controls with 0.25 μ l DMSO added were also set up, after which each was incubated at room temperature at 14 rpm on a rotating mixer for 24 h. Following incubation, the nematodes were pelleted at 3000 rpm for 3 minutes. The supernatant was pipetted off from each tube, and the nematodes were frozen by immersing the tubes in liquid nitrogen. RNA was extracted using the difficult tissue samples protocol for the EZNA Plant RNA kit (Omega Bio-tek, Georgia, USA).

RNA concentrations were measured on a NanoDrop ND-1000 (Thermo Fisher Scientific, Massachusetts, USA). Reverse transcription reactions were performed using equivalent amounts of RNA, using the Tetro cDNA synthesis kit (Bioline, London, UK).

3.3.5 Quantitative PCR

Primer pairs for qPCR were designed using the Primer3Plus. qPCR was performed on a CFX Connect™ Real-Time PCR Detection System (Bio-Rad, California, USA), with each reaction mixture made up using the SsoAdvanced™ Universal SYBR® Green Supermix as follows:

15.0 μ l	Total reaction volume
7.5 μ l	SsoAdvanced™ Supermix
0.6 μ l	Primer mix (final concentration 300 nM)
3.9 μ l	Nuclease-free water
3.0 μ l	cDNA template

Primer pairs were mixed to give 7.5 μ M of each prior to adding to Master mixes for each primer pair were prepared without addition of cDNA before pipetting into each well.

Calibration curves for each primer were produced using pooled cDNA from the Dazomet-treated nematodes, with a ten-fold dilution series from 5x to 50000x. Primer pairs were rejected if their efficiency was outside the 90-110 % range. A complete list of primers used for qPCR is given in Table 3.2.

Table 3.1 Primers for sequencing of *G. pallida* genes

Primer	Sequence 5'-3'	Target accession number
GP01278F	ATGGACAGCGAGAAAGAG	GPLIN_000127800
GP01278R	ATTCGATCACTTCGGCCTCAT	
GP02040F	CGACCAATGGGACATGAATCA	GPLIN_000204000
GP02040R	GTTGCATCATTTCGTCTCGACT	
GP02405F	AAATGGTCCAATACAAATTGT	GPLIN_000240500
GP02405R	CTCCATCGTTCAGCGGTCCTG	
GP03693F	CATTATGGCACCAAATTG	GPLIN_000369300
GP03693R	GGGAAGTTCCTTGGTAAAGCC	
GP04700F	ATGATTGGTCATTTACGACAC	GPLIN_000470000
GP04700R	TCACCGCCACCAATTCCA	
GP04723F	ATGTGCTTTCACAACCTTGGTGG	GPLIN_000472300
GP04723R	TCAGAGGTCTGCGAGGTTACAAT	
GP04777F	TTTTAAATAGAATATGTTGGAACAT	GPLIN_000477700
GP04777R	TTTCTACCAAATAACTCGAAGG	
GP07079F	ATGTTGTGCCAAGTCAAATTTTCG	GPLIN_000707900
GP07079R	CAATTAATAATGGGCATCGTTTGG	
GP08126F	ATGAATGCACAAAAGACAATAATTG	GPLIN_000812600
GP08126R	TCATTTTGAACCAGCAGCTGTG	
GP08879F	ATGGGCAATGTGAGGCCAAA	GPLIN_000887900
GP08879R	TCAGCGGTCCCTCCCTTTTG	
GP09707F	ATGCTAAATGCAAATGCAGACC	GPLIN_000970700
GP09707R	TTAAAATCCTCCCATTAATAATTG	
GP10083F	ATGAACGCATCAAACAACCAAT	GPLIN_001008300
GP10083R	GTCAACTACAGCTCGTCTCT	
GP10467F	ATGTTGTTGCGGATACAGCTT	GPLIN_001046700
GP10467R	TTAGGTGCAGAATCCGCATG	
GP10686F	GATATAAATAAATGTTGC	GPLIN_001068600
GP10686R	CTTCTTCAGCATCTGGTCCATG	
GP11840F	GGCAAACATGCTGAAATCTTA	GPLIN_001184000
GP11840R	CTTTGTCAAGTAATCGCTGATC	
GP11984F	CGCTAAAATATTATTAATGCC	GPLIN_001198400
GP11984R	CTCCATCGTTCAGCGGTCC	
GP12030F	ATGTTTCTTCTTCGCCGTCCAAC	GPLIN_001203000
GP12030R	CTAATGCTTAGGCTTCTTTCCG	

Table 3.2 qPCR primers

Primer	Primer sequence 5'-3'	% Efficiency	Target
q01278L1	TGCGGTTGGAATGCAAACCTG	98.0	GPLIN_000127800
q01278R1	TTCAAGGGCATGCGAACAAC		
q02040L1	AAAAACAGGGCGACCGGAATG	97.1	GPLIN_000204000
q02040R1	TCGGCCAAAGTGAAAAGCTC		
q02405L1	ATTTGCATTGGCCGGGAAAG	99.9	GPLIN_000240500
q02405R1	TTTCTCTGTCGCCAGTTTG		
q03693L1	ACGCCAAATTGTTGCCCTTC	93.8	GPLIN_000369300
q03693R1	TTCGTCCAACGCGTAATTGC		
q04700L1	AATGGACACTTTGGCAACGC	96.1	GPLIN_000470000
q04700R1	TCTCTCAGCTTTTCGTGCAG		
q04723L1	AATGTGCCGGCCTGAAAAAC	97.8	GPLIN_000472300
q04723R1	TGAAACCCGCCGATTTGAAG		
q04777L1	TGCACTGTCCAACCTCATTGC	126.2	GPLIN_000477700
q04777R1	TGTTGATTCCGCTGCGTTTG		
q07079L1	TGACCACGAGCAAATTTGCG	100.6	GPLIN_000707900
q07079R1	TTCGGCTCTCCAACCTCATTG		
q08126L1	AATAATTGTCGCCGCGTTGG	104.3	GPLIN_000812600
q08126R1	AGGCAATTGTCACAGCAACC		
q08879L1	AATGTGAGGCCAAAGGGAAC	113.9	GPLIN_000887900
q08879R1	AGTTTTGCGAAGACGATGCG		
q09707L1	TCAAATGCCATGCGAGTCG	128.9	GPLIN_000970700
q09707R1	TGTCGTTTTAAGCGCGTTGG		
q10083L1	AACGCGTTGGAGTGCATTTG	96.3	GPLIN_001008300
q10083R1	ACAATGGCGTTGAACAGTGC		
q10467L1	TCAATTTGTCACCGCACTGC	102.1	GPLIN_001046700
q10467R1	TCGCAACACTTGGAACCTTGC		
q10686L1	ATCATGCTTGCCCAATGTG	110.4	GPLIN_001068600
q10686R1	AAACGCACAAACTCGTCCAC		
q11840L1	AATCATTGCTGGCCAGAAGC	96.8	GPLIN_001184000
q11840R1	TTTTTCGTGCCATCCGCTTC		
q11984L1	TTGCCCGTACATTTTTGCC	98.8	GPLIN_001198400
q11984R1	AACGGGAAAATGCGCTTGAC		
q12030L1	ACTTCGGCCAACTGCAAATG	102.0	GPLIN_001203000
q12030R1	ACGCCACACGTAATTCTTG		
qEFT-1L1	ATCGAAAAACGGCCAAACGC	91.0	GPLIN_000541000
qEFT-1R1	TTGCAAGCGACGATGAGTTG		

3.4 Results

3.4.1 RNAseq analysis

The normalised RNAseq data presented 163 up-regulated and 28 down-regulated genes following Dazomet exposure ($P < 0.01$). In total, 3192 genes with no detectable reading in either condition were excluded. At the higher confidence threshold for genes with a 10-fold increase in exposure under Dazomet exposure, 18 genes of interest were identified ($P < 0.005$, Figure 3.1). A heatmap was produced and principal components analysis was performed, confirming a pattern of differential expression in Dazomet-exposed nematodes (Figure 3.2).

3.4.2 Confirmation of gene models and bioinformatics

3.4.2.1 *GP01278*

The assembly of 8 pair-wise sequencing runs, corresponding to 4 copies of the GP01278 amplicon, resulted in two consensus sequences that differed from the predicted CDS in a number of single nucleotide substitutions that resulted in one of the translated ORFs differing from that of the predicted gene by a single amino acid, E144D (Figure 3.3). The resultant protein of 501 amino acids was orthologous to *C. elegans* tyrosine aminotransferase, confirmed by BLAST homology and InterPro protein analysis.

3.4.2.2 *GP02040*

Attempted cloning of GP02040 resulted in a sequence that was shorter than the predicted CDS (1173 bp cf. 1719 bp). The translated sequence was shorter than the predicted, at 390 amino acids (cf. 572 predicted a.a.s). Analysis of the sequence suggested a pyroxidal phosphate-dependent transferase enzyme with a role in cysteine/methionine metabolism. BLAST analysis highlighted strong homology with cystathionine gamma-lyase genes in a number of nematode species. Sequence repetition identified towards the N-terminus of the predicted amino acid sequence was absent in that cloned from cDNA, but the repeated sequence was present (Figure 3.4). BLAST analysis matched each repetition to a single region of several cystathionine gamma-lyase genes, in which no such repetition was observed. InterPro analysis of this region alone identifies it as the major domain of pyroxidal phosphate-dependent transferases.

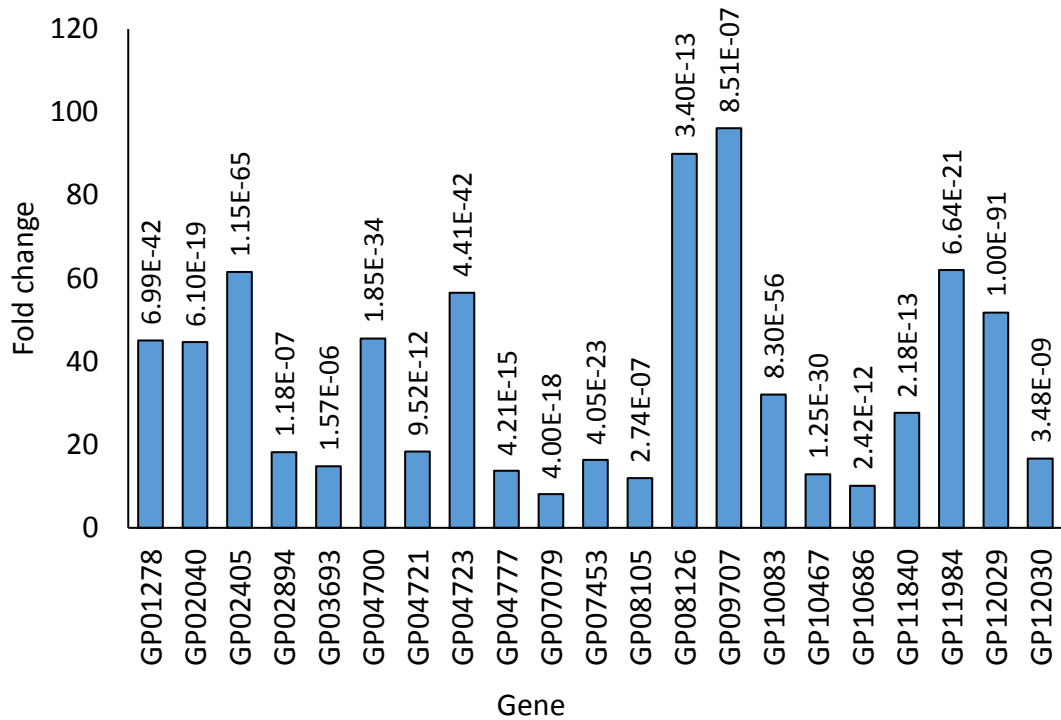


Figure 3.1 Fold changes of genes of interest identified from RNAseq analysis. Fold changes in expression are based on the output of RNAseq analysis of *G. pallida* J2s exposed to 0.12 mM Dazomet, contrasted with expression values from nematodes incubated with 0.5 % DMSO. Each treatment was carried out in triplicate, n = 5000 J2s. Data labels give the P-value for the change in expression.

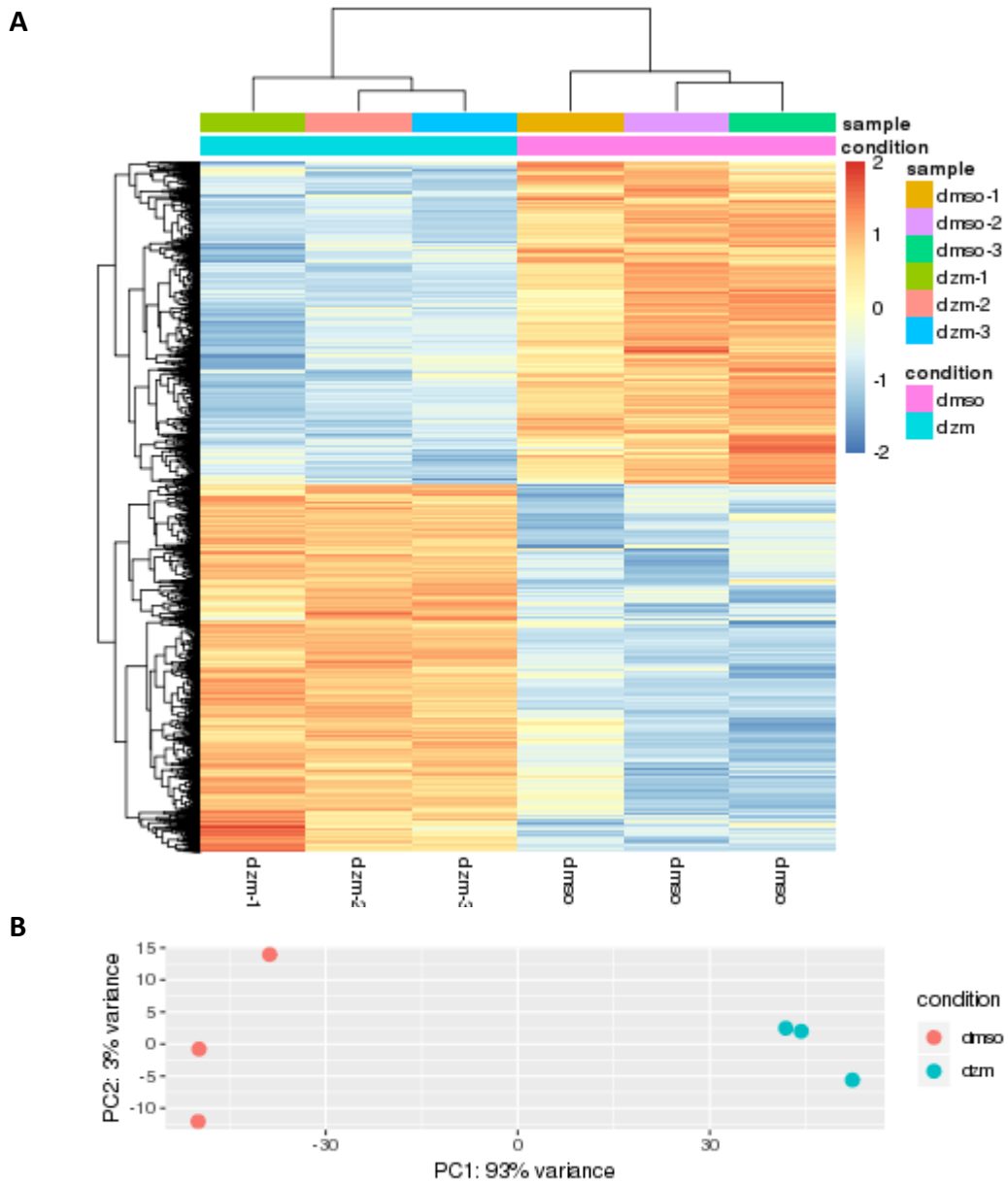


Figure 3.2 Heatmap and principal components analysis showing clustering of gene regulation in Dazomet-exposed *G. pallida*. A, heatmap of gene expression demonstrates broadly differential expression in nematodes incubated with and without 0.12 mM Dazomet. Each horizontal row represents a single gene and each column representing a sample, with the three dazomet treatments grouped on the left and the three DMSO control treatments on the right. The scale represents \log_2 fold change, with maximum values capped at ± 2 for clarity; the range of values ran from -5.32 to 9.13. B, principal components analysis further demonstrates differential clustering of gene expression: PC1 gives the variance between the two treatments; PC2 gives the variance between samples within the treatments..

```

GP01278seqcDNA1      MVVTSPPIALAQHSRRQQRALPKASALENRCYSAMAAPIKTPKKAKMHLNAPKRHQINE 60
GP01278seqcDNA2      MVVTSPPIALAQHSRRQQRALPKASALENRCYSAMAAPIKTPKKAKMHLNAPKRHQINE 60
GP01278predicted     *****

GP01278seqcDNA1      HSEWTTLRSSKHSRDTVNPIRRVTDSL SVAPNPKRPIQLNLGDPTLTGCLPPSESVVAA 120
GP01278seqcDNA2      HSEWTTLRSSKHSRDTVNPIRRVTDSL SVAPNPKRPIQLNLGDPTLTGCLPPSESVVAA 120
GP01278predicted     HSEWTTLRSSKHSRDTVNPIRRVTDSL SVAPNPKRPIQLNLGDPTLTGCLPPSESVVAA 120
*****

GP01278seqcDNA1      LRDAIDSHRFDGYGPAVGMQTARDAVAEFFSSREAPISADDVVLASGCSHALEMAIVAIA 180
GP01278seqcDNA2      LRDAIDSHRFDGYGPAVGMQTAREAVA EFFSSREAPISADDVVLASGCSHALEMAIVAIA 180
GP01278predicted     LRDAIDSHRFDGYGPAVGMQTAREAVA EFFSSREAPISADDVVLASGCSHALEMAIVAIA 180
*****

GP01278seqcDNA1      DPGQNVLVPCPGFPLYSTLCQPNGIKTRQYRLKMEEDGLIDLQHLES LIDDQTRAIIVNN 240
GP01278seqcDNA2      DPGQNVLVPCPGFPLYSTLCQPNGIKTRQYRLKMEEDGLIDLQHLES LIDDQTRAIIVNN 240
GP01278predicted     DPGQNVLVPCPGFPLYSTLCQPNGIKTRQYRLKMEEDGLIDLQHLES LIDDQTRAIIVNN 240
*****

GP01278seqcDNA1      PSNPTGVVFPREHLEQILRLAQKYLKLP IIADEIYGDLYAEGAKFHALATLSPRVPIITC 300
GP01278seqcDNA2      PSNPTGVVFPREHLEQILRLAQKYLKLP IIADEIYGDLYAEGAKFHALATLSPRVPIITC 300
GP01278predicted     PSNPTGVVFPREHLEQILRLAQKYLKLP IIADEIYGDLYAEGAKFHALATLSPRVPIITC 300
*****

GP01278seqcDNA1      DGI GKR YLVPGWFLGWLIVHNRFVLS DVKAGIVSLSQKIVGPCALIQGALPRILRDT PQ 360
GP01278seqcDNA2      DGI GKR YLVPGWFLGWLIVHNRFVLS DVKAGIVSLSQKIVGPCALIQGALPRILRDT PQ 360
GP01278predicted     DGI GKR YLVPGWFLGWLIVHNRFVLS DVKAGIVSLSQKIVGPCALIQGALPRILRDT PQ 360
*****

GP01278seqcDNA1      SFFDNIKNLLSQNAQIVYDILARV PGLKPLRPQGAMYMMVGFDP ELYGDETSFVQSLISE 420
GP01278seqcDNA2      SFFDNIKNLLSQNAQIVYDILARV PGLKPLRPQGAMYMMVGFDP ELYGDETSFVQSLISE 420
GP01278predicted     SFFDNIKNLLSQNAQIVYDILARV PGLKPLRPQGAMYMMVGFDP ELYGDETSFVQSLISE 420
*****

GP01278seqcDNA1      ESVYCLPGSAFSLPNWFRVLVLA FPEETREACERISAFCTRR LRPCRQLALWGSVPDEE 480
GP01278seqcDNA2      ESVYCLPGSAFSLPNWFRVLVLA FPEETREACERISAFCTRR LRPCRQLALWGSVPDEE 480
GP01278predicted     ESVYCLPGSAFSLPNWFRVLVLA FPEETREACERISAFCTRR LRPCRQLALWGSVPDEE 480
*****

GP01278seqcDNA1      DGGGSEGAERTAESTSDEDET 501
GP01278seqcDNA2      DGGGSEGAERTAESTSDEDET 501
GP01278predicted     DGGGSEGAERTAESTSDEDET 501
*****

```

Figure 3.3 Amino acid sequence alignment for GP01278. One of the cloned genes was identical with the predicted sequence, with a variant that resulted in a single amino acid substitution, E144D. The tyrosine aminotransferase domain is highlighted in yellow, while the residues that form the pyridoxal 5'-phosphate binding site are highlighted in red, with the lysine (K305) residue that binds to pyridoxal phosphate underlined.

```

GP02040predicted      MGHESGRRCCLVFMESLATSSIPNARA GRATNFVVSTTYKQFKPEELKGGHDYSRAGNPTRD 60
GP02040seqcDNA      ----- 0

GP02040predicted      ELQENIASLEGARFSRVFSSGLGATAAMANWLRAGDHLI MADDGYGGTQRYFR CMVWFES 120
GP02040seqcDNA      ----- 0

GP02040predicted      PSNPLLKVIDIEAVSKLVKAHSSSEIVVVDNTFMSPPFQNPALGADVVLHSLTKYINGH 180
GP02040seqcDNA      -----M 1

GP02040predicted      SDVVMGCLVTNSEQLDAHFLFQQL GRATNFVVSTTYKPEELKGGHDYSRAGNPTRDELQEN 240
GP02040seqcDNA      LPAAMAAAGIRFDQWDMNQVPPISL---STTYKQSKGEPKGGHDYSRAGNPTRDELQEN 58
      ..*.. .:* * :.:. :. . . . * * * ***** * * *

GP02040predicted      IASLEGARFSRVFSSGLGATAAMANWLRAGDHLI MADDGYGGTQRYFR DVSAHHGVQLS 300
GP02040seqcDNA      IASLEGARFSRVFSSGLGATAAMANWLRAGDHLI MADDGYGGTQRYFR DVSAHHGVQLS 118
      *****

GP02040predicted      FVDMTKLDDLRALRPNTKMWVFESPSNPLLKVIDIEAVSKAVKAHNPEIVVVDNTFMS 360
GP02040seqcDNA      FVDMTKLDDLRALRPNTKMWVFESPSNPLLKVIDIEAVSKAVKAHNPEIVVVDNTFMS 178
      *****

GP02040predicted      PFFQNPALGADVVLHSLTKYINGHSDVVMGSLVTNSERLDAHFLFQQLAVGSPSSFDV 420
GP02040seqcDNA      PFFQNPALGADVVLHSLTKYINGHSDVVMGSLVTNSERLDAHFLFQQLAVGSPSSFDV 238
      *****

GP02040predicted      YLVLRGIKTLHLRMGQHQTNAVARWLKTDPRVEKVLVPALKCHPQHEVHKKQATGMSG 480
GP02040seqcDNA      YLVLRGIKTLHLRMGQHQTNAVARWLETDPREKVLYPELESHPPQHKVHKKQATGMSG 298
      *****

GP02040predicted      MISFYLRTDLEGSQKFLANLELFTLAESLGGYESLAELPALMTHASVPSEIHQKLGISNN 540
GP02040seqcDNA      MISFYLRTDLEGSQKFLANLQVFTLAESLGGYESLAELPALMTHASVPQEIIRKLGISNN 358
      *****

GP02040predicted      LIRLSVGCEYIRD LIRLDLIAMNVATGRSRDE 572
GP02040seqcDNA      LIRLSVGCEDRLDLIRLDLIAMEVATGRSRDE 390
      *****

>1st predicted repetition
GRATNFVVSTTYKQFKPEELKGGHDYSRAGNPTRDELQENIASLEGARFSRVFSSGLGATAAMANWLRAGDHLI MADDGYGGTQRYFR
>2nd predicted repetition
GRATNFVVSTTYK---PEELKGGHDYSRAGNPTRDELQENIASLEGARFSRVFSSGLGATAAMANWLRAGDHLI MADDGYGGTQRYFR
>translated cDNA sequence
-----STTYKQSKGEPKGGHDYSRAGNPTRDELQENIASLEGARFSRVFSSGLGATAAMANWLRAGDHLI MADDGYGGTQRYFR

```

Figure 3.4 Comparison of cloned and predicted amino acid sequences for GP02040.

Repetition of a region present in the predicted protein is not repeated in the cloned sequence, with a similar sequence appearing only once. The first repetition is highlighted in yellow and the second in green on the predicted sequence, while the corresponding residues in the N-terminal end of the cloned sequence are highlighted in purple. Alignment of the repeated region is replicated below the main alignment.

3.4.2.3 GP02405

Sequencing of GP02405 resulted in a sequence identical to the predicted gene model from the genome assembly. The sequence has strong homology to sigma-class glutathione S-transferase genes from nematodes and broader clades, with strongest homology to *Meloidogyne incognita gst-1* (Figure 3.5). This was supported by InterPro protein domain analysis.

3.4.2.4 GP02984

Attempted amplification of GP02984 from *G. pallida* cDNA was unsuccessful, though amplification from gDNA resulted in a sequence similar to the region of the gene model in the genome assembly. Alignment of either the predicted CDS or the sequenced genomic region gave no homology to known genes.

3.4.2.5 GP03693

The cDNA sequence cloned here was translated to identify the most likely ORF and this was then compared with that of the predicted gene model, minor divergence from the gene model was observed, e.g. E42dup, but did not affect the putative active site (residues 233-248) (Figure 3.6). GP03693 was orthologous to carboxylic esterase sequences from a number of nematode species, based on its ParaSite entry, and these associations were confirmed through amino acid sequence homology and InterPro analysis.

```

GP02405seqcDNA      MVQYKLYYFDLRGIGEPIRLLHLYVGQQFEDVRFMGMEEWPTKYKSKFFYGGKAPVLEVDGK 60
MincGST1            MVQYKLYYFDLPGRAEAIRMLFYKQPPFEDYRIKKEDWPTI-KSNYIFGQVPVLEVDGK 59
*****:***** * . * **:::* ** ** * : *:* ** **:::*:*****

GP02405seqcDNA      QLGQSSVILRFLAEKFFALAGKDEWEKAKADEIINFQDANTEELAFYLYTKLG----DREK 116
MincGST1            QLAQAGVILQFLGKRFDLAGKNEWEEAKAMEIIFLNDEFGVAVGTYIGAKFGFREGNVEQ 119
**.*:***:**::* *****:**:*** ** *::: . . :** ::* * : *

GP02405seqcDNA      LRTEVLEPGVKRIFPLFEALLKESGDYMLPSGLSMVDFQVGNLYFTKLEPDMIKAYP 176
MincGST1            LRKDVFLPAIERYFPFYEKRLAESNSGFILPSGLSFVDFSVAFFTMMIEMEKDIMAKYP 179
**.*: * .:* **:* *:*:*:*****:**.*:* : ::* ** : **

GP02405seqcDNA      ELVKYVERVHALPQLQKYLQQRPODR      202
MincGST1            KLVDFSNRFYSLPQLKEYLSKKKC--      203
:*.*: *.*:*****:**.*:

```

Figure 3.5 GP02405 sequence homology with *M. incognita* GST-1. The residues that make up the GSH-binding site are highlighted in yellow in each sequence. The substrate binding site of GP02405 is highlighted in blue, and the *M. incognita* *gst-1* substrate binding site is highlighted in green.

GP03693predicted	MAPKLSNSHNELLFFLILCPALIKFASSSAFVPIIEEFSTVNE-EESIPSIVTVRNGKIRG	59
GP03693seqcDNA	MAPKLSNSHNELLFFLILCPALIKFASSSAFVPIIEEFSTVNEEEESIPSIVTVRNGKIRG *****	60
GP03693predicted	FRRELEPALDADKVLFEQADIFLGIPFAQPPVDKLRRLERPLAASNWTGTLDATALPAPCV	119
GP03693seqcDNA	FRRELEPALDADKVLFEQADIFLGIPFAQPPVDKLRRLERPLAASNWTGTLDATALPAPCV *****	120
GP03693predicted	PQQLLTALNFDENCLQLNVMRPASAPSGDASPYQLPVLVFIHGGAFIIGGTFVEGYANIS	179
GP03693seqcDNA	PQQMLTALNFDENCLQLNVMRPASAPSGDASPYQLPVLVFIHGGAFIIGGTFVEGYANIS ***:*****	180
GP03693predicted	NNFVAQGIVVVTQYRLNFLGFFTDGTERNPGNLGLWDQRQALLWVRDNIGAFGGDPNRV	239
GP03693seqcDNA	NNFVAQGIVVVTQYRLNFLGFFTDGTERNPGNLGLWDQRQALLWVRDNIGAFGGDPNRV *****	240
GP03693predicted	TVWGQSAGAASTSILAL SPLTRDLFQQTIQMSGASLCPWAMNDLVRDESARTAEIIGCGM	299
GP03693seqcDNA	TVWGQSAGAASTSILAL SPLTRDLFQQTIQMSGASLCPWAMNDLVRDESARTAEIIGCGM *****	300
GP03693predicted	KGEQSVRDCVCRVELEDLVDIAIQQLELFRLLDLAMTRFNPRVDGEFVPSANLSVLFRTAPP	359
GP03693seqcDNA	KGEQSVRDCVCRVELEDLVDIAIQQLELFRLLDLAMTRFNPRVDGEFVPSANLSVLFRTAPP *****	360
GP03693predicted	KPTLMGFTPHEALFLTIQNPNSLLSFASPLTVSNLSEFGRDRFVKIIQRIVHLESIGRNA	419
GP03693seqcDNA	KPTLMGFTPHEALFLTIQNPNSLLSFDSPLTVSNLSEFGRDRFVKIIQRIVHLESIGRNA *****	420
GP03693predicted	NVREAEKQRQILEELIQFYASEPPTNNDTAHWLKRYTLFLSDALFIMPILAEARLKAEL	479
GP03693seqcDNA	NVREAEKQRQILEELIQFYASEPPTNNDTAHWLKRYTLFLSDALFIMPILAEARLKAEL *****	480
GP03693predicted	GWPVFLHQFDHVNKGHAKLLPFPGVAHTAEYAFTLGVPLLGNALDEEDKRVRAHAY	539
GP03693seqcDNA	GWPVFLHQFDHVNKGHAKLLPFPGVAHTAEYAFTLGVPLLGNALDEEDKRVRAHAY *****	540
GP03693predicted	GTFVKNGVPNTLNGETNWPRLGSDRRRSLQLTRIKYPNPVTETEPTDVAEKLKFWRKLSL	599
GP03693seqcDNA	GTFVKNGVPNTLNGETNWPRLGSDRRRSLQLTRIKYPNPVTETEPTDVAEKLKFWRKLSL *****:*****	600
GP03693predicted	LKGYGGMTGFTKELP	614
GP03693seqcDNA	LKGYGGMPGFTKELP *****	615

Figure 3.6 Amino acid sequence alignment for GP03693. Comparing data from the genome assembly with sequenced cDNA.

3.4.2.6 GP04700

Two distinct consensus sequences were generated from attempts to clone GP04700, with each containing the predicted CDS. The two sequences were broadly similar apart from a 159 bp break in the second sequence. Translation of the DNA sequences resulted in ORFs containing the predicted protein (Figure 3.7), which appears to feature an S-adenosylmethionine synthetase domain.

3.4.2.7 GP04723

Sequencing of GP04723 resulted in a consensus sequence that produced an amino acid sequence which was broadly homologous to the translation of the predicted protein, with the N and C termini being identical (Figure 3.8). Neither sequence was found to have homology to known protein domains, based on InterPro analysis. A BLAST search identified poor homology to unidentified and hypothetical proteins in other nematode species.

3.4.2.8 GP04777

The WormBase ParaSite entry for GP04777 indicated homology with *C. elegans* *lpr-3*, a lipocalin related protein. Sequencing of the GP04777 region resulted in two disparate consensus sequences, with homologous regions at either end but little homology elsewhere. InterPro analysis of the predicted sequence suggested homology with the calycin superfamily, which include lipocalin and lipocalin related proteins. Of the largest complete ORFs from each of the cloned sequence consensus, one was predicted to belong to the phosphoenolpyruvate synthase family, and contained a PEP/pyruvate-binding domain typical of the family; the other translated sequence had no identifiable domains and a BLAST search identified only poor homology to unidentified proteins.

3.4.2.9 GP07079

The consensus sequence from cloning of GP07079 gave a longer ORF than the predicted gene model (Figure 3.9). Where the predicted 78-a.a. protein had no domain homology and aligned poorly to predicted proteins from *Heterodera spp.* and *Globodera rostochiensis*, the longer ORF had a carbohydrate-binding domain and a signal peptide, as well as homology to *Heterodera avenae* predicted effectors. The signal peptide prediction was further reinforced by SignalP 4.1 analysis (Petersen et al., 2011) (Figure 3.9).

3.4.2.10 *GP08126*

The largest translated ORF from the cloned GP08126 sequence matched that of the predicted protein, a short (86 a.a.) protein with poor homology to known enzymes and domains, but with a predicted signal peptide in the 28 N-terminal residues (Figure 3.10).

3.4.2.11 *GP08879*

Sequences cloned for GP08879 matched the 5' region of the predicted CDS, but were otherwise mismatched. Two distinct consensus sequences were generated, which translated to give short ORFs that matched the start codon of the predicted gene; the longest ORFs generated from each cloned cDNA sequence bore little homology to the predicted sequence or one another (Figure 3.11). The sequence designated as GP08879contig1 returned no homologous domains. GP08879contig2 contained domains with homology to acyltransferase family proteins, and BLAST aligned the sequence to bacterial acyltransferase proteins with high sequence conservation.


```

GP04700Contig1      MHPTRWELSHMVDLQAAANSLVIMVTHFGSSPINERDLLQIIESNFDLRPGAIKQLGLT 60
GP04700Contig2      MHPTRWELSHMVDLQAAANSLVIMVTHFGSSPINERDLLQIIESNFDLRPGAIKQLGLT 60
GP04700predicted     -----MVTHFGSSPINERDLLQIIESNFDLRPGAIKQLGLT 37
                      *****

GP04700Contig1      RPIYQRTAENGHFGNAEFPWERPKTLILPKNLHEKLRDVQVG 102
GP04700Contig2      RPIYQRTAENGHFGNAEFPWERPKTLILPKNLHEKLRDVQVG 102
GP04700predicted     RPIYQRTAENGHFGNAEFPWERPKTLILPKNLHEKLRDVQVG 79
                      *****

```

Figure 3.7 GP04700 predicted ORFs. The longest predicted reading frames from the consensus sequences for GP04700 are aligned with the predicted protein. A predicted S-adenosylmethionine synthetase domain is highlighted in yellow.

```

GP04723seqcDNA      MCFHNLVEMDAKHMRQMEEDRMRGMDREHPQSMDMRGMDMKHSRSMIDIEHMRGMDMKQQS 60
GP04723predicted    MCFHNLVEMDAKHMRQMEEDRMRGMDREHPQSMDMRSMDMKHSRSMIDIEHMRGMDMKQQS 60
                    *****:*****.****.****.*****:***:*****

GP04723seqcDNA      MDMKHSR-IDMELLQGMMDRMDMKHSRSMIDMK-----HMRGMDMKHSR 103
GP04723predicted    MDMKHSRSMIDMELLQRMMDRMDMKHSRSMIDMEHMRGMDMKHSRSMIDMEHMRGMDMKHSR 120
                    *****:*****.****.*****:*****

GP04723seqcDNA      SMDMEHMRGMNDDEMRAWKTRSNLLRVDAKGGSPVKQSSKSNETKSGEIKEAQQPGTMQ 163
GP04723predicted    SMDMEHMRGMNDDEMRAWKARSNLLRVDAKGGSPVKQSSKSNETESNEIKAPSSPGQC- 179
                    *****:*****:*****:*****:*.***.***

GP04723seqcDNA      GEGGKHGDKQAEQKPKKCKLNAECYSNAQCGKRSTCEPVSFADKKKVGTCDCGICGXKI 223
GP04723predicted    -----RAKCKLNAECYSNAQCGKRSTCEPVGFADKKKVGTCDCGICGMKI 225
                    *****:*****.*****.*****

GP04723seqcDNA      PLTMFCNLNKGPIAFKPKIAIRQCAGLKNACRKDSLFTALETTRKCNCEEGFKSAGFKNLE 283
GP04723predicted    PLTMFCNFKNGPIALKPKIAIRQCAGLKNACRKDSLFTALETTRKCNCEEGFKSAGFKNLE 285
                    *****:*****:*****:*****:*****

GP04723seqcDNA      DGQKKKLCDEQQCDGEKDTCHGMKCTAGKCNCNLADL 320
GP04723predicted    DGQK-KLCNEQQCDGEKDTCHGMKCTAGKCNCNLADL 321
                    ****.***:*****:*****

```

Figure 3.8 Comparison of predicted and sequenced protein models for GP04723. The proteins are of similar length and are highly homogenous, possibly indicating splice variants. Poor homology with known proteins prevents prediction of gene function.

```

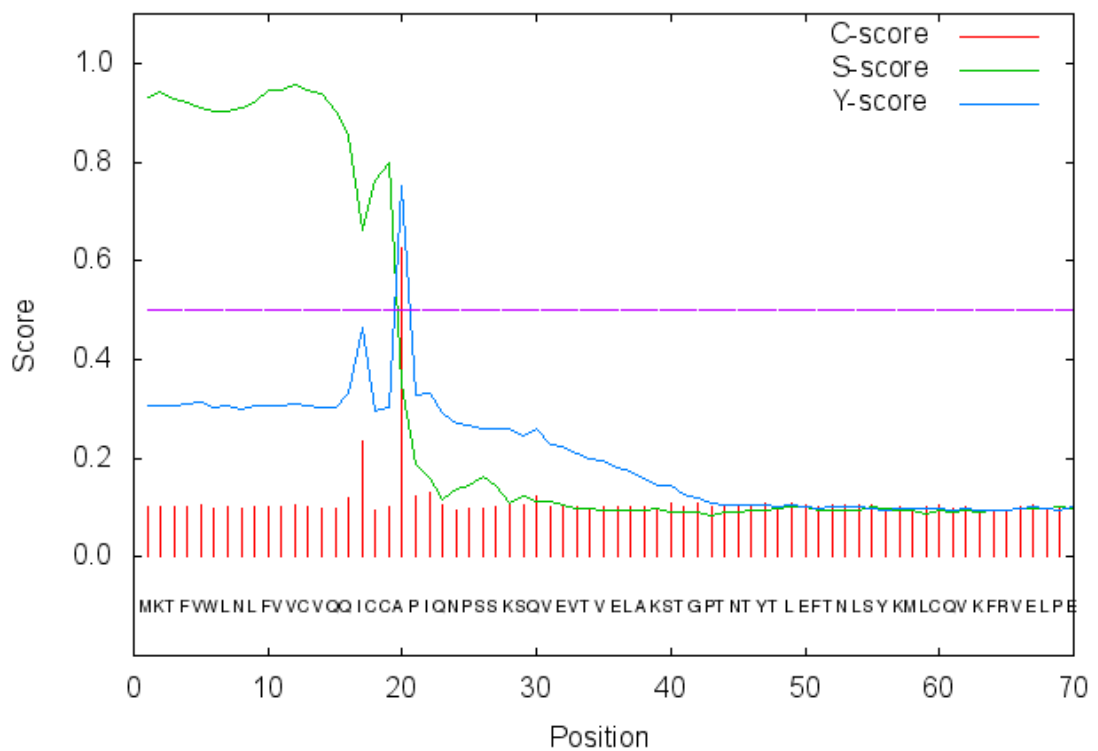
GP07079seqcDNA      MKTFVWLNLFVVCVQQICCAPIQNSSKQVEVTVELAKSTGPTNTYLEFTNLSYKMLC 60
GP07079predicted    -----MLC 3
                                     ***

GP07079seqcDNA      QVKFRVELPETATLVKYWNLSPVSGTTDHFTLPDHEQISPGQAFAYAGIKVNGVGEPKIT 120
GP07079predicted    QVKFRVELPETATLVKYWNLSPVSGTTDHFTLPDHEQISPGQAFAYAGIKVNGVGEPKIT 63
*****

GP07079seqcDNA      ILDTVKVLSTKRCPF 135
GP07079predicted    ILDTVKVLSTKRCPF 78
*****

```

SignalP-4.1 prediction (euk networks): GP07079



#	Measure	Position	Value	Cutoff	signal peptide?
	max. C	20	0.627		
	max. Y	20	0.750		
	max. S	12	0.955		
	mean S	1-19	0.894		
	D	1-19	0.828	0.450	YES

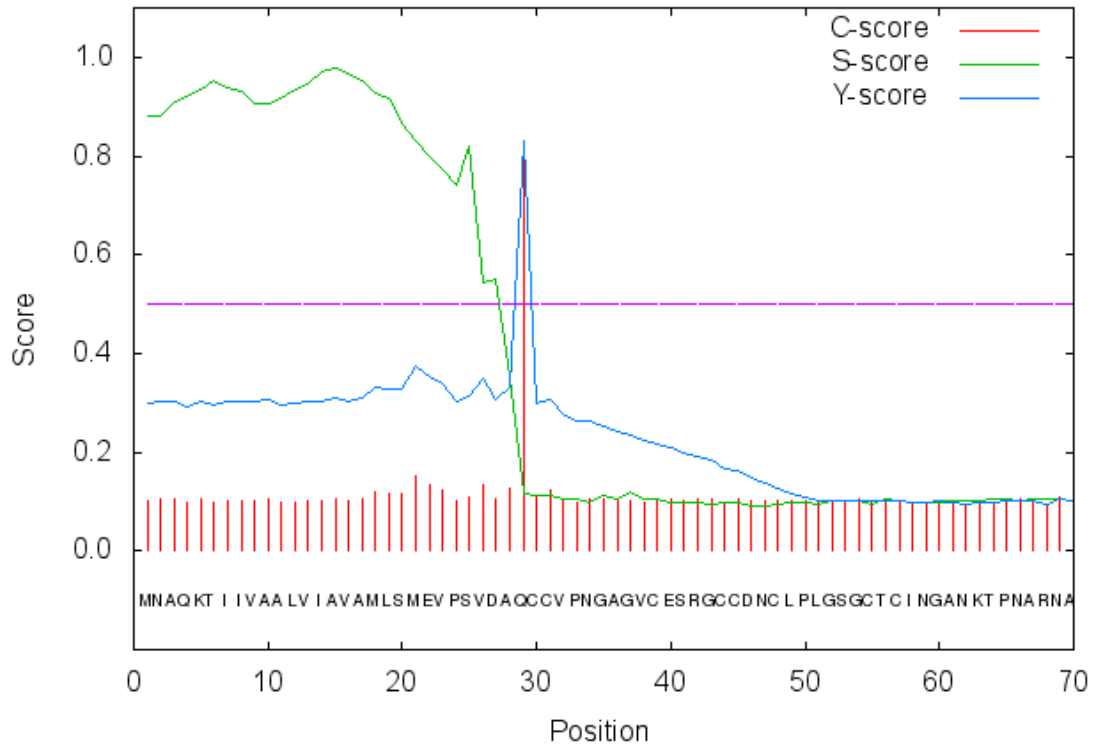
Cleavage site between pos. 19 and 20: ICC-AP D=0.828 D-cutoff=0.450

Figure 3.9 GP07079 amino acid sequence alignment. The predicted signal peptide is highlighted in yellow in the alignment, and the SignalP 4.1 output is given below.

GP08126 **MNAQKTIIVAAALVIAVAMLSMEVPSVDA**QCCVPNGAGVCEESRGCCDNC LPLGSGCTCING 60

GP08126 ANKTPNARNAVEAAAAADGTAAGSK 86

SignalP-4.1 prediction (euk networks): GP08126



# Measure	Position	Value	Cutoff	signal peptide?
max. C	29	0.824		
max. Y	29	0.832		
max. S	15	0.977		
mean S	1-28	0.855		
D	1-28	0.845	0.450	YES

Cleavage site between pos. 28 and 29: VDA-QC D=0.845 D-cutoff=0.450

Figure 3.10 Signal peptide identified in the GP08126 sequence. The 28-a.a. signal peptide in the sequence is highlighted in yellow, and the SignalP 4.1 readout is given below (Petersen et al., 2011).

A

GP08879pred	MGNVRPKGTIYMAAQKGGKQKLSSTSSASSQNSQIKQELKRRTKLANKKNKKAAPAMGM	60
GP08879contig1	MGNVRPRPVVREHVGSTPGCHCPKCPREPAPFALV-----	35
GP08879contig2	MGNVRPNPKYATTEGVQKFDALGSRLRHRDSLRFPAH-----	39
	***** *	
GP08879pred	SGNGREKRKETKGRDR	76
GP08879contig1	-----	35
GP08879contig2	-----	39

B

GP08879c1ORF	MSPLQLQTRPPSKFGYRAGILTIELWFAPNHLSSAPHTTANCSSMPPHNSIHTPPRS	60
GP08879c1ORF	TISPSEQTVNQVNHGVFGSALLRIFSPVLVQLVKKLLSGFFGSMASQLKLLTAQSRNAPAA	120
GP08879c1ORF	VRNTHKKDEITENNENEADYFSACSDTSYIEELERSSSGESVSTADAIGFKLLHYQAALE	180
GP08879c1ORF	VVNEILKQNSKPDANISLEEFSSLIIDRAASALREKQSQNISFDNTSIKQIGGGKHKRSKI	240
GP08879c1ORF	TDVFRQFKREQTALVHAGTWGSGIPESTRHVHVRTALASHCP	282

C

GP08879c2ORF	MTLCILCPGQGSQTVDMPLPRLGEPHLEPLLDAMPFDAMAVSQNSELCFVNAHAQP	60
BetaproMDC-E	MTLCILCPGQGSQTVDMPLPRLGEPHLEPLLDAMPFDAMAVSQNSELCFVNAHAQP	60

GP08879c2ORF	LIVAAGAAVAQALKAHGIHADLSAGYSIGELTAHTVAGSLQALDGVGLAVKRAQCMDQAA	120
BetaproMDC-E	LIVAAGAAVAQALKAHGIHADLSAGYSIGELTAHTVAGSLQALDGVGLAVKRAQCMDQAA	120

GP08879c2ORF	PAAHGMMAVKGVRIIDRLGAIQEHGLAVAIVNDEQHAVLAGPTAVMKSICKGMERELGAH	180
BetaproMDC-E	PAAHGMMAVKGVRIIDRLGAIQEHGLAVAIVNDEQHAVLAGPTAVMKSICKGMERELGAH	180

GP08879c2ORF	VVHLNVQVPSHTVWLI EASVQFKNALDAASWRGFDCPVLSALDGSFVENRDGAI DCLARQ	240
BetaproMDC-E	VVHLNVQVPSHTVWLS EASVQFKNALDAASWRGFDCPVLSALDGSFVENRDGAI DCLARQ	240
	***** *****↑*****	
GP08879c2ORF	ISEPLQWSRTL DLASHCP-----	258
BetaproMDC-E	ISEPLQWSRTL DLASEMGATVYFEVGPGNL TRMVRERFPAAQARSLSEFQ TLEGALNWL	300

GP08879c2ORF	-	258
BetaproMDC-E	N	301

Figure 3.11 GP08879 sequence alignments. A, alignments of the short peptide ORFs from the two cloned GP08879 sequences with the predicted protein, showing poor homology. B, the largest ORF translated from GP08879 consensus sequence one, the sequence had poor homology to known proteins. C, GP08879 consensus sequence 2 largest ORF, aligned with a malonate carboxylase protein from *Betaproteobacteria bacterium*, an acyltransferase domain-containing protein.

3.4.2.12 GP09707

The predicted gene sequence for GP09707 is listed as orthologous to phosphoethanolamine methyl transferase (PMT) genes described in *Caenorhabditis spp.* on WormBase ParaSite. The cloned cDNA has a sequence that was homologous to the predicted CDS, with an extra 75 bp region near the middle of the sequence. Translating the sequence gave a complete open reading frame that matched the predicted protein, with a corresponding extra 25-a.a. insertion at residue 257 of the predicted sequence. The cloned gene had strong homology to methyltransferase proteins, including *C. elegans pmt-1*. InterPro analysis identified domain homology for S-adenosyl-L-methionine-dependent methyltransferases, with an S-adenosylmethionine binding site highlighted (Figure 3.12).

3.4.2.13 GP10083

The cloned sequence for GP10083 was nearly identical to the predicted sequence, with 11 single nucleotide mismatches. Mismatched nucleotides largely maintained the amino acid sequence, with only one corresponding residue substitution, R58K (Figure 3.13). WormBase suggested orthology with sodium/nucleoside co-transporters in a number of species, which was confirmed by BLAST alignment and InterPro analysis of the cloned sequence. The gene encodes a likely membrane protein, with Phobius analysis predicting 13 transmembrane domains (Kall et al., 2004).

3.4.2.14 GP10467

Cloning of GP10467 confirmed the gene model, and identified strong homology with a *G. rostochiensis* predicted gene, *Gros_g4372*, and a *C. elegans* carboxypeptidase gene, *ZC434.9*. InterPro analysis of the sequence confirmed homology to carboxypeptidase domains, identifying a metallo-carboxypeptidase binding site and a nematode six-cysteine domain (SXC, associated with secreted toxins in *Toxocara canis*), and SignalP 4.1 suggested a probable 23 residue signal peptide (Petersen et al., 2011). The identified domains, except for the signal peptide of GP10467, were conserved across the *G. pallida* and *G. rostochiensis* (Figure 3.14).

GP09707seqcDNA	MLNANADQIEALDRANILALLPPVNGKFFVVDIGAGIGRFTTVFAQSEASKVVATDEVHSF	60
GP09707pred	MLNANADQIEALDRANILALLPPVNGKFFVVDIGAGIGRFTTVFAQSEASKVVATDEVHSF	60

GP09707seqcDNA	VEKNRERNSEYANVEWRVGDATGLQFDEGSVDLVFTNWLMLYMSDEETVQFVANALQWLR	120
GP09707pred	VEKNRERNSEYANVEWRVGDATGLQFDEGSVDLVFTNWLMLYMSDEETVQFVANALQWLR	120

GP09707seqcDNA	PDGYLHLRESCSEPSTKKSVDNNSSSSSSLHNKSQPNPTRYRFSSAYIQLLRNIRHIEDE	180
GP09707pred	PDGYLHLRESCSEPSTKKSVDNNSSSSSSLHNKSQPNPTRYRFSSAYIQLLRNIRHIEDE	180

GP09707seqcDNA	SGKIWRFDVQWACSVGVYIERQLNWRQVHVLARKVPATDNNAISIPKSVETLAKQFADQW	240
GP09707pred	SGKIWRFDVQWACSVGVYIERQLNWRQVHVLARKVPATDNNAISIPKSVETLAKQFADQW	240

GP09707seqcDNA	PAEQREFDHRMDVQKPGWMQKAFDRCLDEMEFNGDGIMFGFSGRKIFTEFGVDAEALAQR	300
GP09707pred	PAEQREFDHRMDVQKPG-----GRKIFTEFGVDAEALAQR	275

GP09707seqcDNA	VGRRIWAVETDPFAYRNALTRANQCGDRRVRLAWHFNLESALDFWGNAGQSMPMFEAVVG	360
GP09707pred	VGRRIWAVETDPFAYRNALTRANQCGDRRVRLAWHFNLESALDFWGNAGQSMPMFEAVVG	335

GP09707seqcDNA	TEMLAQLQDERIVNKFARMLAGGAQFASVELVKPGKDQSDKFRANLKLRSRFIVNEEIE	420
GP09707pred	TEMLAQLQDERIVNKFARMLAGGAQFASVELVKPGKDQSDKFRANLKLRSRFIVNEEIE	395

GP09707seqcDNA	VDQLENGYKILIVMAKLRSTKDFWDGDENNQTRQLLMGGF	460
GP09707pred	VDQLENGYKILIVMAKLRSTKDFWDGDENNQTRQLLMGGF	435

Figure 3.12 GP09707 sequence alignment. The cloned sequence is aligned with the predicted sequence, resulting in a 25-aa insertion from residue 257 of the predicted sequence. The S-adenosylmethionine binding site is highlighted in yellow.

GP10083seqcDNA	MNASNNQYANENGVIELRQKQQPVKRNDANSRRSWDLMEWVEQAQQSLLQIFDENQRLI	60
GP10083pred	MNASNNQYANENGVIELRQKQQPVKRNDANSRRSWDLMEWVEQAQQSLLQIFDENQKLI *****: **	60
GP10083seqcDNA	NAFILLIILFLYHALIGFALFHNFNKAATLFTITVFGWLVVIYQQLSPFLKRQKLVGQI	120
GP10083pred	NAFILLIILFLYHALIGFALFHNFNKAATLFTITVFGWLVVIYQQLSPFLKRQKLVGQI *****	120
GP10083seqcDNA	KMQLLEHWTQLKANAIMTRLFYGFAGLPILFVVWDTRHNLERLSGLFGLIVFLIVMCLI	180
GP10083pred	KMQLLEHWTQLKANAIMTRLFYGFAGLPILFVVWDTRHNLERLSGLFGLIVFLIVMCLI *****	180
GP10083seqcDNA	SHKPTKVNWRPVLWGFLQFIFGIMVLRWEYGARKFVDLSNMAILFLDFTKNGTDFTYGF	240
GP10083pred	SHKPTKVNWRPVLWGFLQFIFGIMVLRWEYGARKFVDLSNMAILFLDFTKNGTDFTYGF *****	240
GP10083seqcDNA	LSAPPNICGMEPVLAFTIQVIIVVGAIVSVLYFYGIVQAVLKRMAMLQLTLGTATES	300
GP10083pred	LSAPPNICGMEPVLAFTIQVIIVVGAIVSVLYFYGIVQAVLKRMAMLQLTLGTATES *****	300
GP10083seqcDNA	LNACACVLLGNAESPLLIRPYIEKMTASELHAVMTGFSCFAGAVFAAYISFGACPRYLL	360
GP10083pred	LNACACVLLGNAESPLLIRPYIEKMTASELHAVMTGFSCFAGAVFAAYISFGACPRYLL *****	360
GP10083seqcDNA	SAAVMSAPGSLACSKLLYPETEKSSVKNVKDLELPPSKESNALECI SNGSLMSVHLITAV	420
GP10083pred	SAAVMSAPGSLACSKLLYPETEKSSVKNVKDLELPPSKESNALECI SNGSLMSVHLITAV *****	420
GP10083seqcDNA	CANLVSFMAIMALFNAIVGVGTLIGYTDWSLELFLGYTFFPVAYMIGVTENAEQTFLLVA	480
GP10083pred	CANLVSFMAIMALFNAIVGVGTLIGYTDWSLELFLGYTFFPVAYMIGVTENAEQTFLLVA *****	480
GP10083seqcDNA	RLLGVKIVINDFMAYQRLGVMLKQNLTPRSAMISTYALCSFSDPIAAGIQLAVLSEMAP	540
GP10083pred	RLLGVKIVINDFMAYQRLGVMLKQNLTPRSAMISTYALCSFSDPIAAGIQLAVLSEMAP *****	540
GP10083seqcDNA	TRRTLIARLVLRLALLAGCISCFMSAAIAGILIEVPVACKPSGGDGGAKCFDLSVHQRFME	600
GP10083pred	TRRTLIARLVLRLALLAGCISCFMSAAIAGILIEVPVACKPSGGDGGAKCFDLSVHQRFME *****	600
GP10083seqcDNA	DVLNSTSMVNLRDEL 615	
GP10083pred	DVLNSTSMVNLRDEL 615 *****	

Figure 3.13 Cloned GP10083 sequence aligns well with the predicted sequence, post-translation. The gene encodes a 615-a.a. protein with 13 transmembrane domains, marked in grey. The N-terminal region is cytoplasmic and the C-terminus is extracellular, according to Phobius prediction (Kall et al., 2004).

GP10467seqcDNA	-----MLLRIQQLVLFVLSYQIQFVTALLKAEDEA	31
Gros_g04732	MFGIVRGANVPAGAKSIPKGLSRMLLKTMLLRIQQLVLFVLSYQIQFVTALLKAEDEA	60

GP10467seqcDNA	ATAGKFQVLRIVPQKQDELALLRRLTYKVAQEFELDFWKAPTLDIGAFVDVMVPEFVNTFS	91
Gros_g04732	ATAGKFQVLRIVPQKQDELALLRRLTYKVAQEFELDFWKAPTLDIGAFVDVMVPEFVNTFS	120

GP10467seqcDNA	DLNKRQRIQYNTIIEDVQSMIVQREKATGGRNHHAHKGNLSESVLLNQFKLFGKMRDDA	151
Gros_g04732	DLNKRQHIQYNTIIEDVQNMIVQREKAAGGRHQHAKGNLSESVLLNQFKLFGKMRDDA	180

GP10467seqcDNA	SSTGTRNKAVFGFDYHSYDEIVRWLEDVERFYQPMAQFTTIGTTYEGRSIRGIKIGSPI	211
Gros_g04732	SSTSSRNKAIFGFDYHSYDEIVRWLEDVERFYQPMAQFTTIGTTYEGRSIRGIKIGSPI	240

GP10467seqcDNA	SDTKRIVWVDGGMHAREWASVHTALWFIEQLIVQYGVDPQITSYMDTLNIFYFVVPANPD	271
Gros_g04732	SDTKRIVWVDGGMHAREWASVHTALWFIEQLIVQYGVDPQITAYVDTLNFYFVVPANPD	300

GP10467seqcDNA	GFEYSRSDVNPQTRFWRKNRGAQVCKKDRWRRCGGVDLNRNFDHGWETGSSSDMCS	331
Gros_g04732	GFEYSRSDVNPQTRFWRKNRGAQVCKKDRWRRCGGVDLNRNFDHGWETGSSSDMCS	360

GP10467seqcDNA	DIYQGAYAFSEPEPSRAIRDKMLSPELFGKVDAFLTLHTYSQMWHHPFNHERKSFNDIED	391
Gros_g04732	DIYQGAYAFSEPEPSRAIRDKMLSPELFGKVDAFLTLHTYSQMWHHPFNHERKSFNDIED	420

GP10467seqcDNA	LQEVGRRGVRALEQVYGTRYRFGTGADILYPSAGGSDDWAKSKAGVKYVYLLELRPGEEL	451
Gros_g04732	LQEVGRRGVRALEQVYGTRYRFGTGADILYPSAGGSDDWAKSKAGVKYVYLLELRPGEEL	480

GP10467seqcDNA	WDGFLDDRQLIPTGRETWEGVKVVIDAVMKRAKELQPWRVPVAVATTTAVAPLPQRPPP	511
Gros_g04732	WDGFLDDRQLIPTGRETWEGVKVVIDAVMKRAKELQPWRVPVAVATTTAAAPLPQRPPP	539

GP10467seqcDNA	AVAVTPPASFPRAVLPDVPVQTPATARLQNFVPSSEFQQKSRVDSSSTDNSQASTLR	571
Gros_g04732	AVAVTPPASFPRAVLPDVPVQTLPATARLNFVPSSEFQQKSRVDSSADNSQASTLR	599

GP10467seqcDNA	QALHMLRLARLRSQLEAKREFERNMQMKTNAAPQQSSSPCFDRSPWCSGWIQSSPLICR	631
Gros_g04732	QALHMLRLARLRSQLEAKREFERNMQAKTNAASQ-QSSSPCFDRSPWCSGWIQSSPLICR	658

GP10467seqcDNA	TSSIYMRQDCAKSCGFCT	649
Gros_g04732	TSSIYMRQDCSKSCGFCT	676

Figure 3.14 GP10467 compared with *G. rostochiensis* g04732. The predicted signal peptide of GP10467 is highlighted in blue. A carboxypeptidase activation site is highlighted in green, while the residues of the metalloprotease inhibitor-binding interface are marked in yellow, and the six-cysteine site is highlighted in magenta.

3.4.2.15 GP10686

The cloned sequence for GP10686 was nearly identical to the predicted sequence, with 14 nucleotide mismatches that resulted in no changes to amino acid composition (Figure 3.15). The predicted protein has homology with a number of glycoside hydrolase family genes in other nematode species, with the strongest homology and InterPro analysis suggesting a role in either galactose or maltase metabolism.

3.4.2.16 GP11840

Sequencing of GP11840 produced two consensus sequences that were broadly identical, with a number of mismatched single nucleotides and 3 corresponding mismatched residues. The sequenced genes were also largely homologous with the predicted gene apart from a mismatched region including a gap, corresponding to residues 154-240 of the cloned and translated sequence, and for an extension of the sequence in the C-terminus, resulting in 82 extra C-terminal residues in the cloned sequence (Figure 3.16). InterPro analysis suggested a role as a serine/threonine protein kinase, which was affirmed by BLAST homology to described serine/threonine kinases in other nematode species.

3.4.2.17 GP11984

The predicted sequence for GP11984 matched with that of GP02405, at both the DNA and amino acid sequence level. PCR primers specific to the slight variation in the 3' end of the GP11984 sequence resulted in amplification of the GP02405 sequence. Translating the predicted sequence results in a similar protein to GP02405, with an insertion of 4 amino acids as well as a number of substitutions (Figure 3.17); GP11984 therefore had similar homology, aligning well with *M. incognita* GST-1 and likely being a sigma-class GST.

3.4.2.18 GP12030

Cloning the GP12030 CDS resulted in an amplicon that gave the predicted amino acid sequence when translated. The short sequence had poor homology to known proteins other than putative gland proteins and effectors predicted in *Heterodera glycines* and *M. incognita*. Potential as a secreted protein was supported by SignalP 4.1 analysis (Figure 3.18).

GP10686	MLLLFLLLCGSI	<u>LPCHAIVDEPQRVDCLPNEHEISKACLETGCIWDGNYDQYNPSVPMC</u>	60	
GP10686	<u>YYPPEEC</u> YTIQSSVPGNVQLKWTSTLQ	<u>NPYSRPNLDVQVQHQMKGDIYVRIGREDRWL</u>	120	
GP10686	<u>PPLNELRNPTNFQKI</u> ISSNSLHFELGNMDGTF	<u>SFAIKRNDTNKANIWDTSIGGFVFGDQF</u>	180	
GP10686	<u>LQIATFI</u> ASDRLYGLGENMHHELKHFTRYTTWGAFSRDQ	NEYVPGPYNGYGVHPPFYV	240	
GP10686	GLEPSGKAHGVLIILNSNAQEYITGPGPHFVYRTVGGQ	LELFFFPGFTPEEVIRQYQQIIG	300	
GP10686	TPYLPAYWAFGRFLCRWGYRSAEDAKNTVQRVRDAKI	PFVQYADIDYMERYKDFTYDSE	360	
GP10686	KWAGLPEFAEQLSWDMKLVLIWDPVQANYSSFQRAIEK	GVSFIEWPNESMVQKEINDL	420	
GP10686	YPLTRNTNIMLGPMWPDHHCFFDFLDPLPNTTDWWV	DEFVRFHDKVNF	<u>GIWIDMNEPS</u>	480
GP10686	VFGTNEQQPWYFDPAAFGKKPPIAPLMCPKPNNNLD	YPPYRTWNSYQWDWDKSTKSLNDK	540	
GP10686	TLCMIGKSGRRKLSMYDTHSLYGWSEMIATQKALRA	STGKRSITSRSTFPSSGHYGGHW	600	
GP10686	LGDNHSRWPDLRLSIIGVMEFNMFGIPQIGADVCGFI	GDTEELCLRWQQLGAFHSYRNL	660	
GP10686	HNDVNSHMDQDPAQWKS VATATRVANLFRYQHLPY	LYSLHFRASLYGGTVIRPLFFEFPL	720	
GP10686	DTNTHSLSFQFMWGSAMVVVVISPNVDSVHAYLPV	NETWYSMSDAHEYGTRITPGYSTF	780	
GP10686	NAPRNTPLPTFLRGGYII	PRQEPDMTTVASRKKPFQLLAGLKPLSCPCTMVATGELFWDD	840	
GP10686	GETIVDDFAAHPPYHYIQFSVKATHSATTIVANRTH	SSSKEPLPSLEQIVILGHHFTPKLG	900	
GP10686	TATLNGIPVTLDPALSEFVPEKGALTVQCADLIKLD	DLAHDVWVTLSWHNEGKHGPDAEEE	960	
GP10686	K		961	

Figure 3.15 GP10686 structural features. The glycoside hydrolase family domain is underlined with the active site highlighted in yellow. A P-type trefoil sequence is highlighted in blue and an N-terminal barrel associated with galactose-metabolising proteins is highlighted in green.

GP11840pred	MLKSYKISSTSTPTLTSSTSTSDSDSGEIERQQFQQQSDDIKRVNGEMKSRNASYGDKSL	60
GP11840contig1	MLKSYKISSTSTPTLTSSTSTSDSDSGEIERQQFQQQSDDIKRVNGEMKSRNASYGDKSL	60
GP11840contig2	MLKSYKISSTSTPTLTSSTSTSDSDSGEIERQQFQQQSDDIKRVNGEMKSRNASYGDKSL *****	60
GP11840pred	LARSEQGSVWKSIAATEADGTTKCVTIKLLRAPFHSPGTAKYALREVALLSALNHPNLIAL	120
GP11840contig1	LARSKQGSVWKSIAATEADGTTKCVTIKLLRAPFHSPGTAKYALREVALLSALNHPNLIAL	120
GP11840contig2	LARSEQGSVWKSIAATEADGTTKCVTIKLLRAPFHSPGTAKYALREVALLSALNHPNLIAL ****:*****	120
GP11840pred	YDVRLPSKVKPLKKFDDLHLVTEYFGKNLRERINCHTVS-----FKFYVASI	167
GP11840contig1	YDVRLPSKVKPLKKFDDLHLVTEYFGKNLRERIVEKLNCTLWTHQELSYCIIQILCGVN	180
GP11840contig2	YDVRLPSKVKPLKKFDDLHLVTEYFGKNLRERIVEKLNCTLWTHQELSYCIIQILCGVN ***** : . :: .	180
GP11840pred	FLHAGSIVHRDLKPTNIVMSDRGNVKILDYGIARDIVPENLTTEAGTPIYRAPEIYLGID	227
GP11840contig1	FLHAGSIVHRDLKPTNIVMSDRGNVKILDYGIARDIVPENLTTEAGTPIYRAPEIYLGID	240
GP11840contig2	YLHAGSIVHRDLKPTNIVMSDRGNVKILDYGIARDIVPENLTTEAGTPIYRAPEIYLGID :*****	240
GP11840pred	SYDKKVDLWSVGCIFAELILARILFHGTTLATQWKLNFNEVLGTPDLKFLDSLGVKETNKQ	287
GP11840contig1	SYDKKVDLWSVGCIFAELILARILFHGTTLATQWKLNFNEVLGTPDLKFLDSLGVKETNKQ	300
GP11840contig2	SYDKKVDLWSVGCIFAELILARILFHGTTLATQWKLNFNEVLGTPDLKFLDSLGVKETNKQ *****	300
GP11840pred	IVMDMPKRESADWTQMIADNAVPKLISDYLT-----	319
GP11840contig1	IVMEMPKRESADWTQMIADNAVPKLISDYLTINVRALLSSMLVLDPAQRTSAEQALKNA	360
GP11840contig2	IVMDMPKRESADWTQMIADNAVPKLISDYLTINVRALLSSMLVLDPAQRTSAEQALKNA ***:*****	360
GP11840pred	-----	319
GP11840contig1	YFDIYRGYLSANLLATPQKVYCTEEFKQLMKDNNIDHFKEKILEQIATFKTKL	413
GP11840contig2	YFDIYRGYLSANLLATPQKVYCTEEFKQLMKDNNIDHFKEKILEQIATFKTKL	413

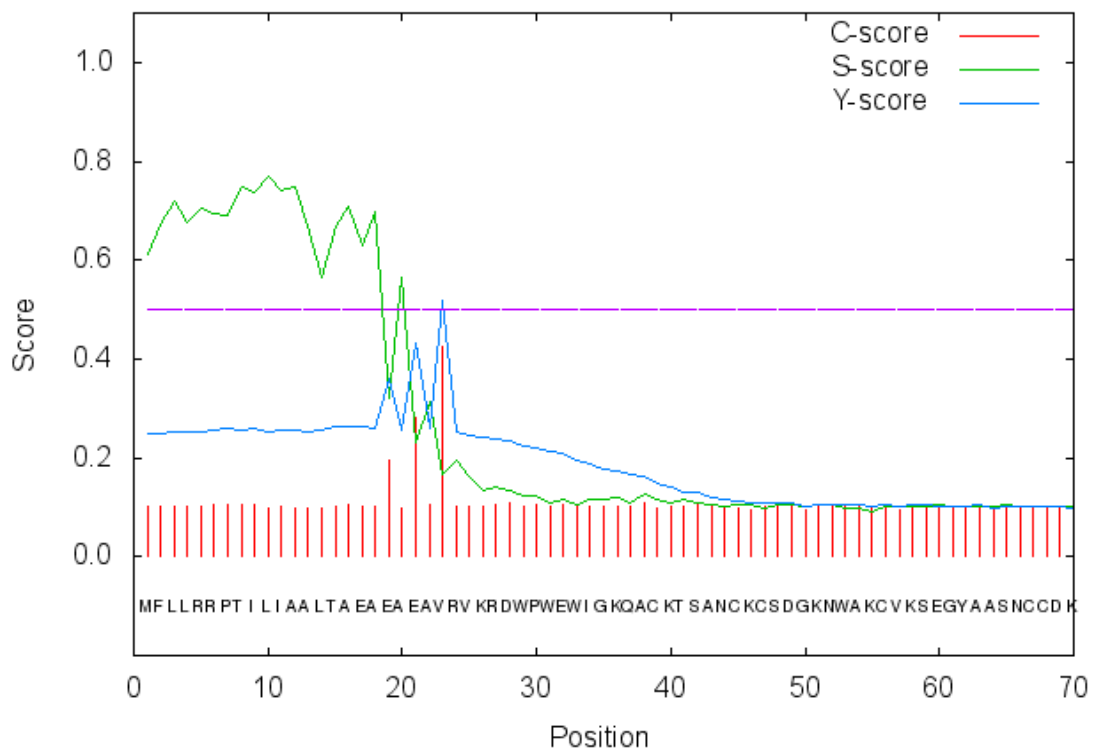
Figure 3.16 GP11840 sequence alignments. The amino acid sequences corresponding to the cloned genes were largely similar to the predicted protein sequence, with a mismatched region in the centre and an additional 83 amino acids at the C-terminus. The serine/threonine-protein kinase active site is highlighted in yellow.

GP11984pred	MVQYKLYYFDLRGIGEPiRLLHLYVGQQFEDVRFGKEEWPtKYKSKFFYgKAPVLEVDGK	60
GP02405seq	MVQYKLYYFDLRGIGEPiRLLHLYVGQQFEDVRFGMEEWPtKYKSKFFYgKAPVLEVDGK *****	60
GP11984pred	QLGQSTTiLRFLAEKfALAGKDEWEKAKADEiINFQKDANTEfAPYiFAKLGFREGDLdK	120
GP02405seq	QLGQSSViLRFLAEKfALAGKDEWEKAKADEiINFQKDANTElAPYLYTKLG----DREK *****:*****:***:*** * :*	116
GP11984pred	LRTEVLEPGVKRiFPLFEALLKESGSDYMLPSGLSMVDFQVGNFLYtFTKLEPDTiKAYP	180
GP02405seq	LRTEVLEPGVKRiFPLFEALLKESGSDYMLPSGLSMVDFQVGNFLYtFTKLEPDMiKAYP *****	176
GP11984pred	ELVKYVERVHALPQLQKYLQQRpQDR	206
GP02405seq	ELVKYVERVHALPQLQKYLQQRpQDR *****	202

Figure 3.17 Predicted GP11984 amino acid sequence compared with the cloned GP02405 sequence. The two sequences are similar enough that attempted amplification of the GP11984 cDNA resulted in amplification of GP02405.

GP12030seq MFLRRPTILIAALTAEEAEAEAVRVKRDWPWEWIGKQACKTSANCKSDGKNWAKCVKSE 60
 GP12030seq GYAASNCCDKNYVWACCGKKPKH 83

SignalP-4.1 prediction (euk networks): GP12030seqcDNA



#	Measure	Position	Value	Cutoff	signal peptide?
	max. C	23	0.425		
	max. Y	23	0.518		
	max. S	10	0.771		
	mean S	1-22	0.631		
	D	1-22	0.579	0.450	YES

Cleavage site between pos. 22 and 23: AEA-VR D=0.579 D-cutoff=0.450

Figure 3.18 GP12030 sequence and signal peptide prediction. A 23-a.a. likely signal peptide was identified with SignalP4.1 software (Petersen et al., 2011).

3.4.5 Quantification of expression in Dazomet-treated second-stage juveniles

17 genes of interest were investigated by qPCR, to confirm their up-regulation and evaluate the fold-change values given by the RNAseq analysis – GP02984 was excluded from the analysis as no satisfactory CDS sequence could be confirmed. 12 out of 17 genes were confirmed to be significantly up-regulated in Dazomet-exposed *G. pallida* J2s (Figure 3.19). The difference between fold-change values given by RNAseq and qPCR were inconsistent across genes: RNAseq analysis overestimated up-regulation response to Dazomet exposure in most cases (Table 3.3).

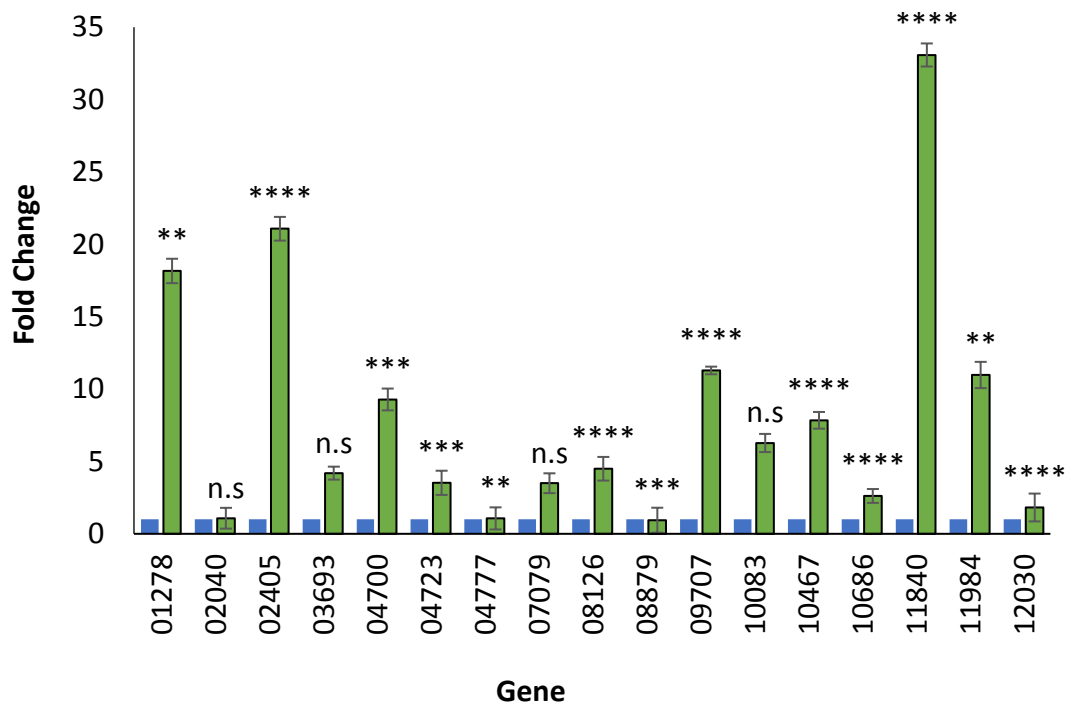


Figure 3.19 Fold change in gene expression in *G. pallida* second-stage juveniles following exposure to Dazomet. Differential gene expression was measured by qPCR comparing J2s exposed to 0.12 μ M Dazomet for 24 h with J2s incubated only with 0.5 % DMSO. The blue bars represent a fold change of 1, no change in expression. Error bars give the standard error. Significance levels are indicated by data labels above each bar: *, $P < 0.05$; **, $P < 0.01$; ***, $P < 0.001$; ****, $P < 0.0001$.

Table 3.3 Comparison of the fold changes reported by RNAseq and qPCR. Of the 17 genes measured with both techniques, RNAseq overestimated the fold-changes in expression of 14 of the genes and underestimated the fold-change of two. There was no correlation between the magnitude of the fold-change reported by RNAseq and the discrepancy between the expression changes reported by the two techniques.

Gene	RNAseq	qPCR	Ratio qPCR:RNAseq
GP01278	14.07654	18.16045	1.290122
GP02040	9.543149	1.07682	0.112837
GP02405	17.59692	21.07513	1.19766
GP03693	5.518074	4.192492	0.759774
GP04700	12.78629	9.281929	0.725928
GP04723	14.11655	3.52291	0.249559
GP04777	8.529677	1.063041	0.124629
GP07079	9.336028	3.495806	0.374443
GP08126	90.01018	4.49	0.049928
GP08879	11.7083	0.941272	0.080394
GP09707	96.10079	11.29	0.117441
GP10083	32.04867	6.27	0.19576
GP10467	12.88022	7.842178	0.608854
GP10686	10.1236	2.616015	0.258408
GP11840	27.63534	33.0807	1.197043
GP11984	62.01283	10.97279	0.176944
GP12030	16.6988	1.818418	0.108895

3.5 Discussion

3.5.1 Genes implicated in *Globodera pallida* xenobiotic metabolism

A number of genes likely involved in the detoxification of methyl isothiocyanate (as the bioactive breakdown product of Dazomet) were identified.

The principal candidates for identification as phase II xenobiotic metabolism enzymes are GP02405 and GP11984. GP2405 had strong homology to the *M. incognita gst-1* gene, which was further supported by InterPro analysis identifying the protein as belonging to the sigma class of GSTs; this coupled with its strong up-regulation in response to Dazomet suggest that GP02405 is a glutathione S-transferase, congruent with the idea that GSTs are the principal breakdown route of ITCs (Jiao et al., 1996, Jones et al., 2013b, Kolm et al., 1995, Øverby et al., 2015, Zhang, 2000). GP11984 was strongly homologous to GP02405, such that amplification of the CDS proved difficult, suggesting the possibility of errant duplication of GP02405 in the genome assembly. However, qPCR primers designed for GP11984 resulted in a differential fold change in expression in response to Dazomet, indicating that it may exist as a paralogue of GP2405 with a similar role.

Identification of GP09707 as a methyltransferase could imply a role in xenobiotic metabolism, however the presence of an S-adenosylmethionine binding site and its homology to *C. elegans* phosphoethanolamine methyltransferase 2 (PMT-2) indicate that it is more likely involved in phosphocholine biosynthesis (Palavalli et al., 2006). *C. elegans* with PMT-2 production suppressed by RNAi are unviable, due to the essential role the enzyme plays in phospholipid membrane maintenance (Palavalli et al., 2006). A host defence-suppressive role for PMT was identified in filarial nematodes, in which phosphocholine was conjugated to proteins to be secreted into the host (Lovell et al., 2007). As phosphocholine biosynthesis is essential to proper cell function and division, PMTs have been investigated as potential drug targets for control of nematodes, though the targeting of plant-parasitic nematode PMTs has not been studied directly (Bobenchik et al., 2011). Any future development of PMTs as a control target in PPN would depend on sufficient divergence of the *pmt* genes of target nematodes with other soil organisms and humans, to ensure biosafety. As a putative S-adenosylmethionine synthetase, GP04700 is likely involved in producing the substrate for PMTs (Markham

and Pajares, 2009); it is logical that up-regulation of an S-adenosylmethionine-dependent methyltransferase would be accompanied by a similar up-regulation of an S-adenosylmethionin synthetase, as well as other enzymes involved in the phosphocholine synthase pathway. The up-regulation of PMT in response to cytotoxic isothiocyanates could be related to the roles of PMTs in signalling or modulation of gene expression (Bobenchik et al., 2011), or simply as a mechanism for repairing damaged phospholipid membranes.

GP03693, identified as a carboxylesterase, could play a role in phase I xenobiotic metabolism. Carboxylesterases have a range of catalytic activities, principally cleavage of carboxyesters (RCOOR') into their constituent carboxylic acids and alcohols (RCOOH and R'OH) but also including esterification and hydrolysis reactions with a wide substrate range (Aranda et al., 2014). The potential role of carboxylesterases in xenobiotic metabolism is considered overlooked in comparison to CYPs (Laizure et al., 2013).

Identification of GP01278 as a putative tyrosine aminotransferase (TAT) does not suggest a role in xenobiotic metabolism, as TATs form part of the breakdown pathway for tyrosine (Mehere et al., 2010). However, studies on *C. elegans* TAT identified a role for tyrosine and tyrosine breakdown products in cell-signalling (Ferguson et al., 2013), such that indicators of cell damage could be communicated to neighbouring cells via metabolism of TAT.

The proteins likely encoded by GP07079, GP08126 and GP12030 were identified as potential effectors, based on sequence homology and presence of signal peptides. While poor sequence homology prevents identification of putative roles for the genes, production of effectors in response to what could be host defence compounds is congruent with the role of many effectors in suppression of host defence (Quentin et al., 2013). The cellular stress caused by Dazomet-exposure could be interpreted by *G. pallida* as the stress induced by contact with the host's defences. Similarly, in response to general stress, GP10686 encodes a protein involved in sugar metabolism. If stress is associated with entry into the host tissues, up-regulation of genes GP10686 could aid in energy metabolism and prepare the parasite for contact with the food source. GP11840, encoding a serine/threonine kinase, could have multiple roles in response both to biotic stress and to contact with a host plant. Serine/threonine kinases

are implicated in a number of signal transduction pathways (Motley and Lory, 1999). Further investigation of GP11840 could elucidate a role in signalling and activation of xenobiotic metabolism, especially given its high up-regulatory response to Dazomet. GP10083 is a putative sodium/nucleoside transporter, implied by sequence homology and prediction of several transmembrane domains. These are concentrative co-transporters that import nucleosides in an energy dependent manner, and are implicated in facilitation of intracellular signalling, as nucleosides are recruited as important signal molecules (Parkinson et al., 2011).

Metalloproteases, as encoded by GP10467, are typically involved in protein processing within the cell, cleaving specific C-terminal residues from nascent proteins to allow proper folding and functionality (Gomis-Ruth, 2008). The increase in expression of GP10467 could therefore indicate a role in post-translational modification of proteins involved either in xenobiotic metabolism or in repairing cellular damage.

Of the examined genes, three were found to have no change in expression when measured with qPCR: GP02040, GP04777 and GP08879. Cysteine/methionine metabolism-related pyridoxal transferases, as encoded by GP02040, are involved in the biosynthesis of cysteine from methionine, and as such contribute to amino acid and protein turnover in the cell (Noji and Saito, 2003). Lipocalin and lipocalin-related proteins (GP04777) are extracellular enzymes typically involved in intracellular signalling (Flower, 1996). GP08879 appears to be a malonate decarboxylase enzyme subunit, which forms part of a complex that catalyses the turnover of malonate to acetate (Chohnan et al., 1998); interestingly, the sequence has strongest homology to genes of bacterial origin, possibly indicating incorporation into the nematode genome through horizontal transfer, as identified for a number of genes present in the genomes of *Globodera* and *Heterodera* species (Danchin et al., 2016, Danchin et al., 2010, Noon and Baum, 2016). The likely roles of these proteins and their apparent lack of up-regulation when checked with qPCR indicated that they are unlikely to be directly involved in xenobiotic metabolism.

3.5.2 Identification of genes through exposure to known xenobiotics

The approach taken in this chapter has been to expose a plant-parasitic nematode to a known toxin that mimics the activity of biofumigation, in an effort to identify genes

involved in defence against that toxin. Elucidation of the mechanisms by which *G. pallida* detoxifies isothiocyanates is important towards fully understanding how biofumigation affects nematodes in the soil. Additionally, by subjecting nematodes to a specific stressor, genes involved in important biological processes, that may be crucial to survival of the parasite in the host environment, can be identified and designated as potential targets for control.

Further study of the genes identified in this chapter could focus on knockdown of the genes by RNAi, to assess what impact this has on viability and parasitism. Investigation of the regulation of these genes through a system such as a yeast 1-hybrid assay (ref) could elucidate the transcription factors associated with the activation of xenobiotic metabolism in *G. pallida*, which could then be investigated as potential targets for control.

3.5.3 Potential for RNAi-based control of *G. pallida*

As discussed in the introduction to this chapter, RNAi has good potential for providing target-specific control localised to the point of contact that the parasite has with the plant host. Of the genes analysed here, those with the greatest potential for control of *G. pallida* as delivered by plant roots are the putative GSTs GP02405 and GP11984, due to their role in detoxification, the PMT GP09707, due to its essential role in cell maintenance, and the putative effectors, GP07079, GP08126, and GP12030. By disrupting either the defences of the parasite, its basic cellular processes, or the methods by which it communicates with and manipulates its host, the maintenance of the host-parasite interaction could be detrimentally perturbed.

3.5.4 Differences in fold-change observed from RNAseq and qPCR data

The fold changes observed in genes when analysed by qPCR differed greatly from those identified by RNAseq, with most of the observed genes having a reduced up-regulatory response relative to the RNAseq data. This could be due to differences in sensitivity and specificity between the two protocols (ref), and highlights the need to validate observations gleaned from one method before biological significance can be conferred to the result.

3.5.5 Conclusions

Analysis of gene regulation in response to exposure to xenobiotic compounds has been identified as a method for investigating the xenobiotic metabolism response of plant-parasitic nematodes to known stressors. A number of genes elucidated in this study were predicted to have important roles, in direct detoxification of the applied xenobiotics, to essential cellular processes, and also in more general response to biotic stress. Investigation of gene expression modulation in response to xenobiotic compounds is therefore posited as a potential tool for the identification of novel control targets for important agricultural pests. This framework can be applied to other plant and animal parasites.

3.6 Summary

-
- A number of genes implicated in *G. pallida* were identified by RNAseq analysis and analysis of sequence data.
 - Strong candidates for glutathione S-transferases involved in detoxification of isothiocyanates in *G. pallida* were identified, GP02405 and GP11984.
 - Investigation of changes in gene regulation in response to biotic stress is revealed as a useful tool for the elucidation of genes involved in xenobiotic metabolism.
 - Future work targeting the regulation of genes identified here could provide novel methods of control of potato cyst nematodes.
-

4 Utilising *C. elegans* reporter lines to identify xenobiotic activity in plants

4.1 Introduction

Biofumigation as an agricultural practice is associated with the use of brassicas, and frequently centres on the use of a small subset of plants of the brassicaceae, typically cultivars of those already used in agriculture such as *Brassica juncea*, *B. oleracea* or *Sinapis alba* (Aires et al., 2009, McSorley, 2011, Meyer et al., 2011). The effectiveness of each tested cultivar varies, however, as demonstrated by the great variation in biofumigation efficacy observed in the literature (see Chapter 1.3.5 for review). Among the Brassicaceae, the glucosinolate profile and leaf concentration may vary considerably between species and cultivars (Fahey et al., 2001). Outside of the brassicas, a number of plant species are purported to have nematicidal effects, including marigolds, *Tagetes* spp. (Ploeg, 2002), and lupins, *Lupinus* spp. (Yildiz, 2011). Given the time, effort, and cost associated with testing the ability of green manures to suppress plant-parasitic nematodes, development of a simple method to assess the potential of a plant to act as a biofumigant would allow for the rapid screening of various plant accessions for their biofumigation potential. A quick, affordable assessment of biofumigation potential could hasten and reduce wastage in the process of trialling crop species for biofumigation.

Caenorhabditis elegans is a nematode model organism for which a broad range of research techniques is available, and was the first multicellular organism to have a full genome published (The *C. elegans* Sequencing Consortium, 1998). Study of *C. elegans* as a model organism for metazoan development and neurobiology has continued since it first began in the 1960s (Ankeny, 2001), and a number of techniques developed through this process have had far-reaching outcomes for biological research, such as the use of green fluorescent protein (GFP) as a marker for biological processes in animal models (Chalfie et al., 1994). The up-regulation of genes implicated in specific stress responses can be used as an indicator of particular stimuli: by generating transgenic nematodes with markers, such as GFP, under the control of promoters associated with such responses, their activation can be quickly visualised. This has been used to indicate

toxic levels of heavy metals for monitoring of environmental hazards (Wah Chu and Chow, 2002), and combined with RNAi to investigate the regulatory processes associated with activation of genes implicated in xenobiotic metabolism (Jones et al., 2013b).

Reporter organisms that respond to stimuli associated with biofumigation, such as the presence of bioactive isothiocyanates, can be used as a marker for biofumigant activity. A number of reporter lines generated previously in the lab have the potential to be used in this manner, in particular a *gfp::gst-31* line that produces GFP when induced by Dazomet, a methyl isothiocyanate liberator (Jones et al., 2013b). *Gst-31* encodes a glutathione S-transferase (GST) enzyme – as discussed in Chapter 3, GSTs are the principal route by which isothiocyanates are detoxified in a eukaryotic cell (Shapiro et al., 2001). The response of ITC-specific reporter lines to exposure to a given plant extract can therefore be used as an indicator of the presence or absence of ITCs in that extract. However, given the differential response of different nematode species both to biofumigants and to specific isothiocyanates (see Chapter 1.3.5), the inferences that can be drawn from *C. elegans* reporters to other species are limited. Methodologies that incorporate both the test species and *C. elegans* have been demonstrated in the past, with the roles of *Globodera spp.* heat shock proteins investigated alongside their equivalents in *C. elegans* (Jones et al., 2018b). Where an experiment requires a tractable model organism such as *C. elegans*, efforts must be made to bridge the gap between the model and the species of interest.

With transgenic model organisms, it is possible to incorporate genes and their regulatory elements from a test species into a model system for which there are more techniques available for investigation of their functions. Transcription factor binding for homologous genes is frequently conserved across distantly related species, such that the expression profile of a gene in one species can be inferred from expression of a homologous gene in another (Hemberg and Kreiman, 2011). Transgenic *C. elegans* carrying reporter genes under control of promoters for genes implicated in *G. pallida* xenobiotic metabolism may therefore act as reporters for potato cyst nematode-specific responses to stresses. Development of such a tool would also allow for investigation of

the regulatory apparatus associated with those genes, as demonstrated with RNAi performed on reporters for *C. elegans* xenobiotic metabolism (Jones et al., 2013b).

Further to generating *C. elegans* lines carrying genetic material from species such as *G. pallida*, it would be preferable to develop tools for direct study of plant-parasitic nematodes. Model organisms are studied in place of species of interest due to experimental tractability and the availability of forward- and reverse-genetic techniques (Ankeny and Leonelli, 2011). *Caenorhabditis elegans* is a convenient model system, well-suited to *in vitro* study, and has been studied at the forefront of both research into nematodes and into animal life more broadly (Ankeny, 2001). However, there are drawbacks to focusing on model organism research: *C. elegans* is a specialised organism and is therefore divergent in many ways from the organisms it is used to study (Ankeny and Leonelli, 2011). It has been suggested that many model organisms may become obsolete within 30 years, as the sophistication of molecular biological techniques advances (Hunter, 2008); therefore, the organism of interest should be studied directly whenever possible. Attempts to generate transgenic plant-parasitic nematodes have been so far unsuccessful. One advantage of *C. elegans* is that the majority of its reproduction is through hermaphroditic self-fertilisation – stable transgenic lines can therefore be established from a single transgenic individual. *Globodera* spp. are ill-suited to transgenesis as they reproduce sexually and have a lengthy life cycle requiring both a suitable host and a long period of dormancy (see Chapter 1.2.4). The related Southern root-knot nematode *Meloidogyne incognita*, may prove to be a better candidate for transformation: *M. incognita* reproduces through apomictic parthenogenesis, resulting in clonal offspring (Trudgill and Blok, 2001) – any successfully transformed individual should then also have the potential to produce a clonal transgenic line. The broad host range of *M. incognita* (Trudgill, 1997) would also be of benefit, as transgenic individuals could be used to infect transgenic host plants, allowing for investigation of specific interactions between parasite and host. It could therefore be of merit to attempt to generate transgenic *Meloidogyne incognita* to advance the study of plant-parasitic nematodes.

4.2 Aims

1. Investigate the use of transgenic *Caenorhabditis elegans* reporter lines as indicators of potential biofumigant activity.
2. Develop transformation vectors and attempt to generate transgenic *C. elegans* lines expressing fluorescent proteins under control of promoters implicated in *Globodera pallida* xenobiotic metabolism.
3. Attempt to transform *Meloidogyne incognita*, potentially leading to the development of a new model system.

4.3 Materials & methods

4.3.1 Source of reporter lines

The *C. elegans* reporter line *gst-31::gfp* was obtained from Dr Laura M Jones (Jones et al., 2013b). Nematodes were maintained according to the methods set out in Chapter 2.2.

4.3.2 Toxicity of isothiocyanates to *C. elegans*

To determine the range of isothiocyanate concentrations at which up-regulation of GFP would occur in reporter lines, toxicity tests were performed. For each concentration, wells in a 96-well plate were set up in triplicate each containing 50-100 adult *C. elegans* N2 in 200 μ l sterile M9 buffer. Nematodes were exposed to concentrations of 500 μ M, 100 μ M, 50 μ M and 10 μ M of a number of isothiocyanates and Dazomet in DMSO over a 16h time period, and the number of active nematodes counted to give a percentage viability score; DMSO-only and non-treatment controls were performed alongside chemical exposures. The concentrations chosen were based on the concentration of Dazomet that elicited an up-regulatory response in *gst-31::gfp* reporters (Jones et al., 2013b). Table 4.1 gives the isothiocyanates used in chemical exposures throughout this chapter, with their chemical structures and respective sources.

4.3.3 Reporter line chemical exposures

Reporter nematodes (*gst-31::gfp* reporters and those transformed lines generated as in method 4.3.10) were exposed to 10 μ M allyl isothiocyanate and 10 μ M Dazomet as above, and fluorescence measured after 1 h, 2 h, 4 h, 8 h and 16 h. Subsequent exposures were performed with a full range of isothiocyanates (Table 4.1) over 16 h, after which nematodes were imaged and fluorescence intensity calculated. To compare the fluorescence induced by methyl isothiocyanate and Dazomet, reporters exposed to a 10-fold dilution series (from 0.1 μ M to 1 mM, based on observed toxicities) over 16 h were imaged and fluorescence quantified.

4.3.4 Imaging fluorescent nematodes

Nematodes were mounted on glass microscope slides with an agar pad. A 5% agar solution was autoclaved, to which sodium azide was added to give a final concentration of 10 mM. A drop of this solution was pipetted onto a clean glass slide and pressed down

with a second glass slide to give an agar pad approximately 0.4 mm thick. These pads were used soon after being made, to prevent drying. Nematodes to be imaged were removed from the 96-well plate into 0.6 ml maximum recovery microcentrifuge tubes and placed on ice for 5 minutes to settle. A 10 µl aliquot was then pipetted from the bottom of the tube onto an agar pad, and a glass coverslip was placed over this. Slides were viewed on a Leica DMRB microscope (Leica, Germany) illuminated by a mercury vapour bulb and images were captured using a QImaging QICAM Fast 1394 CCD and QCapture software.

4.3.5 Quantification of GFP response

Images were analysed using FIJI, an ImageJ package (Schindelin et al., 2012, Schneider et al., 2012). To quantify GFP response, the body of an individual nematode was isolated using the 'Freehand selections' tool and the pixel intensity measured. The average pixel intensity for the nematode was used as a measure of the level of fluorescence due to GFP, and the value from a number of nematodes from each treatment was averaged to give a representative figure.

4.3.6 Generating leaf extracts

Leaf extracts were generated according to a method used previously in the lab (Lord et al., 2011). Tomato (*Solanum lycopersicum*), cotton (*Gossypium hisutum*), wheat (*Triticum aestivum*), Indian mustard (*Brassica juncea*), white mustard (*Sinapis alba*), dog mustard (*Erucastrum gallicum*), and shield mustard (*Biscutella didyma*) were grown for 6-8 weeks in compost, in 20 °C green houses with watering three times per week, before sampling. From each plant, 3-5 leaves were taken and immediately snap-frozen in liquid nitrogen. Samples were kept at -80 °C before being freeze-dried in a vacuum chamber. Each sample was then ground with a mortar and pestle to a fine powder. To produce the extract, 30 mg of tissue powder was then transferred to a 15 ml centrifuge tube containing 15 ml sterile tap water, which was then incubated at 37 °C and 200 rpm on a rotary incubator for 200 min. Extracts were then sterilised by filtration through a 0.22 µm syringe filter to remove insoluble tissue debris. This resulted in a 2 mg/ml leaf tissue extract that could then be stored at -20 °C for later use.

4.3.7 Plant tissue extract exposures

Reporter nematodes were exposed to plant tissue extracts over a period of 16 h. 50-100 adult *C. elegans* *gst-31::gfp* reporters were added to wells of a 96-well plate in 20 μ l M9 buffer, to which was added 180 μ l of plant tissue extract. After incubation for 16 h in the dark at 20 °C, nematodes were mounted on slides and imaged as above.

4.3.8 Generation of transformation vectors for nematode bombardment

For transformation of *C. elegans* *unc-119* mutants, the pJM119 vector backbone (Figure 4.1) was used. This had been developed by Dr Jess Marvin from the pPD95_75 vector (Figure 4.2) by insertion of a *C. briggsae* *unc-119* sequence that acts as a rescue gene (pPD95_75 was a gift from Andrew Fire (Addgene plasmid # 1494)). The rescue gene acts to restore mutant nematodes to wild-type phenotype. Vector maps were generated using ApE (A plasmid Editor, M. Wayne Davis, 2018). The *unc-119* gene from *C. briggsae* completely rescues *unc-119* phenotype *C. elegans* (Maduro and Pilgrim, 1996), and is used preferentially to the native gene in transformation vectors as it is more compact (Maduro, 2015). Promoter regions from *G. pallida* genes of interest identified in Chapter 3 were cloned using primers designed to amplify the region 1-3 kb upstream of each gene's predicted start codon. Primers were designed to fit the criteria of being at least 18 nt in length, having T_m 60 ± 4 °C and GC content ≥ 35 %, after which appropriate restriction sites were added to the 5' end of each primer with 4 random bases upstream of this (Table 4.1). Where possible, the reverse complement primer was designed with an MscI restriction site rather than a KpnI site, to preserve the artificial intron present upstream of the GFP sequence. Primers were checked with BLAST to ensure specificity to the desired region. Following amplification of the target region, double restriction digests were set up of both the insert and the pJM119 vector, digesting a molar ratio of at least 3:1 insert:vector. Digests were performed in a 50 μ l reaction volume, using restriction enzymes from New England BioLabs, as follows:

50.0 μl Total reaction volume

5.0 μl CutSmart[®] buffer

x μl 5' restriction enzyme (to give 20 U)

y μl 3' restriction enzyme (20 U)

z μl DNA > 1 mg

(45- x - y - z) μl Sterile water

Following the restriction digest, agarose gel electrophoresis was performed with the digested vector, in order to separate the backbone from the fragment to be replaced by the insert, and to separate the DNA from restriction enzymes. After electrophoresis, the fragment of gel containing the band for the backbone was excised and gel extraction was performed using the EZNA[®] MicroElute Gel Extraction kit (Omega Bio-Tek, D6294). The insert DNA reaction volume was heated to 95 °C for 30 min to heat inactivate the restriction enzymes.

Ligation reactions were performed with T4 DNA ligase (New England BioLabs, M0202):

10.0 μl Total reaction volume

1.0 μl CutSmart[®] buffer

x μl Vector DNA (>100 ng)

y μl Insert DNA ($\geq 3x$ molar mass of vector)

0.5 μl T4 DNA ligase

(8.5- x - y) μl Sterile water

The reaction volume was incubated at 16 °C overnight to allow complete ligation. An aliquot of 5 μl of the ligation mixture was added to 50 μl ultra-competent *E. coli* DH5 α (Method 2.4.1) and the cells were spread on LB-Agar plates with 100 $\mu\text{g}/\text{ml}$ carbenicillin. After overnight incubation at 37 °C, colony PCR was performed to identify colonies that carried the vector with the desired insert (Method 2.4.7), using an insert-specific forward primer and the GFP frame check reverse primer (Table 4.1).

Inserting fragments into the pPDmCh vector was performed in the same manner, utilising appropriate restriction site (Figure 4.2) and the mCherry frame check reverse primer for colony PCR.

Promoter regions were amplified using Phusion High-Fidelity DNA Polymerase (New England BioLabs, M0530) as per Method 2.4.6.

Restriction digests were performed simultaneously, using the enzymes appropriate to the primer pair and the desired insertion site in the vector.

The vector pPDmCh was generated by cloning the mCherry sequence from pBCN22 (a gift from Ben Lehner (Addgene plasmid # 26302) (Semple et al., 2010)) with added restriction sites and inserting the fragment into the pPD95_75 (Fire, 1995) backbone with the GFP sequence removed

4.3.9 Preparation of vector for transformation of nematodes

Gold beads were first prepared for the binding of DNA by suspending 30 mg 0.3-3.0 μm gold particles (Chempur, Karlsruhe, Germany) in 1 ml sterile 70 % ethanol in a sterile 1.6 ml microcentrifuge tube, then mixing at 1800 rpm for 5 min in an Eppendorf MixMate vortex mixer. The particles were then left to settle for 15 min, centrifuged briefly to pellet, and the supernatant removed by pipette. The pellet was then re-suspended in 1 ml 70 % ethanol, vortexed at 1800 rpm for 1 min, settled for 1 min, then centrifuged briefly to pellet. The supernatant was then removed and the process repeated a further two times. After the final removal of the supernatant, the particles were re-suspended in 500 μl sterile 50 % glycerol. Gold particles prepared in this way could be stored at 4 °C for up to 2 months.

The transformation plasmid was linearised before binding to the gold particles. A 35 μl restriction digest was prepared, with 2.5 μl restriction enzyme (appropriate to the plasmid to be linearised), 3.5 μl 10X digest buffer (appropriate to the enzyme), x μl plasmid DNA (where x is a volume that give ~ 7 μg total plasmid DNA) and $(29 - x)$ μl ddH₂O; this was incubated at 37 °C for 2 h. Before binding, the gold particles were re-suspended by vortexing at 1800 rpm for 20 min. For each bombardment, 70 μl gold particles in glycerol were added to a 1.6 ml maximum recovery microcentrifuge tube, kept on the vortex mixer to prevent settling. 30 μl of the digested plasmid was

added to the gold suspension after which two separate aliquots of 150 μ l 2.5 M CaCl₂ and an aliquot of 112 μ l spermidine were added, drop-wise, to each tube. Each tube was vortexed at 1800 rpm for 5 min to ensure even coating of the gold beads, then briefly centrifuged to form a pellet. The supernatant was removed and the gold re-suspended in 800 μ l 70 % ethanol, then pelleted once more, and re-suspended in 70 μ l absolute ethanol. The gold was then kept in suspension on the vortex mixer.

4.3.10 Bombardment protocol

C. elegans were grown in 50 ml liquid culture (according to Method 2.2) until they reached a population density of approximately 1000 young adult nematodes per millilitre. For transformation with a rescue plasmid, *unc-119* mutant nematodes were grown. Each culture was poured into a sterile 50 ml centrifuge tube and set in a rack, allowing the nematodes to settle for 10 min at room temperature. The juvenile nematodes remain in suspension while the young adults settle out. The supernatant was then poured into a second 50 ml centrifuge tube and placed on ice; after settling for 20 min the settled worms could be used to seed a new liquid culture.

The system used for bombardment was the PDS-1000/HE Biolistic[®] Particle Delivery System (Bio-Rad) with Hepta[™] Adaptor (Bio-Rad). The procedure was performed in a laminar flow hood, and all equipment was sterilised with 70 % ethanol where not otherwise specified. For each bombardment, approximately half of the total volume of settled young adult *C. elegans* from a single 50 ml culture was distributed evenly between seven target regions on a 9 cm NGM-lite plate, seeded with *E. coli* HT115.

DNA-coated gold beads were applied evenly between seven macrocarrier discs (Bio-Rad), which had been cleaned by immersion in isopropanol and allowed to dry beforehand. After the gold had dried, the macrocarrier discs were inserted into the macrocarrier holder with the stopping screen and this was placed in the microcarrier launch assembly. A rupture disc (1350 psi, Bio-Rad) was briefly immersed in isopropanol and inserted into the retaining cap of the Hepta[™] Adaptor, which was then screwed into place in the bombardment chamber. The microcarrier launch assembly was then put into place, and rotated so that the openings in the holder aligned with the openings in the Hepta[™] Adaptor. The plate with *C. elegans* young adults was then placed in the chamber on the target shelf, aligning the seven patches of *C. elegans* with the

macrocarrier discs and the adaptor. The lid of the *C. elegans* plate was then removed. The chamber was sealed and evacuated to 27 inHg, and the bombardment was fired. Plates were checked for evidence of the delivery of the gold beads and 1 ml sterile M9 buffer was added, to rehydrate the nematodes. After resting for 30 min, 4 ml M9 buffer was added to each plate, and the resulting suspension of nematodes distributed across 8 seeded 9 cm NGM-lite plates.

4.3.11 Selection of positive transformants

In the case of *unc-119* mutants, transformants were selected based on the rescue of the *unc-119* phenotype. This could either be performed by identifying rescued individuals and picking them individually onto fresh, seeded NGM-lite plates, or by allowing plates to starve for 4-5 weeks following bombardment, after which rescued worms will enter into the dauer stage, and placing a chunk of NGM-lite taken from a separate seeded plate onto the starved plate. Rescued nematodes will exit dauer arrest and move onto the chunk of seeded media, from which they can be picked individually onto fresh seeded plates. These plates were then monitored for the presence of nematodes that reverted to the *unc-119* mutant phenotype, as this indicates that the line of transformants is not stable. Stable transformants were kept and non-stable transformants discarded.

4.3.12 Double plasmid bombardment protocol

A protocol was developed for transformation of wild-type *C. elegans*, and for selection of transformants in the absence of an obvious differential phenotype. For this, a pair of transformation plasmids were used in each bombardment. A plasmid expressing red fluorescent protein (RFP) under the control of promoter of the constitutively expressed *myo-2* gene was developed and named pPDmCh, designed to act as a marker for selection of transformed nematodes.

4.3.13 Data analysis

One-way ANOVA with post-hoc Student-Newman-Keuls analyses were used to determine the significance of groupings in Figures 4.4 and 4.7, based on a confidence level of $P < 0.05$.

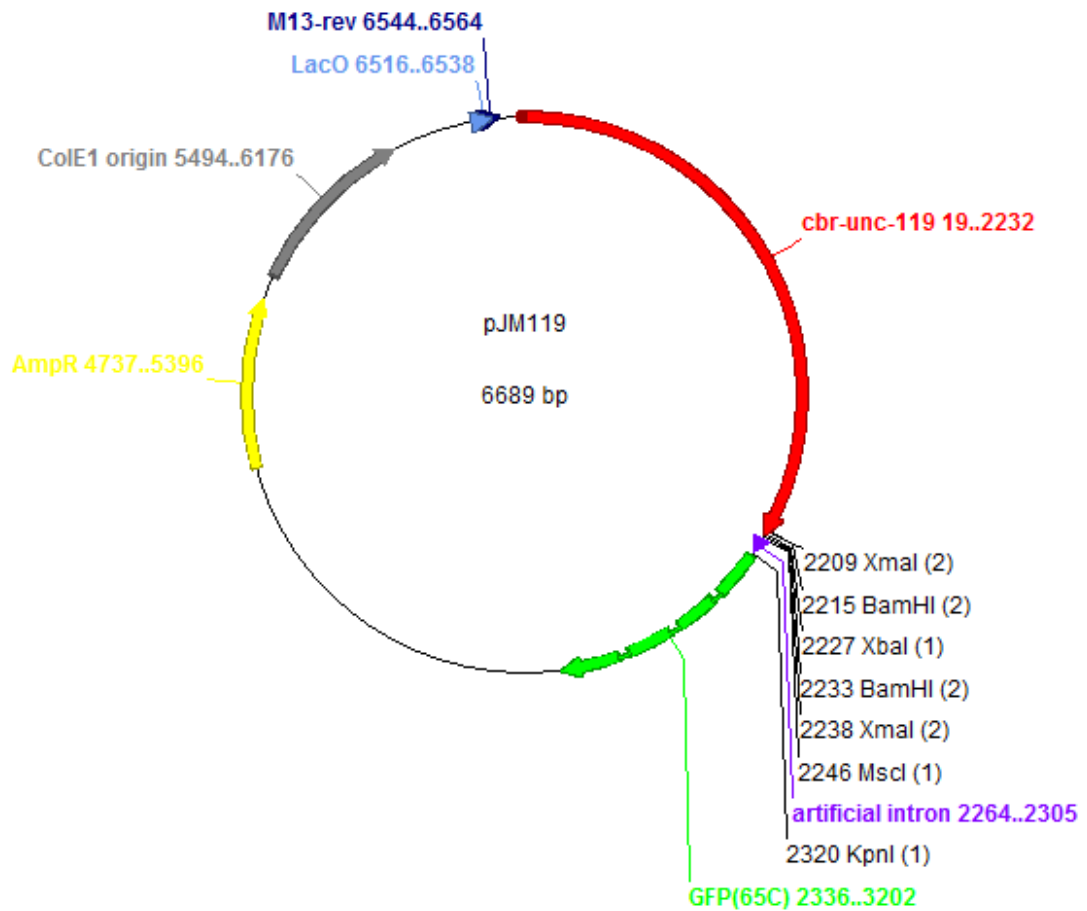


Figure 4.1 Annotated schematic of the pJM119 vector backbone with restriction sites in the multiple cloning site highlighted. The vector conveys resistance to ampicillin and carbenicillin, allowing for growth of transformed bacteria on selective media. The *Cbr-unc-119* gene rescues *C. elegans unc-119* mutants, allowing for phenotypic selection of transgenic animals. The multiple cloning site contains an artificial intron that enhances expression of GFP. The GFP sequence carries the S65C alteration, enhancing brightness relative to wild-type GFP (Reichel et al., 1996).

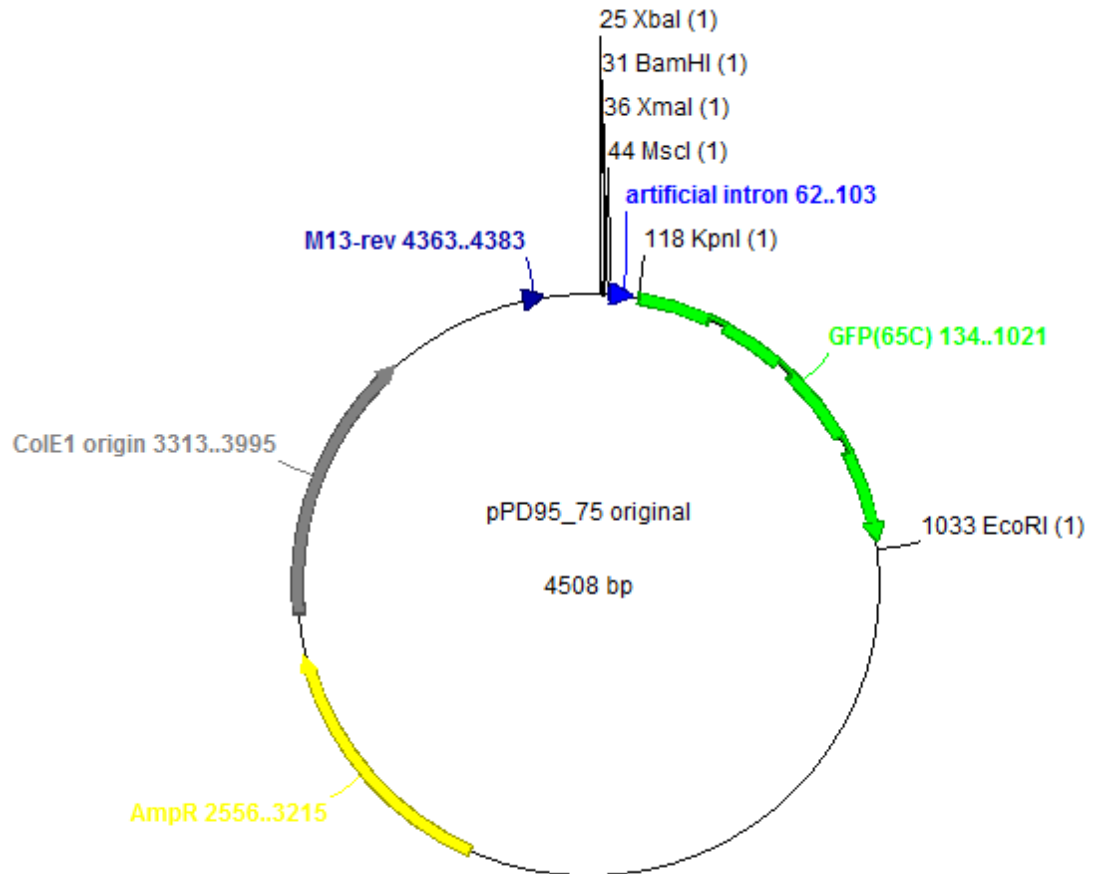


Figure 4.2 pPD95_75 vector backbone with restriction sites highlighted. The basic structure is identical to that of pJM119 without the *Cbr-unc-119* gene and with different availability of restriction sites in the multiple cloning site.

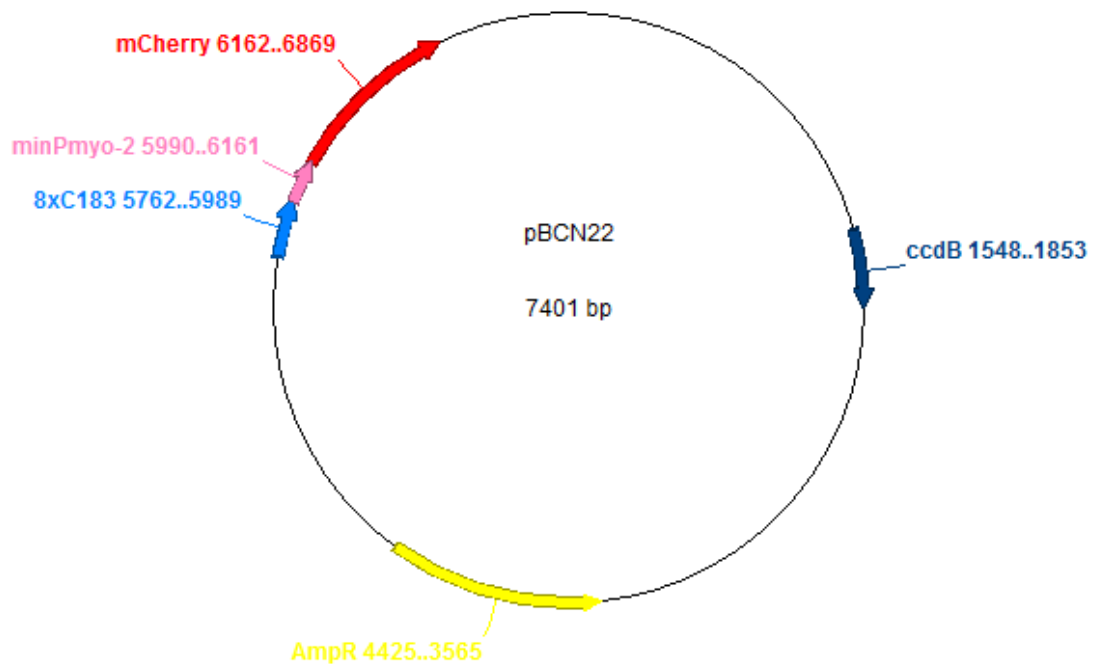


Figure 4.3 Structure of plasmid pBCN22. The plasmid carries an mCherry sequence under control of a promoter construct consisting of 8 repeats of the C183 pharynx-specific promoter enhancer upstream of a minimal *myo-2* promoter region, to drive high, pharynx-specific expression (Semple et al., 2010, Thatcher et al., 1999). The plasmid is designed for use in Gateway cloning, and the *ccdB* region acts as a negative selection element for bacterial cells transformed with the plasmid without the desired insert. The *ccdB* region encodes a toxin that kills cells by interacting with DNA gyrase to induce double-strand DNA breaks (Bernard, 1996, Bernard and Couturier, 1992). The plasmid was used as a source of the mCherry sequence and the *myo-2* promoter region.

Table 4.1 Isothiocyanates used in ITC-screens with *C. elegans* reporter lines

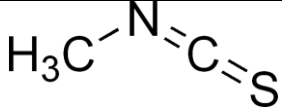
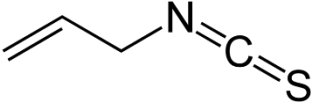
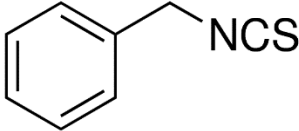
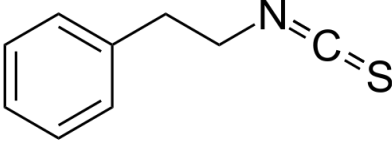
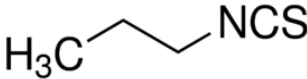
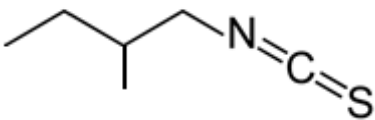
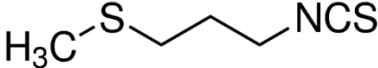
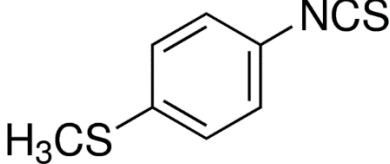
Isothiocyanate (Abbreviation)	IUPAC name	Molar mass (g mol ⁻¹)	Structure
Methyl (MITC)	Methylisothiocyanate	73.12	
Allyl (AITC)	3-isothiocyanato-1-propene	99.15	
Benzyl (BITC)	Isothiocyanatomethylbenzene	149.21	
Phenethyl (PhITC)	(2-isothiocyanatoethyl)benzene	163.24	
Propyl (PrITC)	1-isothiocyanatopropane	101.17	
2-methylbutyl (2MBITC)	1-isothiocyanato-2-methylbutane	129.23	
3-(methylthio)propyl (3(MT)PITC)	1-isothiocyanato-3-(methylthio)propane	147.26	
4-(methylthio)phenyl (4(MT)PITC)	1-isothiocyanato-4-(methylsulfanyl)benzene	181.28	
Sources: ^a , Sigma-Aldrich, MO, USA; ^b , Alfa Aesar MA, USA; ^c , Fluorochem, UK.			

Table 4.2 Primers used for generating and checking promoter constructs

Primer	Sequence 5'-3'
mCherryframechkR	TCGCCCTTGCTCACCAT
GFPframechkR	GAAAAGTTCTTCTCCTTTACTCAT
GP02405promoterF	TCTCAAATCTCATATCCGCG
GP02405promoterR	GACCATTTTGGATATTGATTG
GP03693promoterF	CGAGCATATCGTCCGTTG
GP03693promoterR	CAATTTTGGTGCCATAATGAA
GP09707promoterF	CAGTCTCAGTACCGGATAGCTC
GP09707promoterR	CCGAGTTGTCTGCTCGTC
GP11840promoterF	CGATAAAGTGTTTATTGAGGAGG
GP11840promoterR	AGGCAAAATCCGTAGTTAATCC
GP11984promoterF	CAACTCGTTTGCGCCTCC
GP11984promoterR	TGTTGCAATAAAGCAACTCG
GpGAPDHpromoterF	AACTCGGAAGTCGGAATTACC
GpGAPDHpromoterR	TTTTGCTATGTTTAGCAGGAAAAT
CeminPmyo-2BamHiF	ATATGGATCCGATATCGAATTCCTGCAGGC
CeminPmyo-2HindIII R	ATATAAGCTTGGTCGAGGGTTAAAATGAAAAGT
CeGST31promoterF	ATTAGTTGATTGGAAGAAG
CeGST31promoterR	AGTGGTTTCACTGAAACTATAA

Where necessary to facilitate restriction digests and ligations, appropriate restriction sites were added to the 5' end of each primer

4.4 Results

4.4.1 Toxicity of isothiocyanates to *C. elegans* N2 adults

Differential toxicity of a number of isothiocyanates was observed. The isothiocyanates with the highest activity were allyl ITC, benzyl ITC, 4-(methylthio)-phenyl ITC and methyl ITC (MITC), while all tested isothiocyanates were found to have greater bioactivity than Dazomet at concentrations $\geq 50 \mu\text{M}$ (Figure 4.4).

4.4.2 *gst-31::gfp* reporter lines

4.4.2.1 *GFP induction from exposure to Dazomet and isothiocyanates*

Reporter lines for *gst-31* exposed to Dazomet and AITC showed greatest fluorescence at 16 h exposure, after which fluorescence declined (Figure 4.5). Exposures were performed over 16 h thereafter. Dose-dependent induction of GFP was also observed, though sufficiently high MITC concentration resulted in no fluorescence, as nematodes were killed before a response could be induced (Figure 4.6). When exposed to a range of ITCs of the same concentration, differential induction of GFP was observed (Figure 4.7).

4.4.2.2 *Up-regulation of *gst-31* in response to plant leaf extracts*

Having confirmed the response of the reporter line to pure isothiocyanates, nematodes were exposed to plant tissue extracts of a range of plant leaf extracts. Response was specific to brassicaceous leaf extracts, with tomato, cotton and wheat extracts inducing no up-regulation of *gst-31* (Figure 4.8). Induction of GFP was dose-dependent, indicating that the intensity of fluorescence observed may be indicative of the isothiocyanate concentration of the extract and therefore glucosinolate content of the extract (Figure 4.9). Differential responses to leaf extracts of the same concentration from different brassicas could therefore be indicative of the total glucosinolate content of the leaves of tested plants.

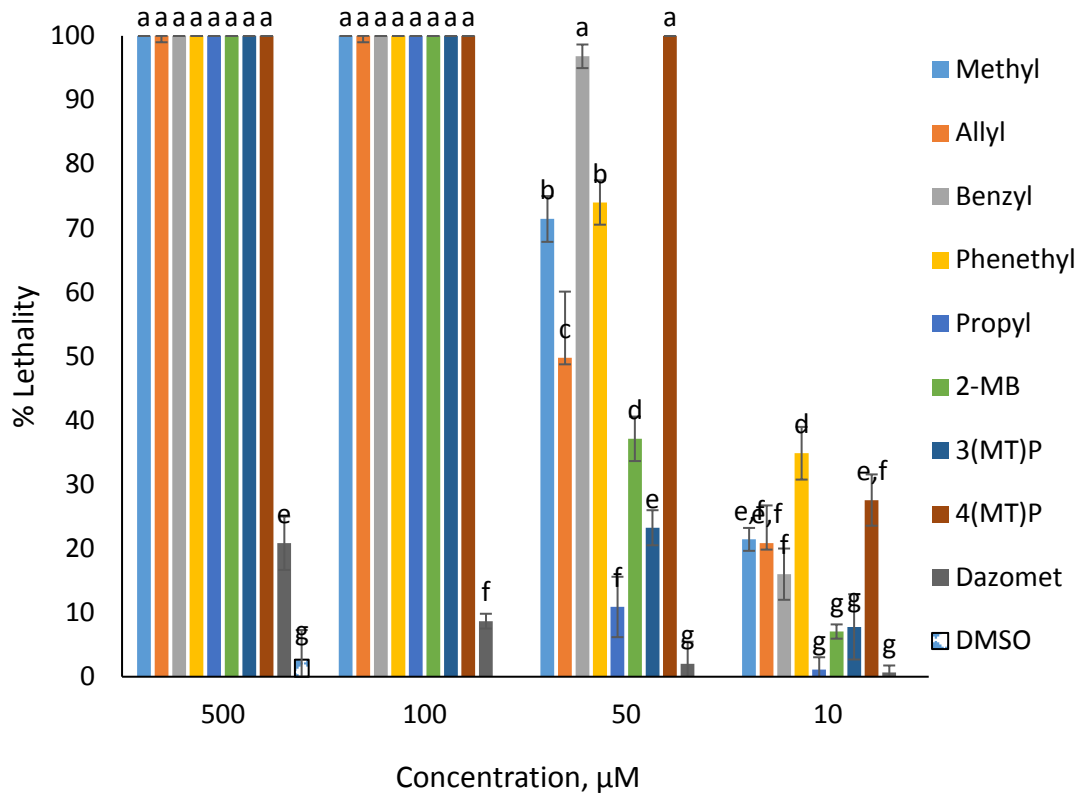


Figure 4.4 Viability of *C. elegans* N2 adults after 16h exposure to isothiocyanates. Isothiocyanates in DMSO were added to N2 adults in M9 buffer and viability was assessed after 16h at room temperature, 150 rpm. Dazomet was included for comparison, and two control conditions of DMSO-treated and non-treated nematodes were included. No loss of viability was observed in the no-treatment control. Wells were made up in triplicate, $n = 54 \pm 8$, error bars = ± 1 SD. Letters above bars indicate groups that were not significantly different from one another; groups are based on a Student-Newman-Keuls analysis, $P \leq 0.05$

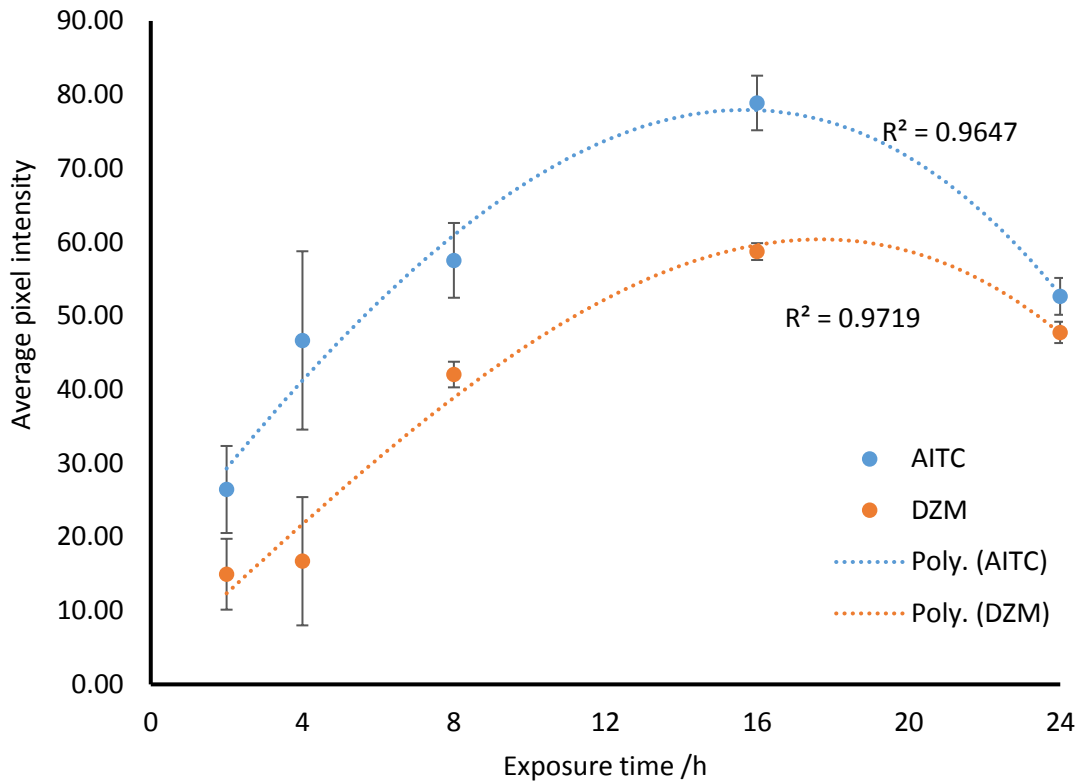


Figure 4.5 Quantification of GFP response in allyl isothiocyanate and Dazomet-exposed *gst-31::gfp* reporters over time. *C. elegans gst-31::gfp* reporters exposed to 10 μ M allyl isothiocyanate and 10 μ M Dazomet. Greatest GFP induction was observed in 16h exposures. Exposures were performed in triplicate. For each time point, 5 individual nematodes were analysed and mean pixel intensity calculated. Polynomial trendlines are plotted. Error bars = \pm SD reporters exposed to 10 μ M allyl isothiocyanate and 10 μ M Dazomet. Greatest GFP induction was observed in 16h exposures. Exposures were performed in triplicate. For each time point, 5 individual nematodes were analysed and mean pixel intensity calculated. Polynomial trendlines are plotted. Error bars = \pm SD

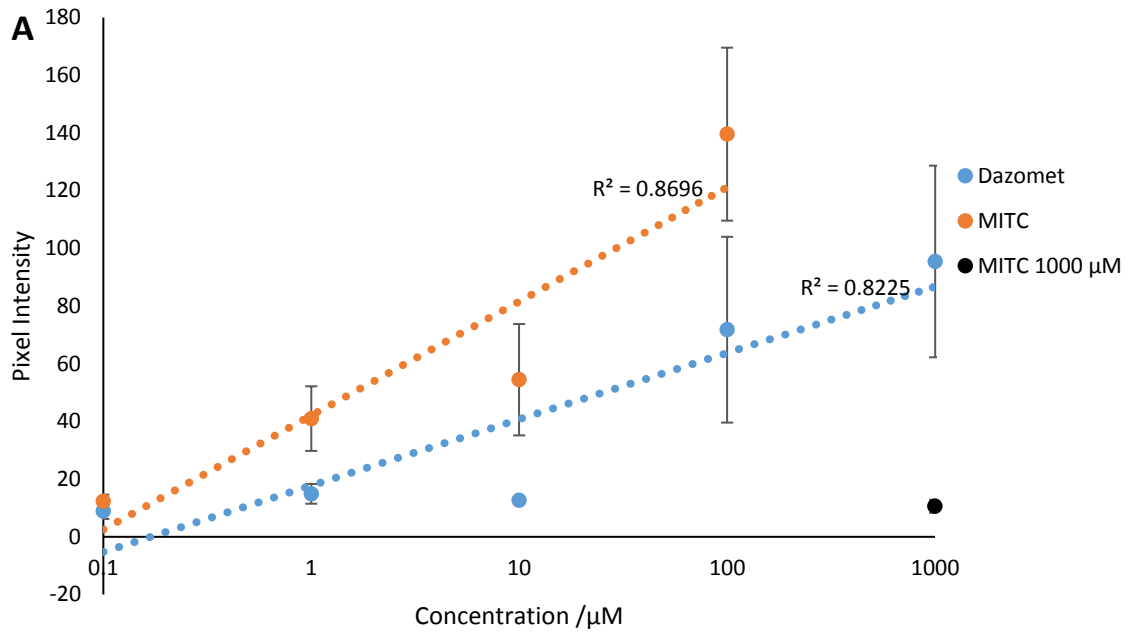


Figure 4.6 (continues on next page) Dose-dependent response of *C. elegans gst-31::gfp* reporters to methyl isothiocyanate and Dazomet. A, Chemical exposures induced dose-dependent responses in reporter worms after 16 h – no fluorescence was observed at 1000 μ M methyl isothiocyanate as all trialed individuals were killed, error bars = \pm SEM.

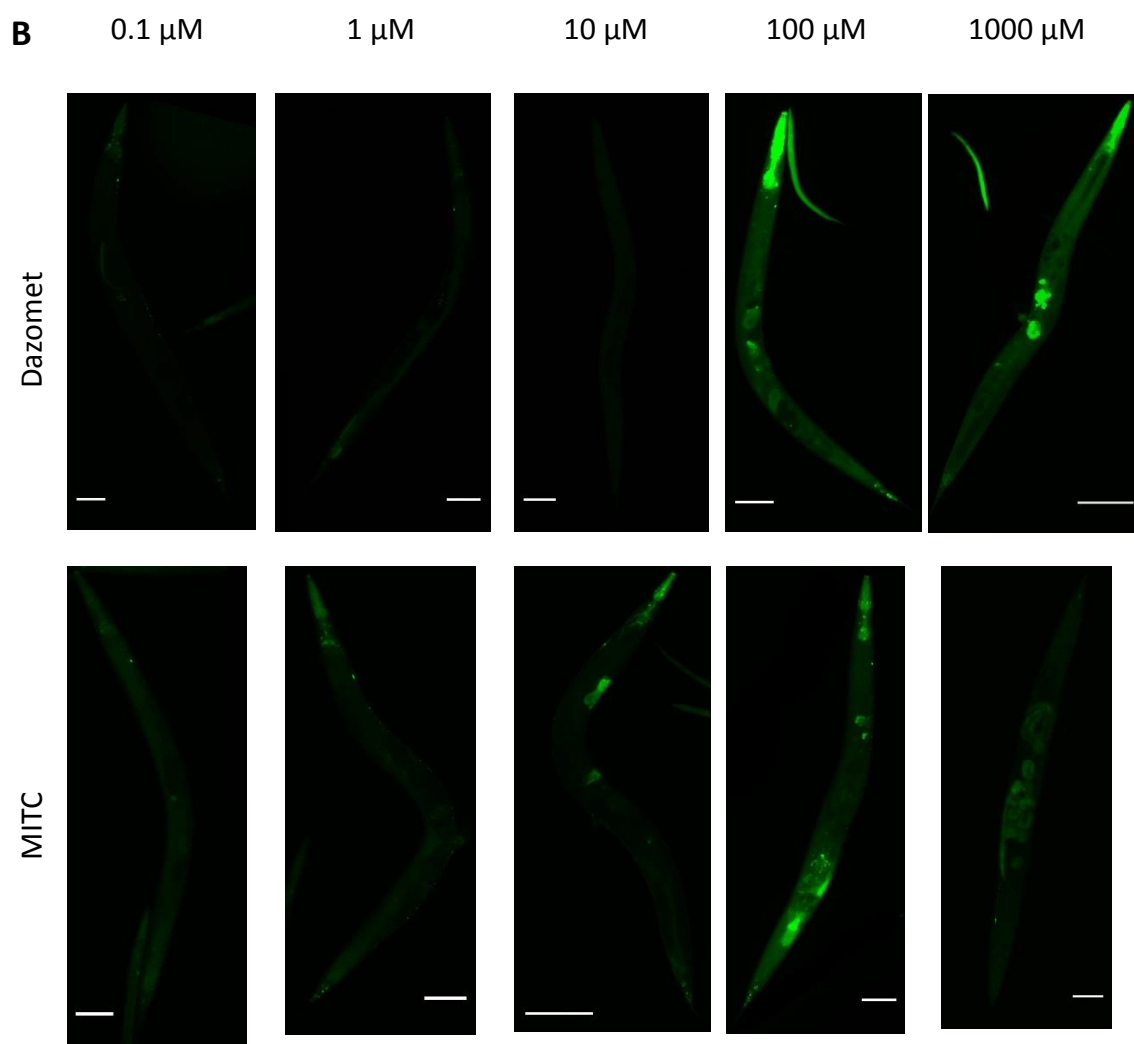


Figure 4.6 (continued) Dose-dependent response of *C. elegans* *gst-31::gfp* reporters to methyl isothiocyanate and Dazomet. B, Representative images of MITC and Dazomet-exposed reporters, scale bar = 150 μ m. Exposures were performed in triplicate. For each concentration, 5 representative individuals were imaged and mean pixel intensity was calculated.

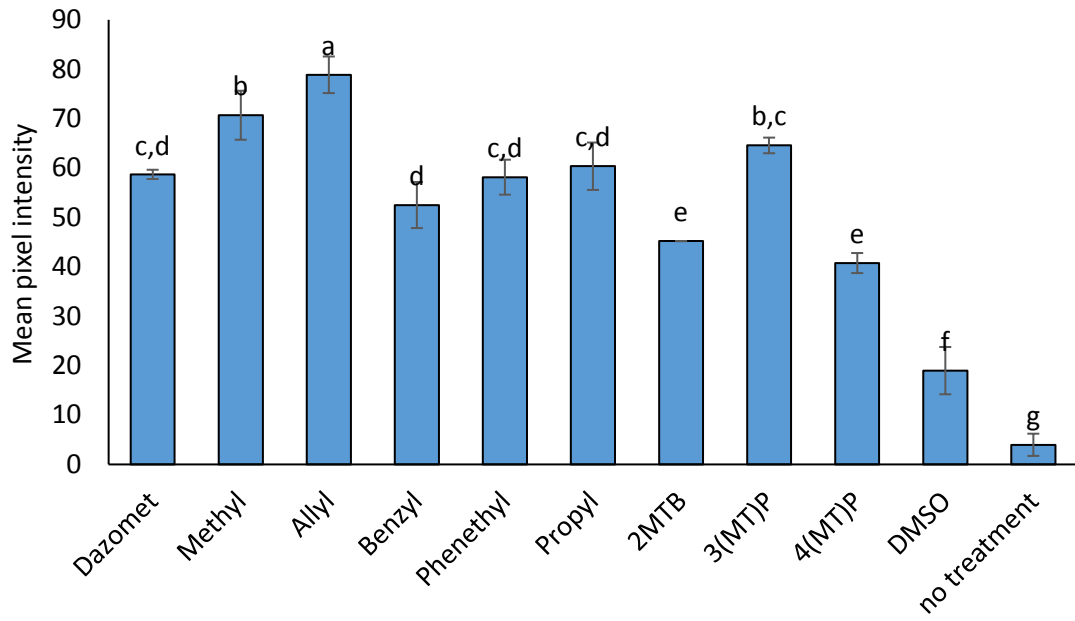


Figure 4.7 (continues on next page) Differential sensitivity of *gst-31::gfp* reporters to isothiocyanates. Reporters exposed to the 10 μ M of a range of isothiocyanates and Dazomet for 16h demonstrated a differential up-regulation of *gst-31*. Letters indicate values that do not differ significantly from one another, based on a Student-Newman-Keuls analysis, $P \leq 0.05$.

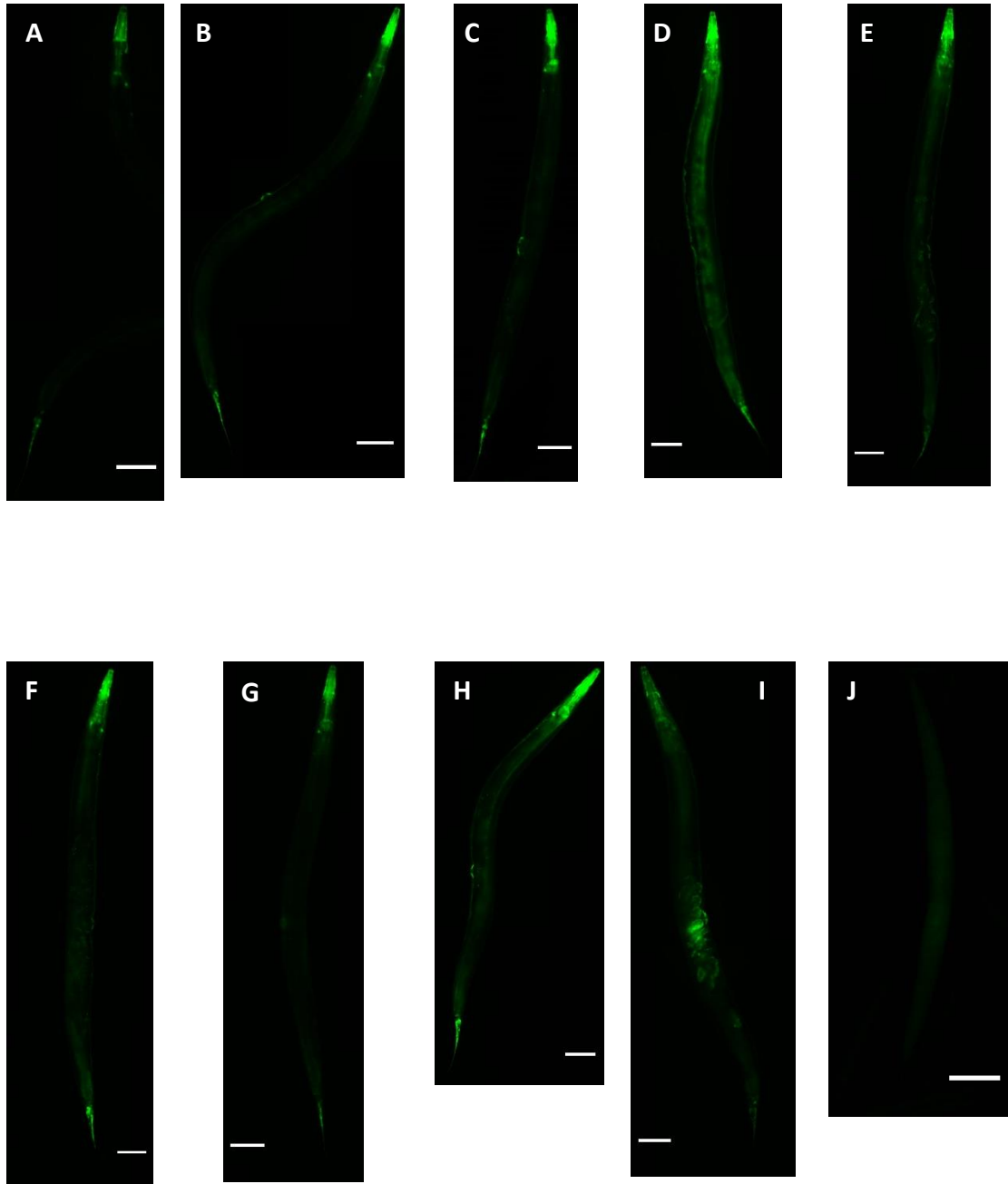


Figure 4.7 (continued) Differential sensitivity of *gst-31::gfp* reporters to isothiocyanates. False colour fluorescence images of representative individuals: A, Dazomet; B, methyl ITC; C, allyl ITC; D, benzyl ITC; E, phenethyl ITC; F, propyl ITC; G, 2-methylbutyl ITC; H, 3-(methylthio)propyl ITC; I, 4-(methylthio)phenyl ITC; and J, DMSO. Scale bars = 150 μm .

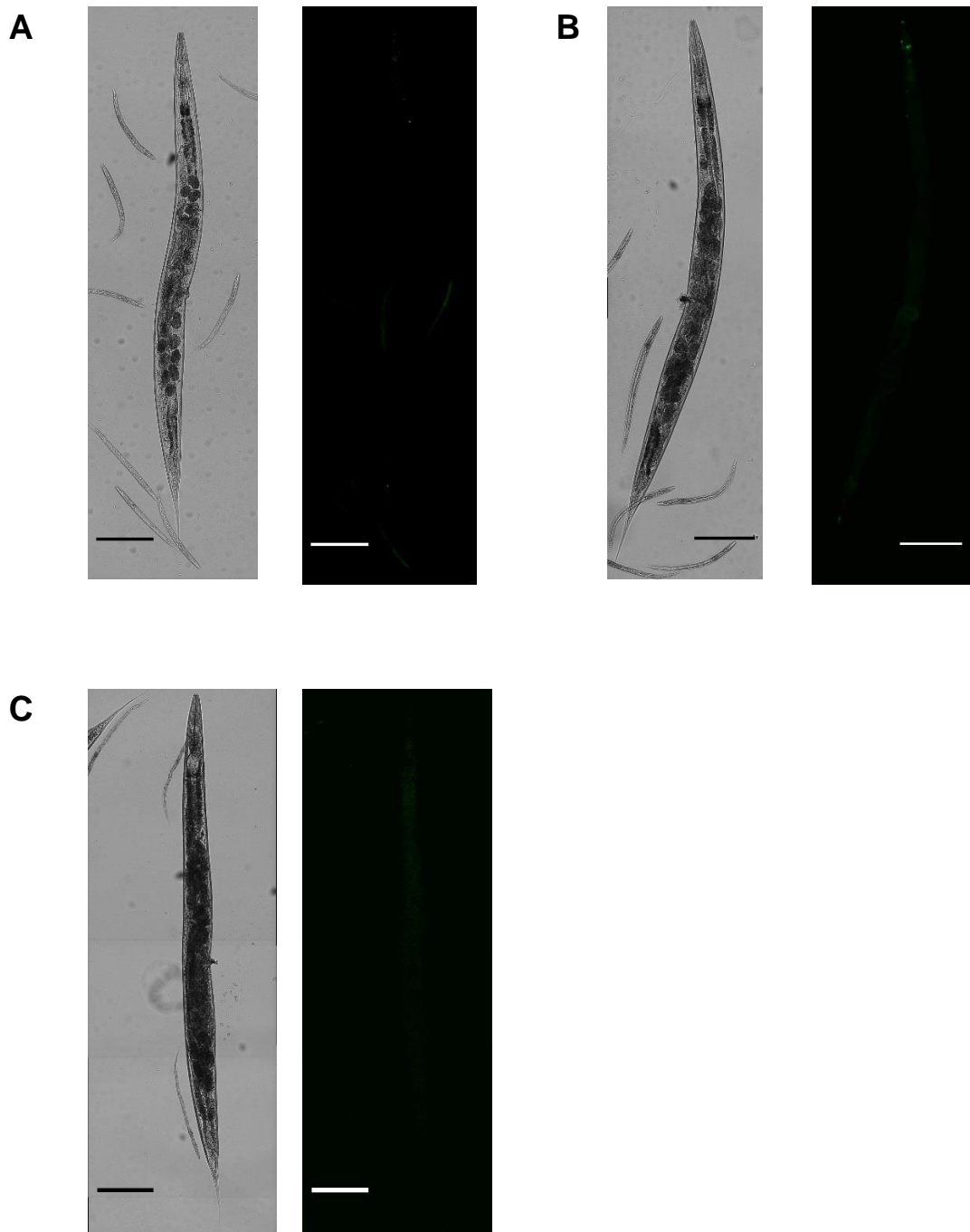


Figure 4.8 Non-brassicaceous leaf extracts induced no up-regulation of *gst-31*. Leaf extracts of A, tomato (*Solanum lycopersicum*); B, wheat (*Triticum aestivum*); and C, cotton (*Gossypium hirsutum*) induced no production of GFP in *gst-31::gfp* reporters when exposed to 1.8 mg/ml leaf extract over 16h. Scale bars = 150 μ m.

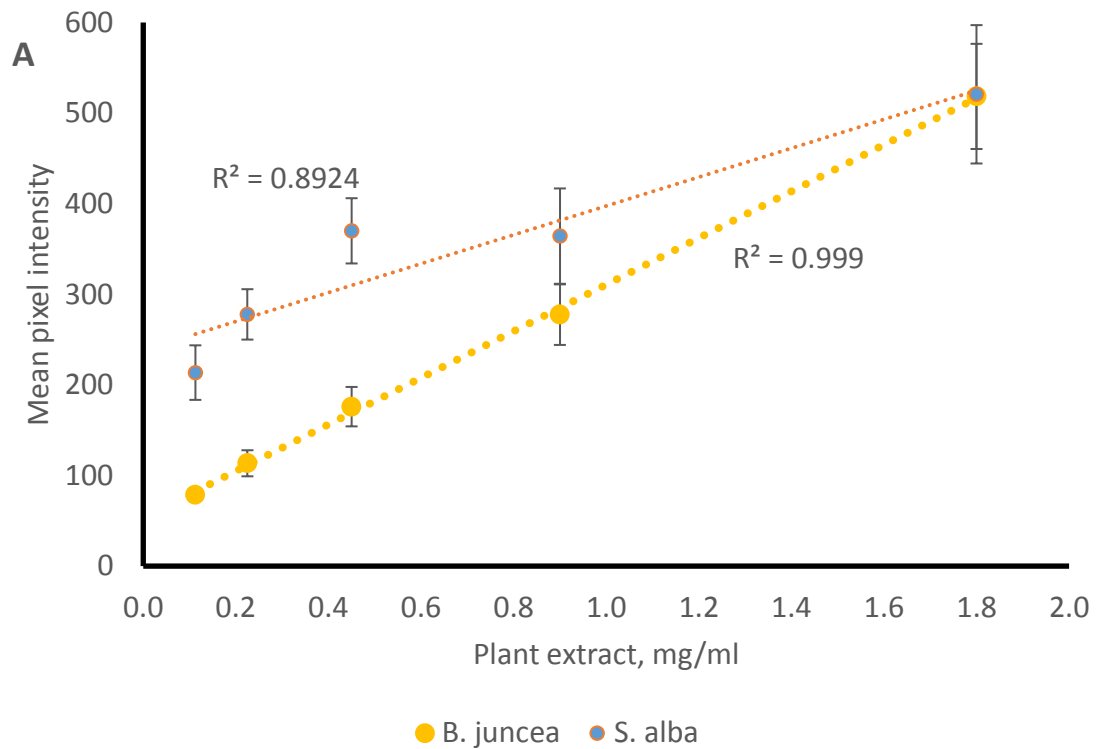


Figure 4.9 (continues on next page) Brassicaceous leaf extracts induce a dose-dependent up-regulation of *gst-31*. A, The intensity of GFP-induction correlated with the concentration of brassicaceous leaf extract that *C. elegans gst-31::gfp* reporters were exposed to after 16h incubation. Exposures were performed in triplicate and at least 5 representative images from each repeat were measured for pixel intensity. B, *gst-31::gfp* reporters responded to exposure to a number of brassicaceous tissue extracts at 1.8 mg/ml.

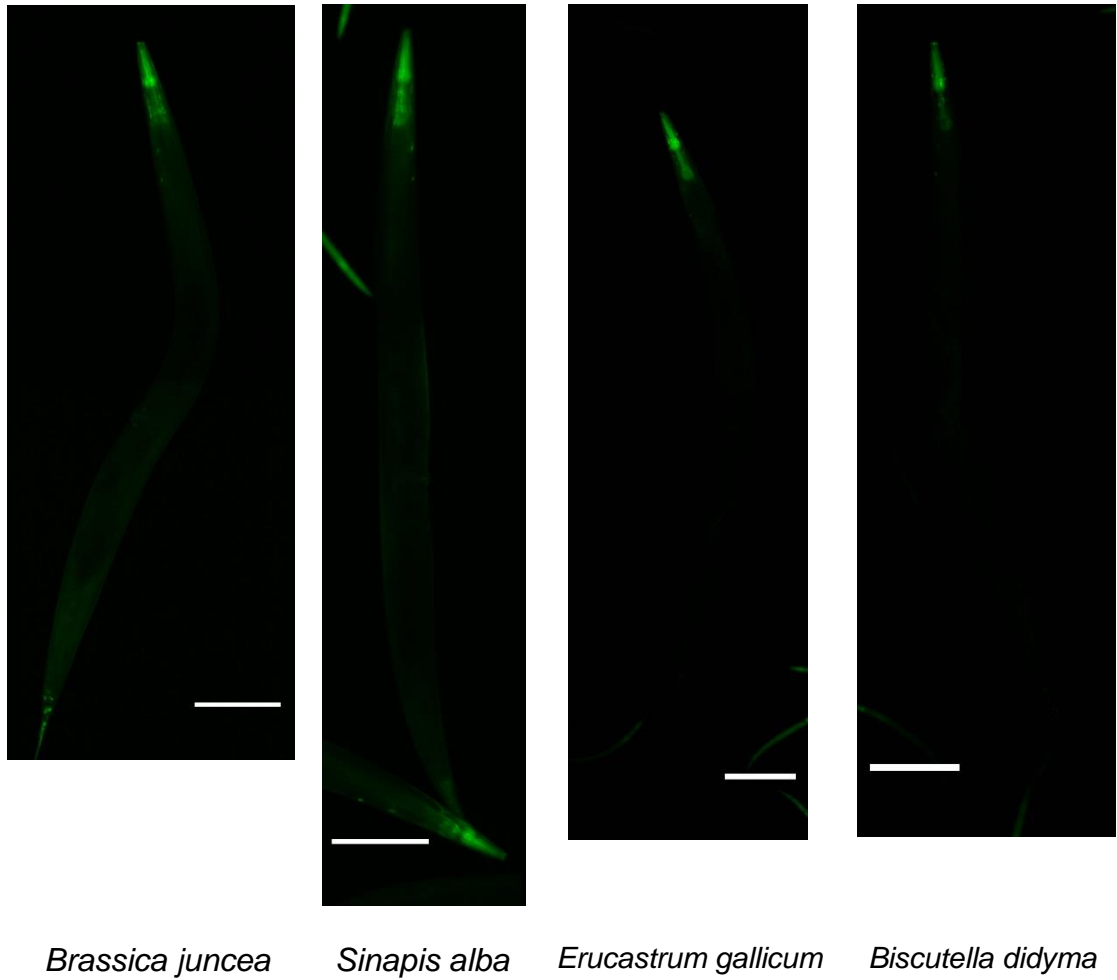


Figure 4.9 (continued) Brassicaceous leaf extracts induce a dose-dependent up-regulation of *gst-31*. B, *gst-31::gfp* reporters responded to exposure to a number of brassicaceous tissue extracts at 1.8 mg/ml. Scale bars = 150 μm.

4.4.3 Transforming *C. elegans* with GFP under control of exogenous promoters

4.4.3.1 Transformation vectors

A modified pPD95_75 vector, with mCherry in place of GFP, was generated (Figure 4.10). Transformation vectors were generated with GFP and RFP under control of a number of *G. pallida* promoters (Table 4.3). The presence of the correct insert in each plasmid was confirmed by sequencing.

4.4.3.2 Results of bombardments

Nematodes that had been successfully transformed with vectors carrying GFP under control of *G. pallida* promoters were identified by rescue from the *unc-119* mutant phenotype. When exposed to 10 mM Dazomet or 10 mM MITC, no induction of GFP was observed in any of the transgenic lines.

4.4.4 Transforming *C. elegans* by microparticle bombardment with two vectors

Double bombardments were performed with three pairings of transformation vectors, and any resulting transgenic animals were recorded (Table 4.4), each bombardment consisted of approximately 50,000 adult *C. elegans*. For bombardments with the pJM119-Gp02405 plasmid and pPDmCh-Ce-my0-2, *unc-119* mutants were bombarded, and rescue of the phenotype taken to indicate successful incorporation of the pJM119 plasmid while observed red fluorescence indicated incorporation of the pPDmCh plasmid. An example of a doubly transformed juvenile is given in Figure 4. . pBCN22 x pPD95_75-Ce-my0-2 bombardment was similarly scored on fluorescence, with successful pBCN22 incorporation resulting in red fluorescence and pPD95_75-ce-my0-2 incorporation resulting in green fluorescence. Fluorescence was observed shortly after bombardment in juvenile nematodes; later observation and attempts to isolate fluorescent individuals revealed that transgenic animals had seemingly died, as no fluorescence was observed.

Table 4.3 Transformation vectors generated for each vector backbone

pJM119	pPDmCh	pPD95_75
<i>Gp-02405</i>	<i>Gp-02405</i>	<i>Ce-gst-31</i>
<i>Gp-03693</i>	<i>Gp-03693</i>	<i>Gp-GAPDH</i>
<i>Gp-09707</i>	<i>Gp-09707</i>	
<i>Gp-11840</i>	<i>Ce-minPmyo-2*</i>	
<i>Gp-11984</i>		
<i>Ce-gst-31</i>		
<p>The inserts successfully ligated into each plasmid backbone are listed.</p> <p>* cloned from the pBCN22 vector</p>		

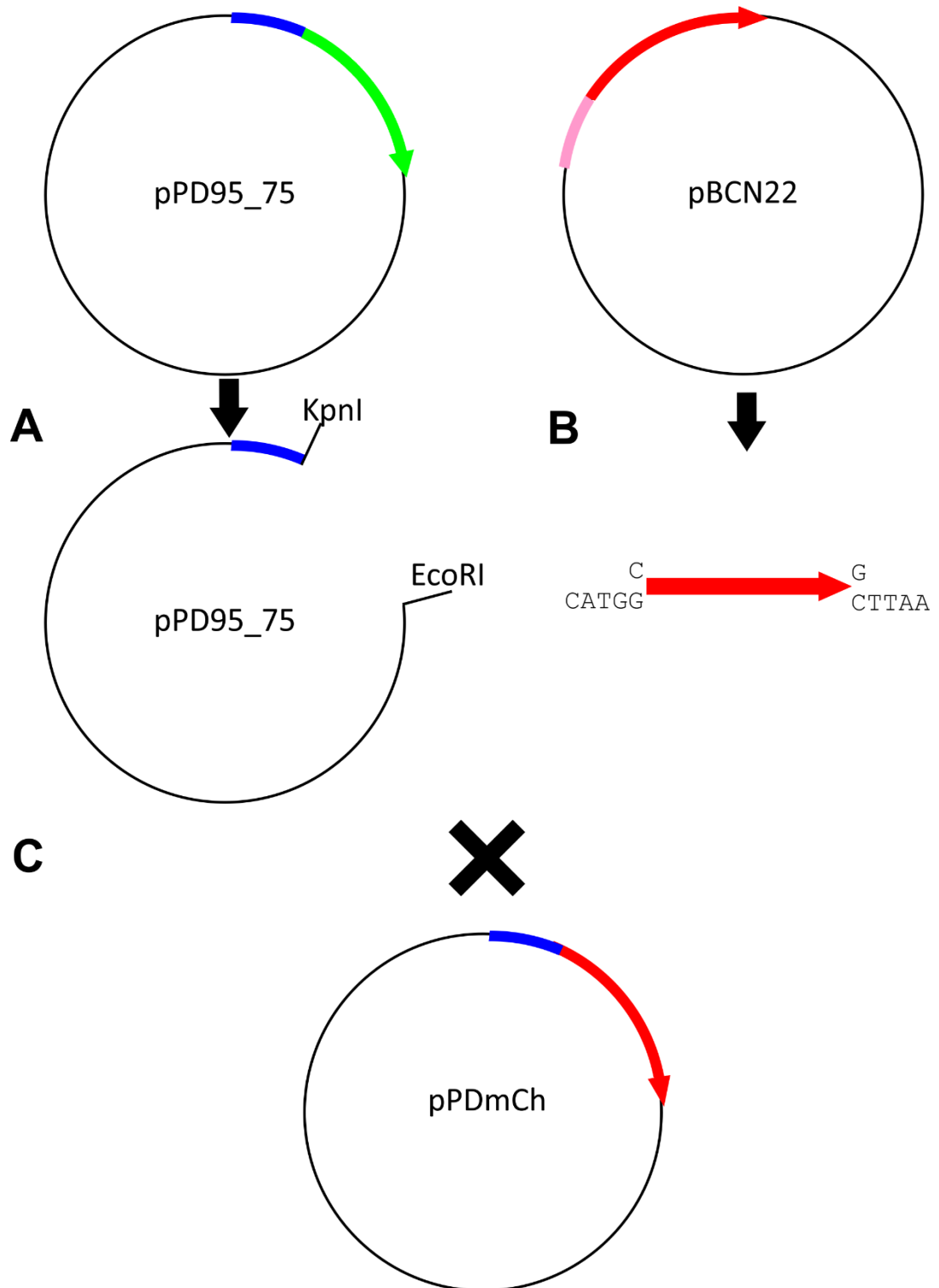


Figure 4.10 Schematic diagram of the generation of pPDmCh. A, the GFP sequence is removed from pPD95_75 by restriction digest. B, mCherry is amplified with added restriction sites and digested. C, the mCherry amplicon is ligated into the empty pPD95_75 backbone, forming pPDmCh.

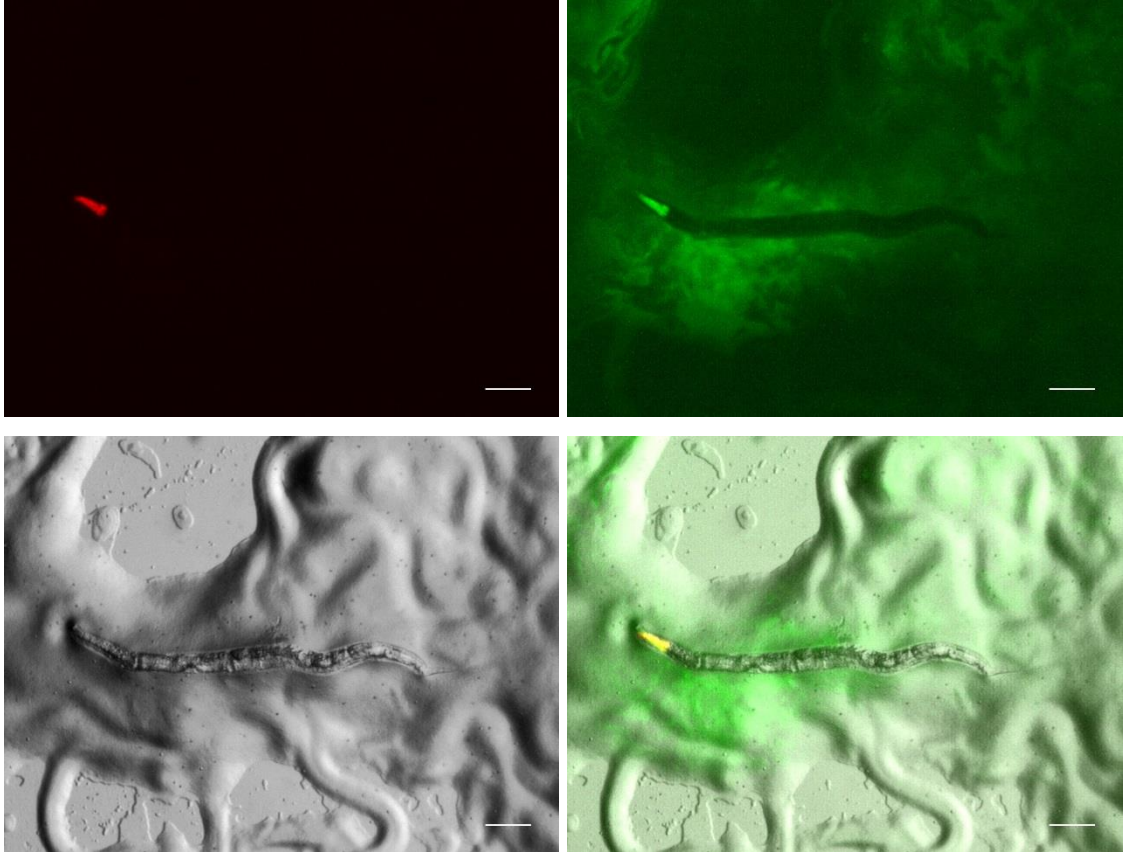


Figure 4.11 *C. elegans unc-119* mutants bombarded simultaneously with pPDmCh-my o -2 and pPD95_75-Ce-my o -2 showed red and green fluorescence in the pharynx. GFP and mCherry expressed under control of the *myo*-2 promoter were visible under fluorescence microscopy in double-bombarded nematodes. Green autofluorescence is observed in the bacteria on the plate.

Table 4.4 Rates of transformation and of inheritance in subsequent generations following double bombardment.

Vector pair	Attempts	Single transformants	Double transformants	Stable lines
pPDmCh- <i>Ce-myo-2</i> x pPDJM119- <i>Gp02405</i>	3	0	8	0
pBCN22 x pPD95_75- <i>Ce-myo-2</i>	2	2	0	0
pPDmCh- <i>Ce-myo-2</i> x pPD95_75- <i>Ce-gst-31</i>	2	0	0	0
pPDmCh- <i>Ce-myo-2</i> x pPD95_75- <i>Ce-myo-2</i>	2	0	1	0

4.4.5 Attempts to transform *Globodera pallida* and *Meloidogyne incognita*

Fluorescence was not observed following attempted bombardment of *G. pallida* juveniles. In one instance, with *M. incognita* eggs bombarded with pPD95_75-GpGAPDH1, a single fluorescent egg was observed (Figure 4.12). The egg was observed daily over the course of a week: no change in fluorescence was observed, though it initially appeared that the cells in the transgenic egg were active and that embryogenesis was progressing. Isolation of the single fluorescent egg from the total bombarded population proved difficult. A week after bombardment, no fluorescence was observed in any egg in the bombarded population.

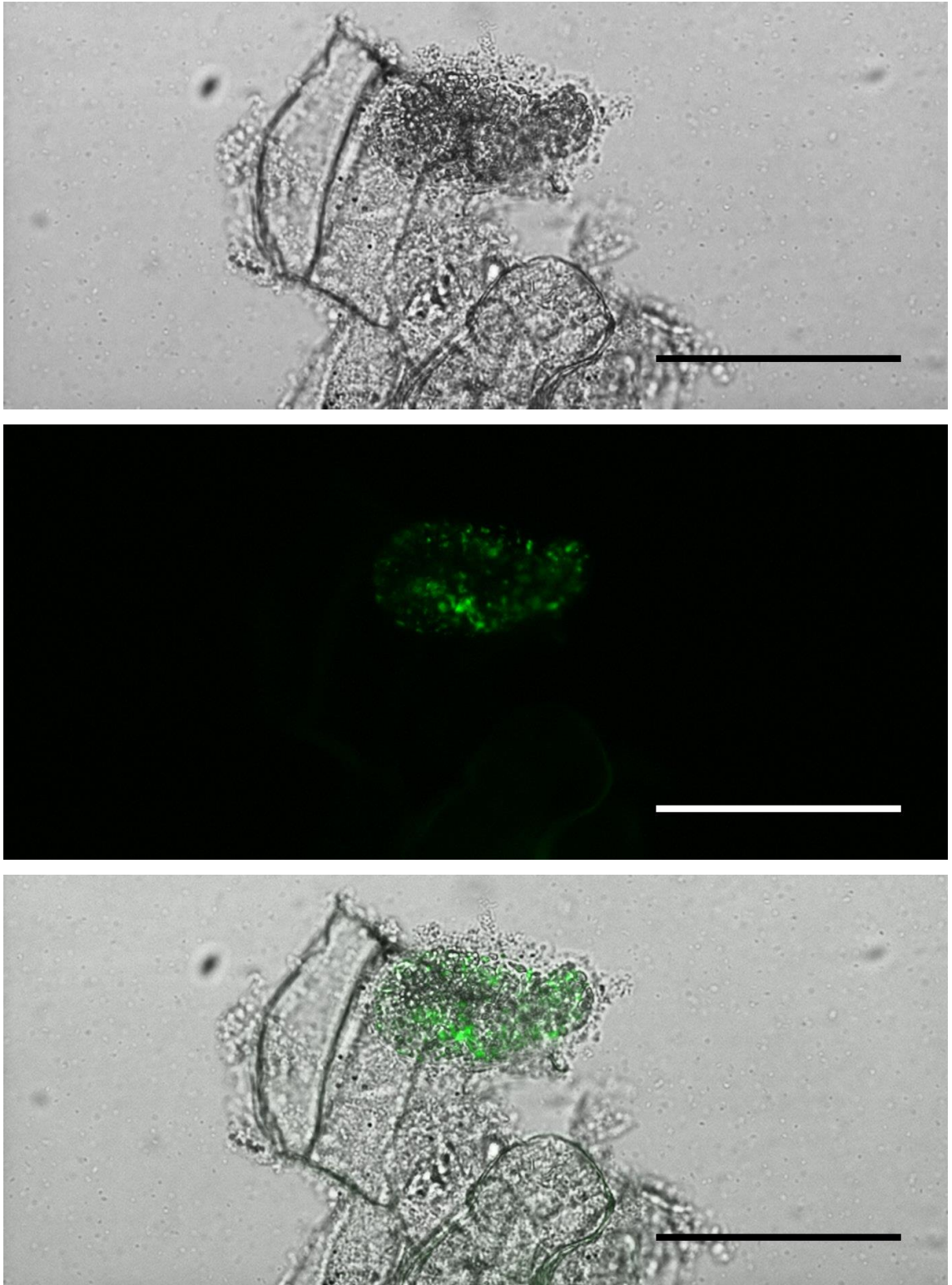


Figure 4.12 Transgenic *Meloidogyne incognita* egg with GFP under control of a *G. pallida* *GAPDH1* promoter. Bright field and false-colour fluorescent images are given, followed by a composite. Scale bar = 100 μ m

4.5 Discussion

4.5.1 *C. elegans* reporter lines as reporters of biofumigant activity

Transgenic nematodes expressing marker proteins under control of reporters for xenobiotic metabolism has been demonstrated to allow detection of indicative bioactivity in plant tissue extracts. Quantification of fluorescence intensity has previously been used to indirectly count cells (Wilson et al., 2018) and to measure gene expression in transgenic *C. elegans* (Mendenhall et al., 2015), as fluorescence is proportional to protein copy number, therefore acting as a proxy measurement of gene expression (Soboleski et al., 2005). Therefore, though the accurate quantification of the constituents of a given solution is not trivial using *C. elegans* reporters, they can be used to differentiate between leaf extracts or chemical solutions of varying strengths.

Reporter lines responded to isothiocyanates in a dose-dependent manner (figure 4.7), indicating a dose-dependent regulatory response of *C. elegans* to contact with isothiocyanates. Up-regulation of a glutathione S-transferase in response to isothiocyanate exposure is in line with previous studies that suggest that GSTs are the principal route of ITC detoxification (Shapiro et al., 2001). The differential effect between isothiocyanates observed, both in compound toxicity and in the up-regulation of *gst-31* (figure 4.6 and 4.7), did not correlate: where Dazomet was the least bioactive of the compounds trialled, it generated strong GFP expression; conversely, 4-(methylthio)phenyl isothiocyanate and phenethyl isothiocyanate demonstrated high toxicity to *C. elegans* adults at 10 uM but did not cause a strong up-regulation of *gst-31* relative to the other compounds tested. This may indicate a level of specificity of response that cannot be represented by *gst-31::gfp* reporters alone: different isothiocyanates may induce specific up-regulatory responses including any number of genes.

The dose-dependent, brassica-specific response of *gst-31::gfp* reporters to leaf extracts suggest that reporter nematodes can be employed as a screen for biofumigation potential. The differential response of reporters to *B. juncea* and *S. alba* leaf extracts (figure 4.9) correlates with the higher toxicity to *G. pallida* J2s previously observed with extracts generated with the same method (Lord et al., 2011). Owing to the response of the reporter line to all tested isothiocyanates, and the differential response to various

compounds, the glucosinolate profile of a plant cannot be inferred from up-regulation of *gst-31*. However, given the broad-spectrum toxicity of isothiocyanates (see Chapter 1.3.5), the potential for bioactivity from a given brassica should roughly correlate with the response of reporter lines to leaf extracts from that plant. Reporters for genes that respond to other stimuli (such as thiabendazole, imidacloprid and chloroquine (Jones et al., 2013b)) could prove useful for screening of plant tissue extracts for various xenobiotic modes of action. Expanding the toolset of available reporters may therefore allow for the screening of myriad plant extracts for a broad range of end uses, limited only by the scope of stimuli for which *C. elegans* demonstrates an inducible response.

4.5.2 Generation of *C. elegans* reporters for *G. pallida* xenobiotic metabolism

No induction of GFP was observed in worms that were successfully transformed with GFP under control of *G. pallida* promoters. Transgenic *C. elegans* expressing GFP under control of *M. hapla* promoters for orthologous genes have been generated by microinjection (Gordon et al., 2015). The promoters drove expression of GFP, but not according to the expected pattern based on the function of the orthologous gene. The authors posit that high divergence in promoter regions over time may have resulted in “resurfacing” of regulatory elements through turnover, resulting in the apparent mismatch in gene expression patterns – they also suggest that a mismatch of *cis*-regulatory elements (promoters and enhancers in the genome) with non-native *trans*-regulatory elements (genes encoding transcription factors) could result in unexpected gene expression in transgenic animals (Gordon et al., 2015). The evolutionary divergence between *C. elegans* and *G. pallida*, both of regulatory elements and of genes involved in xenobiotic metabolism, could therefore explain the lack of gene expression observed in the transgenic animals generated in this study. The promoters used drove expression of proteins with conserved sequences and functions (Gordon et al., 2015), which cannot be said for the *G. pallida* genes that were investigated here (see Chapter 3).

4.5.3 Double bombardment of *C. elegans*

The two major methods for transformation of *C. elegans*, before the recent development of CRISPR-Cas9 (Dickinson and Goldstein, 2016), were microinjection (Mello et al., 1991) and microparticle bombardment (Praitis et al., 2001). Microinjection

involves the direct injection of DNA into the cytoplasm of the distal arm of the gonad – the transgene is then incorporated into newly formed embryos, usually in the form of high copy-number extrachromosomal arrays, though integration can be encouraged by irradiating transformed animals with UV or gamma radiation (Evans, 2006). Advantages of microinjection are quick turnaround and the high success rate, with the majority of injections generating transgenic animals within 10 days of microinjection (Evans, 2006, Mello et al., 1991). The potential disadvantages of the technique are low integration rate, germline silencing of extrachromosomal arrays and the high copy-number of transgenes possibly confusing interpretation of fluorescence (Praitis et al., 2001, Gordon et al., 2015). Bombardment occurs as described in the Materials & Methods section of this chapter, usually involving transformation of *unc-119* mutants with a plasmid carrying a rescue gene (Schweinsberg and Grant, 2013). The major advantages of bombardment are that many thousands of individuals can be subjected to transformation and that successful transformation frequently results in low-copy integration of the transgene, but the efficiency of transformation is poor (Schweinsberg and Grant, 2013). It is this poor efficiency that encourages the use of selection markers such as *unc-119* rescue (Praitis, 2006). Drug-based selection using puromycin resistance genes have been developed recently, in order to simplify the process of selection following bombardment (Semple et al., 2010).

Co-injection of transformation vectors is frequently used when micro-injecting *C. elegans*, as this enables simple combination of transgenes of interest with marker genes, without having to incorporate several elements into a single plasmid; injections can consist of different forms of DNA, including plasmids and PCR products (Evans, 2006). An extensive search of the literature reveals no published articles in which transformation of *C. elegans* by bombardment with more than one transformation construct has been attempted. As negative data is rarely published (Weintraub, 2016), the lack of published data on the subject represents a gap in knowledge when it comes to transgenesis of nematodes. The generation of co-transformed animals was demonstrated here, though stable integration was not observed. The low recovery of transgenic animals and the absence of stable transgenic lines is consistent with poor transformation efficiency previously observed – a principal methods paper generated

58 transgenic lines from a total of 110 bombardments, of which 27 were stable lines, a ratio of 0.25 stable lines per bombardment, with efficiency varying between different constructs (Praitis et al., 2001). As co-bombardment with two constructs was only attempted 3 times, future work should look to develop the technique further – the identification of co-transformation in all transgenic animals is encouraging. The ability of the technique to potentially generate stable transgenic lines carrying independent reporters for two genes, or incorporating gene fusions that take advantage of techniques such as fluorescence complementation (Shyu and Hu, 2008, Zhang et al., 2004), could prove to be a useful method for *C. elegans* research.

4.5.4 Transgenesis of plant-parasitic nematodes

Where no fluorescence was observed in *C. elegans* transformed with *G. pallida* promoters, transgenic *M. incognita* eggs expressed fluorescent proteins under control of a promoter from *G. pallida*. Both *M. incognita* and *G. pallida* are sedentary endoparasites belonging to the superfamily Tylenchida, more closely related to one another than to *C. elegans* (Decraemer and Hunt, 2013). This may account for the ability of a *G. pallida* promoter to drive expression in *M. incognita* cells. *GAPDH* is considered a “housekeeping gene,” required for fundamental cellular processes and therefore assumed to be constitutively expressed (Barber et al., 2005). As such, it might be assumed that regulatory elements controlling expression of orthologous genes in related species are conserved, or that expression of housekeeping genes might not depend on specificity of promoter regions. The latter assumption is supported by reduced sequence conservation observed in housekeeping genes that drive expression throughout the body of an animal, attributed to a simpler mechanism of gene regulation (Farré et al., 2007). A lack of specificity in regulation of *G. pallida* *GAPDH* expression could therefore lend itself to expression in related species.

4.5.5 Conclusions

Caenorhabditis elegans reporter lines expressing GFP under control of native promoters are well-documented. Here, their potential to be employed practically has been demonstrated, echoing previous use of reporters to detect toxins in wastewater (Wah Chu and Chow, 2002). The novel development shown here is the use of reporter lines for screening of plant tissue extracts, which could be further developed, incorporating a

broad range of xenobiotic metabolism reporters for various chemical stimuli, to create a screening pipeline to assess suitability of plant tissues for further study as biofumigants across a range of activities beyond the production of isothiocyanates.

Generation of *C. elegans* reporters for *G. pallida* genes proved unsuccessful. Whether this was due to inherent incompatibility between *cis*- and *trans*-regulatory elements across the two species or to some fault in the transformation procedure is unclear. Transgenic *C. elegans* expressing GFP under control of *M. hapla* promoters suggest that generation of reporters for *G. pallida* genes could be possible, but doubts about correctly representing gene expression patterns across distant phyla (Gordon et al., 2015) could suggest that such reporters would be poor models for *G. pallida* xenobiotic metabolism.

Development of double bombardment as a technique for transforming *C. elegans* could boost the available tools for study of intracellular processes in nematodes, but more work is needed to determine how useful the technique could be.

A more promising development for study of plant-parasitic nematodes would be the successful generation of stable transgenic *M. incognita* lines. As discussed in the introduction to this chapter, *M. incognita* has many traits suited to use as a “model organism,” and expression of GFP under a non-native promoter has been demonstrated here. Further work on transgenesis of *Meloidogyne spp.* could form the basis of a future project with scope to greatly influence the study of plant-parasitic nematodes.

4.6 Summary

-
- Reporters for *C. elegans* xenobiotic metabolism were shown to be useful in detecting biofumigant activity of plant tissues extracts.
 - Generation of *C. elegans* reporters with GFP under control of *G. pallida* promoters was unsuccessful.
 - Double bombardment has potential for use in generating transgenic *C. elegans* that express multiple reporter genes.
 - Future work with *Meloidogyne incognita* could lead to the stable development of transgenic lines, providing a powerful tool for research into plant-parasitic nematodes.
-

Chapter 5 Investigating the volatile emissions of brassicas as a source of pest management

5.1 Introduction

Emission of volatile compounds by plants is a well-documented phenomenon, and the role of volatile compounds in plant defence has been the subject of a number of studies. Plants have been shown to actively release volatiles in response to biotic stress in a dose-dependent manner or to stresses such as insect herbivory or pathogenic fungi (Niinemets et al., 2013). Damage caused by leaf herbivores can induce systemic volatile-release responses (Rostás and Eggert, 2008); these have been observed to deter herbivore egg-laying, as well as acting as attractants for predators of leaf-feeding herbivores such as predatory insects (Kessler and Baldwin, 2001) or entomopathogenic nematodes (Rasmann et al., 2005). Systemic responses have also been observed in root systems that have been attacked by herbivorous beetle larvae, resulting in systemic release of (E)- β -caryophyllene (Hiltpold et al., 2011), an attractant for entomopathogenic nematodes such as *Heterorhabditis megidis* (Turlings et al., 2012). Herbivory-induced defences may also lead to release of defence elicitors into the soil, causing neighbouring plants to release their own defensive volatiles (Dicke and Dijkman, 2001). The direct impact of plant volatile emissions on soilborne pathogens and herbivores is less well understood, however (Pierik et al., 2014).

Plants of the Brassicaceae have been previously observed to emit methyl bromide, a potent ozone depleting agent that has previously been used as a soil fumigant for nematode-infested fields. It has been estimated that global production of oilseed rape, *Brassica napus*, accounts for a notable proportion of methyl bromide sources in the atmosphere: a 1998 analysis suggested that 6.6 ± 1.6 Gg/yr of methyl bromide comes from oilseed, with 0.4 ± 0.2 Gg/yr coming from cabbage growth (Gan et al., 1998); analysis of trends from 1961-2003 found that 5.12 ± 0.85 Gg/yr methyl bromide was produced by oilseed in 2003, and predicted that this would only increase year on year, as production of oilseed also increases (Mead et al., 2008). The latter analysis highlights a potential issue with the monitoring of atmospheric methyl bromide, as the global budget isn't balanced: known sinks of methyl bromide outweigh known sources, both

anthropogenic and biogenic, leading to uncertainty about where methyl bromide is coming from, and hindering efforts to monitor compliance with the Montreal Protocol (Mead et al., 2008). Under the Montreal Protocol on Substances that Deplete the Ozone Layer, ozone-depleting compounds such as methyl bromide are restricted in use, and their atmospheric concentrations must be monitored in order to ensure compliance (UNEP, 2002). A recent example of this comes from a reported 13 ± 5 Gg/yr increase in atmospheric CFC-11 since 2012, coming from somewhere in east Asia (Montzka et al., 2018), despite there being no reported production since 2006 (UNEP, 2012), pointing to un-regulated production of CFC-11. This increase was detected as the global budget of CFC-11 is accounted for, with no biogenic sources; such an increase in methyl bromide emissions may not be readily detected, and whether or not its source is anthropogenic may not be easily determined. It is therefore important to identify and quantify sources of methyl bromide emissions. As growth of brassicas increases both as a cash crop and for purposes such as biofumigation, it will therefore be necessary to consider what impact these increases will have on global halide budgets.

Previous analyses of the volatile emissions from brassicas are based on production of methyl bromide over 24 h from whole young plants in soil (Gan et al., 1998, Mead et al., 2008). Measurements from rice paddies throughout a growing season have shown that emissions of methyl bromide and methyl iodide differ according to growth stage (Redeker et al., 2000). Methyl iodide has been investigated as a possible replacement for methyl bromide in soil fumigation, due to its similar broad spectrum toxicity without the environmental impacts associated with methyl bromide (Pelley, 2009). Other bioactive compounds known to be released from land plants include methyl chloride (Yokouchi et al., 2000), which is recognised as a potential ozone-depleting agent but is not monitored as it is largely biogenic in origin (UNEP, 2012); methane thiol (Saini et al., 1995); and dimethyl sulphide (Bentley and Chasteen, 2004). The production of the methyl halides and methane thiol by plants has been suggested as a way to eliminate halide and HS⁻ ions from cells (Saini et al., 1995). Atmospheric dimethyl sulphide flux comes principally (> 90 %) from the oceans, and is thought to contribute to global climate cooling (Stefels et al., 2007).

Where the impacts of these compounds on the atmosphere have been calculated on regional and global scales, no such analysis has been made on the effects of such plant-emitted volatile compounds on a local scale. As a result of restrictions on pesticide use, particularly of soil fumigants, natural sources of nematode control have been the subject of much recent research (see Chapter 1.3 for review). An analysis into the gaseous emissions of three brassica species was made over the course of growth from vegetative growth to senescence, and the toxicity of these emissions to soilborne nematodes was assessed.

5.2 Aims

1. Determine the quantities of bioactive compounds released by brassicas into the soil and atmosphere.
2. Examine the potential of these compounds for control of soilborne nematodes, such as *Globodera pallida*.
3. Estimate the atmospheric impacts of brassicaceous volatile emissions.

5.3 Materials & methods

5.3.1 Growth of plants for volatile sampling

A number of commonly used biofumigant plant species were grown for sampling of volatiles, including: yellow mustard (*Brassica juncea* cv. ISCI99); radish (*Raphanus sativus* cvs. WeedCheck and Diablo); and rocket (*Eruca sativa* cv. Nemat). Seeds were surface sterilised with 1 % sodium hypochlorite and then germinated in sterile 90 mm petri dishes on filter paper moistened with autoclaved tap water. After germination, 8-12 seedlings were transferred to a pot. Plants were allowed to grow for 7 days, watering every other day with ½-strength Hoagland's No. 2 solution, before transferring individually to 15 cm Ø, 1 litre pots. In order to facilitate removal of soil from the root systems of the plants when sampling, the plants were grown in a 9:1 sand:compost mix throughout their lifecycle. Plants were watered three times a week with a modified Hoagland's No.2 Solution (6.5 mM potassium nitrate, 4.0 mM calcium nitrate, 2.0 mM ammonium dihydrogen phosphate, 2.0 mM magnesium sulphate, 4.6 µM boric acid, 0.5 µM manganese chloride, 0.2 µM zinc sulphate, 0.1 µM ammonium heptamolybdate, 0.2 µM copper sulphate, and 45 µM iron(III) chloride; supplemented with 50 mM sodium chloride, 0.5 mM sodium bromide, and 0.05 mM potassium iodide). The addition of chloride, bromide, and iodide salts was intended to prevent depletion of the halides from the soil in the pots.

5.3.2 Sampling plant volatiles

In order to sample the airspaces of the above and below-ground parts of each plant, a two-chambered sampling box was used (Figure 5.1). The lower chamber was formed of an opaque PVC base with a clear acrylic lid, with a total volume of 10.01 L; the clear acrylic upper chamber gave a sampling volume of 27.25 L. Plants were checked for physical damage or visible signs of disease or malnourishment, and only those plants that were outwardly healthy were sampled. Plants were carefully removed from pots and the roots were washed of soil, taking care not to damage root tissue. The roots were then patted dry and the fresh weight of each plant was recorded.

Plants were first placed into the root sampling chamber, with the roots kept in a pot of water to prevent wilting. A silicone septum was placed around the root-shoot junction and silicone vacuum grease was used to create an airtight seal. The temperature within

the chamber was recorded, using a probe inserted through a hole in the lid of the chamber. Samples were taken 2 minutes, 11 minutes, and 20 minutes after placing the plant into the root chamber by affixing a canister to the glass-coated, stainless steel sampling line, via a length of sampling line filled with Ascarite, and turning the valve to open the canister, allowing air within the chamber to be drawn by pressure differential. The Ascarite trap was constructed using a short length of glass-lined steel tubing filled with Ascarite II Adsorbent, 20-30 mesh sodium hydroxide-coated silica granules (Sigma-Aldrich, 223921), with a piece of coiled silver wire blocking each end, and served to remove moisture and carbon dioxide from the sampled gas as it was drawn into the sampling canister.

The upper chamber was then placed on top of the root chamber, enclosing the aboveground biomass of the plant within. The glass-coated sampling line and Ascarite trap were once more affixed to the sampling port and a temperature probe was inserted through a separate hole on the top of the chamber. Sampling followed the same procedure as with the root chamber, with the chamber temperature recorded at the time of each sampling. The ambient temperature was also noted throughout sampling.

After sampling, the plants were dried and the root and aboveground biomass components were separated and placed in paper bags in a 65 °C incubator to dry. After 4 days in the incubator, plant roots and shoots were separately weighed and returned to the incubator. Samples were weighed again after 24 hours, and if the mass had not changed through subsequent drying, this was recorded as the dry biomass of that sample.

|

A



B



Figure 5.1 Plant volatile sampling chamber. The sampling chamber is depicted in use: A, the assembled sampling chamber set up to sample volatiles from the aboveground biomass of the plant; B, sampling volatiles from the belowground biomass, with the canister and Ascarite trap in place. The hole through which the roots of the plant are separated from the aboveground biomass is covered with a silicon pad and sealed with silicone vacuum grease, to ensure separation of sampling.

5.3.3 Analysis of volatile samples and calculation of flux

The concentrations of gases in the canisters were analysed on an HP GC/MSD fitted with a PoraPlot Q column (25 m, 0.32 ID, 5 μm thickness; Restek, Bellefonte, PA), as used in previous studies measuring plant methyl halide emissions (Redeker and Cicerone, 2004, Redeker et al., 2000).

Once the peaks of each compound of interest had been integrated, these could be used to calculate the concentration of the compound in a sample. The amount of CFC-11 (trichlorofluoromethane) in the sample was used as an internal standard, due to its well-mixed, nearly constant concentration in the atmosphere. This allowed samples to be compared directly and for more precise calculation of the concentration of each compound in each sample. The reading for CFC-11 was set at 240 ppt (parts per trillion), as this represents the global tropospheric average (Hoffmann et al., 2014). Changes in compound concentration over time are then used to calculate the flux according to the equation: $Flux_X = \frac{\Delta[X]}{\Delta t}$, where $\Delta[X]$ gives the change in concentration of a given compound X over the time period Δt . This provides a calculated flux in grams of compound per gram dry biomass (above- and belowground) per day (g/g biomass/day).

5.3.4 Estimating contributions of brassicas to global methyl bromide budgets

The global reported yield values for mustard seed for the year 2016 was taken from the Food and Agricultural Organisation Statistical Database (FAOSTAT, 2017), converted into total dry biomass based on the average proportion taken from a study on mustard responses to different fertiliser treatments (Banerjee et al., 2012). Yield of radishes was given as 7 Mt/yr (Dixon, 2006); this was converted to dry mass by according to the percentage dry mass:fresh mass taken from plants sampled at flowering stage. These dry masses were then divided into above and belowground biomass values based on the proportions observed in sampled plants. Assuming constant output of methyl bromide over an 8 week growing season and consistent growth of the each plant from seed to harvest, an estimate was then produced.

No harvest data specific to *Eruca sativa* was available.

5.3.5 Volatile toxicity assays

Toxicity assays were performed with methyl iodide, dimethyl sulphide and chloroform. The remaining compounds were gaseous at room temperature so were considered unsuited to the assay.

The toxicity of compounds to nematodes in a closed environment was assayed using a nested dish system (Figure 5.2). Initial experiments with *C. elegans* N2 adults assessed the difference in toxicity of methyl iodide applied directly in solution with the nematodes to that of methyl iodide pipetted into the surrounding dish, so that only volatilised compound would come into contact with the nematodes. Subsequent assays applied compounds only to the outer dish. Compounds were pipetted into the dish in 3 μ l aliquots, diluted where necessary with absolute ethanol, and with control treatments of 3 μ l absolute ethanol and with no addition of any compound. Where two compounds were applied to one dish, this was applied as two 3 μ l aliquots, diluted as above, with a 6 μ l absolute ethanol control treatment.

Before application of compounds, both the total number of nematodes in each dish and the number of those nematodes that were dead or inactive was counted in triplicate. Following application of the compounds, the number of inactive or dead nematodes was counted at set timepoints. From these numbers, the percentage lethality or inactivity was calculated for each dish.

A further nested-plate assay was conducted with cysts. The values from the single cultivar that had the highest methyl iodide and dimethyl sulphide flux from the belowground biomass were used, and applied at 1x, 7x and 49x doses from the equivalent of 1 g dry biomass, to give values for 1 day, 7 days, and 7 weeks exposure. After 24 h incubation, cysts were crushed and the eggs were collected and stained with 0.001 % Meldola's blue dye: eggs were incubated for 4 h at room temperature, then washed by centrifugation, removal of the supernatant and resuspension in sterile distilled water, repeated 3 times. Egg suspensions were then made up to 10 ml volume and subsampled (as in Chapter 2.2.3). The total number of nematodes per counting slide was counted as well as the number of stained individuals.

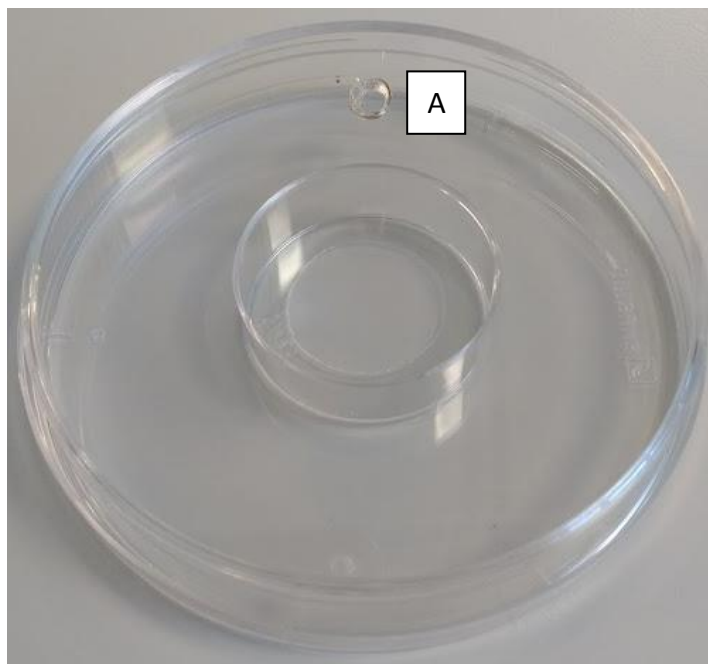


Figure 5.2 The nested dish system used to assay toxicity of volatile compounds. The lower half of a 35 mm petri dish is sealed to the inside of the lid of a 90 mm petri dish using vacuum grease and a hole (A) is burned into the upper section of the larger, outer dish. A known quantity of nematodes is pipetted into the smaller, central dish in a 2 ml aliquot of sterile water, and the larger dish is closed and sealed with vacuum grease. The compound to be tested is pipetted through the hole (A), which is quickly sealed with vacuum grease.

Table 5.1 Compounds investigated in this chapter

Compound	IUPAC name	Abbreviation	Formula	Molar mass (g mol ⁻¹)
Methyl chloride	Chloromethane	MeCl	CH ₃ Cl	50.49
Methane thiol	Methanethiol	MeSH	CH ₃ SH	48.11
Methyl bromide	Bromomethane	MeBr	CH ₃ Br	94.94
Methyl iodide	Iodomethane	MeI	CH ₃ I	141.94
Dimethyl sulphide	(Methylsulfanyl)methane	DMS	(CH ₃) ₂ S	62.13
Chloroform	Trichloromethane	CHCl ₃	CHCl ₃	119.37

Abbreviations used in the text are given

5.3.6 Statistical analyses

Data was analysed for statistical significance using IBM SPSS Statistics 24. Analysis of variance (ANOVA) was performed with post-hoc Student-Newman-Keuls multiple pairwise comparison to identify groups of variables that significantly differed from one another.

5.4 Results

5.4.1 Gaseous compounds emitted by brassicas in a closed environment

The gases produced by the above and below-ground parts of four brassica cultivars were examined for their potential to contribute to pest control. The tested brassicas were found to produce methyl chloride, methyl bromide and methyl iodide, as well as dimethyl sulphide, and chloroform. The growth stage of each plant at the time of sampling was found to have an effect on both the flux of compound per gram of dry biomass, and therefore on the total flux of compound per plant. A one way-ANOVA found significant interaction ($P < 0.005$) between growth stage and the flux of compound across all cultivars for methyl bromide ($P = 0.001$) and methyl iodide ($P = 0.003$) (Table 5.3), while a further analysis found a significant effect ($P < 0.05$) of cultivar on the total output of compound per plant (flux*biomass), again for methyl bromide ($P = 0.049$) and methyl iodide ($P = 0.029$) (Table 5.4).

Table 5.2 One-way ANOVA of compound fluxes against growth stages (vegetative, flowering and senescent) across all cultivars.

		Sum	of			
		Squares	df	Mean Square	F	Sig.
MeCl	Between Groups	.000	2	.000	.384	.683
	Within Groups	.000	75	.000		
	Total	.000	77			
MeSH	Between Groups	.000	2	.000	1.929	.154
	Within Groups	.000	60	.000		
	Total	.000	62			
MeBr	Between Groups	.000	2	.000	7.670	.001**
	Within Groups	.000	75	.000		
	Total	.000	77			
MeI	Between Groups	.000	2	.000	6.356	.003**
	Within Groups	.000	75	.000		
	Total	.000	77			
DMS	Between Groups	.000	2	.000	2.510	.088
	Within Groups	.000	75	.000		
	Total	.000	77			
CHCl₃	Between Groups	.000	2	.000	3.494	.036*
	Within Groups	.000	73	.000		
	Total	.000	75			

*P<0.05 ; **P<0.005; n = 3 in all cases except flowering stage WeedCheck, where n = 5

Table 5.3 One-way ANOVA comparing flux of compounds against cultivar (ISCI99, WeedCheck, Nemat, Diablo) across all growth stages.

		Sum Squares	of df	Mean Square	F	Sig.
MeCl	Between Groups	.000	2	.000	.611	.545
	Within Groups	.000	75	.000		
	Total	.000	77			
MeSH	Between Groups	.000	2	.000	1.979	.147
	Within Groups	.000	60	.000		
	Total	.000	62			
MeBr	Between Groups	.000	2	.000	3.130	.049*
	Within Groups	.000	75	.000		
	Total	.000	77			
Mel	Between Groups	.000	2	.000	3.724	.029*
	Within Groups	.000	75	.000		
	Total	.000	77			
DMS	Between Groups	.000	2	.000	.231	.794
	Within Groups	.000	75	.000		
	Total	.000	77			
CHCl₃	Between Groups	.000	2	.000	.574	.566
	Within Groups	.000	73	.000		
	Total	.000	75			

*P<0.05; n = 3 in all cases except flowering WeedCheck, where n = 5

5.4.1.1 *Brassica juncea* cultivar 'ISCI99'

The average dry mass of plants sampled varied according to growth stage, with root mass increasing from vegetative (0.15 ± 0.02 g) to flowering (0.96 ± 0.06 g) stage and then decreasing from flowering stage to senescence (0.76 ± 0.05 g); ANOVA gave a between groups significance of $P < 0.001$, with Tukey's test finding the same level of significance except in the pairwise comparison of flowering and senescent stage roots, where $P = 0.047$. Shoot masses increased with each growth stage: vegetative (0.85 ± 0.11 g) to flowering (3.42 ± 0.43 g, $P=0.0021$) and flowering to senescent (8.15 ± 1.73 g, $P=0.028$); ANOVA gave $P = 0.007$ for between groups significance, with Tukey's test finding significant differences in pairwise comparisons with senescent aboveground biomass ($P = 0.257$).

The profile of gases emitted by the Indian mustard cultivar 'ISCI99' was found to change with the growth stage of the plant (figure 5.3). The flux of methyl chloride from the roots decreased over successive growth stages, while from the aboveground biomass it went from a negative flux during vegetative growth to a positive flux during flowering, then returned to a negative flux in senescence (figure 5.3A). Methane thiol fluxes varied from sample to sample but were generally positive, and increased from the roots in senescent plants (figure 5.3B). The output of methyl bromide was generally positive, decreasing over successive growth stages from the roots, and peaking in production from the aboveground biomass in the flowering stage, at 0.51 ± 0.02 $\mu\text{g/g}$ dry biomass/day (figure 5.3). Methyl iodide (figure 5.3D) production from the roots fell after the vegetative stage from 2.63 ± 0.82 $\mu\text{g/g}$ biomass/day to 71.61 ± 0.37 ng/g biomass/day in flowering and 154.67 ± 69.31 ng/g biomass/day in senescence; flux from the aboveground biomass was highest in the vegetative stage (12.48 ± 0.68 $\mu\text{g/g}$ biomass/day), falling to less than half that value when flowering (5.73 ± 0.45 $\mu\text{g/g}$ biomass/day), and then reducing further in senescence (79.42 ± 28.3 ng/g biomass/day). Dimethyl sulphide fluxes (figure 5.3E) were negative in the vegetative plant stage, showed high variation in flowering plants, and became positive in senescent roots but with high variability (1.06 ± 0.76 $\mu\text{g/g}$ biomass/day). Output of chloroform (figure 5.3F) appeared high from vegetative stage roots, but with high variation (39.40 ± 74.15 $\mu\text{g/g}$ biomass/day), falling and stabilising in

flowering ($8.09 \pm 4.20 \mu\text{g/g biomass/day}$) and senescent roots ($11.89 \pm 2.04 \mu\text{g/g biomass/day}$).

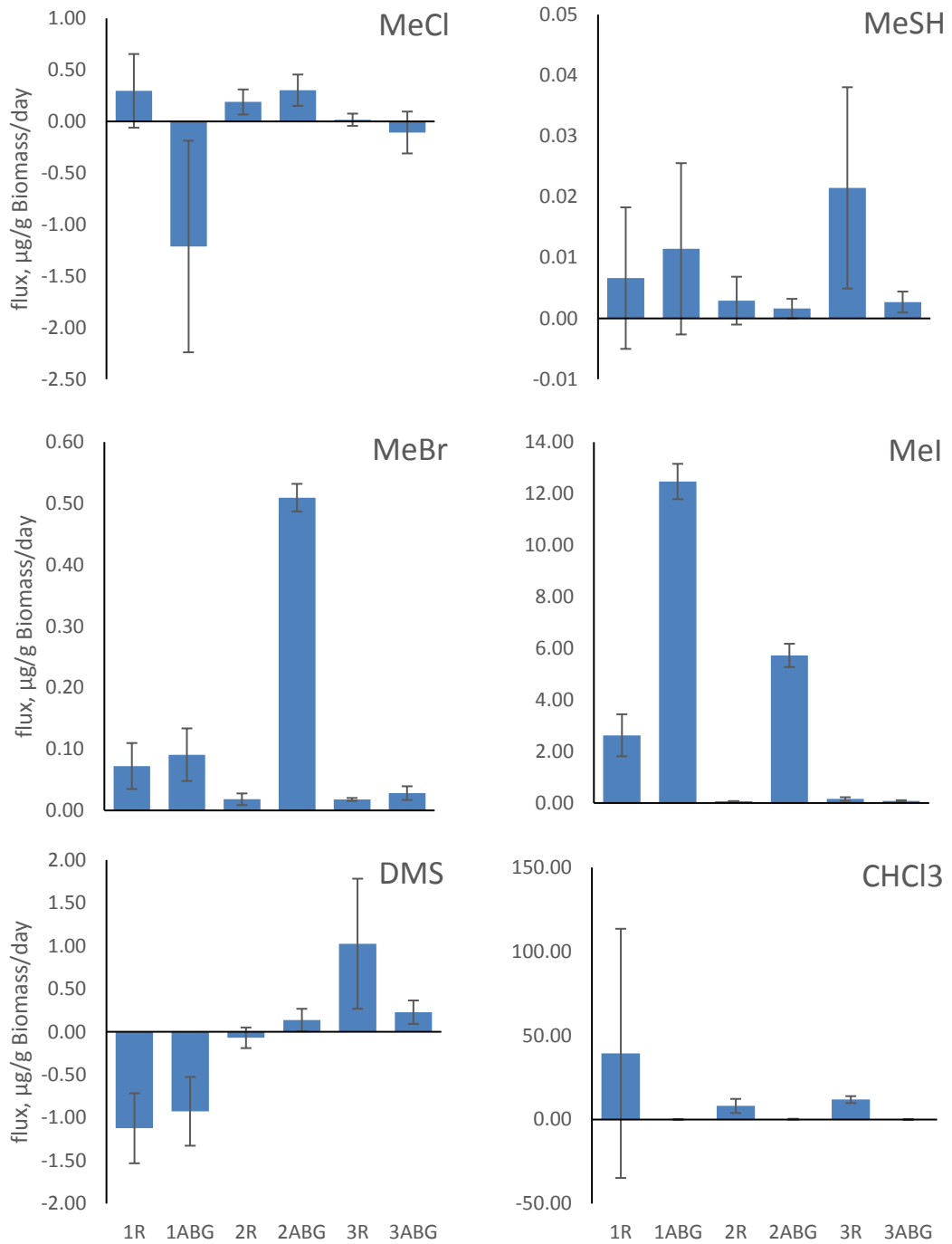


Figure 5.3 Gas fluxes from *Brassica juncea* cv. 'ISCI99' roots and aboveground biomass over 3 growth stages. The change in concentration of gases over a 20 minute period was extrapolated to give a value of micrograms flux per gram plant dry biomass per day. Horizontal axis markers indicate growth stage (1 = vegetative growth, 6 weeks; 2 = flowering, 12 weeks; 3 = senescence, 18 weeks) and section of plant (R = roots; ABG = aboveground biomass). Error bars give ± 1 standard error.

5.4.1.2 *Raphanus sativus* cultivar 'WeedCheck'

Biomass values for 'WeedCheck' radish increased with growth stage. Root biomass increased from 0.23 ± 0.037 g in vegetative plants to 7.14 ± 1.38 g in flowering and 7.78 ± 2.86 g in senescence: differences between growth stages were significant (ANOVA, $P = 0.037$), though Tukey's test separately grouped vegetative and flowering root biomasses and flowering and senescent root biomasses. Shoot biomass also increased with growth stage (vegetative: 1.45 ± 0.20 g; flowering: 16.03 ± 1.48 g; senescent: 17.90 ± 3.07 g). ANOVA suggested a significant difference between groups ($P = 0.001$), with pairwise comparison grouping flowering and senescent biomasses together.

Figure 5.4 gives the fluxes of tested compounds recorded from *R. sativus* cv. 'WeedCheck'. Production of methyl chloride by WeedCheck was variable in the roots of vegetative stage plants (0.31 ± 0.64 $\mu\text{g/g}$ dry biomass/day) but stable in the aboveground biomass. Methane thiol emissions were on the nanogram scale in all samples apart from vegetative stage roots, where there was high variation. Methyl bromide production in the aboveground biomass peaked in flowering plants (0.49 ± 0.04 $\mu\text{g/g}$ dry biomass/day); root production peaked in senescence (0.08 ± 0.07 $\mu\text{g/g}$ dry biomass/day). Methyl iodide production was highest per gram biomass in the vegetative stage and declined thereafter. A similar trend was observed in the production of DMS from roots, whereas a negative flux observed in the aboveground biomass of vegetative plants became positive in later stages. Production of chloroform was principally observed in the roots of vegetative plants (59.87 ± 14.05 $\mu\text{g/g}$ dry biomass/day).

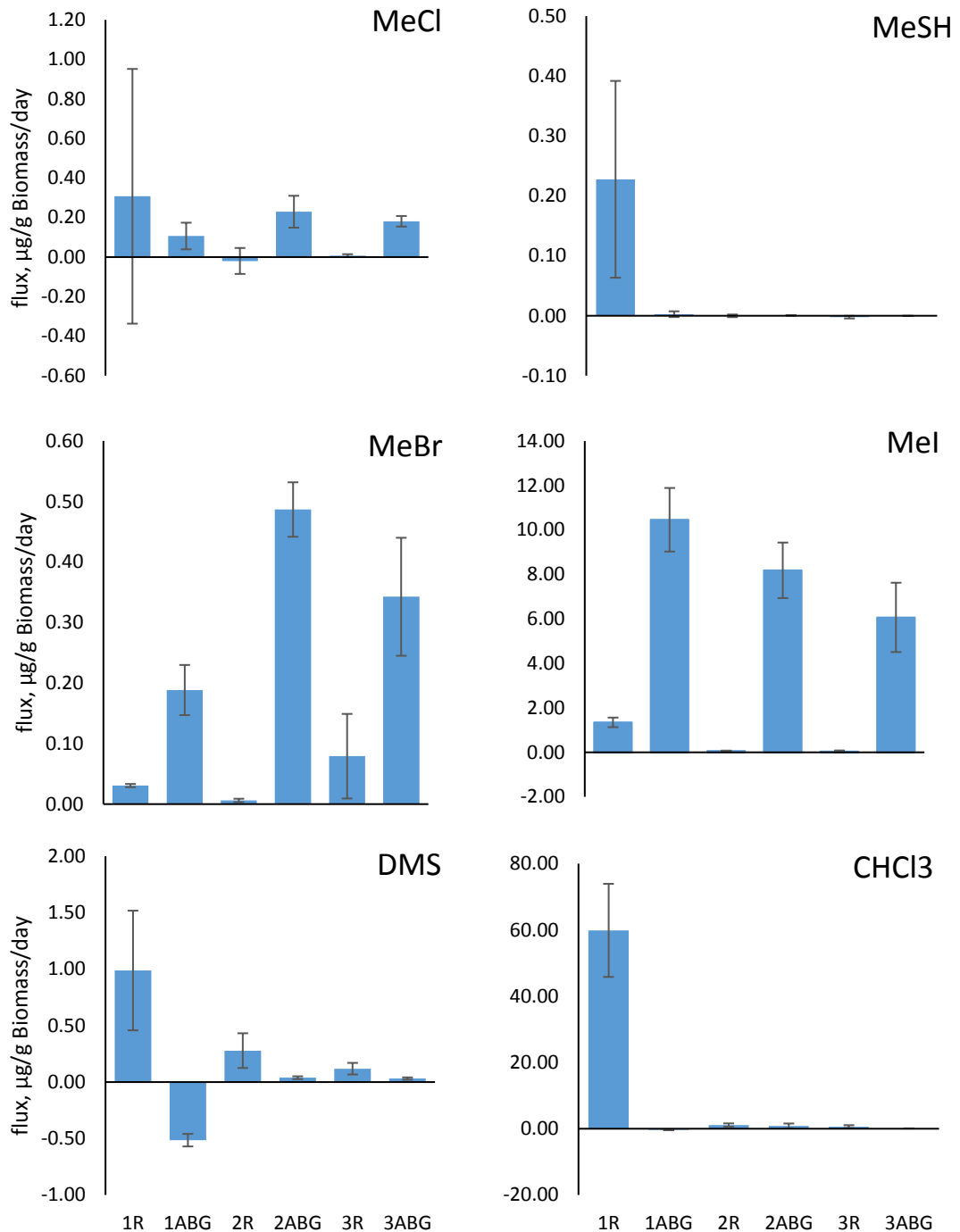


Figure 5.4 Gas fluxes from *Raphanus sativus* cv. 'WeedCheck' roots and aboveground biomass over 3 growth stages. The change in concentration of gases over a 20 minute period was extrapolated to give a value of micrograms flux per gram plant dry biomass per day. Horizontal axis markers indicate growth stage (1 = vegetative growth; 2 = flowering; 3 = senescent) and section of plant (R = roots; ABG = aboveground biomass). Error bars give ± 1 standard error. $n = 3$ for growth stages 1 and 3; $n = 5$ for the flowering stage.

5.4.1.3 *Raphanus sativus* cultivar 'Diablo'

Raphanus sativus cv. 'Diablo' root biomass increased from vegetative (0.42 ± 0.19 g) to flowering (11.01 ± 4.24 g) before decreasing slightly in senescent plants (10.77 ± 3.09 g); ANOVA gave a between groups significance figure of 0.08, indicating that the groups were not significantly different from another. Post-hoc analyses indicated significant differences between vegetative stage root mass and the masses of roots at the later stage ($P < 0.05$). Aboveground biomass followed the same trend (vegetative: 2.53 ± 0.90 g; flowering: 14.78 ± 2.78 g; senescent: 13.32 ± 0.38 g), with ANOVA producing a between groups significance figure of $P = 0.004$; Tukey's test found that flowering and senescent biomass did not significantly differ.

The trends observed in *R. sativus* cv. 'Diablo' were similar to those in 'WeedCheck,' with some notable differences (Figure 5.5). A negative methyl chloride flux was observed in vegetative stage roots, while the aboveground biomass reported positive fluxes at all stages. Methane thiol levels were low in all stages, with high variability. Methyl bromide production peaked in flowering stage plants at nearly double the value observed in 'WeedCheck,' but with high variability (1.16 ± 0.43 $\mu\text{g/g}$ dry biomass/day). Methyl iodide release followed a similar trend to methyl bromide, aboveground biomass emissions peaking in flowering plants at 30.97 ± 11.14 $\mu\text{g/g}$ dry biomass/day; production in the roots was highest per gram biomass in vegetative stage plants (1.15 ± 0.69 $\mu\text{g/g}$ dry biomass/day). DMS emissions were negative in vegetative roots but positive in all other samples, with high variability. Chloroform production was again highest in the roots of vegetative stage plants (53.69 ± 28.31 $\mu\text{g/g}$ dry biomass/day).

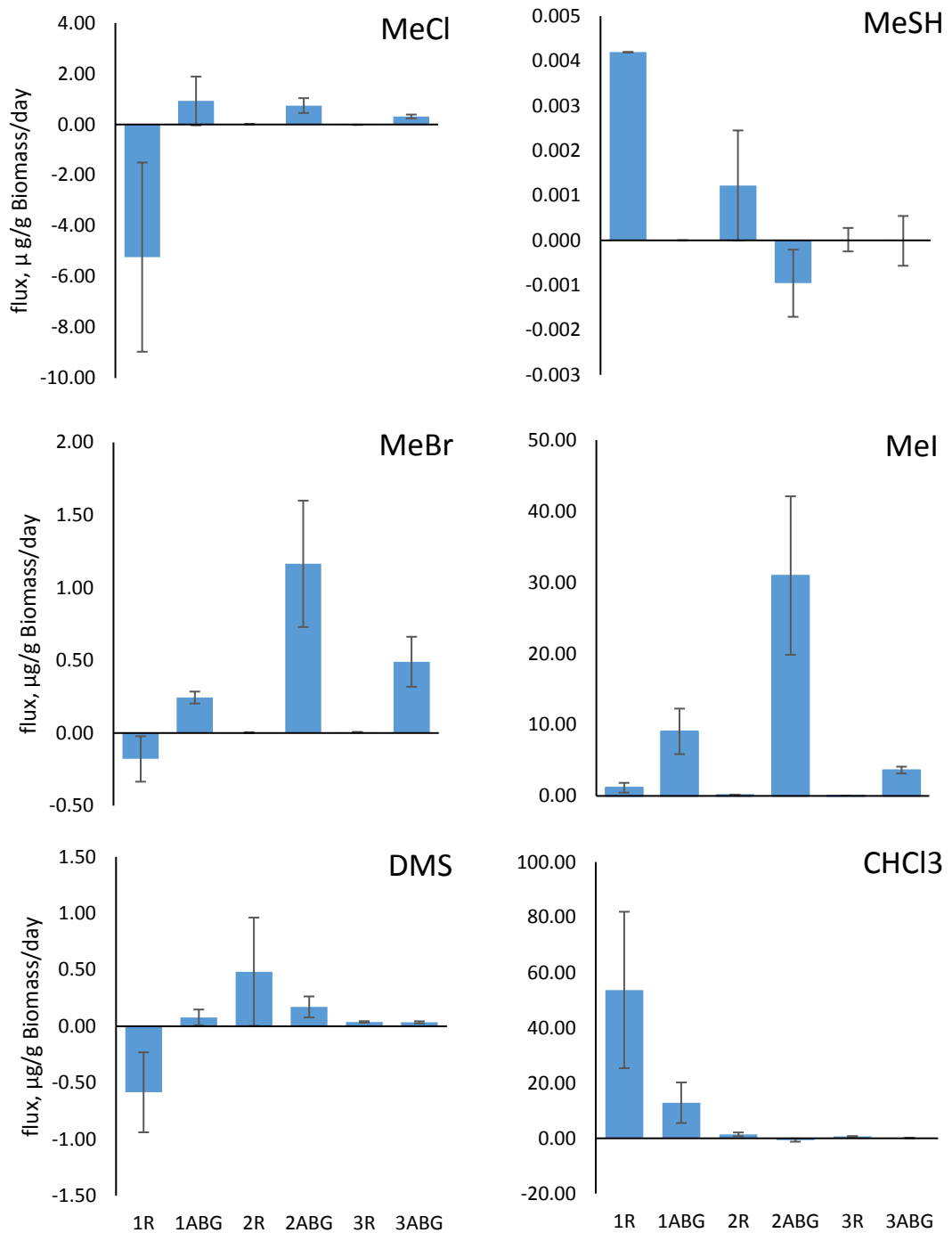


Figure 5.5 Gas fluxes from *Raphanus sativus* cv. 'Diablo' roots and aboveground biomass over 3 growth stages. The change in concentration of gases over a 20 minute period was extrapolated to give a value of micrograms flux per gram plant dry biomass per day. Horizontal axis markers indicate growth stage (1 = vegetative growth; 2 = flowering; 3 = senescent) and section of plant (R = roots; ABG = aboveground biomass). Error bars give ± 1 standard error. The value for methanethiol in vegetative stage roots is taken from a single value. $n = 3$ for all growth stages.

5.4.1.4 *Eruca sativa* cultivar 'Nemat'

Rocket cv. 'Nemat' continued the trend of increased biomass with subsequent growth stages. Root biomass in vegetative plants was 0.16 ± 0.33 g, growing to 1.77 ± 0.38 g in flowering and 2.18 ± 0.65 g in senescent plants (ANOVA $P = 0.037$); pairwise comparison of the groups found a significant difference between vegetative and senescent root biomasses ($P = 0.038$). Aboveground biomass increased from 0.88 ± 0.19 g in vegetative plants to 6.11 ± 0.49 g in flowering plants, and 7.27 ± 1.76 g in senescence. Between groups differences were significant (ANOVA $P = 0.003$), and post-hoc pairwise comparison with Tukey's test found that vegetative stage aboveground biomass differed significantly from the two later growth stages ($P < 0.01$).

The emissions profiles from *Eruca sativa* cv. 'Nemat' at different growth stages varied from those observed in *B. juncea* and *R. sativus*. Methyl chloride flux was highly variable, giving error greater than the average value in vegetative and senescent plants, as well as in the roots of flowering plants. Methane thiol fluxes were in the nanogram range with high error (a single reading is given for vegetative stage above and belowground biomass, resulting in no error bars). Methyl bromide production peaked in both roots and the aboveground biomass at flowering (roots: 0.019 ± 0.009 $\mu\text{g/g}$ dry biomass/day; ABG: 0.29 ± 0.18 $\mu\text{g/g}$ dry biomass/day). Methyl iodide production from the roots was the highest in flowering stage plants of the cultivars tested, at 0.24 ± 0.07 $\mu\text{g/g}$ dry biomass/day – this value was used to generate Figure 5.10; production in the aboveground biomass peaked at flowering (10.02 ± 4.61 $\mu\text{g/g}$ dry biomass/day). DMS fluxes were generally positive in the roots, and negative or near zero in the aboveground biomass. The Flux_{DMS} from *E. sativa* cv. 'Nemat' flowering stage roots was also used for Figure 5.10 (0.66 ± 0.17 $\mu\text{g/g}$ dry biomass/day). Production of chloroform followed a similar pattern to that observed in the other tested species: *E. sativa* vegetative stage roots gave the highest flux recorded, at 153.68 ± 84.74 $\mu\text{g/g}$ dry biomass/day.

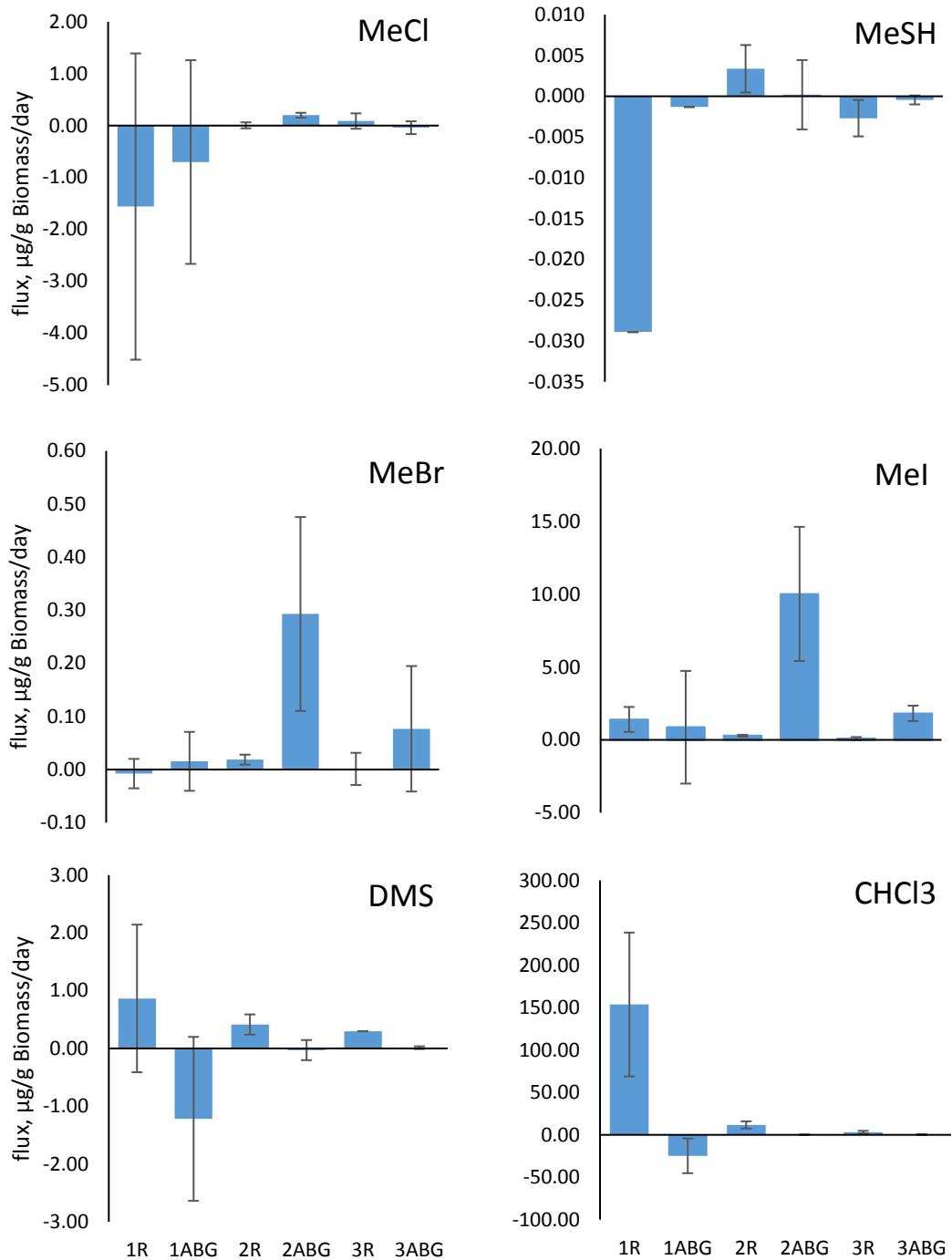


Figure 5.6 Gas fluxes from *Eruca sativa* cv. 'Nemat' roots and aboveground biomass over 3 growth stages. The change in concentration of gases over a 20 minute period was extrapolated to give a value of grams flux per gram plant dry biomass per day. A, methyl chloride; B, methane thiol; C, methyl bromide; D, methyl iodide; E, dimethyl sulphide; and F, chloroform. Horizontal axis markers indicate growth stage (1 = vegetative growth, 6 weeks; 2 = flowering; 3 = senescent) and section of plant (R = roots; S = aboveground biomass). Error bars give ± 1 standard error.

5.4.1.5 Total outputs from plants at each growth stage

The fluxes of each compound from the roots and aboveground biomass at each growth stage were multiplied by the average dry biomass of those sections, to give an estimate of the average per-plant flux (Table 5.4).

5.4.1.6 Estimating contributions of brassicas to global atmospheric budgets

Available data on the yields of mustard seed and radishes were used to calculate the dry mass of commercially produced mustard and radishes, and from there estimate a value for the output of methyl bromide from total commercial production of these crops (Table 5.5). The yield data from 2016 was used for estimation of mustard biomass (FAOSTAT, 2017); the estimate for radish production was taken from a book and gives only the typical global production of radish per annum, accurate at the time of printing (Dixon, 2006).

Table 5.4 Total flux per plant, based on average dry biomass

Species and	Stage	Biomass	Average mass, g	Flux, µg/day per plant												
				MeCl	±	MeSH	±	MeBr	±	MeI	±	DMS	±	CHCl3	±	
<i>Brassica juncea</i>	ISCI99	V	BBG	0.147	0.043	0.052	0.001	0.002	0.011	0.005	0.385	0.120	-0.165	0.060	5.778	10.876
		ABG	0.847	-1.027	0.869	0.010	0.012	0.077	0.036	10.562	0.580	-0.784	0.339	0.051	0.090	
	F	BBG	0.963	0.182	0.117	0.003	0.004	0.017	0.009	0.069	0.004	-0.067	0.116	7.793	4.042	
		ABG	3.420	1.036	0.519	0.006	0.005	1.742	0.077	19.583	1.547	0.469	0.446	0.742	0.805	
	S	BBG	0.763	0.012	0.046	0.016	0.013	0.014	0.002	0.118	0.053	0.783	0.578	9.077	1.556	
		ABG	8.150	-0.874	1.654	0.022	0.014	0.229	0.091	0.647	0.231	1.856	1.117	0.052	0.335	
<i>Raphanus sativus</i>	WeedCheck	V	BBG	0.233	0.072	0.150	0.053	0.038	0.007	0.001	0.314	0.050	0.231	0.124	13.969	3.279
		ABG	1.453	0.155	0.098	0.004	0.007	0.274	0.060	15.198	2.078	-0.748	0.081	-0.540	0.112	
	F	BBG	7.142	-0.141	0.469	-0.001	0.016	0.044	0.020	0.452	0.098	1.988	1.098	7.926	3.517	
		ABG	16.034	3.680	1.292	0.010	0.007	7.803	0.721	131.230	20.018	0.615	0.204	13.441	11.719	
	S	BBG	7.783	0.057	0.057	-0.018	0.017	0.616	0.544	0.299	0.345	0.923	0.399	4.824	3.422	
		ABG	17.903	3.241	0.479	-0.003	0.002	6.132	1.745	108.639	27.902	0.556	0.184	1.474	0.280	
	Diablo	V	BBG	0.423	-2.214	1.579	0.002	0.000	-0.076	0.066	0.487	0.291	-0.248	0.150	22.729	11.984
		ABG	2.533	2.353	2.434	0.000	0.000	0.618	0.105	22.987	8.106	0.199	0.176	32.614	18.598	
	F	BBG	11.013	0.146	0.027	0.013	0.014	0.021	0.031	1.480	0.581	5.318	5.283	16.024	7.304	
		ABG	14.783	11.018	4.337	-0.014	0.011	17.213	6.430	457.801	164.669	2.531	1.373	-9.513	8.716	
S	BBG	10.773	-0.121	0.065	0.000	0.003	0.052	0.026	0.367	0.058	0.414	0.069	7.048	1.664		
	ABG	13.317	4.211	1.005	0.000	0.007	6.528	2.291	48.397	6.405	0.460	0.127	1.431	0.982		
<i>Eruca sativa</i>	Nemat	V	BBG	0.157	-0.244	0.462	-0.005	0.000	-0.001	0.004	0.220	0.134	0.136	0.200	24.076	13.276
		ABG	0.883	-0.621	1.733	-0.001	0.000	0.014	0.049	0.766	3.417	-1.076	1.253	-21.890	18.098	
	F	BBG	1.773	0.009	0.102	0.006	0.005	0.033	0.017	0.507	0.116	0.735	0.309	20.741	7.522	
		ABG	6.110	1.216	0.288	0.001	0.026	1.790	1.115	61.230	28.152	-0.176	1.063	0.664	0.888	
	S	BBG	2.180	0.190	0.323	-0.006	0.005	0.003	0.066	0.198	0.227	0.650	0.004	6.966	3.357	
		ABG	7.273	-0.297	0.897	-0.003	0.004	0.558	0.859	13.248	3.853	0.097	0.168	1.698	0.418	

Stage: V = vegetative, F = flowering, S = senescent; Biomass: BBG = belowground biomass (roots), ABG = aboveground biomass. n = 3 for all sampled plants except WeedCheck F stage, where n = 5

Table 5.5 Estimates of the global yearly methyl bromide flux due to growth of mustard and radish as cash crops

Crop	Yield	Root dry mass /yr	Aboveground dry mass /yr	MeBr production over 8 weeks
Mustard seed	0.7 Mt/yr ¹	475 t/yr	1687 t/yr	0.078 Gg/yr
Radish	7 Mt/yr ²	296 t/yr	663 t/yr	0.012 Gg/yr

1. (Banerjee et al., 2012, FAOSTAT, 2017)
2. (Dixon, 2006)

5.4.2 Toxicity of emitted compounds to nematodes

A nested-dish assay was developed to test the toxicity of emitted compounds to nematodes when in a volatile form. Initial testing compared the toxicity of compounds applied in solution to nematodes suspended in buffer with compounds applied separately to the buffer and allowed to volatilise. Following 18h incubation with methyl iodide, it was found that both treatments resulted in high *C. elegans* mortality ($97.38 \pm 1.27\%$ in solution, $99.38 \pm 0.33\%$ in the outer dish), with no significant difference between the two ($P > 0.05$); both treatments were distinct from the untreated control ($P < 0.001$) (figure 5.7). The initial volume of methyl iodide was explorative, informing subsequent experiments.

To test toxicity for plant-parasitic nematodes, and to investigate any synergistic effect between compounds, *G. pallida* J2s were incubated with methyl iodide diluted in ethanol, with or without an additional aliquot of chloroform (figure 5.8). No statistical difference between treatments at the same concentration of methyl iodide was observed. Chloroform tested alone appeared to have no impact on nematode viability.

The toxicity of dimethyl sulphide (DMS) was then assayed with *G. pallida* J2s (figure 5.9). All concentrations of DMS appeared to result in near 100% mortality for nematodes initially, but some nematodes were able to recover after overnight incubation, suggesting that some individuals experienced a nematostatic rather than nematocidal effect. Volumes of DMS applied to nematodes were made to match those of methyl iodide previously trialled.

The effects of methyl iodide and DMS on encysted eggs was investigated at concentrations estimated to be of biological relevance, and mortality was measured by staining of dead nematodes with Meldola's blue dye (Kroese et al., 2011). Using a dosage based on the maximum output from 1 g dry belowground biomass, toxicity was observed in eggs exposed to 49 times daily flux ($11.91 \mu\text{g}$ of methyl iodide and $32.49 \mu\text{g}$ of dimethyl sulphide, equivalent to 7 weeks cumulative exposure). The effects of DMS and methyl iodide were additive, such that combined application of a 7-week flux of dimethyl sulphide and methyl iodide resulted in significantly higher mortality in eggs than application of dimethyl sulphide alone (Figure 5.10).

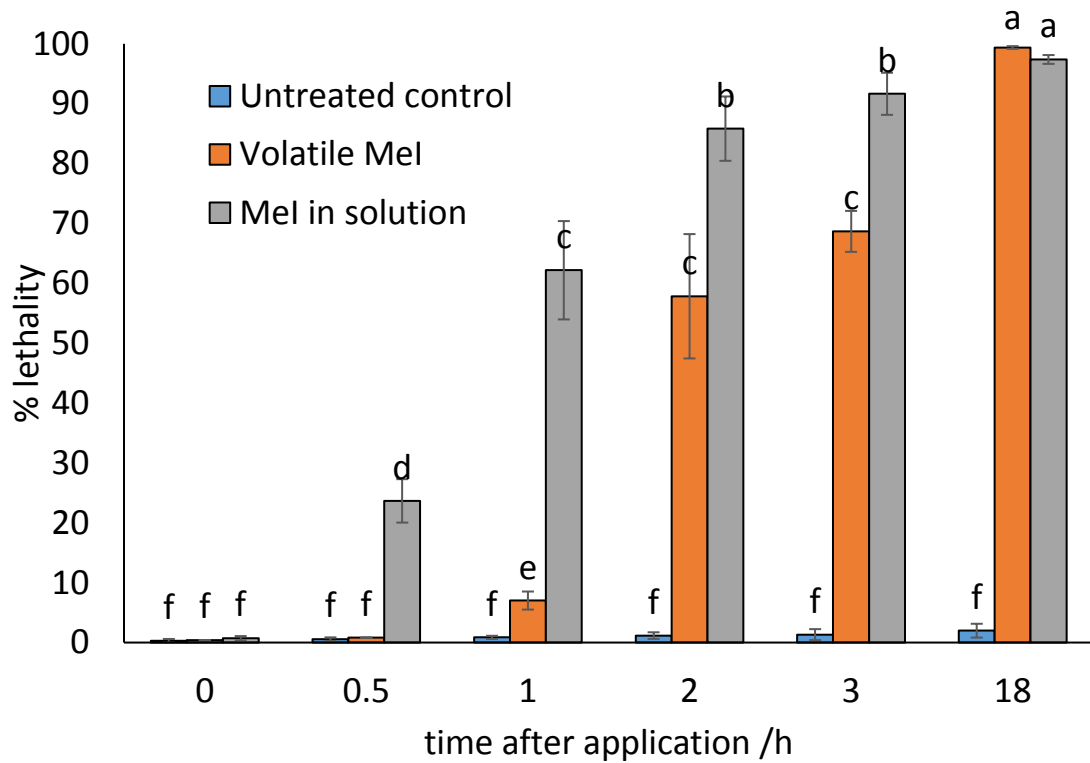


Figure 5.7 Toxicity of methyl iodide to *C. elegans* N2 adults in applied solution and in a volatile form. An aliquot of 3 μ l (6.84 mg) methyl iodide was applied to each of the treatments, and the number of dead nematodes counted before and at 0.5, 1, 2, 3 and 18 hours after application. Methyl iodide appears to act more quickly when applied in solution, but this difference disappeared after overnight incubation. $N = 226 \pm 42$; groups are based on a Student-Newman-Keuls analysis, $P < 0.05$. A t-test indicated $P < 0.001$ for the treatments at 18h versus the non-treatment control.

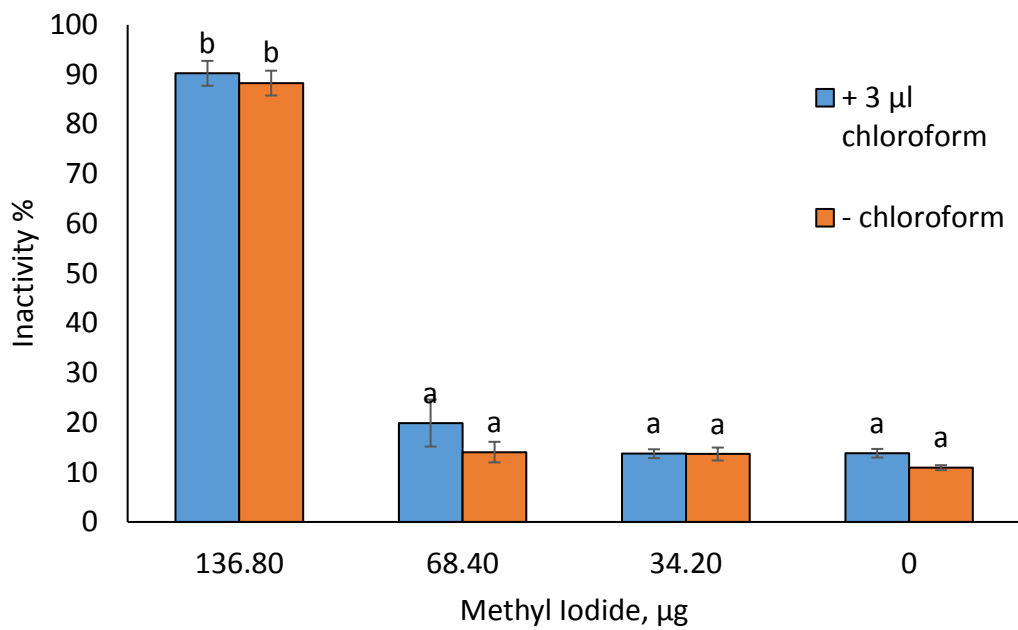


Figure 5.8 Inactivity in *Globodera pallida* J2s after 18h incubation with volatile methyl iodide, with or without additional chloroform. The x-axis displays the total volume of methyl iodide solution in each treatment, applied diluted with absolute ethanol in a 3 µl aliquot. No statistical difference due to addition of chloroform was detected. Exposures were performed in triplicate, $n=151 \pm 28$. Labels give groups based on Student-Newman-Keuls analysis.

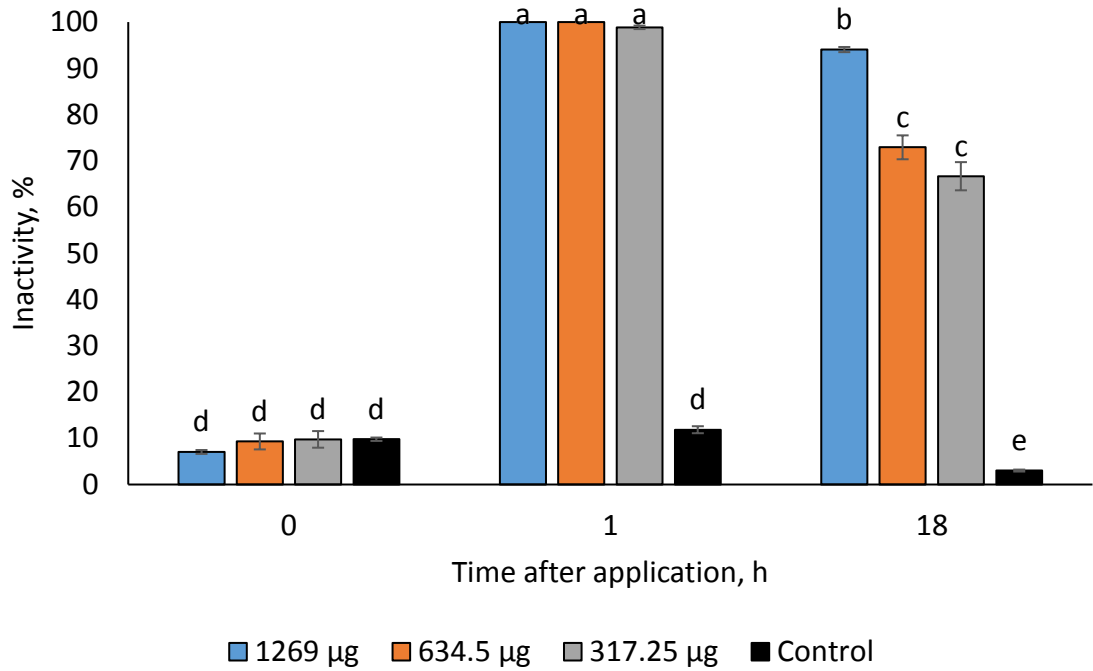


Figure 5.9 Inactivity in *Globodera pallida* J2s after incubation with volatile dimethyl sulphide. DMS was applied diluted in ethanol in 3 µl aliquots. Nematodes initially appeared to have been killed outright at all concentrations of applied DMS, but there was a dose-dependent recovery of some nematodes after overnight incubation. Exposures were performed in triplicate, $n=271 \pm 8$. Groupings are based on a Student-Newman-Keuls analysis, $P < 0.05$

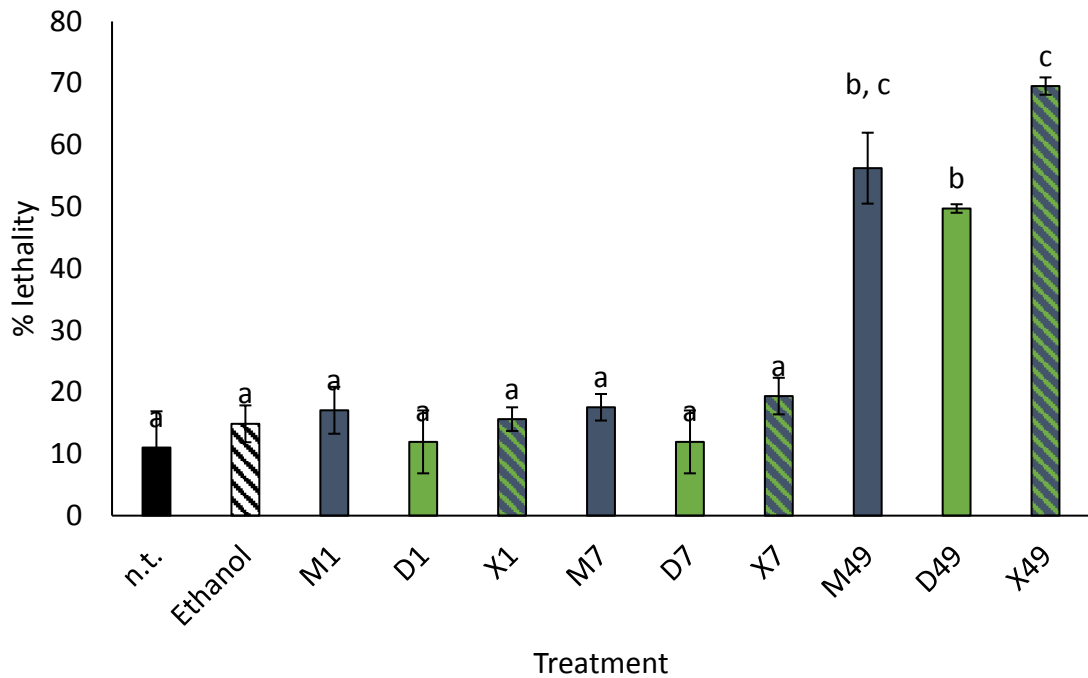


Figure 5.10 Toxicity of methyl iodide and dimethyl sulphide to *Globodera pallida* encysted eggs. Cysts suspended in 2 ml sterile distilled water were exposed to volatilised methyl iodide and dimethyl sulphide, applied in a 14 μ l aliquot diluted in ethanol. Doses were based on the 24h flux from 1 g dry root biomass from flowering stage *R. sativus* cv. 'Diablo': 1 = 1 times the daily flux (methyl iodide = 0.243 μ g; DMS = 0.663 μ g); 7 = 7 times the daily flux; and 49 = 49 times the daily flux; M = methyl iodide in ethanol alone; D = dimethyl sulphide in ethanol alone; X = combined doses of methyl iodide and dimethyl sulphide in ethanol. Data labels give groupings based on a Student-Newman-Keuls analysis, $P \leq 0.05$. Exposures were set up with 3 cysts per plate in triplicate, $n = 433 \pm 92$ eggs per exposure.

5.5 Discussion

5.5.1 Brassicas produce bioactive methyl halides and dimethyl sulphide

It was demonstrated that brassicas emit methyl bromide and methyl iodide reliably, and over the course of their life cycle from seed to senescence. This is in line with previous studies that have noted the production of methyl bromide from *Brassica napus* (Gan et al., 1998, Mead et al., 2008), and methyl iodide from *B. oleracea* (Saini et al., 1995). The genes involved in production of methyl halides and methane thiol have been identified in *Arabidopsis thaliana* as S-adenosyl-L-methionine (SAM) dependent methyltransferases termed HOL (Harmless to Ozone Layer) or HTMT (halide/thiol methyltransferase) genes (Nagatoshi and Nakamura, 2009, Rhew et al., 2003, Saini et al., 1995, Itoh et al., 2009). Phylogenetic and enzymatic studies have confirmed the presence of HTMT activity in plant families including Brassicaceae and Poaceae (including the important food crops wheat, *Triticum aestivum*; rice, *Oryza sativa*; and corn, *Zea mays*) (Itoh et al., 2009, Rhew et al., 2003) with the highest such activity observed in brassicas (Saini et al., 1995). The activity of HTMTs has been suggested as a protective measure, eliminating potentially cytotoxic halide ions from cells (Saini et al., 1995). In brassicas, a role for HTMTs in glucosinolate metabolism has been suggested, with AtHOL1 found to be highly reactive with thiocyanate ions (NCS⁻, a breakdown product of glucosinolates, see Chapter 1.3.3) and *hol1* mutant seedlings showing increased susceptibility to *Pseudomonas syringae* (Nagatoshi and Nakamura, 2009).

The profile of emitted gases changed over the growth period of the plant (Figure 5.3, 5.4, 5.5 and 5.6; Table 5.4). The biomass of plants generally increased with growth period. The plants with highest biomass therefore produced the greatest quantity of compounds. *Raphanus sativus* cv. 'Diablo' aboveground biomass generated the highest total output of methyl chloride, methyl bromide and methyl iodide, while the highest output of dimethyl sulphide was reported from the roots of the same plants. The highest flux for chloroform was seen in vegetative stage 'Diablo' ABG, and in 'Nemat' vegetative roots.

5.5.1.2 Negative flux values

A number of negative flux values were observed in a number of the samples, often accompanied by high error (Figures 5.3, 5.4, 5.5 and 5.6; Table 5.4). Ambient levels of a compound present in the sampling chambers may decrease over time after the chamber is sealed in the absence of the plant releasing the compound, but this does not necessarily imply that the plant is actively taking up the compound. Negative fluxes observed in the roots are likely due to dissolution of the compound into the water in which the roots are suspended. In the upper sampling chamber, compounds may be passively adsorbing onto the plant in the absence of compound emitted from the plant. The presence of microbes able to metabolise a given compound may also explain some of the negative fluxes: the large negative flux value for chloroform in *E. sativa* cv. 'Nemat' vegetative aboveground biomass may be related to the high positive flux observed in the roots (Table 5.4): the abundance of chloroform generated in the roots could lead to an increase in the population of chloroform-metabolising bacteria (Jugder et al., 2017), the presence of which on the surface of the aboveground biomass of the plant would lead to active intake of chloroform.

5.5.2 Atmospheric impacts of brassicaceous crops

Production of methyl bromide has previously been measured in oilseed rape, and the contributions of oilseed rape production to global methyl halide budgets has been estimated (Gan et al., 1998), with the most recent analysis giving a value of 5.5 Gg/yr MeBr from oilseed production, and 0.005 Gg/yr from mustards (Mead et al., 2008). The value estimated from commercial mustard production presented here is higher than those previously given, and no such estimate has been made for radish production. As the tested radish cultivars generated higher fluxes of methyl bromide than mustard, both per g dry biomass (Figures 5.3, 5.4, and 5.5) and per plant (Table 5.4), this may have important implications for monitoring of tropospheric methyl bromide.

The calculated values are necessarily inaccurate. Variation of fluxes based on temperature and varying soil halide concentrations are not factored into the analysis, and the sampled time points likely only give a snapshot of the variation in fluxes over the course of the growing period of a crop, and cannot factor in the variations between different brassica crops and the many cultivars thereof. The differences in emissions

between the two *E. sativa* cultivars suggest that there is much intraspecific as well as interspecific variation. Estimating contributions to atmospheric budgets based on crop production requires accurate data on the yields of each crop produced per annum. The UN's Food and Agricultural Organisation Statistical Database is a valuable resource for monitoring of crop production, but detail on the varieties of brassicas grown beyond separation of mustard seed and "cabbage and other brassicas" is unavailable (FAOSTAT, 2017). Emissions from rice paddies analysed over the course of a growing season have demonstrated variation in output throughout the life of the crop (Redeker et al., 2004). A more granular sampling approach could therefore be taken to analysis of biofumigant crops in the field, with more frequent sampling to allow for a model of the flux profile of a given biofumigant to be generated.

The impacts of biofumigation on atmospheric methyl bromide are impossible to estimate without reporting on the use of biofumigants. Simple reporting of the biofumigant crop used and the seeding density should allow for an estimate of the total dry biomass to be calculated (Doheny-Adams et al., 2018), from which the potential output of methyl bromide can then be determined. No such reporting currently exists, meaning that the potential environmental impacts of growing brassicas for biofumigation or as cover crops are unknown. Future expansion of biofumigation management practices could therefore contribute to uncertainty in monitoring of tropospheric methyl bromide, if not considered in environmental analyses.

5.5.3 Toxicity of volatile compounds emitted by brassicas

The compounds emitted by the tested brassica cultivars were found to be toxic to *C. elegans* adults and to *Globodera pallida* juveniles and encysted eggs (Chapter 5.4.2).

Methyl iodide has been investigated as an alternative fumigant to methyl bromide, apparently preferable because of its low environmental impact, but was rejected in the USA due to worries about local toxicity (Pelley, 2009). The mechanism of methyl iodide toxicity in mammalian cells has been suggested to include depletion of glutathione and disruption of cell membranes (Chamberlain et al., 1999), resulting in severe and long-lasting neurotoxicity following acute exposure (Nair and Chatterjee, 2010) and with less severe effects from chronic, low-level exposure (Chamberlain et al., 1999). Methyl

bromide toxicity represents similarly in mammals (Hustinx et al., 1993), also with effects from chronic exposure (Yang et al., 1995). The mechanisms by which methyl halides cause cytotoxicity, namely excess conjugation of glutathione and disruption of cell membranes, are likely conserved across diverse animal phyla, including nematodes for which conjugation of glutathione is a known response to xenobiotic compounds (see Chapter 3). Inhalation of high concentrations of dimethyl sulphide have been shown to be toxic to humans and mice, both through inducing reduction of available oxygen, and through disruption of the nervous system (Terazawa et al., 1991). Plant-parasitic nematodes have been shown to endure anoxic states for up to 14 days, in the case of *Bursaphelenchus xylophilus* (Kitazume et al., 2018), so this is unlikely to be the mode of action of DMS.

Toxicity of the trialled compounds was observed in nematodes exposed to high concentrations of the compounds in a closed environment, poorly mimicking the soil environment. In soil planted with a given brassica and infested with potato cyst nematodes, encysted eggs located near to brassicas roots could be exposed to a constant but low flux of all of the investigated compounds for the entire growth period of the crop. As the nested-plate assay involved single point applications of compound doses and require the plate to be sealed airtight, a better understanding could be gained from development of an assay in which nematodes or cysts are exposed to chronic, low doses of the compounds emitted by brassicas. Pot and field trials in which *G. pallida* cysts are encapsulated in mesh bags placed into the soil in the vicinity of brassicas could identify if release of compounds from brassica roots into the soil environment contributes to the control of potato cyst nematodes.

The intractability of methyl chloride, methane thiol and methyl bromide also contributes some uncertainty to the conclusions of the presented work. Though the methyl chlorides are known to be broadly bioactive, likely with similar modes of action to methyl iodide, a system in which gaseous compounds can easily be delivered to nematodes would allow for investigation of any interactions between the compounds of interest.

5.6 Summary

-
- Crops grown for biofumigation and as cover crops emit bioactive compounds including methyl halides, methane thiol and dimethyl sulphide
 - The release of the ozone-depleting agents methyl bromide and methyl chloride may have impacts on the atmosphere, and should be considered when expanding growth of brassicas both as cash crops and for biofumigation
 - The compounds emitted from brassicas are toxic to both free-living and plant-parasitic nematodes in a closed environment. An additive effect was observed when nematodes were exposed to both methyl iodide and dimethyl sulphide.
-

Chapter 6 General Discussion

A review of the published literature on biofumigation reveals that the majority of research focuses on the effectiveness of biofumigants as a control method, and on maximisation of the delivery of isothiocyanates into the soil (see Chapter 1.3). The work presented here addresses some of the gaps in knowledge relating to biofumigation, including the effects of isothiocyanates on nematode metabolism and the impact of growing biofumigants on the soil and the environment. An effort was also made to develop a screening process for biofumigant activity, and to develop transgenic reporters with direct relevance to plant-parasitic nematodes.

6.1 Investigating xenobiotic metabolism of *Globodera pallida*

A number of genes were directly implicated in the response of *Globodera pallida* J2s to contact with isothiocyanates. Comparison of sequenced cDNA with the genes predicted in the gene assembly (Cotton et al., 2014) found good overall similarity, with 11 of the 18 investigated genes having strong homology to the predicted sequences; 7 of these translated to amino acid sequences that had >99 % similarity to the predicted protein (GP01278, GP02405, GP08126, GP10083, GP10467, GP10686, and GP12030). While other genes were less well conserved relative to the predicted sequence, only 2 of the 18 genes investigated had poor homology with the predicted gene (GP02984 and GP08879), indicating that the quality of the gene predictions of the genome assembly is generally good.

The amino acid sequences encoded by the investigated genes suggest a range of roles, based on homology to known proteins and to specific domains (see Chapter 3.5.1). A number of genes are implicated in xenobiotic metabolism. GP02405 and GP11984 were identified as glutathione S-transferases, the enzymes most closely associated with detoxification of isothiocyanates (Jiao et al., 1996, Kolm et al., 1995, Zhang, 2000). Given the strong homology of GP02405 to *Mi-gst-1*, its identification as a sigma-class GST, and its apparent role in *G. pallida* xenobiotic metabolism, it is suggested that it be named as *Gp-gst-1*, in-line with suggested naming conventions for parasitic nematode genes (Bird and Riddle, 1994). Further investigation of GP11984 should confirm its role as a GST. GP03693 was identified as a carboxylesterase, implicated in phase I biotransformation

of xenobiotic compounds (Laizure et al., 2013). While carboxylesterases principally hydrolyse carboxyesters, they have been demonstrated to catalyse hydrolysis of a broad range of substrates (Aranda et al., 2014), which could include preparing isothiocyanates for conjugation with reduced glutathione, pending further investigation. Studies on xenobiotic metabolism of isothiocyanates in the context of cancer prevention have identified a modulating effect on a number of phase I and II enzymes, but have largely focused on CYPs and GSTs (Abdull Razis et al.).

Other genes found to be significantly up-regulated in Dazomet-exposed *G. pallida* J2s could have indirect roles in response to contact with isothiocyanates. GP09707 was identified as a putative phosphoethanolamine methyltransferase (PMT), homologous to *C. elegans* PMT-1. PMTs are critical in maintenance of cell membranes such that RNAi knockdown of *C. elegans* PMT-2 results in nematodes with arrested growth that are unable to reproduce (Brendza et al., 2007). GP04700 was predicted as an S-adenosylmethionine synthetase, an enzyme that generates the substrate for PMTs (Markham and Pajares, 2009). The simultaneous up-regulation of both GP04700 and GP09707 suggest that they may be involved in repair of the cell membranes in response to toxin-induced damage, due to the role of PMT in membrane biogenesis (Bobenchik et al., 2011). Investigation of the role of GP09707 in *G. pallida* with RNAi J2s could determine whether or not it plays a crucial role in maintenance of normal cellular function, as in *C. elegans* PMT-1 (Brendza et al., 2007) and PMT-2 (Palavalli et al., 2006). If such a role is identified, GP09707 could provide a valuable target for control of *G. pallida*. PMTs have no homolog in mammals, their equivalent functions being performed by unrelated methyltransferase enzymes (Schubert et al., 2003); targeting of nematode PMTs should therefore be a biosafe approach.

Potential roles in signalling were identified in a number of the genes up-regulated in response to Dazomet. GP01278, as a putative tyrosine aminotransferase (TAT) likely catalyses the breakdown of tyrosine (Mehere et al., 2010, Rettenmeier et al., 1990), the breakdown products of which are involved in cellular communication (Ferguson et al., 2013). GP10083 likely encodes a sodium/nucleoside transporter, facilitators of intercellular signalling (Parkinson et al., 2011). Cell signalling in response to contact with

a toxin prepares neighbouring cells for contact with the toxin, in principle, though some toxins exploit these pathways (Lahiani et al., 2017).

Roles in response to Dazomet could be less reliably predicted for a number of the genes investigated. GP10686 is predicted to be involved in metabolism of sugar, and GP10467 matches well with metalloproteases, involved in protein folding; these could have roles in mobilising energy and proteins for xenobiotic metabolism, but no such link was suggested in the literature. One of the genes could not be cloned from cDNA, and 3 of the 17 remaining genes were found not to be up-regulated when analysed by qPCR: GP02040, GP04777 and GP08879.

Genes identified as putative effectors (GP07079, GP08126 and GP12030) could have a role in response to host defences, as one of the principal roles ascribed to effectors is that of host defence suppression (Quentin et al., 2013). A general response to cytotoxicity in plant-parasitic nematodes could be to up-regulate effectors, as the nematode could respond to all contact with bioactive compounds as an indicator of contact with a host plant. While effectors have been identified through transcriptomic analyses of gene regulation at different life stages (Elling et al., 2009), the stimuli that induce these regulatory changes are unexplored. As the mechanisms by which nematodes recognise that they have reached the host and selected an appropriate feeding site are as yet undescribed (Bohlmann and Sobczak, 2014), contact with xenobiotic compounds could form part of the likely multifaceted complex of triggers that lead to feeding site selection, up-regulation of relevant genes, and induction of the factors that lead to growth and subsequent development of the juvenile nematode.

6.2 Screening plant extracts for biofumigant activity

The use of *C. elegans* reporter lines to detect biofumigant activity was demonstrated, with activity reported even from dilute plant tissue extracts. The response of reporters to several isothiocyanates at low concentrations suggest good sensitivity of the assay, but poor specificity; low concentrations of isothiocyanate activity in plant extracts can therefore be detected, but no identification of specific constituent compounds can be made, and no quantification can be taken from the response. However, relative quantification, by comparison of the differential response of reporters to dilute plant

extracts, can be inferred: in two plant extracts of the same concentration, greater fluorescence observed in the reporters suggests a higher overall concentration of isothiocyanates in the extract, and therefore of glucosinolates in the tissues of the plants, as observed in *B. juncea* and *S. alba* when diluted (Figure 4.9).

Development of reporter lines for different bioactive compounds could allow for screening of various bioactivities among plant extracts, beyond the scope of biofumigation. The study from which the *gst-31::gfp* lines were derived also demonstrated reporters that gave a specific up-regulatory response to chloroquine, imidacloprid and thiabendazole, compounds with distinct modes of action (Jones et al., 2013b). Screening plant extracts for the response related to these compounds could identify sources of similar compounds or help to identify novel compounds with similar activities from plant sources. In the case of chloroquine, an anti-malarial drug for which resistant strains of malaria now exist (Krafts et al., 2012), identification of novel compounds from plant sources could potentially generate new drugs for treatment of malaria, for which no resistance has developed. Novel analogues of thiabendazole and imidacloprid could similarly be identified. As imidacloprid is a neonicotinoid, insecticides implicated in the decline of bees and other insect pollinators (Tsvetkov et al., 2017, Woodcock et al., 2017), there is likely little appetite for development of new compounds of similar activity. Reporter lines that respond to other stimuli, such as nematicides that have been phased out (see Chapter 1.3.2), could be used to identify plant sources of compounds that are known to be active against pest nematodes in the field, which could then be applied in the same fashion as a biofumigant, provided that rigorous testing had been performed to rule out detrimental effects to the environment.

Reports on the efficacy of biofumigants have observed population reductions from plants with no glucosinolate content and therefore no release of isothiocyanates into the soil, such as corn and wheat (Bélair et al., 2016, McSorley, 2011, Vervoort et al., 2014). The observed effects on population are typically ascribed to mechanical disturbance during incorporation or to positive impacts on soil quality from the addition of green manure leading to an increase in organisms that predate or outcompete pests. Screening of these crops using XME reporters could reveal that there are bioactive components in the plant tissues that contribute to nematode control.

For expansion of the biofumigant toolkit, plant extracts that are screened and show various different bioactivities could provide a far more robust method of control against plant-parasitic nematodes and other soilborne pests. Where novel bioactivity is discovered in a plant species through the use of XME reporter nematodes, new biofumigant seed mixes could be developed that incorporate a range of plant crops. These could be designed to deliver a cocktail of bioactive compounds to soilborne pests, mirroring the approaches taken to overcome bacterial resistance, where multiple drugs are administered either simultaneously or in phases, in order to target all members of a population in which resistance to some or all of the drugs exists in separate organisms (Kim et al., 2014, Pal et al., 2015).

Screening of plants for new sources of isothiocyanate-based biofumigation and for methods of control based on separate modes of action could prove to be an important goal for the development of biofumigation as a management practice. The inconsistencies in biofumigation efficacy observed in the field (Chapter 1.3.5) require that research continues until methods are developed that can be applied and guarantee a given result. Expanding the range of traditional and novel biofumigant crops available will provide a greater range of tools that can be used to answer important research questions in the field.

6.3 Developing transgenesis of plant-parasitic nematodes

Attempts were made both to generate *C. elegans* reporters for *G. pallida* genes, and to generate transgenic *G. pallida* and *M. incognita*, in order to provide tools to more directly study cellular processes relating to plant-parasitic nematodes (Chapters 4.4.5 and 4.5.4). Transgenic *C. elegans* with reporter genes (GFP or mCherry) under control of *G. pallida* promoters did not result in expression of the reporter genes, despite confirmation of the presence of transgenes by PCR. Despite conservation of some gene functions, e.g. sequence homology between GP09707 and *C. elegans* PMT-1, this absence of expression could be explained by divergence between trans- and cis-regulatory elements between the species. Where coding DNA sequences may be necessarily conserved across species in order to maintain gene functionality, regulatory elements may diverge while maintaining function. Cis-regulatory elements are those regions of non-coding DNA that sit near to transcribed genes within the genome and act

in some way to regulate expression of those genes, such as promoters and enhancers (Wittkopp and Kalay, 2011), while trans-regulatory elements are those that act on the cis-regulatory elements to modulate changes in expression, including transcription factors and microRNAs (González-Barrios et al., 2015). Over time, divergence in the cis-regulatory elements surrounding a gene will not affect expression as long as those trans-regulatory elements that control expression maintain the modulation of the genes. This potential for divergence of regulatory elements was suggested as an explanation of the unexpected expression patterns observed in *C. elegans* transformed with GFP under the control of promoters from *M. hapla*: promoters for genes of conserved coding sequence resulted in expression patterns inconsistent with the roles of the genes involved (Gordon et al., 2015). The evolutionary distance between *C. elegans* and *M. hapla* is similar to that between *C. elegans* and *G. pallida* (Blaxter, 2011, Blaxter and Koutsovoulos, 2015). Therefore, an analogous variation in regulatory elements might be expected between *C. elegans* and *G. pallida*. The expression of genes with specific roles, such as in xenobiotic metabolism, is necessarily more specifically regulated than genes with constitutive, or “house-keeping,” roles. Transformation of model organisms such as *C. elegans* with reporter genes driven by promoters of plant-parasitic nematode housekeeping genes may prove more fruitful, but would have limited power for further investigation.

More reliable driving of gene expression in transgenic animals might be expected when transgenes are sourced from more closely related animals, such as potato cyst and root-knot nematodes (Decraemer and Hunt, 2013). Expression of GFP under control of the *G. pallida* GAPDH1 promoter was observed in a single transformed *M. incognita* egg (Figure 4.12). As discussed in Chapter 4, parthenogenetic *Meloidogyne spp.* display a number of features, some of these in common with *C. elegans*, which suggest they may be ideal candidates for generation of transgenic plant-parasitic nematodes. For instance, *M. incognita* produces clonal offspring (Trudgill, 1997) – which may be an advantage to generating stable transgenic lines – and can generate hundreds of viable offspring per adult on a broad range of host plant species within a matter of weeks (Trudgill and Blok, 2001), a longer generation time than *C. elegans*, but shorter than cyst nematodes (Turner and Subbotin, 2013). Generation of transgenic *M. incognita* expressing genes

under control of root-knot or cyst nematode promoters could therefore be used to investigate the roles of genes of interest in different life stages of the nematode. As *M. incognita* can utilise arabidopsis as a host, experiments in which transgenic plant-parasitic nematodes are grown within transgenic hosts could be set up, to investigate plant host-parasite relationships both in a biofumigant context (as arabidopsis is a brassica) and more generally, for instance utilising bimolecular fluorescence complementation (Shyu and Hu, 2008) to query host-parasite protein-protein interactions.

As the results here demonstrate that generation of transgenic *M. incognita* is both possible and observable, though difficult, future work should seek to develop the technique in order to generate a tractable system for the study of plant-parasitic nematodes and their interactions with their hosts on a level not yet available.

6.4 Bioactivity of volatile compounds released by plants

A number of bioactive compounds were identified and quantified as emitted from brassicas, including methyl bromide, a regulated soil fumigant that was the principal chemical for control of plant-parasitic nematodes before its regulation under the Montreal Protocol (UNEP, 2012). Testing of their bioactivity against *C. elegans* and *G. pallida* revealed that methyl iodide and dimethyl sulphide (DMS) were toxic to all tested life stages in both liquid and volatile forms (see Chapter 5.4.2). Despite the broad toxicity of chloroform, including to soilborne nematodes (Sarathchandra et al., 1995), no bioactivity was detected at any of the tested volumes. Methyl bromide is also known to be toxic to nematodes (Noling, 2002, Noling and Becker, 1994); however, due to its low boiling point at atmospheric pressure (3.56 °C) and the hazards associated with human exposure (Hustinx et al., 1993), it was deemed inappropriate to attempt to include it in the investigation. Methyl chloride and methane thiol were produced at lower levels and less consistently across the examined cultivars, and were similarly unsuited to study in the work presented here, as each is gaseous at room temperature (with boiling points of -23.8 °C and 5.95 °C respectively).

An additive effect was observed when applying methyl iodide and dimethyl sulphide concurrently to nematodes in a closed, “nested-plate” system, while combination of

either methyl iodide or DMS with chloroform resulted in no effect on activity. It was hypothesised that a synergistic effect, in which the bioactivity of paired compounds would be greater than the sum of their parts, might be observed when combining compounds emitted by brassicas, but no such effect was demonstrated. Compound synergy is sought after in treatment of human infection and disease (Foucquier and Guedj, 2015, Lewis et al., 2015, Tallarida, 2011), and has been a goal in studies into combinations of soil treatments for nematode control (Mao et al., 2014, Mao et al., 2012). Though synergy for nematode control was not observed between three pairings of the compounds emitted by brassicas, the additive effect between methyl iodide and DMS suggest that the full profile of gases emitted by brassica root tissues may have an effect on soil organisms. Further investigation of more complex combinations could elucidate potential interactions between compounds. Development of a system in which methyl bromide can be safely assayed for bioactivity would improve understanding of the impacts brassicas have on the soil environment.

The limitations of the nested-plate assay used here to assess toxicity of volatiles is that nematodes were exposed to a single point application of each given compound, rather than a steady dose over a long period of time, and that the experiments took place in a closed environment. These conditions differ to those experienced by nematodes in the soil: brassicas are constantly emitting bioactive compounds in a continuous low dose, into a relatively open environment. The soil airspace surrounding the roots of a brassica are heterogeneous, porous, moist, and populated with organic matter (O'Brien et al., 2018). The soil microbiome will vary based on soil type, climate, and other abiotic factors (Bates et al., 2011), impacting the fate of gaseous compounds in the soil. While the potential for brassicas to have a controlling effect on soilborne pests has been demonstrated, the validity of these reactions in field conditions have yet to be assessed. Assessment of plant volatile toxicity *in vitro* would be improved by development of a method that could reliably deliver gaseous compounds to a closed environment, at a constant dose. This would allow for the chronic effects of exposure to low concentrations of the compounds to be investigated, while a gas delivery system would enable methyl bromide, methyl chloride and methane thiol to be incorporated into the experiment.

Future work should look to examine the effect of growing brassicas in soil containing potato cyst nematode cysts without then incorporating the brassicas as a green manure, as well as examining the gases released into and from the surface of the soil with the plants *in situ*. Different soil types and moisture contents should be investigated, to assess how these factors affect both the release and the ultimate fate of volatile compounds emitted from brassica roots. Experiments in field conditions could be performed using cysts contained in mesh bags placed in the soil near to the root systems of brassicas, which could be harvested after a period of growth and assessed for egg viability.

The aboveground biomass of brassicas emitted a greater mass of the principal bioactive emissions observed from the belowground biomass. This is unlikely to have any impact on soilborne pests, but could impact how aboveground pests select targets for herbivory. Research into the gaseous emissions of plants largely focus on the release of volatile organic compounds (VOCs), particularly in response to herbivory (Fürstenberg-Hägg et al., 2013, Holopainen and Blande, 2013, Kigathi et al., 2009). Methyl halide emissions from rice plants have been suggested as a possible defence against herbivory, though this is unverified (Redeker et al., 2004). Further investigation should therefore focus on the responses of aboveground herbivores to the gases released by brassicas. Members of the Lepidopterae have developed nitrile-specifier proteins (NSPs) that manipulate breakdown of glucosinolates by brassicas to favour harmless nitriles instead of bioactive isothiocyanates (Wittstock et al., 2004); similar mechanisms of detoxification for contact with toxic methyl halides may also have arisen in brassica-specific herbivores.

6.5 Environmental impacts of biofumigation

The levels of methyl bromide emitted from brassicas were calculated to be higher than previous estimates for brassicas other than *B. napus*, which remains the greatest source of atmospheric methyl bromide from brassicas (Gan et al., 1998, Mead et al., 2008), due to a greater biomass of rapeseed being grown, for a longer growth period, each year (FAOSTAT, 2017). The need for monitoring of sources of ozone-depleting agents was outlined in the Montreal Protocol on Substances that Deplete the Ozone Layer, the treaty that established global monitoring of such compounds and led to the withdrawal

of methyl bromide and artificial compounds such as CFCs (UNEP, 2012); among the compounds identified as emitted from brassicas, only methyl bromide is monitored. Although iodine radicals have strong reactive potential with ozone, iodine compounds react readily in the lower atmosphere and so never reach the stratosphere (Pelley, 2009). Chlorine atoms also react with ozone in the stratosphere, and methyl chloride contributes 16% of atmospheric chlorine atoms (WMO, 2014). However, only ~1% of methyl chloride is thought to be anthropogenic (WMO, 2014), with the remainder coming from natural sources such as oceans and coastal plant-life (Yokouchi et al., 2000); methyl chloride is therefore not a scheduled substance under the Montreal Protocol (UNEP, 2012). Future monitoring of ozone-depleting substances could look to factor in crop production as an anthropogenic source of methyl chloride.

Where crops grown for produce are reported or can be measured based on trade outputs (FAOSTAT, 2017). From these reports, the biomass of brassicas grown for produce can be estimated, and from there the resultant release of methyl bromide into the atmosphere can be calculated (Chapter 5.4.3). However, no such reporting is made for growth of cover crops or for biofumigation. Given the need for adequate monitoring of ozone-depleting compounds (UNEP, 2012), the sources and sinks of such compounds, termed the atmospheric budget, need to be identified (Butler, 2000). The current known sinks of methyl bromide outweigh the known sources, meaning the budget is unbalanced (Mead et al., 2008). While current trends show that atmospheric methyl bromide is decreasing year on year (WMO, 2014), uncertainty of the sources of methyl bromide complicate monitoring. An increase in atmospheric CFC-11 was detected in 2018, and could be located to production in East Asia (Montzka et al., 2018), possible due to the wholly anthropogenic nature of CFC-11. An increase in anthropogenic methyl bromide may not be detected due to the lack of balance in the atmospheric budget. It is recommended therefore that biofumigation practices should be reported to governments for the purposes of improved methyl bromide monitoring.

There remain a number of unanswered questions in the science of biofumigation. The method of green tissue incorporation is evidently a factor in efficacy (Valdes et al., 2012). The traditional focus on isothiocyanates as the principal factor in suppressing nematode populations is undermined by reports on actual isothiocyanate release being far lower

than the calculated potential (Morra and Kirkegaard, 2002), and measurement of isothiocyanates in the soil peaking immediately after incorporation and dissipating thereafter (Dr Kelly Redeker, personal communication). The work presented here has identified a number of genes directly implicated in *Globodera pallida* xenobiotic metabolism, as well as a gene involved in crucial cellular maintenance. These can be targeted with techniques such as RNAi to enable control of potato cyst nematodes in a specific and biosafe manner. A biologically relevant screening process for identification of biofumigant activity in plant tissue extracts has been developed, and should allow for the expansion of available biofumigant crops, potentially allowing for the identification of more effective alternatives to the crops currently employed. The potential for transgenesis of plant-parasitic nematodes has been demonstrated; development of the technique will greatly expand the tools available for study of plant-parasitic nematodes. The gaseous emissions of brassicas have been examined in greater depth than before, identifying bioactive compounds with demonstrable toxicity to plant-parasitic nematodes released from both the aboveground and belowground biomass of the plants. Ozone-depleting agents among these emissions should be considered when expanding biofumigation practice in future. The results presented here indicate that there is promise in the continued investigation of brassicas for the control of plant-parasitic nematodes, but indicate that the focus could shift away from isothiocyanates to other avenues of study.

Chapter 7 References

- ABAD, P., GOUZY, J., AURY, J.-M., CASTAGNONE-SERENO, P., DANCHIN, E. G. J., DELEURY, E., PERFUS-BARBEOCH, L., ANTHOUARD, V., ARTIGUENAVE, F., BLOK, V. C., CAILLAUD, M.-C., COUTINHO, P. M., DASILVA, C., DE LUCA, F., DEAU, F., ESQUIBET, M., FLUTRE, T., GOLDSTONE, J. V., HAMAMOUCHE, N., HEWEZI, T., JAILLON, O., JUBIN, C., LEONETTI, P., MAGLIANO, M., MAIER, T. R., MARKOV, G. V., MCVEIGH, P., PESOLE, G., POULAIN, J., ROBINSON-RECHAVI, M., SALLET, E., SEGURENS, B., STEINBACH, D., TYTGAT, T., UGARTE, E., VAN GHELDER, C., VERONICO, P., BAUM, T. J., BLAXTER, M., BLEVE-ZACHEO, T., DAVIS, E. L., EWBANK, J. J., FAVERY, B., GRENIER, E., HENRISSAT, B., JONES, J. T., LAUDET, V., MAULE, A. G., QUESNEVILLE, H., ROSSO, M.-N., SCHIEX, T., SMANT, G., WEISSENBACH, J. & WINCKER, P. 2008. Genome Sequence of the Metazoan Plant-Parasitic Nematode *Meloidogyne Incognita*. *Nat Biotech*, 26, 909-915.
- ABDULL RAZIS, A. F., KONSUE, N. & IOANNIDES, C. Isothiocyanates and Xenobiotic Detoxification. *Molecular Nutrition & Food Research*, 0, 1700916.
- AGHAJANZADEH, T., HAWKESFORD, M. J. & DE KOK, L. J. 2014. The Significance of Glucosinolates for Sulfur Storage in Brassicaceae Seedlings. *Front Plant Sci*, 5.
- AHDB. 2018. *Potato Variety Database* [Online]. Agriculture and Horticulture Development Board. Available: <http://varieties.ahdb.org.uk/> [Accessed 20th February 2018].
- AHMAD, R. & SRIVASTAVA, A. 2008. Inhibition of Filarial Glutathione-S-Transferase by Various Classes of Compounds and Their Evaluation as Novel Antifilarial Agents. *Helminthologia* 45, 114.
- AIRES, A., CARVALHO, R., DA CONCEICAO BARBOSA, M. & ROSA, E. 2009. Suppressing Potato Cyst Nematode, *Globodera rostochiensis*, with Extracts of Brassicacea Plants.
- AISSANI, N., TEDESCHI, P., MAIETTI, A., BRANDOLINI, V., GARAU, V. L. & CABONI, P. 2013. Nematicidal Activity of Allylisothiocyanate from Horseradish (*Armoracia rusticana*) Roots against *Meloidogyne Incognita*. *Journal of Agricultural and Food Chemistry*, 61, 4723-4727.
- AL-REHIAYANI, S. & HAFEZ, S. 1998. Host Status and Green Manure Effect of Selected Crops on *Meloidogyne chitwoodi* Race 2 and *Pratylenchus neglectus*. *Nematropica*, 28, 213-230.
- ALI, M. A., WIECZOREK, K., KREIL, D. P. & BOHLMANN, H. 2014. The Beet Cyst Nematode *Heterodera schachtii* Modulates the Expression of WRKY Transcription Factors in Syncytia to Favour Its Development in Arabidopsis Roots. *PLOS ONE*, 9, e102360.
- ALTSCHUL, S. F., GISH, W., MILLER, W., MYERS, E. W. & LIPMAN, D. J. 1990. Basic Local Alignment Search Tool. *J Mol Biol*, 215, 403-10.
- ANDERSSON, D., CHAKRABARTY, R., BEJAI, S., ZHANG, J., RASK, L. & MEIJER, J. 2009. Myrosinases from Root and Leaves of *Arabidopsis thaliana* Have Different Catalytic Properties. *Phytochemistry*, 70, 1345-1354.
- ANDREASSON, E., JORGENSEN, L. B., HOGLUND, A. S., RASK, L. & MEIJER, J. 2001. Different Myrosinase and Idioblast Distribution in Arabidopsis and *Brassica napus*. *Plant Physiology*, 127, 1750-1763.

- ANKENY, R. A. 2001. The Natural History of *Caenorhabditis elegans* Research. *Nature Reviews Genetics*, 2, 474.
- ANKENY, R. A. & LEONELLI, S. 2011. What's So Special About Model Organisms? *Studies in History and Philosophy of Science Part A*, 42, 313-323.
- APT, W. J. & CASWELL, E. P. 1988. Application of Nematicides Via Drip Irrigation. *Journal of Nematology*, 20, 1-10.
- ARANDA, J., CERQUEIRA, N. M. F. S. A., FERNANDES, P. A., ROCA, M., TUÑÓN, I. & RAMOS, M. J. 2014. The Catalytic Mechanism of Carboxylesterases: A Computational Study. *Biochemistry*, 53, 5820-5829.
- ARMSTRONG, M. R., BLOK, V. C. & PHILLIPS, M. S. 2000. A Multipartite Mitochondrial Genome in the Potato Cyst Nematode *Globodera pallida*. *Genetics*, 154, 181-92.
- AUMA, J. & HASHEM, M. 1993. Studies on Substances with Sex Pheromone Activity Produced by *Heterodera schachtii* Females. *Fundam. appl. Nematol*, 16, 43-46.
- BANERJEE, A., DATTA, J. K. & MONDAL, N. K. 2012. Changes in Morpho-Physiological Traits of Mustard under the Influence of Different Fertilizers and Plant Growth Regulator Cycocel. *Journal of the Saudi Society of Agricultural Sciences*, 11, 89-97.
- BANERJEE, S., GILL, S. S., GAWADE, B. H., JAIN, P. K., SUBRAMANIAM, K. & SIROHI, A. 2017. Host Delivered Rnai of Two Cuticle Collagen Genes, Mi-Col-1 and Lemmi-5 Hampers Structure and Fecundity in *Meloidogyne incognita*. *Front Plant Sci*, 8, 2266.
- BANKS, N. C., HODDA, M., SINGH, S. K. & MATVEEVA, E. M. 2012. Dispersal of Potato Cyst Nematodes Measured Using Historical and Spatial Statistical Analyses. *Phytopathology*, 102, 620-626.
- BARBER, R. D., HARMER, D. W., COLEMAN, R. A. & CLARK, B. J. 2005. GAPDH as a Housekeeping Gene: Analysis of GAPDH mRNA Expression in a Panel of 72 Human Tissues. *Physiol Genomics*, 21, 389-95.
- BARDOU-VALETTE, S., GRENIER, E. & MONTARRY, J. 2016. Occurrence of the Tobacco Cyst Nematode Subspecies *Globodera tabacum subsp. virginiae* in France. *European Journal of Plant Pathology*, 144, 199-203.
- BARRETT, J. 2009. Forty Years of Helminth Biochemistry. *Parasitology*, 136, 1633-1642.
- BATES, S. T., BERG-LYONS, D., CAPORASO, J. G., WALTERS, W. A., KNIGHT, R. & FIERER, N. 2011. Examining the Global Distribution of Dominant Archaeal Populations in Soil. *ISME J*, 5, 908-17.
- BEEKWILDER, J., VAN LEEUWEN, W., VAN DAM, N. M., BERTOSSI, M., GRANDI, V., MIZZI, L., SOLOVIEV, M., SZABADOS, L., MOLTHOFF, J. W., SCHIPPER, B., VERBOCHT, H., DE VOS, R. C. H., MORANDINI, P., AARTS, M. G. M. & BOVY, A. 2008. The Impact of the Absence of Aliphatic Glucosinolates on Insect Herbivory in Arabidopsis. *PLoS ONE*, 3, e2068.
- BÉLAIR, G., DAUPHINAIS, N. & MIMÉE, B. 2016. Evaluation of Cultural Methods for the Management of the Golden Nematode (*Globodera rostochiensis*) in Quebec, Canada. *Canadian Journal of Plant Pathology*, 38, 209-217.
- BELLAFIORE, S., SHEN, Z., ROSSO, M.-N., ABAD, P., SHIH, P. & BRIGGS, S. P. 2008. Direct Identification of the *Meloidogyne incognita* Secretome Reveals Proteins with Host Cell Reprogramming Potential. *PLoS Pathogens*, 4, e1000192.

- BENTLEY, R. & CHASTEEN, T. G. 2004. Environmental VOCs—Formation and Degradation of Dimethyl Sulfide, Methanethiol and Related Materials. *Chemosphere*, 55, 291-317.
- BERNARD, P. 1996. Positive Selection of Recombinant DNA by *ccdB*. *Biotechniques*, 21, 320-3.
- BERNARD, P. & COUTURIER, M. 1992. Cell Killing by the F Plasmid *ccdB* Protein Involves Poisoning of DNA-Topoisomerase II Complexes. *J Mol Biol*, 226, 735-45.
- BIRD, D. M. & RIDDLE, D. L. 1994. A Genetic Nomenclature for Parasitic Nematodes. *Journal of Nematology*, 26, 138-143.
- BLAXTER, M. 2011. Nematodes: The Worm and Its Relatives. *PLOS Biology*, 9, e1001050.
- BLAXTER, M. & KOUTSOVOULOS, G. 2015. The Evolution of Parasitism in Nematoda. *Parasitology*, 142, S26-S39.
- BOBENCHIK, A. M., AUGAGNEUR, Y., HAO, B., HOCH, J. C. & BEN MAMOUN, C. 2011. Phosphoethanolamine Methyltransferases in Phosphocholine Biosynthesis: Functions and Potential for Antiparasite Therapy. *FEMS microbiology reviews*, 35, 609-619.
- BOHLMANN, H. & SOBCHAK, M. 2014. The Plant Cell Wall in the Feeding Sites of Cyst Nematodes. *Frontiers in Plant Science*, 5.
- BONES, A. & ROSSITER, J. 1996. The Myrosinase-Glucosinolate System, Its Organisation and Biochemistry. *Physiologia Plantarum*, 97, 194-208
- BONES, A. M. & ROSSITER, J. T. 2006. The Enzymic and Chemically Induced Decomposition of Glucosinolates. *Phytochemistry*, 67, 1053-1067.
- BOUCHER, A. C., MIMÉE, B., MONTARRY, J., BARDOU-VALETTE, S., BÉLAIR, G., MOFFETT, P. & GRENIER, E. 2013. Genetic Diversity of the Golden Potato Cyst Nematode *Globodera rostochiensis* and Determination of the Origin of Populations in Quebec, Canada. *Molecular Phylogenetics and Evolution*, 69, 75-82.
- BRENDZA, K. M., HAAKENSEN, W., CAHOON, R. E., HICKS, L. M., PALAVALLI, L. H., CHIAPELLI, B. J., MCLAIRD, M., MCCARTER, J. P., WILLIAMS, D. J., HRESKO, M. C. & JEZ, J. M. 2007. Phosphoethanolamine N-Methyltransferase (PMT-1) Catalyses the First Reaction of a New Pathway for Phosphocholine Biosynthesis in *Caenorhabditis Elegans*. *Biochem J*, 404, 439-48.
- BRESLAUER, K. J., FRANK, R., BLOCKER, H. & MARKY, L. A. 1986. Predicting DNA Duplex Stability from the Base Sequence. *Proc Natl Acad Sci U S A*, 83, 3746-50.
- BRIDGE, J. & PAGE, S. L. J. 1980. Estimation of Root-Knot Nematode Infestation Levels on Roots Using a Rating Chart. *Tropical Pest Management*, 26, 296-298.
- BROLSMA, K. M., VAN DER SALM, R. J., HOFFLAND, E. & DE GOEDE, R. G. M. 2014. Hatching of *Globodera pallida* Is Inhibited by 2-Propenyl Isothiocyanate in Vitro but Not by Incorporation of *Brassica juncea* Tissue in Soil. *Applied Soil Ecology*, 84, 6-11.
- BROPHY, P. M. & BARRETT, J. 1990. Glutathione Transferase in Helminths. *Parasitology*, 100 Pt 2, 345-9.
- BROWN, P. D., TOKUHISA, J. G., REICHEL, M. & GERSHENZON, J. 2003. Variation of Glucosinolate Accumulation among Different Organs and Developmental Stages of *Arabidopsis thaliana*. *Phytochemistry*, 62, 471-481.
- BURMEISTER, W. P., COTTAZ, S., ROLLIN, P., VASELLA, A. & HENRISSAT, B. 2000. High Resolution X-Ray Crystallography Shows That Ascorbate Is a Cofactor for

- Myrosinase and Substitutes for the Function of the Catalytic Base. *Journal of Biological Chemistry*, 275, 39385-39393.
- BUROW, M., BERGNER, A., GERSHENZON, J. & WITTSTOCK, U. 2007. Glucosinolate Hydrolysis in *Lepidium sativum*—Identification of the Thiocyanate-Forming Protein. *Plant Molecular Biology*, 63, 49-61.
- BUTLER, J. H. 2000. Better Budgets for Methyl Halides? *Nature*, 403, 260.
- BUXDORF, K., YAFFE, H., BARDA, O. & LEVY, M. 2013. The Effects of Glucosinolates and Their Breakdown Products on Necrotrophic Fungi. *PLOS ONE*, 8, e70771.
- CHALFIE, M., TU, Y., EUSKIRCHEN, G., WARD, W. & PRASHER, D. 1994. Green Fluorescent Protein as a Marker for Gene Expression. *Science*, 263, 802-805.
- CHAMBERLAIN, M. P., STURGESS, N. C., LOCK, E. A. & REED, C. J. 1999. Methyl Iodide Toxicity in Rat Cerebellar Granule Cells in Vitro: The Role of Glutathione. *Toxicology*, 139, 27-37.
- CHAN, M. K. Y. & CLOSE, R. C. 1987. Aphanomyces Root Rot of Peas 3. Control by the Use of Cruciferous Amendments. *New Zealand Journal of Agricultural Research*, 30, 225-233.
- CHITWOOD, D. J. 2002. Phytochemical Based Strategies for Nematode Control. *Annu Rev Phytopathol*, 40, 221-49.
- CHOHNAN, S., FUJIO, T., TAKAKI, T., YONEKURA, M., NISHIHARA, H. & TAKAMURA, Y. 1998. Malonate Decarboxylase of *Pseudomonas Putida* Is Composed of Five Subunits. *FEMS Microbiol Lett*, 169, 37-43.
- CLARK, S. E., RUNNING, M. P. & MEYEROWITZ, E. M. 1995. Clavata3 Is a Specific Regulator of Shoot and Floral Meristem Development Affecting the Same Processes as Clavata1. *Development*, 121, 2057-2067.
- COTTON, J. A., LILLEY, C. J., JONES, L. M., KIKUCHI, T., REID, A. J., THORPE, P., TSAI, I. J., BEASLEY, H., BLOK, V., COCK, P. J., EVES-VAN DEN AKKER, S., HOLROYD, N., HUNT, M., MANTELIN, S., NAGHRA, H., PAIN, A., PALOMARES-RIUS, J. E., ZAROWIECKI, M., BERRIMAN, M., JONES, J. T. & URWIN, P. E. 2014. The Genome and Life-Stage Specific Transcriptomes of *Globodera pallida* Elucidate Key Aspects of Plant Parasitism by a Cyst Nematode. *Genome Biology*, 15, R43.
- DANCHIN, E. G., GUZEEVA, E. A., MANTELIN, S., BEREPIKI, A. & JONES, J. T. 2016. Horizontal Gene Transfer from Bacteria Has Enabled the Plant-Parasitic Nematode *Globodera pallida* to Feed on Host-Derived Sucrose. *Mol Biol Evol*, 33, 1571-9.
- DANCHIN, E. G. J., ROSSO, M.-N., VIEIRA, P., DE ALMEIDA-ENGLER, J., COUTINHO, P. M., HENRISSAT, B. & ABAD, P. 2010. Multiple Lateral Gene Transfers and Duplications Have Promoted Plant Parasitism Ability in Nematodes. *Proceedings of the National Academy of Sciences*, 107, 17651-17656.
- DE WAELE, D. & ELSEN, A. 2007. Challenges in Tropical Plant Nematology. *Annual Review of Phytopathology*, 45, 457-485.
- DECRAEMER, W. & HUNT, D. 2013. Structure and Classification. In: PERRY, R. N. & MOENS, M. (eds.) *Plant Nematology, 2nd Edition*. CAB International.
- DICKE, M. & DIJKMAN, H. 2001. Within-Plant Circulation of Systemic Elicitor of Induced Defence and Release from Roots of Elicitor That Affects Neighbouring Plants. *Biochemical Systematics and Ecology*, 29, 1075-1087.
- DICKINSON, D. J. & GOLDSTEIN, B. 2016. CRISPR-Based Methods for *Caenorhabditis elegans* Genome Engineering. *Genetics*, 202, 885-901.

- DIXON, G. 2006. *Vegetable Brassicas and Related Crucifers*, Wallingford, Oxfordshire, CABI.
- DOS SANTOS MARQUES, C.T., SILVA GAMA, E.V., DA SILVA, F., TELES, S., CAIAFA, A.N. & LUCCHESI, A.M. 2017. Improvement of Biomass and Essential Oil Production of *Lippia alba* (Mill) N.E. Brown with Green Manures in Succession. *Industrial Crops and Products*, **112**: 113-118
- DOHENY-ADAMS, T., LILLEY, C. J., BARKER, A., ELLIS, S., WADE, R., ATKINSON, H. J., URWIN, P. E., REDEKER, K. & HARTLEY, S. E. 2018. Constant Isothiocyanate-Release Potentials across Biofumigant Seeding Rates. *Journal of Agricultural and Food Chemistry*, **66**, 5108-5116.
- EDWARDS, S. & PLOEG, A. 2014. Evaluation of 31 Potential Biofumigant Brassicaceous Plants as Hosts for Three *Meloidogyne* Species. *Journal of Nematology*, **46**, 287-295.
- ELLENBY, C. 1946. Nature of the Cyst Wall of the Potato-Root Eelworm *Heterodera rostochiensis*, Wollenweber and Its Permeability to Water. *Nature*, **157**, 302-303.
- ELLENBY, C. 1968. Desiccation Survival in the Plant Parasitic Nematodes, *Heterodera rostochiensis* Wollenweber and *Ditylenchus dipsaci* (Kuhn) Filipjev. *Proceedings of the Royal Society B: Biological Sciences*, **169**, 203-213.
- ELLING, A. A., MITREVA, M., GAI, X., MARTIN, J., RECKNOR, J., DAVIS, E. L., HUSSEY, R. S., NETTLETON, D., MCCARTER, J. P. & BAUM, T. J. 2009. Sequence Mining and Transcript Profiling to Explore Cyst Nematode Parasitism. *BMC Genomics*, **10**, 58.
- ERBACH, G. 2012. Pesticide Legislation in the EU. *Library Briefing 120291REV1*. Library of the European Parliament. URL: http://www.europarl.europa.eu/RegData/bibliotheque/briefing/2012/120291/LDM_BRI%282012%29120291_REV1_EN.pdf
- ERIKSSON, S., ANDRÉASSON, E., EKBOM, B., GRANÉR, G., PONTOPPIDAN, B., TAIPALENSUU, J., ZHANG, J., RASK, L. & MEIJER, J. 2002. Complex Formation of Myrosinase Isoenzymes in Oilseed Rape Seeds Are Dependent on the Presence of Myrosinase-Binding Proteins. *Plant Physiology*, **129**, 1592-1599.
- ETTLINGER, M. G., DATEO, G. P., JR., HARRISON, B. W., MABRY, T. J. & THOMPSON, C. P. 1961. Vitamin C as a Coenzyme: The Hydrolysis of Mustard Oil Glucosides. *Proc Natl Acad Sci U S A*, **47**, 1875-80.
- ETTLINGER, M. G. & LUNDEEN, A. J. 1957. First Synthesis of a Mustard Oil Glucoside; the Enzymatic Lossen Rearrangement. *Journal of the American Chemical Society*, **79**, 1764-1765.
- EUROPEAN COMMISSION 2003. Council Decision of 18 March 2003 Concerning the Non-Inclusion of aldicarb in Annex I to Council Directive 91/414/Eec and the Withdrawal of Authorisations for Plant Protection Products Containing This Active Substance. In: COMMISSION, E. (ed.). European Commission.
- EUROPEAN UNION 1957. Treaty on the Functioning of the European Union - PART THREE: UNION POLICIES AND INTERNAL ACTIONS - TITLE XX: ENVIRONMENT - Article 191. Official Journal **115**: 0132-0133 URL: <https://eur-lex.europa.eu/legal-content/EN/ALL/?uri=CELEX:12008E191>
- EUROSTAT 2017. Economic Accounts for Agriculture - Values at Current Prices [Aact_Eaa01]. European Commission, © European Union 1995-2017.
- EVANS, K. & HAYDOCK, P. P. J. 2000. Potato Cyst Nematode Management - Present and Future. *Aspects of Applied Biology*, 91-97.

- EVANS, T. 2006. Transformation and Microinjection. *In: COMMUNITY, T. C. E. R. (ed.) Wormbook.*
- EVES-VAN DEN AKKER, S., LAETSCH, D. R., THORPE, P., LILLEY, C. J., DANCHIN, E. G. J., DA ROCHA, M., RANCUREL, C., HOLROYD, N. E., COTTON, J. A., SZITENBERG, A., GRENIER, E., MONTARRY, J., MIMEE, B., DUCEPPE, M.-O., BOYES, I., MARVIN, J. M. C., JONES, L. M., YUSUP, H. B., LAFOND-LAPALME, J., ESQUIBET, M., SABEH, M., ROTT, M., OVERMARS, H., FINKERS-TOMCZAK, A., SMANT, G., KOUTSOVOULOS, G., BLOK, V., MANTELIN, S., COCK, P. J. A., PHILLIPS, W., HENRISSAT, B., URWIN, P. E., BLAXTER, M. & JONES, J. T. 2016. The Genome of the Yellow Potato Cyst Nematode, *Globodera rostochiensis*, Reveals Insights into the Basis of Parasitism and Virulence. *Genome Biology*, 17, 124.
- EVES-VAN DEN AKKER, S., LILLEY, C. J., REID, A., PICKUP, J., ANDERSON, E., COCK, P. J. A., BLAXTER, M., URWIN, P. E., JONES, J. T. & BLOK, V. C. 2015. A Metagenetic Approach to Determine the Diversity and Distribution of Cyst Nematodes at the Level of the Country, the Field and the Individual. *Molecular Ecology*, 24, 5842-5851.
- FAHEY, J. W., ZALCMANN, A. T. & TALALAY, P. 2001. The Chemical Diversity and Distribution of Glucosinolates and Isothiocyanates among Plants. *Phytochemistry*, 56, 5-51.
- FALK, K. L., TOKUHISA, J. G. & GERSHENZON, J. 2007. The Effect of Sulfur Nutrition on Plant Glucosinolate Content: Physiology and Molecular Mechanisms. *Plant Biol (Stuttg)*, 9, 573-81.
- FAOSTAT 2017. Crops. 15/12/2017 ed.: Food and Agriculture Organisation of the United Nations.
- FARRÉ, D., BELLORA, N., MULARONI, L., MESSEGUER, X. & ALBÀ, M. M. 2007. Housekeeping Genes Tend to Show Reduced Upstream Sequence Conservation. *Genome Biology*, 8, R140.
- FASKE, T. R. & HURD, K. 2015. Sensitivity of *Meloidogyne incognita* and *Rotylenchulus reniformis* to Fluopyram. *Journal of Nematology*, 47, 316-321.
- FENWICK, D. W. 1940. Methods for the Recovery and Counting of Cysts of *Heterodera schachtii* from Soil. *Journal of Helminthology*, 18, 155-172.
- FERGUSON, A. A., ROY, S., KORMANIK, K. N., KIM, Y., DUMAS, K. J., RITOV, V. B., MATERN, D., HU, P. J. & FISHER, A. L. 2013. TATN-1 Mutations Reveal a Novel Role for Tyrosine as a Metabolic Signal That Influences Developmental Decisions and Longevity in *Caenorhabditis elegans*. *PLoS Genetics*, 9, e1004020.
- FINKERS-TOMCZAK, A., BAKKER, E., DE BOER, J., VAN DER VOSSSEN, E., ACHENBACH, U., GOLAS, T., SURYANINGRAT, S., SMANT, G., BAKKER, J. & GOVERSE, A. 2010. Comparative Sequence Analysis of the Potato Cyst Nematode Resistance Locus H1 Reveals a Major Lack of Co-Linearity between Three Haplotypes in Potato (*Solanum tuberosum* ssp.). *Theoretical and Applied Genetics*, 122, 595-608.
- FINN, R. D., ATTWOOD, T. K., BABBITT, P. C., BATEMAN, A., BORK, P., BRIDGE, A. J., CHANG, H. Y., DOSZTANYI, Z., EL-GEBALI, S., FRASER, M., GOUGH, J., HAFT, D., HOLLIDAY, G. L., HUANG, H., HUANG, X., LETUNIC, I., LOPEZ, R., LU, S., MARCHLER-BAUER, A., MI, H., MISTRY, J., NATALE, D. A., NECCI, M., NUKA, G., ORENGO, C. A., PARK, Y., PESSEAT, S., PIOVESAN, D., POTTER, S. C., RAWLINGS, N. D., REDASCHI, N., RICHARDSON, L., RIVOIRE, C., SANGRADOR-VEGAS, A., SIGRIST, C., SILLITOE, I., SMITHERS, B., SQUIZZATO, S., SUTTON, G., THANKI, N.,

- THOMAS, P. D., TOSATTO, S. C., WU, C. H., XENARIOS, I., YEH, L. S., YOUNG, S. Y. & MITCHELL, A. L. 2017. Interpro in 2017-Beyond Protein Family and Domain Annotations. *Nucleic Acids Res*, 45, D190-d199.
- FIRE, A., XU, S., MONTGOMERY, M. K., KOSTAS, S. A., DRIVER, S. E. & MELLO, C. C. 1998. Potent and Specific Genetic Interference by Double-Stranded RNA in *Caenorhabditis elegans*. *Nature*, 391, 806.
- FLOWER, D. R. 1996. The Lipocalin Protein Family: Structure and Function. *Biochemical Journal*, 318, 1-14.
- FOUCQUIER, J. & GUEDJ, M. 2015. Analysis of Drug Combinations: Current Methodological Landscape. *Pharmacology Research & Perspectives*, 3, e00149.
- FÜRSTENBERG-HÄGG, J., ZAGROBELNY, M. & BAK, S. 2013. Plant Defense against Insect Herbivores. *International Journal of Molecular Sciences*, 14, 10242-10297.
- GAN, J., YATES, S. R., OHR, H. D. & SIMS, J. J. 1998. Production of Methyl Bromide by Terrestrial Higher Plants. *Geophysical Research Letters*, 25, 3595-3598.
- GHEDIN, E., WANG, S., SPIRO, D., CALER, E., ZHAO, Q., CRABTREE, J., ALLEN, J. E., DELCHER, A. L., GIULIANO, D. B., MIRANDA-SAAVEDRA, D., ANGIUOLI, S. V., CREASY, T., AMEDEO, P., HAAS, B., EL-SAYED, N. M., WORTMAN, J. R., FELDBLYUM, T., TALLON, L., SCHATZ, M., SHUMWAY, M., KOO, H., SALZBERG, S. L., SCHOBEL, S., PERTEA, M., POP, M., WHITE, O., BARTON, G. J., CARLOW, C. K., CRAWFORD, M. J., DAUB, J., DIMMIC, M. W., ESTES, C. F., FOSTER, J. M., GANATRA, M., GREGORY, W. F., JOHNSON, N. M., JIN, J., KOMUNIECKI, R., KORF, I., KUMAR, S., LANEY, S., LI, B. W., LI, W., LINDBLOM, T. H., LUSTIGMAN, S., MA, D., MAINA, C. V., MARTIN, D. M., MCCARTER, J. P., MCREYNOLDS, L., MITREVA, M., NUTMAN, T. B., PARKINSON, J., PEREGRIN-ALVAREZ, J. M., POOLE, C., REN, Q., SAUNDERS, L., SLUDER, A. E., SMITH, K., STANKE, M., UNNASCH, T. R., WARE, J., WEI, A. D., WEIL, G., WILLIAMS, D. J., ZHANG, Y., WILLIAMS, S. A., FRASER-LIGGETT, C., SLATKO, B., BLAXTER, M. L. & SCOTT, A. L. 2007. Draft Genome of the Filarial Nematode Parasite *Brugia malayi*. *Science*, 317, 1756-60.
- GIBSON, T., BLOK, V. C. & DOWTON, M. 2007a. Sequence and Characterization of Six Mitochondrial Subgenomes from *Globodera rostochiensis*: Multipartite Structure Is Conserved among Close Nematode Relatives. *Journal of Molecular Evolution*, 65, 308-315.
- GIBSON, T., BLOK, V. C., PHILLIPS, M. S., HONG, G., KUMARASINGHE, D., RILEY, I. T. & DOWTON, M. 2007b. The Mitochondrial Subgenomes of the Nematode *Globodera pallida* Are Mosaics: Evidence of Recombination in an Animal Mitochondrial Genome. *J Mol Evol*, 64, 463-71.
- GILLET, F.-X., BOURNAUD, C., ANTONINO DE SOUZA JÚNIOR, J. D. & GROSSI-DE-SA, M. F. 2017. Plant-Parasitic Nematodes: Towards Understanding Molecular Players in Stress Responses. *Annals of Botany*, 119, 775-789.
- GIMSING, A. L. & KIRKEGAARD, J. A. 2006. Glucosinolate and Isothiocyanate Concentration in Soil Following Incorporation of Brassica Biofumigants. *Soil Biology and Biochemistry*, 38, 2255-2264.
- GOMIS-RUTH, F. X. 2008. Structure and Mechanism of Metalloprotease. *Crit Rev Biochem Mol Biol*, 43, 319-45.
- GONZÁLEZ-BARRIOS, M., FIERRO-GONZÁLEZ, J. C., KRPELANOVA, E., MORA-LORCA, J. A., PEDRAJAS, J. R., PEÑATE, X., CHAVEZ, S., SWOBODA, P., JANSEN, G. & MIRANDA-

- VIZUETE, A. 2015. Cis- and Trans-Regulatory Mechanisms of Gene Expression in the Asj Sensory Neuron of *Caenorhabditis elegans*. *Genetics*, 200, 123-134.
- GORDON, K. L., ARTHUR, R. K. & RUVINSKY, I. 2015. Phylum-Level Conservation of Regulatory Information in Nematodes Despite Extensive Non-Coding Sequence Divergence. *PLOS Genetics*, 11, e1005268.
- GOV.UK. 2018. *Importing Food - 3. Genetically Modified Foods* [Online]. Available: <https://www.gov.uk/food-safety-as-a-food-distributor/genetically-modified-foods> [Accessed 20th February 2018].
- GREEN, J., WANG, D., LILLEY, C. J., URWIN, P. E. & ATKINSON, H. J. 2012. Transgenic Potatoes for Potato Cyst Nematode Control Can Replace Pesticide Use without Impact on Soil Quality. *PLoS ONE*, 7, e30973.
- GRENIER, E., ANTHOINE, G., FOURNET, S. & PETIT, E. 2010. A Cyst Nematode 'Species Factory' Called the Andes. *Nematology*, 12, 163-169.
- GRISHOK, A. 2005. Rnai Mechanisms in *Caenorhabditis Elegans*. *FEBS Lett*, 579, 5932-9.
- GRUNDLER, F., BETKA, M. & WYSS, U. 1991. Influence of Changes in the Nurse Cell System (Syncytium) on Sex Determination and Development of the Cyst Nematode *Heterodera-Schachtii* - Total Amounts of Proteins and Amino-Acids. *Phytopathology*, 81, 70-74.
- GRUNDLER, F. M. W., SOBCZAK, M. & GOLINOWSKI, W. 1998. Formation of Wall Openings in Root Cells of *Arabidopsis thaliana* Following Infection by the Plant-Parasitic Nematode *Heterodera schachtii*. *European Journal of Plant Pathology*, 104, 545-551.
- GUMZ, F., KRAUSZE, J., EISENSCHMIDT, D., BACKENKÖHLER, A., BARLEBEN, L., BRANDT, W. & WITTSTOCK, U. 2015. The Crystal Structure of the Thiocyanate-Forming Protein from *Thlaspi arvense*, a Kelch Protein Involved in Glucosinolate Breakdown. *Plant Molecular Biology*, 89, 67-81.
- HALKIER, B. A. & GERSHENZON, J. 2006. Biology and Biochemistry of Glucosinolates. *Annual Review of Plant Biology*, 57, 303-333.
- HANDOO, Z. A., CARTA, L. K., SKANTAR, A. M. & CHITWOOD, D. J. 2012. Description of *Globodera ellingtonae* n. sp. (Nematoda: Heteroderidae) from Oregon. *J Nematol*, 44, 40-57.
- HAVERKORT, A. J. & HILLIER, J. G. 2011. Cool Farm Tool – Potato: Model Description and Performance of Four Production Systems. *Potato Research*, 54, 355-369.
- HEMBERG, M. & KREIMAN, G. 2011. Conservation of Transcription Factor Binding Events Predicts Gene Expression across Species. *Nucleic Acids Research*, 39, 7092-7102.
- HENDERSON, D. R., RIGA, E., RAMIREZ, R. A., WILSON, J. & SNYDER, W. E. 2009. Mustard Biofumigation Disrupts Biological Control by *Steinernema spp.* Nematodes in the Soil. *Biological Control*, 48, 316-322.
- HEUNGENS, K., MUGNIERY, D., VANMONTAGU, M., GHEYSEN, G. & NIEBEL, A. 1996. A Method to Obtain Disinfected *Globodera* Infective Juveniles Directly from Cysts. *Fundamental and Applied Nematology*, 19, 91-93.
- HILTPOLD, I., ERB, M., ROBERT, C. A. & TURLINGS, T. C. 2011. Systemic Root Signalling in a Belowground, Volatile-Mediated Tritrophic Interaction. *Plant Cell Environ*, 34, 1267-75.
- HOFFMANN, L., HOPPE, C. M., MÜLLER, R., DUTTON, G. S., GILLE, J. C., GRIESSBACH, S., JONES, A., MEYER, C. I., SPANG, R., VOLK, C. M. & WALKER, K. A. 2014.

- Stratospheric Lifetime Ratio of CFC-11 and CFC-12 from Satellite and Model Climatologies. *Atmos. Chem. Phys.*, 14, 12479-12497.
- HOFMANN, J., EL ASHRY, A. E. N., ANWAR, S., ERBAN, A., KOPKA, J. & GRUNDLER, F. 2010. Metabolic Profiling Reveals Local and Systemic Responses of Host Plants to Nematode Parasitism. *The Plant Journal*, 62(6), 1058-1071.
- HOLOPAINEN, J. K. & BLANDE, J. D. 2013. Where Do Herbivore-Induced Plant Volatiles Go? *Frontiers in Plant Science*, 4, 185.
- HUANG, G., ALLEN, R., DAVIS, E. L., BAUM, T. J. & HUSSEY, R. S. 2006. Engineering Broad Root-Knot Resistance in Transgenic Plants by RNAi Silencing of a Conserved and Essential Root-Knot Nematode Parasitism Gene. *Proceedings of the National Academy of Sciences of the United States of America*, 103, 14302-14306.
- HUBER, W., CAREY, V. J., GENTLEMAN, R., ANDERS, S., CARLSON, M., CARVALHO, B. S., BRAVO, H. C., DAVIS, S., GATTO, L., GIRKE, T., GOTTARDO, R., HAHNE, F., HANSEN, K. D., IRIZARRY, R. A., LAWRENCE, M., LOVE, M. I., MACDONALD, J., OBENCHAIN, V., OLES, A. K., PAGES, H., REYES, A., SHANNON, P., SMYTH, G. K., TENENBAUM, D., WALDRON, L. & MORGAN, M. 2015. Orchestrating High-Throughput Genomic Analysis with Bioconductor. *Nat Methods*, 12, 115-21.
- HUNTER, P. 2008. The Paradox of Model Organisms. The Use of Model Organisms in Research Will Continue Despite Their Shortcomings. *EMBO Reports*, 9, 717-720.
- HUSTINX, W. N., VAN DE LAAR, R. T., VAN HUFFELEN, A. C., VERWEY, J. C., MEULENBELT, J. & SAVELKOUL, T. J. 1993. Systemic Effects of Inhalational Methyl Bromide Poisoning: A Study of Nine Cases Occupationally Exposed Due to Inadvertent Spread During Fumigation. *British Journal of Industrial Medicine*, 50, 155-159.
- IGC. 2017. International Grains Council Market Report 23 November 2017. [Accessed 11th January 2018].
- INDARTI, S., RTP, B., MULYADI & TRIMAN, B. 2004. First Record of Potato Cyst Nematode *Globodera rostochiensis* in Indonesia. *Australasian Plant Pathology*, 33, 325-326.
- INOUE, H., NOJIMA, H. & OKAYAMA, H. 1990. High Efficiency Transformation of *Escherichia coli* with Plasmids. *Gene*, 96, 23-8.
- ISHIDA, M., HARA, M., FUKINO, N., KAKIZAKI, T. & MORIMITSU, Y. 2014. Glucosinolate Metabolism, Functionality and Breeding for the Improvement of Brassicaceae Vegetables. *Breeding Science*, 64, 48-59.
- ITOH, N., TODA, H., MATSUDA, M., NEGISHI, T., TANIGUCHI, T. & OHSAWA, N. 2009. Involvement of S-Adenosylmethionine-Dependent Halide/Thiol Methyltransferase (HTMT) in Methyl Halide Emissions from Agricultural Plants: Isolation and Characterization of an HTMT-Coding Gene from *Raphanus Sativus* (Daikon Radish). *BMC Plant Biology*, 9, 116-116.
- JAFFE, H., HUETTEL, R. N., DEMILO, A. B., HAYES, D. K. & REBOIS, R. V. 1989. Isolation and Identification of a Compound from Soybean Cyst Nematode, *Heterodera glycines*, with Sex Pheromone Activity. *J Chem Ecol*, 15, 2031-43.
- JANCOVA, P., ANZENBACHER, P. & ANZENBACHEROVA, E. 2010. Phase II Drug Metabolizing Enzymes. *Biomed Pap Med Fac Univ Palacky Olomouc Czech Repub*, 154, 103-16.
- JAOUANNET, M., MAGLIANO, M., ARGUEL, M. J., GOURGUES, M., EVANGELISTI, E., ABAD, P. & ROSSO, M. N. 2013. The Root-Knot Nematode Calreticulin Mi-CRT Is a Key Effector in Plant Defense Suppression. *Mol Plant Microbe Interact*, 26, 97-105.

- JIAO, D., CONAWAY, C. C., WANG, M. H., YANG, C. S., KOEHL, W. & CHUNG, F. L. 1996. Inhibition of N-Nitrosodimethylamine Demethylase in Rat and Human Liver Microsomes by Isothiocyanates and Their Glutathione, L-Cysteine, and N-Acetyl-L-Cysteine Conjugates. *Chem Res Toxicol*, 9, 932-8.
- JOHNSON, A. W., GOLDEN, A. M., AULD, D. L. & SUMNER, D. R. 1992. Effects of Rapeseed and Vetch as Green Manure Crops and Fallow on Nematodes and Soil-Borne Pathogens. *Journal of Nematology*, 24, 117-126.
- JOHNSTONE, I. L. 1999. 10. Molecular Biology. In: HOPE, I. (ed.) *C. Elegans: A Practical Approach*. Oxford University Press.
- JONES, J. G., KLECZEWSKI, N. M., DESAEGER, J., MEYER, S. L. F. & JOHNSON, G. C. 2017a. Evaluation of Nematicides for Southern Root-Knot Nematode Management in Lima Bean. *Crop Protection*, 96, 151-157.
- JONES, J. T., HAEGEMAN, A., DANCHIN, E. G. J., GAUR, H. S., HELDER, J., JONES, M. G. K., KIKUCHI, T., MANZANILLA-LÓPEZ, R., PALOMARES-RIUS, J. E., WESEMAEL, W. M. L. & PERRY, R. N. 2013a. Top 10 Plant-Parasitic Nematodes in Molecular Plant Pathology. *Molecular Plant Pathology*, 14, 946-961.
- JONES, J. T., KUMAR, A., PYLYPENKO, L. A., THIRUGNANASAMBANDAM, A., CASTELLI, L., CHAPMAN, S., COCK, P. J., GRENIER, E., LILLEY, C. J., PHILLIPS, M. S. & BLOK, V. C. 2009. Identification and Functional Characterization of Effectors in Expressed Sequence Tags from Various Life Cycle Stages of the Potato Cyst Nematode *Globodera pallida*. *Mol Plant Pathol*, 10, 815-28.
- JONES, L. M., EVES-VAN DEN AKKER, S., VAN-OOSTEN HAWLE, P., ATKINSON, H. J. & URWIN, P. E. 2018a. Duplication of hsp-110 Is Implicated in Differential Success of *Globodera* Species under Climate Change. *Molecular Biology and Evolution*, 35(10), 2401-2413.
- JONES, L. M., KOEHLER, A.-K., TRNKA, M., BALEK, J., CHALLINOR, A. J., ATKINSON, H. J. & URWIN, P. E. 2017b. Climate Change Is Predicted to Alter the Current Pest Status of *Globodera pallida* and *G. rostochiensis* in the United Kingdom. *Global Change Biology*, 23, 4497-4507.
- JONES, L. M., RAYSON, S. J., FLEMMING, A. J. & URWIN, P. E. 2013b. Adaptive and Specialised Transcriptional Responses to Xenobiotic Stress in *Caenorhabditis elegans* Are Regulated by Nuclear Hormone Receptors. *PLoS ONE*, 8, e69956.
- JONES, P. W., TYLKA, G. L. & PERRY, R. N. 1998. Hatching. In: PERRY, R. N. & WRIGHT, D. J. (eds.) *The Physiology and Biochemistry of Free-Living and Plant-Parasitic Nematodes*. UK: CABI.
- JUGDER, B. E., BOHL, S., LEBHAR, H., HEALEY, R. D., MANEFIELD, M., MARQUIS, C. P. & LEE, M. 2017. A Bacterial Chloroform Reductive Dehalogenase: Purification and Biochemical Characterization. *Microb Biotechnol*, 10, 1640-1648.
- KALL, L., KROGH, A. & SONNHAMMER, E. L. 2004. A Combined Transmembrane Topology and Signal Peptide Prediction Method. *J Mol Biol*, 338, 1027-36.
- KEARN, J., LUDLOW, E., DILLON, J., O'CONNOR, V. & HOLDEN-DYE, L. 2014. Fluensulfone is a Nematicide with a Mode of Action Distinct from Anticholinesterases and Macrocyclic Lactones. *Pesticide Biochemistry and Physiology*, 109: 44-57
- KELLY, P. J., BONES, A. & ROSSITER, J. T. 1998. Sub-Cellular Immunolocalization of the Glucosinolate Sinigrin in Seedlings of Brassica Juncea. *Planta*, 206, 370-7.
- KERRY, B., BARKER, A. & EVANS, K. 2003. Investigation of Potato Cyst Nematode Control. *Report HH31111TPO for DEFRA*. Rothamstead Research.

- KESSLER, A. & BALDWIN, I. T. 2001. Defensive Function of Herbivore-Induced Plant Volatile Emissions in Nature. *Science*, 291, 2141-2144.
- KIGATHI, R. N., UNSICKER, S. B., REICHEL, M., KESSELMEIER, J., GERSHENZON, J. & WEISSER, W. W. 2009. Emission of Volatile Organic Compounds after Herbivory from *Trifolium pratense* (L.) under Laboratory and Field Conditions. *Journal of Chemical Ecology*, 35, 1335-1348.
- KIKUCHI, T., AKKER, S. E.-V. D. & JONES, J. T. 2017. Genome Evolution of Plant-Parasitic Nematodes. *Annual Review of Phytopathology*, 55, 333-354.
- KIM, S., LIEBERMAN, T. D. & KISHONY, R. 2014. Alternating Antibiotic Treatments Constrain Evolutionary Paths to Multidrug Resistance. *Proc Natl Acad Sci U S A*, 111, 14494-9.
- KIONTKE, K. & FITCH, D. 2005. The Phylogenetic Relationships of *Caenorhabditis* and Other Rhabditids. In: COMMUNITY, T. C. E. R. (ed.) *Wormbook*.
- KIRKEGAARD, J. A. & SARWAR, M. 1998. Biofumigation Potential of Brassicas - I. Variation in Glucosinolate Profiles of Diverse Field-Grown Brassicas. *Plant and Soil*, 201, 71-89.
- KITAZUME, H., DAYI, M., TANAKA, R. & KIKUCHI, T. 2018. Assessment of the Behaviour and Survival of Nematodes under Low Oxygen Concentrations. *PLoS ONE*, 13, e0197122.
- KLIEBENSTEIN, D. J., KROYMANN, J., BROWN, P., FIGUTH, A., PEDERSEN, D., GERSHENZON, J. & MITCHELL-OLDS, T. 2001. Genetic Control of Natural Variation in Arabidopsis Glucosinolate Accumulation. *Plant Physiol*, 126, 811-25.
- KOLDE, R. 2018. Pheatmap: Pretty Heatmaps.
- KOLM, R. H., DANIELSON, U. H., ZHANG, Y., TALALAY, P. & MANNERVIK, B. 1995. Isothiocyanates as Substrates for Human Glutathione Transferases: Structure-Activity Studies. *Biochem J*, 311 (Pt 2), 453-9.
- KONG, X. Y., KISSEN, R. & BONES, A. M. 2012. Characterization of Recombinant Nitrile-Specifier Proteins (Nsps) of *Arabidopsis thaliana*: Dependency on Fe(II) Ions and the Effect of Glucosinolate Substrate and Reaction Conditions. *Phytochemistry*, 84, 7-17.
- KORT, J., ROSS, H., RUMPENHORST, H. J. & STONE, A. R. 1977. An International Scheme for Identifying and Classifying Pathotypes of Potato Cyst-Nematodes *Globodera rostochiensis* and *G. pallida*. *Nematologica*, 23, 333-339.
- KRAFTS, K., HEMPELMANN, E. & SKÓRSKA-STANIA, A. 2012. From Methylene Blue to Chloroquine: A Brief Review of the Development of an Antimalarial Therapy. *Parasitology Research*, 111, 1-6.
- KROESE, D., ZASADA, I. A. & INGHAM, R. E. 2011. Comparison of Meldola's Blue Staining and Hatching Assay with Potato Root Diffusate for Assessment of *Globodera* sp. Egg Viability. *Journal of Nematology*, 43, 182-186.
- KUCHERNIG, J. C., BACKENKÖHLER, A., LUBBECKE, M., BUROW, M. & WITTSTOCK, U. 2011. A Thiocyanate-Forming Protein Generates Multiple Products Upon Allylglucosinolate Breakdown in *Thlaspi arvense*. *Phytochemistry*, 72, 1699-709.
- KYNDT, T., VIEIRA, P., GHEYSEN, G. & DE ALMEIDA-ENGLER, J. 2013. Nematode Feeding Sites: Unique Organs in Plant Roots. *Planta*, 238, 807-818.
- LAHIANI, A., YAVIN, E. & LAZAROVICI, P. 2017. The Molecular Basis of Toxins' Interactions with Intracellular Signaling Via Discrete Portals. *Toxins*, 9, 107.

- LAIZURE, S. C., HERRING, V., HU, Z., WITBRODT, K. & PARKER, R. B. 2013. The Role of Human Carboxylesterases in Drug Metabolism: Have We Overlooked Their Importance? *Pharmacotherapy*, 33, 210-222.
- LARKIN, R. P. & GRIFFIN, T. S. 2007. Control of Soilborne Potato Diseases Using Brassica Green Manures. *Crop Protection*, 26, 1067-1077.
- LAZZERI, L., CURTO, G., LEONI, O. & DALLAVALLE, E. 2004. Effects of Glucosinolates and Their Enzymatic Hydrolysis Products Via Myrosinase on the Root-Knot Nematode *Meloidogyne incognita* (Kofoid Et White) Chitw. *J Agric Food Chem*, 52, 6703-7.
- LAZZERI, L., MALAGUTI, L., CINTI, S., UGOLINI, L., DE NICOLA, G. R., BAGATTA, M., CASADEI, N., D'AVINO, L., MATTEO, R. & PATALANO, G. 2013. The Brassicaceae Biofumigation System for Plant Cultivation and Defence. An Italian Twenty-Year Experience of Study and Application. *Acta Horticulturae*, 1005, 375-382.
- LEE, C., CHRONIS, D., KENNING, C., PERET, B., HEWEZI, T., DAVIS, E. L., BAUM, T. J., HUSSEY, R., BENNETT, M. & MITCHUM, M. G. 2011. The Novel Cyst Nematode Effector Protein 19c07 Interacts with the Arabidopsis Auxin Influx Transporter LAX3 to Control Feeding Site Development. *Plant Physiol*, 155, 866-80.
- LEMBRIGHT, H. W. 1990. Soil Fumigation: Principles and Application Technology. *Journal of Nematology*, 22, 632-644.
- LEWIS, K., TZILIVAKIS, J., WARNER, D. & GREEN, A. 2016. An International Database for Pesticide Risk Assessments and Management. *Human and Ecological Risk Assessment: An International Journal*, 22, 1050-1064.
- LEWIS, R., GUHA, R., KORCSMAROS, T. & BENDER, A. 2015. Synergy Maps: Exploring Compound Combinations Using Network-Based Visualization. *Journal of Cheminformatics*, 7, 36.
- LILJEROTH, E., LANKINEN, Å., WIJK, L., BURRA, D. D., ALEXANDERSSON, E. & ANDREASSON, E. 2016. Potassium Phosphite Combined with Reduced Doses of Fungicides Provides Efficient Protection against Potato Late Blight in Large-Scale Field Trials. *Crop Protection*, 86, 42-55.
- LILLEY, C. J., ATKINSON, H. J. & URWIN, P. E. 2005. Molecular Aspects of Cyst Nematodes. *Molecular Plant Pathology*, 6, 577-588.
- LILLEY, C. J., DAVIES, L. J. & URWIN, P. E. 2012. Rna Interference in Plant Parasitic Nematodes: A Summary of the Current Status. *Parasitology*, 139, 630-640.
- LILLEY, C. J., URWIN, P. E., JOHNSTON, K. A. & ATKINSON, H. J. 2004. Preferential Expression of a Plant Cystatin at Nematode Feeding Sites Confers Resistance to *Meloidogyne incognita* and *Globodera pallida*. *Plant Biotechnol J*, 2, 3-12.
- LIMA-DYBAL, K. 2016, Survey of PCN in England and Wales, *Unpublished*
- LORD, J. S., LAZZERI, L., ATKINSON, H. J. & URWIN, P. E. 2011. Biofumigation for Control of Pale Potato Cyst Nematodes: Activity of Brassica Leaf Extracts and Green Manures on *Globodera pallida* in Vitro and in Soil. *Journal of Agricultural and Food Chemistry*, 59, 7882-7890.
- LOVE, M. I., HUBER, W. & ANDERS, S. 2014. Moderated Estimation of Fold Change and Dispersion for RNA-seq Data with DESEQ2. *Genome Biology*, 15, 550.
- LOVELL, T. M., WOODS, R. J., BUTLIN, D. J., BRAYLEY, K. J., MANYONDA, I. T., JARVIS, J., HOWELL, S. & LOWRY, P. J. 2007. Identification of a Novel Mammalian Post-Translational Modification, Phosphocholine, on Placental Secretory Polypeptides. *Journal of Molecular Endocrinology*, 39, 189-198.

- LU, P., GILARDI, G., GULLINO, M.L. & GARIBALDI, A. 2010. Biofumigation with *Brassica* Plants and its Effect on the Inoculum Potential of *Fusarium* Yellowings of *Brassica* crops. *Eur J Plant Pathol* 126, 387.
- MACLEOD, A. J. & ROSSITER, J. T. 1985. The Occurrence and Activity of Epithiospecifier Protein in Some Cruciferae Seeds. *Phytochemistry*, 24, 1895-1898.
- MADDEN, T. L., TATUSOV, R. L. & ZHANG, J. 1996. Applications of Network Blast Server. *Methods Enzymol*, 266, 131-41.
- MADURO, M. & PILGRIM, D. 1996. Conservation of Function and Expression of Unc-119 from Two *Caenorhabditis* Species Despite Divergence of Non-Coding DNA. *Gene*, 183, 77-85.
- MADURO, M. F. 2015. 20 Years of unc-119 as a Transgene Marker. *Worm*, 4, e1046031.
- MAI, W. F. 1977. Worldwide Distribution of Potato-Cyst Nematodes and Their Importance in Crop Production. *J Nematol*, 9, 30-4.
- MAIER, T. R., HEWEZI, T., PENG, J. & BAUM, T. J. 2013. Isolation of Whole Esophageal Gland Cells from Plant-Parasitic Nematodes for Transcriptome Analyses and Effector Identification. *Mol Plant Microbe Interact*, 26, 31-5.
- MAO, L., YAN, D., WANG, Q., LI, Y., OUYANG, C., LIU, P., SHEN, J., GUO, M. & CAO, A. 2014. Evaluation of the Combination of Dimethyl Disulfide and Dazomet as an Efficient Methyl Bromide Alternative for Cucumber Production in China. *J Agric Food Chem*, 62, 4864-9.
- MAO, L. G., WANG, Q. X., YAN, D. D., XIE, H. W., LI, Y., GUO, M. X. & CAO, A. C. 2012. Evaluation of the Combination of 1,3-Dichloropropene and Dazomet as an Efficient Alternative to Methyl Bromide for Cucumber Production in China. *Pest Manag Sci*, 68, 602-9.
- MARAHATTA, S. P., WANG, K.-H., SIPES, B. S. & HOOKS, C. R. R. 2010. Strip-Tilled Cover Cropping for Managing Nematodes, Soil Mesarthropods, and Weeds in a Bitter Melon Agroecosystem. *Journal of Nematology*, 42, 111-119.
- MARKHAM, G. D. & PAJARES, M. A. 2009. Structure-Function Relationships in Methionine Adenosyltransferases. *Cellular and molecular life sciences : CMLS*, 66, 636-648.
- MATILE, P. 1980. The Mustard Oil Bomb. Compartmentation of the Myrosinase System. *Biochem. Physiol. Pflanzen.*, 1758, 722-731.
- MATOUŠKOVÁ, P., VOKŘÁL, I., LAMKA, J. & SKÁLOVÁ, L. 2016. The Role of Xenobiotic-Metabolizing Enzymes in Anthelmintic Deactivation and Resistance in Helminths. *Trends in Parasitology*, 32, 481-491.
- MCSORLEY, R. 2011. Assessment of Rotation Crops and Cover Crops for Management of Root-Knot Nematodes (*Meloidogyne spp.*) in the Southeastern United States. *Nematropica*, 41, 200-214.
- MEAD, M. I., WHITE, I. R., NICKLESS, G., WANG, K.-Y. & SHALLCROSS, D. E. 2008. An Estimation of the Global Emission of Methyl Bromide from Rapeseed (*Brassica napus*) from 1961 to 2003. *Atmospheric Environment*, 42, 337-345.
- MEHERE, P., HAN, Q., LEMKUL, J. A., VAVRICKA, C. J., ROBINSON, H., BEVAN, D. R. & LI, J. 2010. Tyrosine Aminotransferase: Biochemical and Structural Properties and Molecular Dynamics Simulations. *Protein & Cell*, 1, 1023-1032.
- MEI, Y., THORPE, P., GUZHA, A., HAEGEMAN, A., BLOK, V. C., MACKENZIE, K., GHEYSEN, G., JONES, J. T. & MANTELIN, S. 2015. Only a Small Subset of the SPRY Domain

- Gene Family in Is Likely to Encode Effectors, Two of Which Suppress Host Defences Induced by the Potato Resistance Gene. *Nematology*, 17, 409-424.
- MELILLO, M. T., LEONETTI, P., LEONE, A., VERONICO, P. & BLEVE-ZACHEO, T. 2011. ROS and NO Production in Compatible and Incompatible Tomato-*Meloidogyne incognita* Interactions. *European Journal of Plant Pathology*, 130, 489-502.
- MELLO, C. C., KRAMER, J. M., STINCHCOMB, D. & AMBROS, V. 1991. Efficient Gene Transfer in *C. elegans*: Extrachromosomal Maintenance and Integration of Transforming Sequences. *Embo j*, 10, 3959-70.
- MENDENHALL, A. R., TEDESCO, P. M., SANDS, B., JOHNSON, T. E. & BRENT, R. 2015. Single Cell Quantification of Reporter Gene Expression in Live Adult *Caenorhabditis elegans* Reveals Reproducible Cell-Specific Expression Patterns and Underlying Biological Variation. *PLoS ONE*, 10, e0124289.
- MENEZ, C., ALBERICH, M., KANSO, D., BLANCHARD, A. & LESPINE, A. 2016. Acquired Tolerance to Ivermectin and Moxidectin after Drug Selection Pressure in the Nematode *Caenorhabditis elegans*. *Antimicrobial Agents and Chemotherapy*, 60, 4809-4819.
- MEYER, S. L. F., ZASADA, I. A., ORISAJO, S. B. & MORRA, M. J. 2011. Mustard Seed Meal Mixtures: Management of *Meloidogyne incognita* on Pepper and Potential Phytotoxicity. *Journal of Nematology*, 43, 7-15.
- MINNIS, S. T., HAYDOCK, P. P. J., IBRAHIM, S. K., GROVE, I. G., EVANS, K. & RUSSELL, M. D. 2002. Potato Cyst Nematodes in England and Wales - Occurrence and Distribution. *Annals of Applied Biology*, 140, 187-195.
- MOJTAHEDI, H., SANTO, G. S. & INGHAM, R. E. 1993. Suppression of *Meloidogyne chitwoodi* with Sudangrass Cultivars as Green Manure. *Journal of Nematology*, 25, 303-311.
- MONFORT, W. S., CSINOS, A. S., DESAEGER, J., SEEBOLD, K., WEBSTER, T. M. & DIAZ-PEREZ, J. C. 2007. Evaluating Brassica Species as an Alternative Control Measure for Root-Knot Nematode (*M. incognita*) in Georgia Vegetable Plasticulture. *Crop Protection*, 26, 1359-1368.
- MONTZKA, S. A., DUTTON, G. S., YU, P., RAY, E., PORTMANN, R. W., DANIEL, J. S., KUIJPERS, L., HALL, B. D., MONDEEL, D., SISO, C., NANCE, J. D., RIGBY, M., MANNING, A. J., HU, L., MOORE, F., MILLER, B. R. & ELKINS, J. W. 2018. An Unexpected and Persistent Increase in Global Emissions of Ozone-Depleting Cfc-11. *Nature*, 557, 413-417.
- MORRA, M. J. & KIRKEGAARD, J. A. 2002. Isothiocyanate Release from Soil-Incorporated Brassica Tissues. *Soil Biology and Biochemistry*, 34, 1683-1690.
- MORRISON, C. A., COLIN, T., SEXTON, J. L., BOWEN, F., WICKER, J., FRIEDEL, T. & SPITHILL, T. W. 1996. Protection of Cattle against *Fasciola hepatica* Infection by Vaccination with Glutathione S-Transferase. *Vaccine*, 14, 1603-12.
- MOTA, M. M. & EISENBACK, J. D. 1993. Morphometrics of *Globodera tabacum tabacum*, *G. t. virginiae*, and *G. t. solanacearum* (Nemata: Heteroderinae). *Journal of Nematology*, 25, 148-160.
- MOTLEY, S. T. & LORY, S. 1999. Functional Characterization of a Serine/Threonine Protein Kinase of *Pseudomonas Aeruginosa*. *Infection and Immunity*, 67, 5386-5394.
- MOXNES, J. F. & HAUSKEN, K. 2007. The Population Dynamics of Potato Cyst Nematodes. *Ecological Modelling*, 207, 339-348.

- MÜLLER, J. 1999. The Economic Importance of *Heterodera Schachtii* in Europe. *Helminthologia*, 36, 205-213.
- NAGATOSHI, Y. & NAKAMURA, T. 2009. Arabidopsis Harmless to Ozone Layer Protein Methylates a Glucosinolate Breakdown Product and Functions in Resistance to *Pseudomonas syringae* sv. *maculicola*. *The Journal of Biological Chemistry*, 284, 19301-19309.
- NAIR, J. R. & CHATTERJEE, K. 2010. Methyl Iodide Poisoning Presenting as a Mimic of Acute Stroke: A Case Report. *Journal of Medical Case Reports*, 4, 177.
- NELSON, D. R. 2009. The Cytochrome P450 Homepage. *Human Genomics*, 4, 59-65.
- NGALA, B. M., HAYDOCK, P. P. J., WOODS, S. & BACK, M. A. 2014. Biofumigation with *Brassica juncea*, *Raphanus sativus* and *Eruca sativa* for the Management of Field Populations of the Potato Cyst Nematode *Globodera pallida*. *Pest Management Science*, 75(5), 759-769.
- NICOL, J. M., TURNER, S. J., COYNE, D. L., NIJS, L. D., HOCKLAND, S. & MAAFI, Z. T. 2011. Current Nematode Threats to World Agriculture. In: JONES, J., GHEYSEN, G. & FENOLL, C. (eds.) *Genomics and Molecular Genetics of Plant-Nematode Interactions*. Springer Netherlands.
- NIELSEN, E., BALTENSPERGER, D., KERR, E. & RIFE, C. 2003. Host Suitability of Rapeseed for *Heterodera Schachtii*. *Journal of Nematology*, 35, 35-38.
- NIINEMETS, Ü., KÄNNASTE, A. & COPOLOVICI, L. 2013. Quantitative Patterns between Plant Volatile Emissions Induced by Biotic Stresses and the Degree of Damage. *Frontiers in Plant Science*, 4, 262.
- NOJI, M. & SAITO, K. 2003. Sulphur Amino Acids: Biosynthesis of Cysteine and Methionine. In: ABROL, Y. P. & AHMAD, A. (eds.) *Sulphur in Plants*. Dordrecht: Springer Netherlands.
- NOLING, J. W. 2002. The Practical Realities of Alternatives to Methyl Bromide: Concluding Remarks. *Phytopathology*, 92, 1373-5.
- NOLING, J. W. & BECKER, J. O. 1994. The Challenge of Research and Extension to Define and Implement Alternatives to Methyl Bromide. *J Nematol*, 26, 573-86.
- NOON, J. B. & BAUM, T. J. 2016. Horizontal Gene Transfer of Acetyltransferases, Invertases and Chorismate Mutases from Different Bacteria to Diverse Recipients. *BMC Evolutionary Biology*, 16, 74.
- NORSHIE, P.M., GROVE, I.G., & BACK, M.A. 2016. Field Evaluation of the Nematicide Fluensulfone for Control of the Potato Cyst Nematode *Globodera pallida*. *Pest Manag Sci.* **72**(10): 2001-2007
- O'BRIEN, F. J. M., DUMONT, M. G., WEBB, J. S. & POPPY, G. M. 2018. Rhizosphere Bacterial Communities Differ According to Fertilizer Regimes and Cabbage (*Brassica oleracea* var. *Capitata* L.) Harvest Time, but Not Aphid Herbivory. *Frontiers in Microbiology*, 9, 1620.
- OKA, Y. 2014. Nematicidal Activity of Fluensulfone against Some Migratory Nematodes under Laboratory Conditions. *Pest Management Science*, 70, 1850-1858.
- OKA, Y., SHUKER, S. & TKACHI, N. 2009. Nematicidal Efficacy of MCW-2, a New Nematicide of the Fluoroalkenyl Group, against the Root-Knot Nematode *Meloidogyne javanica*. *Pest Management Science*, 65, 1082-1089.
- OMIECINSKI, C. J., VANDEN HEUVEL, J. P., PERDEW, G. H. & PETERS, J. M. 2011. Xenobiotic Metabolism, Disposition, and Regulation by Receptors: From

- Biochemical Phenomenon to Predictors of Major Toxicities. *Toxicological Sciences*, 120, S49-S75.
- OSMAN, KA; Al-Rehiayani, SM; Al-Deghairi, MA; Salama, AK. 2009. Bioremediation of Oxamyl in Sandy Soil Using Animal Manures, *International Biodeterioration & Biodegradation* 63(3): 341-346
- ØVERBY, A., STOKLAND, R. A., ÅSBERG, S. E., SPORSHEIM, B. & BONES, A. M. 2015. Allyl Isothiocyanate Depletes Glutathione and Upregulates Expression of Glutathione S-Transferases in *Arabidopsis thaliana*. *Frontiers in Plant Science*, 6, 277.
- PAL, C., PAPP, B. & LAZAR, V. 2015. Collateral Sensitivity of Antibiotic-Resistant Microbes. *Trends Microbiol*, 23, 401-7.
- PALAVALLI, L. H., BRENDZA, K. M., HAAKENSON, W., CAHOON, R. E., MCLAIRD, M., HICKS, L. M., MCCARTER, J. P., WILLIAMS, D. J., HRESKO, M. C. & JEZ, J. M. 2006. Defining the Role of Phosphomethylethanolamine N-Methyltransferase from *Caenorhabditis elegans* in Phosphocholine Biosynthesis by Biochemical and Kinetic Analysis. *Biochemistry*, 45, 6056-65.
- PALOMARES-RIUS, J. E., HEDLEY, P., COCK, P. J. A., MORRIS, J. A., JONES, J. T. & BLOK, V. C. 2016. Gene Expression Changes in Diapause or Quiescent Potato Cyst Nematode, *Globodera pallida*, Eggs after Hydration or Exposure to Tomato Root Diffusate. *PeerJ*, 4, e1654.
- PALOMARES-RIUS, J. E., HEDLEY, P. E., COCK, P. J., MORRIS, J. A., JONES, J. T., VOVLAS, N. & BLOK, V. 2012. Comparison of Transcript Profiles in Different Life Stages of the Nematode *Globodera pallida* under Different Host Potato Genotypes. *Mol Plant Pathol*, 13, 1120-34.
- PALOMARES-RIUS, J. E., JONES, J. T., COCK, P. J., CASTILLO, P. & BLOK, V. C. 2013. Activation of Hatching in Diapaused and Quiescent *Globodera pallida*. *Parasitology*, 140, 445-54.
- PARKINSON, F. E., DAMARAJU, V. L., GRAHAM, K., YAO, S. Y., BALDWIN, S. A., CASS, C. E. & YOUNG, J. D. 2011. Molecular Biology of Nucleoside Transporters and Their Distributions and Functions in the Brain. *Curr Top Med Chem*, 11, 948-72.
- PARRA, G., BRADNAM, K., NING, Z., KEANE, T. & KORF, I. 2009. Assessing the Gene Space in Draft Genomes. *Nucleic Acids Research*, 37, 289-297.
- PELLEY, J. 2009. Methyl Iodide, a Fumigant under Fire. *Environmental Science & Technology*, 43, 6898-6898.
- PERRY, R. 2002. Hatching. *The Biology of Nematodes*. CRC Press.
- PERRY, R. N. 1996. Chemoreception in Plant Parasitic Nematodes. *Annual Review of Phytopathology*, 34, 181-199.
- PERRY, R. N. 1997. Plant Signals in Nematode Hatching and Attraction. In: FENOLL, C., GRUNDLER, F. M. W. & OHL, S. A. (eds.) *Cellular and Molecular Aspects of Plant-Nematode Interactions*. Dordrecht: Springer Netherlands.
- PETERSEN, T. N., BRUNAK, S., VON HEIJNE, G. & NIELSEN, H. 2011. SIGNALP 4.0: Discriminating Signal Peptides from Transmembrane Regions. *Nature Methods*, 8, 785.
- PHILLIPS, M. S. & TRUDGILL, D. L. 1998. Variation of Virulence, in Terms of Quantitative Reproduction of *Globodera pallida* Populations, from Europe and South America, in Relation to Resistance from *Solanum vernei* and *S. tuberosum ssp. andigena* CPC 2802. *Nematologica*, 44, 409-423.

- PIEKARSKA, A., KUSZNIEREWICZ, B., MELLER, M., DZIEDZIUL, K., NAMIEŚNIK, J. & BARTOSZEK, A. 2013. Myrosinase Activity in Different Plant Samples; Optimisation of Measurement Conditions for Spectrophotometric and PH-STAT Methods. *Industrial Crops and Products*, 50, 58-67.
- PIERIK, R., BALLARE, C. L. & DICKE, M. 2014. Ecology of Plant Volatiles: Taking a Plant Community Perspective. *Plant Cell Environ*, 37, 1845-53.
- PLANTARD, O., PICARD, D., VALETTE, S., SCURRAH, M., GRENIER, E. & MUGNIÉRY, D. 2008. Origin and Genetic Diversity of Western European Populations of the Potato Cyst Nematode (*Globodera pallida*) Inferred from Mitochondrial Sequences and Microsatellite Loci. *Molecular Ecology*, 17, 2208-2218.
- PLOEG, A. T. 2002. Effects of Selected Marigold Varieties on Root-Knot Nematodes and Tomato and Melon Yields. *Plant Disease*, 86, 505-508.
- POSTMA, W. J., SLOOTWEG, E. J., REHMAN, S., FINKERS-TOMCZAK, A., TYTGAT, T. O., VAN GELDEREN, K., LOZANO-TORRES, J. L., ROOSIEN, J., POMP, R., VAN SCHAIK, C., BAKKER, J., GOVERSE, A. & SMANT, G. 2012. The Effector SPRYSEC-19 of *Globodera rostochiensis* Suppresses CC-NB-LRR-Mediated Disease Resistance in Plants. *Plant Physiol*, 160, 944-54.
- POULIN, R. & RANDHAWA, H. S. 2015. Evolution of Parasitism Along Convergent Lines: From Ecology to Genomics. *Parasitology*, 142, S6-S15.
- PRAITIS, V. 2006. Creation of Transgenic Lines Using Microparticle Bombardment Methods. In: STRANGE, K. (ed.) *C. Elegans: Methods and Applications*. Totowa, NJ: Humana Press.
- PRAITIS, V., CASEY, E., COLLAR, D. & AUSTIN, J. 2001. Creation of Low-Copy Integrated Transgenic Lines in *Caenorhabditis elegans*. *Genetics*, 157, 1217-26.
- PRUETT, S. B., MYERS, L. P. & KEIL, D. E. 2001. Toxicology of Metam Sodium. *J Toxicol Environ Health B Crit Rev*, 4, 207-22.
- PYLYPENKO, LA. 2002. Resistance and Tolerance to Potato Cyst Nematodes among Ukrainian Potato Cultivars and Breeding Materials. *Plant Protec. Sci.* **38** (Special Issue 1): 189-194
- QIN, S. J., GAN, J. Y., LIU, W. P. & BECKER, J. O. 2004. Degradation and Adsorption of Fosthiazate in Soil. *Journal of Agricultural and Food Chemistry*, 52, 6239-6242.
- QUENTIN, M., ABAD, P. & FAVERY, B. 2013. Plant Parasitic Nematode Effectors Target Host Defense and Nuclear Functions to Establish Feeding Cells. *Frontiers in Plant Science*, 4, 53.
- R CORE TEAM 2018. R: A Language and Environment for Statistical Computing. Vienna, Austria: R Foundation for Statistical Computing.
- RAMIREZ, R. A. I., HENDERSON, D. R., RIGA, E., LACEY, L. A. & SNYDER, W. E. 2009. Harmful Effects of Mustard Bio-Fumigants on Entomopathogenic Nematodes. *Biological Control*, 48, 147-154.
- RAO, U., SHARMA, A., TYAGI, N., BANAKAR, P. & KUMAR, M. 2013. Characterization of Genetic Homogeneity of an Indian Population of Cereal Cyst Nematode, *Heterodera avenae* Using Sequencing and PCR-RFLP of Ribosomal DNA. *Bioinformation*, 9, 67-71.
- RASK, L., ANDRÉASSON, E., EKBOM, B., ERIKSSON, S., PONTOPPIDAN, B. & MEIJER, J. 2000. Myrosinase: Gene Family Evolution and Herbivore Defense in Brassicaceae. *Plant Molecular Biology*, 42, 93-114.

- RASMANN, S., KÖLLNER, T. G., DEGENHARDT, J., HILTPOLD, I., TOEPFER, S., KUHLMANN, U., GERSHENZON, J. & TURLINGS, T. C. J. 2005. Recruitment of Entomopathogenic Nematodes by Insect-Damaged Maize Roots. *Nature*, 434, 732.
- REDEKER, K. R. & CICERONE, R. J. 2004. Environmental Controls over Methyl Halide Emissions from Rice Paddies. *Global Biogeochemical Cycles*, 18.
- REDEKER, K. R., MANLEY, S. L., WALSER, M. & CICERONE, R. J. 2004. Physiological and Biochemical Controls over Methyl Halide Emissions from Rice Plants. *Global Biogeochemical Cycles*, 18.
- REDEKER, K. R., WANG, N.-Y., LOW, J. C., MCMILLAN, A., TYLER, S. C. & CICERONE, R. J. 2000. Emissions of Methyl Halides and Methane from Rice Paddies. *Science*, 290, 966-969.
- REICHEL, C., MATHUR, J., ECKES, P., LANGENKEMPER, K., KONCZ, C., SCHELL, J., REISS, B. & MAAS, C. 1996. Enhanced Green Fluorescence by the Expression of an Aequorea Victoria Green Fluorescent Protein Mutant in Mono- and Dicotyledonous Plant Cells. *Proceedings of the National Academy of Sciences of the United States of America*, 93, 5888-5893.
- RETTENMEIER, R., NATT, E., ZENTGRAF, H. & SCHERER, G. 1990. Isolation and Characterization of the Human Tyrosine Aminotransferase Gene. *Nucleic Acids Research*, 18, 3853-3861.
- RHEW, R. C., OSTERGAARD, L., SALTZMAN, E. S. & YANOFSKY, M. F. 2003. Genetic Control of Methyl Halide Production in Arabidopsis. *Curr Biol*, 13, 1809-13.
- ROBERTS, A. F., DEVOS, Y., LEMGO, G. N. Y. & ZHOU, X. 2015. Biosafety Research for Non-Target Organism Risk Assessment of RNAi-Based Ge Plants. *Frontiers in Plant Science*, 6, 958.
- ROSTÁS, M. & EGGERT, K. 2008. Ontogenetic and Spatio-Temporal Patterns of Induced Volatiles in Glycine Max in the Light of the Optimal Defence Hypothesis. *Chemoecology*, 18, 29-38.
- ROTT, M., LAWRENCE, T., BELTON, M., SUN, F. & KYLE, D. 2010. Occurrence and Detection of *Globodera rostochiensis* on Vancouver Island, British Columbia: An Update. *Plant Disease*, 94, 1367-1371.
- RUIZ-SUÁREZ, N., BOADA, L. D., HENRÍQUEZ-HERNÁNDEZ, L. A., GONZÁLEZ-MOREO, F., SUÁREZ-PÉREZ, A., CAMACHO, M., ZUMBADO, M., ALMEIDA-GONZÁLEZ, M., DEL MAR TRAVIESO-AJA, M. & LUZARDO, O. P. 2015. Continued Implication of the Banned Pesticides Carbofuran and Aldicarb in the Poisoning of Domestic and Wild Animals of the Canary Islands (Spain). *Science of The Total Environment*, 505, 1093-1099.
- SAINI, H. S., ATTIEH, J. M. & HANSON, A. D. 1995. Biosynthesis of Halomethanes and Methanethiol by Higher Plants Via a Novel Methyltransferase Reaction. *Plant, Cell & Environment*, 18, 1027-1033.
- SALAZAR, A. & RITTER, E. 1993. Effects of Daylight During Cyst Formation, Storage Time and Temperature of Cysts on the *in Vitro* Hatching of *Globodera rostochiensis* and *G. pallida*. *Fundamental and Applied Nematology*, 16, 567-572.
- SAMUNI-BLANK, M., IZHAKI, I., DEARING, M. D., GERCHMAN, Y., TRABELCY, B., LOTAN, A., KARASOV, WILLIAM H. & ARAD, Z. 2012. Intraspecific Directed Deterrence by the Mustard Oil Bomb in a Desert Plant. *Current Biology*, 22, 1218-1220.

- SARATHCHANDRA, S. U., DI MENNA, M. E., BURCH, G., BROWN, J. A., WATSON, R. N., BELL, N. L. & COX, N. R. 1995. Effects of Plant-Parasitic Nematodes and Rhizosphere Microorganisms on the Growth of White Clover (*Trifolium repens* L.) and Perennial Ryegrass (*Lolium perenne* L.). *Soil Biology and Biochemistry*, 27, 9-16.
- SCHINDELIN, J., ARGANDA-CARRERAS, I., FRISE, E., KAYNIG, V., LONGAIR, M., PIETZSCH, T., PREIBISCH, S., RUEDEN, C., SAALFELD, S. & SCHMID, B. 2012. Fiji: An Open-Source Platform for Biological-Image Analysis. *Nature methods*, 9, 676.
- SCHNEIDER, C. A., RASBAND, W. S. & ELICEIRI, K. W. 2012. NIH Image to ImageJ: 25 Years of Image Analysis. *Nature Methods*, 9, 671-675.
- SCHUBERT, H. L., BLUMENTHAL, R. M. & CHENG, X. 2003. Many Paths to Methyltransfer: A Chronicle of Convergence. *Trends Biochem Sci*, 28, 329-35.
- SCHWEINSBERG, P. & GRANT, B. 2013. *C. Elegans* Gene Transformation by Microparticle Bombardment. In: COMMUNITY, T. C. E. R. (ed.) *Wormbook*.
- SEMPLE, J. I., GARCIA-VERDUGO, R. & LEHNER, B. 2010. Rapid Selection of Transgenic *C. Elegans* Using Antibiotic Resistance. *Nat Methods*, 7, 725-7.
- SHAPIRO, T. A., FAHEY, J. W., WADE, K. L., STEPHENSON, K. K. & TALALAY, P. 2001. Chemoprotective Glucosinolates and Isothiocyanates of Broccoli Sprouts. *Metabolism and Excretion in Humans*, 10, 501-508.
- SHROFF, R., VERGARA, F., MUCK, A., SVATOŠ, A. & GERSHENZON, J. 2008. Nonuniform Distribution of Glucosinolates in *Arabidopsis Thaliana* Leaves Has Important Consequences for Plant Defense. *Proceedings of the National Academy of Sciences of the United States of America*, 105, 6196-6201.
- SHYU, Y. J. & HU, C.-D. 2008. Fluorescence Complementation: An Emerging Tool for Biological Research. *Trends in Biotechnology*, 26, 622-630.
- SIES, H. 1997. Oxidative Stress: Oxidants and Antioxidants. *Experimental Physiology*, 82, 291-295.
- SIJMONS, P. C., GRUNDLER, F. M. W., MENDE, N., BURROWS, P. R. & WYSS, U. 1991. *Arabidopsis thaliana* as a New Model Host for Plant-Parasitic Nematodes. *The Plant Journal*, 1, 245-254.
- SKANTAR, A. M., HANDOO, Z. A., ZASADA, I. A., INGHAM, R. E., CARTA, L. K. & CHITWOOD, D. J. 2011. Morphological and Molecular Characterization of *Globodera* Populations from Oregon and Idaho. *Phytopathology*, 101, 480-91.
- SKELSEY, P; KETTLE, H; MACKENZIE, K; & BLOK, V. 2018. Potential Impacts of Climate Change on the Threat of Potato Cyst Nematode Species in Great Britain. *Plant Pathology* 67, 909-919
- SMANT, G., STOKKERMANS, J. P., YAN, Y., DE BOER, J. M., BAUM, T. J., WANG, X., HUSSEY, R. S., GOMMERS, F. J., HENRISSAT, B., DAVIS, E. L., HELDER, J., SCHOTS, A. & BAKKER, J. 1998. Endogenous Cellulases in Animals: Isolation of Beta-1, 4-Endoglucanase Genes from Two Species of Plant-Parasitic Cyst Nematodes. *Proc Natl Acad Sci U S A*, 95, 4906-11.
- SOBCZAK, M. & GOLINOWSKI, W. 2011. Cyst Nematodes and Syncytia. *Genomics and Molecular Genetics of Plant-Nematode Interactions*. Springer Netherlands.
- SOBOLESKI, M. R., OAKS, J. & HALFORD, W. P. 2005. Green Fluorescent Protein Is a Quantitative Reporter of Gene Expression in Individual Eukaryotic Cells. *The FASEB journal : official publication of the Federation of American Societies for Experimental Biology*, 19, 440-442.

- SØNDERBY, I. E., GEU-FLORES, F. & HALKIER, B. A. 2010. Biosynthesis of Glucosinolates – Gene Discovery and Beyond. *Trends in Plant Science*, 15, 283-290.
- SONTHEIMER, E. J. 2005. Assembly and Function of Rna Silencing Complexes. *Nat Rev Mol Cell Biol*, 6, 127-38.
- SPIETH, J., LAWSON, D., DAVIS, P., WILLIAMS, G. & HOWE, K. 2014. Overview of Gene Structure in *C. Elegans*. In: COMMUNITY, T. C. E. R. (ed.) *Wormbook*.
- SPOONER, D. M., MCLEAN, K., RAMSAY, G., WAUGH, R. & BRYAN, G. J. 2005. A Single Domestication for Potato Based on Multilocus Amplified Fragment Length Polymorphism Genotyping. *Proceedings of the National Academy of Sciences of the United States of America*, 102, 14694-14699.
- STARR, J. L., KOENNING, S. R., KIRKPATRICK, T. L., ROBINSON, A. F., ROBERTS, P. A. & NICHOLS, R. L. 2007. The Future of Nematode Management in Cotton. *Journal of Nematology*, 39, 283-294.
- STATES, D. J. & GISH, W. 1994. Combined Use of Sequence Similarity and Codon Bias for Coding Region Identification. *J Comput Biol*, 1, 39-50.
- STEFELS, J., STEINKE, M., TURNER, S., MALIN, G. & BELVISO, S. 2007. Environmental Constraints on the Production and Removal of the Climatically Active Gas Dimethylsulphide (DMS) and Implications for Ecosystem Modelling. *Biogeochemistry*, 83, 245-275.
- STIERNAGLE, T. 1999. 4. Maintenance of *C. elegans*. In: HOPE, I. (ed.) *C. Elegans: A Practical Approach*. Oxford University Press.
- STIRLING, G. R. & STIRLING, A. M. 2003. The Potential of *Brassica* Green Manure Crops for Controlling Root-Knot Nematode (*Meloidogyne javanica*) on Horticultural Crops in a Subtropical Environment. *Australian Journal of Experimental Agriculture*, 43, 623-630.
- TALLARIDA, R. J. 2011. Quantitative Methods for Assessing Drug Synergism. *Genes & Cancer*, 2, 1003-1008.
- TERAZAWA, K., MIZUKAMI, K., WU, B. & TAKATORI, T. 1991. Fatality Due to Inhalation of Dimethyl Sulfide in a Confined Space: A Case Report and Animal Experiments. *International Journal of Legal Medicine*, 104, 141-144.
- THATCHER, J. D., HAUN, C. & OKKEMA, P. G. 1999. The *daf-3* SMAD Binds DNA and Represses Gene Expression in the *Caenorhabditis Elegans* Pharynx. *Development*, 126, 97-107.
- THE *C. ELEGANS* SEQUENCING CONSORTIUM 1998. Genome Sequence of the Nematode *C. Elegans*: A Platform for Investigating Biology. *Science*, 282, 2012-2018.
- THORNALLEY, P. J. 2003. Glyoxalase I – Structure, Function and a Critical Role in the Enzymatic Defence against Glycation. *Biochemical Society Transactions*, 31, 1343-1348.
- THORPE, P., MANTELIN, S., COCK, P. J., BLOK, V. C., COKE, M. C., EVES-VAN DEN AKKER, S., GUZEEVA, E., LILLEY, C. J., SMANT, G., REID, A. J., WRIGHT, K. M., URWIN, P. E. & JONES, J. T. 2014. Genomic Characterisation of the Effector Complement of the Potato Cyst Nematode *Globodera pallida*. *BMC Genomics*, 15, 923.
- TOOKEY, H. L. 1973. Crambe Thioglucoside Glucohydrolase (EC 3.2.3.1): Separation of a Protein Required for Epithiobutane Formation. *Can J Biochem*, 51, 1654-60.
- TORRES, M. A., JONES, J. D. G. & DANGL, J. L. 2006. Reactive Oxygen Species Signaling in Response to Pathogens. *Plant Physiology*, 141, 373-378.

- TRUDGILL, D. L. 1997. Parthenogenetic Root-Knot Nematodes (*Meloidogyne spp.*); How Can These Biotrophic Endoparasites Have Such an Enormous Host Range? *Plant Pathology*, 46, 26-32.
- TRUDGILL, D. L. & BLOK, V. C. 2001. Apomictic, Polyphagous Root-Knot Nematodes: Exceptionally Successful and Damaging Biotrophic Root Pathogens. *Annual Review of Phytopathology*, 39, 53-77.
- TSVETKOV, N., SAMSON-ROBERT, O., SOOD, K., PATEL, H. S., MALENA, D. A., GAJIWALA, P. H., MACIUKIEWICZ, P., FOURNIER, V. & ZAYED, A. 2017. Chronic Exposure to Neonicotinoids Reduces Honey Bee Health near Corn Crops. *Science*, 356, 1395-1397.
- TURLINGS, T. C. J., HILTPOLD, I. & RASMANN, S. 2012. The Importance of Root-Produced Volatiles as Foraging Cues for Entomopathogenic Nematodes. *Plant and Soil*, 358, 51-60.
- TURNER, S. J. 1996. Population Decline of Potato Cyst Nematodes (*Globodera rostochiensis*, *G. pallida*) in Field Soils in Northern Ireland. *Annals of Applied Biology*, 129, 315-322.
- TURNER, S. J. & SUBBOTIN, S. A. 2013. Cyst Nematodes. In: PERRY, R. N. & MOENS, M. (eds.) *Plant Nematology, 2nd Edition*. CABI.
- TYLER, J. 1933. Development of the Root-Knot Nematode as Affected by Temperature. *Hilgardia*, 7, 389-415.
- UNEP 2002. United Nations Environment Programme, Fourteenth Meeting of the Parties to the Montreal Protocol on Substances That Deplete the Ozone Layer. In: UNEP (ed.) *Pro14/3*.
- UNEP 2005. Effects of trade liberalization on agriculture in Lebanon: with special focus on products where methyl bromide is used. 1st ed. United Nations Environmental Programme.
- UNEP 2012. Handbook for the Montreal Protocol on Substances That Deplete the Ozone Layer. In: SECRETARIAT, O. (ed.) 9 ed.
- UNEP. 2017. Critical-Use Exemptions for Methyl Bromide for 2018 and 2019. Twenty-Ninth Meeting of the Parties to the Montreal Protocol on Substances that Deplete the Ozone Layer, 2017 Montreal, Canada. United Nations Environment Programme.
- UNFCCC 2016. The Paris Agreement, C.N.92.2016.Treaties-Xxvii.7.D. In: UNTS (ed.). New York: United Nations.
- URWIN, P. E., ATKINSON, H. J., WALLER, D. A. & MCPHERSON, M. J. 1995. Engineered Oryzacystatin-I Expressed in Transgenic Hairy Roots Confers Resistance to *Globodera Pallida*. *Plant J*, 8, 121-31.
- VALDES, Y., VIAENE, N. & MOENS, M. 2012. Effects of Yellow Mustard Amendments on the Soil Nematode Community in a Potato Field with Focus on *Globodera Rostochiensis*. *Applied Soil Ecology*, 59, 39-47.
- VAN DOORN, H. E., VAN DER KRUK, G. C., VAN HOLST, G.-J., RAAIJMAKERS-RUIJS, N. C. M. E., POSTMA, E., GROENEWEG, B. & JONGEN, W. H. F. 1998. The Glucosinolates Sinigrin and Progoitrin Are Important Determinants for Taste Preference and Bitterness of Brussels Sprouts. *Journal of the Science of Food and Agriculture*, 78, 30-38.
- VAN MEGEN, H., HOLOVACHOV, O., BONGERS, T., BAKKER, J., HELDER, J., VAN DEN ELSEN, S., HOLTERMAN, M., KARSSSEN, G. & MOOYMAN, P. 2009. A Phylogenetic

- Tree of Nematodes Based on About 1200 Full-Length Small Subunit Ribosomal DNA Sequences. *Nematology*, 11, 927-950.
- VERVOORT, M. T. W., VONK, J. A., BROLSMA, K. M., SCHÜTZE, W., QUIST, C. W., DE GOEDE, R. G. M., HOFFLAND, E., BAKKER, J., MULDER, C., HALLMANN, J. & HELDER, J. 2014. Release of Isothiocyanates Does Not Explain the Effects of Biofumigation with Indian Mustard Cultivars on Nematode Assemblages. *Soil Biology and Biochemistry*, 68, 200-207.
- WAH CHU, K. & CHOW, K. L. 2002. Synergistic Toxicity of Multiple Heavy Metals Is Revealed by a Biological Assay Using a Nematode and Its Transgenic Derivative. *Aquatic Toxicology*, 61, 53-64.
- WANG, X., MITCHUM, M. G., GAO, B., LI, C., DIAB, H., BAUM, T. J., HUSSEY, R. S. & DAVIS, E. L. 2005. A Parasitism Gene from a Plant-Parasitic Nematode with Function Similar to CLAVATA3/ESR (Cle) of Arabidopsis Thaliana. *Mol Plant Pathol*, 6, 187-91.
- WARNOCK, N. D., WILSON, L., PATTEN, C., FLEMING, C. C., MAULE, A. G. & DALZELL, J. J. 2017. Nematode Neuropeptides as Transgenic Nematicides. *PLoS Pathogens*, 13, e1006237.
- WEINTRAUB, P. G. 2016. The Importance of Publishing Negative Results. *Journal of Insect Science*, 16, 109.
- WHITEHEAD, A. G., TITE, D. J., FRASER, J. E. & NICHOLS, A. J. F. 1984. Differential Control of Potato Cyst-Nematodes, *Globodera rostochiensis* and *G. pallida* by Oxamyl and the Yields of Resistant and Susceptible Potatoes in Treated and Untreated Soils. *Annals of Applied Biology*, 105, 231-244.
- WIESNER, R. J., RÜEGG, J. C. & MORANO, I. 1992. Counting Target Molecules by Exponential Polymerase Chain Reaction: Copy Number of Mitochondrial DNA in Rat Tissues. *Biochemical and Biophysical Research Communications*, 183, 553-559.
- WILLIAMS, R. T. 1959. *Deoxygenation Mechanisms: The Metabolism and Detoxication of Drugs, Toxic Substances and Other Organic Compounds*, Chapman and Hall.
- WILSON, E., OKUOM, M., KYES, N., MAYFIELD, D., WILSON, C., SABATKA, D., SANDOVAL, J., FOOTE, J., KANGAS, M., HOLMES, A. & SUTLIEF, A. 2018. Using Fluorescence Intensity of Enhanced Green Fluorescent Protein to Quantify Pseudomonas Aeruginosa. *Chemosensors*, 6, 21.
- WITTKOPP, P. J. & KALAY, G. 2011. Cis-Regulatory Elements: Molecular Mechanisms and Evolutionary Processes Underlying Divergence. *Nat Rev Genet*, 13, 59-69.
- WITTSTOCK, U., AGERBIRK, N., STAUBER, E. J., OLSEN, C. E., HIPPLER, M., MITCHELL-OLDS, T., GERSHENZON, J. & VOGEL, H. 2004. Successful Herbivore Attack Due to Metabolic Diversion of a Plant Chemical Defense. *Proc Natl Acad Sci U S A*, 101, 4859-64.
- WITTSTOCK, U. & BUROW, M. 2007. Tipping the Scales - specifier Proteins in Glucosinolate Hydrolysis. *IUBMB Life*, 59, 744-751.
- WMO, W. M. O. 2014. Assessment for Decision-Makers: Scientific Assessment of Ozone Depletion: 2014. *Global Ozone Research and Monitoring Project*. Geneva, Switzerland.
- WOOD, C., KENYON, D. M. & COOPER, J. M. 2017. Allyl Isothiocyanate Shows Promise as a Naturally Produced Suppressant of the Potato Cyst Nematode In Biofumigation Systems. *Nematology*, 19, 389-402.

- WOODCOCK, B. A., BULLOCK, J. M., SHORE, R. F., HEARD, M. S., PEREIRA, M. G., REDHEAD, J., RIDDING, L., DEAN, H., SLEEP, D., HENRYS, P., PEYTON, J., HULMES, S., HULMES, L., SÁROSPATAKI, M., SAURE, C., EDWARDS, M., GENERSCH, E., KNÄBE, S. & PYWELL, R. F. 2017. Country-Specific Effects of Neonicotinoid Pesticides on Honey Bees and Wild Bees. *Science*, 356, 1393-1395.
- WRATHER, J. A., ANDERSON, T. R., ARSYAD, D. M., TAN, Y., PLOPER, L. D., PORTA-PUGLIA, A., RAM, H. H. & YORINORI, J. T. 2001. Soybean Disease Loss Estimates for the Top Ten Soybean-Producing Countries in 1998. *Canadian Journal of Plant Pathology*, 23, 115-121.
- WU, H., WANG, C.-J., BIAN, X.-W., ZENG, S.-Y., LIN, K.-C., WU, B., ZHANG, G.-A. & ZHANG, X. 2011. Nematicidal Efficacy of Isothiocyanates against Root-Knot Nematode *Meloidogyne javanica* in Cucumber. *Crop Protection*, 30, 33-37.
- XU, Z. W., ESCAMILLA-TREVINO, L. L., ZENG, L. H., LALGONDAR, M., BEVAN, D. R., WINKEL, B. S. J., MOHAMED, A., CHENG, C. L., SHIH, M. C., POULTON, J. E. & ESEN, A. 2004. Functional Genomic Analysis of *Arabidopsis thaliana* Glycoside Hydrolase Family 1. *Plant Molecular Biology*, 55, 343-367.
- XUE, J., LENMAN, M., FALK, A. & RASK, L. 1992. The Glucosinolate-Degrading Enzyme Myrosinase in Brassicaceae Is Encoded by a Gene Family. *Plant Molecular Biology*, 18, 387-398.
- YANG, R. S., WITT, K. L., ALDEN, C. J. & COCKERHAM, L. G. 1995. Toxicology of Methyl Bromide. *Rev Environ Contam Toxicol*, 142, 65-85.
- YILDIZ, S. 2011. Rotational and Nematicidal Effect of Lupine (*Lupinus Albus* L.: Leguminosae).
- YOKOUCHI, Y., NOIJIRI, Y., BARRIE, L. A., TOOM-SAUNTRY, D., MACHIDA, T., INUZUKA, Y., AKIMOTO, H., LI, H. J., FUJINUMA, Y. & AOKI, S. 2000. A Strong Source of Methyl Chloride to the Atmosphere from Tropical Coastal Land. *Nature*, 403, 295.
- ZASADA, I. A. & FERRIS, H. 2003. Sensitivity of *Meloidogyne javanica* and *Tylenchulus semipenetrans* to Isothiocyanates in Laboratory Assays. *Phytopathology*, 93, 747-750.
- ZASADA, I. A., MEYER, S. L. F. & MORRA, M. J. 2009. Brassicaceous Seed Meals as Soil Amendments to Suppress the Plant-Parasitic Nematodes *Pratylenchus penetrans* and *Meloidogyne incognita*. *Journal of Nematology*, 41, 221-227.
- ZHANG, S., MA, C. & CHALFIE, M. 2004. Combinatorial Marking of Cells and Organelles with Reconstituted Fluorescent Proteins. *Cell*, 119, 137-144.
- ZHANG, W., WANG, W., LIU, Z., XIE, Y., WANG, H., MU, Y., HUANG, Y. & FENG, Y. 2016. Crystal Structure of the Epithiospecifier Protein, ESP from *Arabidopsis thaliana* Provides Insights into Its Product Specificity. *Biochemical and Biophysical Research Communications*, 478, 746-751.
- ZHANG, W., ZHOU, Y., WANG, K., DONG, Y., WANG, W. & FENG, Y. 2017. Crystal Structure of the Nitrile-Specifier Protein NSP1 from *Arabidopsis thaliana*. *Biochemical and Biophysical Research Communications*, 488, 147-152.
- ZHANG, Y. 2000. Role of Glutathione in the Accumulation of Anticarcinogenic Isothiocyanates and Their Glutathione Conjugates by Murine Hepatoma Cells. *Carcinogenesis*, 21, 1175-82.